Identification and characterization of regulatory factors and regulatory RNA elements controlling the expression of the primary invasion factors invasin and YadA in *Yersinia pseudotuberculosis*

Von der Fakultät für Lebenswissenschaften

der Technischen Universität Carolo-Wilhelmina

zu Braunschweig

zur Erlangung des Grades einer

Doktorin der Naturwissenschaften

(Dr. rer. nat.)

genehmigte

D i s s e r t a t i o n

von Katja Böhme

aus Dresden

1. Referentin oder Referent: Professor Dr. Petra Dersch

2. Referentin oder Referent: Professor Dr. Michael Steinert

eingereicht am: 10. 11. 2010

mündliche Prüfung (Disputation) am: 22. 12.2010

Druckjahr 2011

Vorveröffentlichungen der Dissertation

Teilergebnisse aus dieser Arbeit wurden mit Genehmigung der Fakultät für Lebenswissenschaften, vertreten durch die Mentorin der Arbeit, in folgenden Beiträgen vorab veröffentlicht:

Publikationen

Böhme K., Heroven A. K., Sievers S., Schaake J. & Dersch P.: YmoA activates expression of the regulatory RNA CsrC, and induces synthesis of the virulence regulator RovA in *Yersinia pseudotuberculosis*. In preparation.

Böhme K., Steinmann R., Opitz W., Heroven A. K., Kortmann J., Pisano F., Dornbusch E., Ritter S., Fehse S., Eitel J., Wolf-Watz H. & Narberhaus F.: A coupled RNA thermometer and cell contact sensor controls virulence gene expression in *Yersinia pseudotuberculosis*. In preparation.

Heroven A. K., Böhme K., Rohde M. & Dersch P.: A Csr-type regulatory system, including small non-coding RNAs, regulates the global virulence regulator RovA of *Yersinia pseudotuberculosis* through RovM. Mol Microbiol. 2008 Jun; 68(5):1179-95.

Heroven A. K., Böhme K., Tran-Winkler H. & Dersch P.: Regulatory elements implicated in the environmental control of invasin expression in enteropathogenic *Yersinia.* (Review) Adv Exp Med Biol. 2007; 603:156-66.

Tagungsbeiträge

Heroven A. K., Böhme K. & Dersch P.: Different strategies of invasion of *Yersinia pseudotuberculosis* into host cells. (Vortrag) 10th International Symposium "*Yersinia* 2010". Recife, Brasilien (2010).

Böhme K., Heroven A. K. & Dersch P.: The nucleoid-associated protein YmoA is a key regulator for the control of Csr-type regulatory RNAs and for switching virulence gene expression in *Yersinia pseudotuberculosis*. (Vortrag) 10th International Symposium "*Yersinia* 2010". Recife, Brasilien (2010).

Steinmann R., Böhme K. & Dersch P.: Regulation of the virulence regulator LcrF in *Yersinia pseudotuberculosis* (Vortrag). 2. Nationale *Yersinia*-Konferenz. München (2010).

Böhme K., Heroven A. K., Steinmann R., Opitz W., Kortmann J., Narberhaus F. & Dersch P.: The synthesis of important virulence factors in *Yersinia pseudotuberculosis* underlies the control of a complex regulatory network during the infection process. (Poster) Jahrestagung der Vereinigung Allgemeiner und Angewandter Mikrobiologie. Hannover (2010).

Böhme K., Dornbusch E., Fehse S. & Dersch P.: Complex network regulates synthesis of invasin and YadA in *Y. pseudotuberculosis*. (Poster) International Conference "Sensory and regulatory RNAs in prokaryotes". Berlin (2009).

Böhme, K., Heroven A. K. & Dersch P.: YmoA regulates the synthesis of the adhesins Invasin and YadA in *Yersinia pseudotuberculosis*. (Vortrag) International Workshop of the International Graduate School "Molecular Complexes of Biomedical Relevance". Braunschweig (2009).

Böhme, K., Heroven A. K. & Dersch P.: YmoA activates expression of the virulence regulator gene *rovA* in *Yersinia pseudotuberculosis* through the Csr regulatory system. (Vortrag) Jahrestagung der Vereinigung Allgemeiner und Angewandter Mikrobiologie (2009).

Heroven A. K., Böhme K. & Dersch P.: The *Yersinia pseudotuberculosis* Csr system is a key regulatory system for the control of virulence, motility and metabolism. (Poster) Jahrestagung der Vereinigung Allgemeiner und Angewandter Mikrobiologie. Bochum (2009).

Böhme K., Dornbusch E., Fehse S. & Dersch P.: The *Yersinia* virulence modulator "YmoA" in the control of *rovA* and *virF* expression. (Poster) 1. Nationale *Yersinia*-Konferenz. Braunschweig (2008).

Böhme K., Dornbusch E., Fehse S. & Dersch P.: The *Yersinia* virulence modulator "YmoA" in the control of *rovA* and *virF* expression. (Poster) Symposium der Fachgruppe „Mikrobielle Pathogenität" der DGHM. Bad Urach (2008).

Böhme K., Dornbusch E. & Dersch P.: Synthesis of the transcription activator VirF in *Yersinia* is regulated by an RNA thermometer. (Poster) Schwerpunkttreffen des SPP 1258, Sensorische und regulatorische RNAs in Prokaryoten. Bochum (2008).

Heroven A. K, Böhme K. & Dersch P.: A CsrC-type non-coding RNA and a CsrA-type regulatory factor control virulence gene expression, environmental adaptation, motility and general fitness of *Yersinia pseudotuberculosis.* (Poster) 9th International Symposium on *Yersinia*. Lexington, USA (2007).

Danksagung

Diese Dissertation war möglich, dank der vielfältigen Unterstützung durch Kollegen, Freunde und im Besonderen meiner Familie. Bei Prof. Dr. Petra Dersch möchte ich mich besonders für die zahlreichen Diskussionen und motivierenden Worte während der vergangenen Jahre bedanken. Weiterhin danke ich dem Internationalen Graduiertenkolleg „Molecular Complexes of Biomedical Relevance“ für die zusätzliche abwechslungsreiche Ausbildung und die Finanzierung meiner Promotion. Jens Kortmann und Prof. Franz Narberhaus sei herzlich gedankt, dass ich in ihrer Arbeitsgruppe an der Ruhruniversität Bochum einen Teil der Experimente dieser Arbeit mit Hilfe ihres Fachwissens durchführen konnte. Bei der gesamten Arbeitsgruppe „Molekulare Infektionsbiologie“ am Helmholtz-Zentrum möchte ich mich für die motivierende, inspirierende Arbeitsatmosphäre danken, inbesondere Dr. Ann Kathrin Heroven, Tanja Thiermann und Rebekka Steinmann. Und nicht zuletzt ein Dankeschön an Prof. Dr. Michael Steinert für die Übernahme des Koreferats.

Table of contents

List of figures

List of tables

Abbreviation

A	adenine
AHT	anhydrotetracycline
Ap	ampicillin
aqua bidest.	double-destilled water
ATP	adenosine triphosphate
BCIP	5-bromo-4-chloro-3-indolyl phosphate
bp	base pair
C	cytosine
Cm	chloramphenicol
CV	column volume
Da	dalton
DMF	dimethylformamide
DNA	desoxyribonucleic acid
DTT	dithiothreitol
DYT	double yeast tryptone medium
EDTA	ethylenediaminetetraacetic acid
G	guanine
IS	insertion sequence
kb	kilobase
kDa	kilo-Dalton
Kn	kanamycin
kV	kilovolt
lacZ	reporter gene encoding for β-galactosidase
LB	Luria-Bertani medium
M	molare
mA	milliampere
µF	microfarad
µg	microgram
mg	milligram
min	minute
µl	microliter
ml	milliliter
mM	millimolare
MMA	minimal medium A
NBT	nitro blue tetrazolium
ng	nanogram
nm	nanometer

nM	nanomolare
nt	nucleotides
dNTP	deoxynucleotide triphosphate
OD	optical density
Ω	ohm
ONPG	o-nitrophenyl-β-galactosidase
PAGE	polyacrylamide gelelectrophoresis
PCR	polymerase chain reaction
pmol	picomol
PNK	T4 polynucleotide kinase
rbs	ribosomal binding site
RNA	ribonucleic acid
rpm	rotations per minute
SD	Shine-Dalgarno
SDS	sodium dodecyl sulfate
t	time
T	thymine
TAE	tris-acetate buffer
Taq	DNA polymerase of *Thermus aquaticus*
TBE	Tris/Borate/EDTA
TEMED	tetramethylethylenediamine
Tet	tetracycline
Tris	trishydroxymethylaminomethane
U	uridine
U/µl	units/microliter
UTR	untranslated region
V	volume

1 Introduction

Pathogenic *Enterobacteriaceae* such as *Salmonella* spp., *E. coli* spp., or *Yersinia* spp. are not only found in the gastrointestinal tract but also in soil or water (Fremaux, *et al*. 2008; Guan and Holley 2003; Sherman, *et al*. 2010). Throughout their infectious lifecycle, they face numerous rapidly changing environmental conditions, which include changing temperatures, pH, oxygen content, altering nutrients and ion concentrations. Thus, the bacteria need to adapt their metabolism immediately according to their new living circumstances. Moreover, environmental signals trigger the expression of virulence determinants for optimally survival and colonisation of the pathogen within the host organism.

1.1 The genus *Yersinia*

Yersiniae are described as rod-shaped and gram negative bacteria of which some species are motile. The bacteria grow at temperatures up to 43°C and at moderate temperature down to 4°C, which characterizes them as psychrophil. The genus comprises 14 species but only three species, i.e. *Y. enterocolitica*, *Y. pseudotuberculosis* and *Y. pestis,* cause diseases in humans with a common tropism. The pathogens preferentially colonize the lymphoid tissues of their host and form microcolonies and microabscesses. They circumvent the host immune system by inhibiting phagocytosis through macrophages or polymorphonuclear leukocytes and impair lysis by the complement system. Their infection process, however, differs greatly (Autenrieth, *et al*. 1993; Bergsbaken and Cookson 2009; Heesemann, *et al*. 2006; Hurst, *et al*. 2010; Li and Yang 2008; Murros-Kontiainen, *et al*. 2010a; Murros-Kontiainen, *et al*. 2010b; Sebbane, *et al*. 2006).

Y. pestis, which evolved from *Y. pseudotuberculosis* 1,500 to 20,000 years ago, represents the etiological agent of bubonic, septemic or pneumonic plaque. *Y. pestis* is found living zoonotically in rodents from where it is transmitted to humans by bites of infected fleas. *Y. pestis* still causes outbreaks lately reported from North America, Africa and Asia (Butler 2009; Perry and Fetherston 1997; WHO 2009).

Y. enterocolitica and *Y. pseudotuberculosis* have been isolated from soil, water, plants or domestic and wildlife animals, especially pigs. They occur primarily in the temperate zone of the northern hemisphere. The species *Y. enterocolitica* includes a variety of serotypes differing in virulence. They comprise serotypes O:3 or O:9 predominantly found in Europe and serotypes O:8 or O:13 isolated in North America. In contrast, *Y. pseudotuberculosis* serotypes show comparable infectivity and virulence (Bottone 1997; Bottone 1999; Rosner, *et al*. 2010). Both species cause gut-associated diseases ranging from enteritis and terminal ileitis to mesenterial lymphadenitis also known as yersiniosis (Dube 2009; Pepe, *et al*. 1995; Trulzsch, *et al*. 2007).

1.1.1 Route of infection of *Y. pseudotuberculosis*

Alike *Y. enterocolitica*, *Y. pseudotuberculosis* is taken up by contaminated food or water. The bacteria pass the gastrointestinal tract and encounter the ileum which represents the final part of the small intestine. During this **early infection phase**, the pathogen is able to adhere and to invade into specialized cells of the host immune system, intercalated within the epithelial cell layer, the so-called M-cells (Fig. 1).

In general, M-cells take up macromolecules as well as pathogenic material by endocytosis or phagocytosis. In contrast to neighbouring epithelial cells they lack microvilli at the apical side and form a pocket-like structure at their basolateral side containing dendritic cells, macrophages and lymphocytes. Thereby, antigenic material is delivered from the lumen towards cells of the host immune system (Jang, *et al*. 2004; Neutra, *et al*. 1996). *Y. pseudotuberculosis* translocates through the M-cells and reaches the underlying lymphoid tissue, the Peyer's patches (Grutzkau, *et al*. 1990; Hanski, *et al*. 1989; Sansonetti and Phalipon 1999). In the **later infection phases**, the bacteria are able to proliferate extracellularly and cause microabscesses. Within these, yersiniae form microcolonies to sustain resistance against phagocytosing neutrophils as well as macrophages (Oellerich, *et al*. 2007; Simonet, *et al*. 1990). The genus *Yersinia* has shown to be able to survive in macrophages and dendritic cells which might be used as carriers to transfer to the mesenteric lymph nodes. Eventually, the bacteria disseminate into deeper lymphatic tissues such as liver, spleen and kidney (Marra and Isberg 1996; Pepe and Miller 1993; Pujol and Bliska 2005). Finally, a yersiniae infection can result in auto-immune diseases, for example reactive arthritis, in particular in hosts carrying the major histocompatibility complex HLA-B27 (Carter and Hudson 2009; Girschick, *et al*. 2008; Toivanen and Toivanen 2004). Few infections in patients with underlying disorders such as HIV, diabetes or hepatic cirrhosis have shown that enteropathogenic yersiniae may lead to septemic infections (Ljungberg, *et al*. 1995; Paglia, *et al*. 2005).

Throughout the infection process, *Y. pseudotuberculosis* faces different tissues which present a variety of different surface molecules and components of the host immune system. The pathogen therefore needs to produce specific virulence factors allowing an efficient adaptation to these different tissue components. In the early infection phase, *Y. pseudotuberculosis* carries flagella and smooth lipopolysaccharides. To translocate efficiently through the M-cells to the lymphoid-follicle tissue yersiniae expose the non-fimbrial protein invasin (Fig. 1).

For long-term colonisation in the Peyer's patches and deeper lymphatic tissues yersiniae require a set of virulence factors involving the *Yersinia* adhesin A (YadA), a type III secretion system (*Yersinia* secretion – Ysc) and the thereby transported effector proteins, the *Yersinia* outer protein (Yops) (Fig. 1).

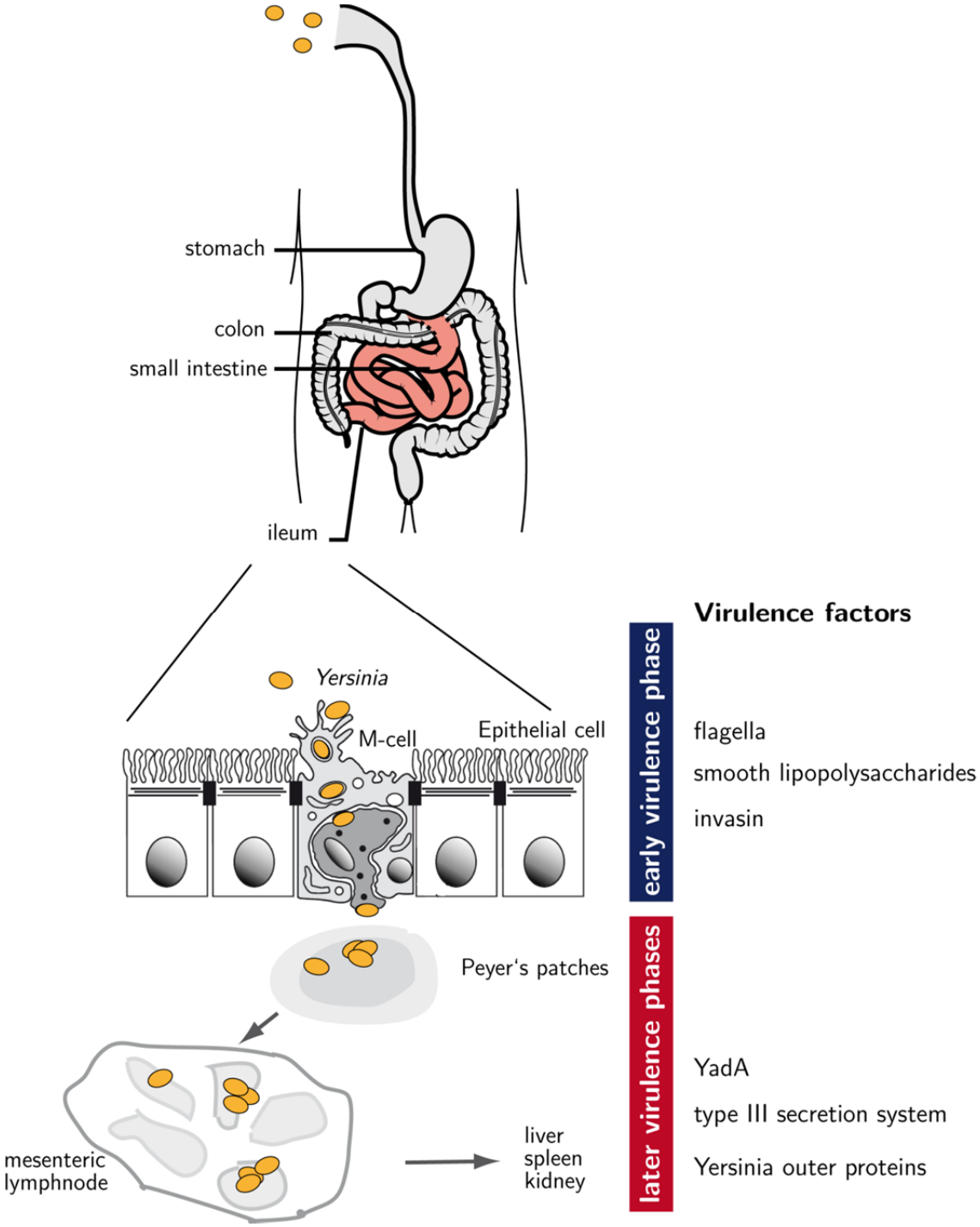

Fig. 1. *Yersinia* infection route. *Yersinia* (in yellow) enters the human host by contaminated food or water and passes the intestinal tract to the small intestine (in red). In the ileum, the bacteria translocate through the gut epithelium by invading the M-cells to reach the underlying Peyer's patches. There, *Yersinia* proliferates and disseminates to the mesenteric lymph nodes and further to liver, spleen or kidney. Early and later infection phases are marked on the right, indicating the important virulence factors expressed during these stages (according to Sansonetti 2002).

1.1.2 Important virulence factors of *Y. pseudotuberculosis*

In the beginning of the infection, the enteric pathogens *Y. pseudotuberculosis* and *Y. enterocolitica* need to penetrate the first epithelial barrier in the distal ileum escaping a fast recognition by cells of the innate immune response in the gut lumen. This process is mediated by the primary virulence factor invasin.

Invasin is chromosomally encoded by the *inv* gene and represents an outer membrane protein of the intimin family of adhesins. The 100 kDa molecule comprises a N-terminus anchored to the bacterial membrane and five extracellular C-terminal domains D1 to D5. Domains D1 to D4 show topological similarities to the Ig superfamily whereas D5 is characterized by a C-terminal-lectin-domain (CTLD) (Marra and Isberg 1997; Niemann, *et al.* 2004). Though invasin shows no sequence homology to fibronectin its three dimensional structure is very similar to the receptor binding domain of the extracellular matrix component (Stebbins and Galan 2001).

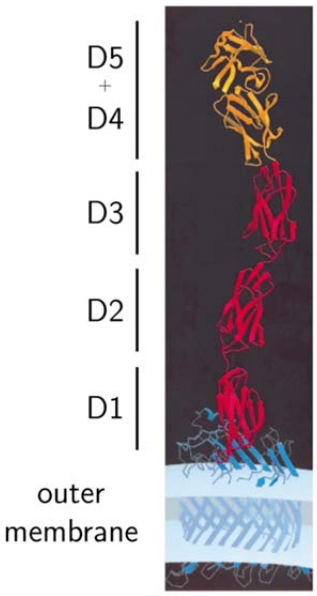

Fig. 2. Crystal structure of the *Y. pseudotuberculosis* invasin. The molecule is located on a bacterial cell with a membrane spanning domain in blue. Domains D1 to D4 show homologies to the Ig superfamily. D5 at the C-terminus represents a C-type lectin like-domain, which together with D4 forms the adhesion complex of invasin (Isberg, *et al.* 2000).

Domains D4 and D5 allow invasin a direct high-affinity binding to $\alpha_5\beta_1$ integrins at the luminal side of the M-cells. Integrins are receptor molecules on the surface of mammalian cells usually involved in cell-cell-interaction. An extracellular domain recognizes the RGD (Arg-Gly-Asp) motif within the substrate, which is resembled by two aspartate residues in D4 and D5 (Fig. 2). An intracellular integrin domain is able to induce a signaling cascade which leads to polymerization of actin filaments. Such actin polymerization restructures the cytoskeleton and activates pseudopod formation at the bacterial contact site. The invasin protein of *Y. pseudotuberculosis* is able to form multimers mediated by the D2 domain (Fig. 2). This clustering induces β_1 integrin-clustering and results in the uptake of the bacterium into non-

phagocytic cells by the zippering mechanism due to an amplification of the intracellular signaling events. *Y. enterocolitica* is missing this D2 domain, so that it internalizes less efficiently into human cells (Grassl, *et al*. 2003; Isberg and Barnes 2001; Isberg, *et al*. 2000; Uliczka, *et al*. 2009; Wong and Isberg 2005). *Y. pestis* is unable to express invasin because of an IS200 element encoded within the *inv* gene (Simonet, *et al*. 1996). Deletion of the *inv* gene in *Y. pseudotuberculosis* resulted in a reduced colonization of the Peyer's patches early during the infection but did not influence the virulence in the mouse after several days post infection. Hence, invasin seems only important for the initial infection stages (Marra and Isberg 1996; Pepe and Miller 1993). Indeed, after two to four hours post infection, *Y. pseudotuberculosis* seems to turn off the synthesis of invasin (J. Eitel, unpublished data).

As mentioned before, *Y. pseudotuberculosis* synthesizes different virulence factors during the ongoing infection phases, which are YadA, a type III secretion system and the Yop effector proteins. These are encoded on the 70 kDa *Yersinia* virulence plasmid pYV. Strains cured from pYV proliferate transiently in the mesenterial lymph nodes and spleen but are eventually eliminated within granulomas by the host immune system (Pujol and Bliska 2005).

The outer membrane protein **Yersinia adhesin A** belongs to the group of trimeric autotransporters which have also been found in other organisms such as *Escherichia coli*, *Moraxella* spp. or *Neisseria* spp. (Cotter, *et al*. 2005; Roggenkamp, *et al*. 2003). The protein has a size of 200 to 240 kDa and forms homotrimers. Its lollipop-like structure is assembled of a C-terminal membrane anchor of β-barrels, a right handed coiled-coil shaped stalk-neck and a surface-exposed head domain (Fig. 3A). The polypeptide interactions of YadA are based on the ionic or hydrophobic nature of the molecules (El Tahir and Skurnik 2001; Hoiczyk, *et al*. 2000; Koretke, *et al*. 2006). The head domain of YadA in *Y. enterocolitica* has been described to form nine-coiled left-handed parallel β-roll (Nummelin, *et al*. 2004). In *Y. pestis*, YadA synthesis is impaired by a frame shift mutation within the gene as well as IS and transposon elements located in the *yadA* promoter region (El Tahir and Skurnik 2001).

Adhesion of *Yersinia* to mammalian cells is mediated by binding of the YadA head domain to $\alpha\beta_1$ integrins using the extracellular matrix proteins fibronectin, collagen or laminin as bridging molecules. This binding leads to the activation of signalling pathways in the host cell producing proinflammatory cytokines such as interleukin 8 (IL-8) and serum resistance of enteric yersiniae (Eitel, *et al*. 2005; Kirjavainen, *et al*. 2008; Schmid, *et al*. 2004; Uliczka, *et al*. 2009).

The N-terminal part of YadA determines different binding specificities to mammalian cells. The YadA head domain of *Y. enterocolitica* binds to $\alpha_2\beta_1$ or $\alpha_3\beta_1$ integrins via collagen and laminin leading to tight adhesion but not cell entry of the pathogen. The head domain of *Y. pseudotuberculosis* contains an additional motif of 30 amino acids which mediates binding to fibronectin as a bridging molecule. This leads to $\alpha_5\beta_1$ integrin binding and uptake into the host cell (Fig. 3B). In the mouse model, colonization of a *Y. enterocolitica yadA* mutant in the deeper tissues was found to be significantly reduced (Schutz, *et al*. 2010).

The YadA head domain of *Y. pseudotuberculosis* mediates autoagglutination and hemagglutination of the bacteria, which enables them to form microcolonies to sustain neutrophil attacks in the lymphatic tissue (Eitel and Dersch 2002; Heise and Dersch 2006; Nummelin, *et al.* 2004).

The outer membrane protein YadA helps *Yersinia* to colonize and to proliferate within the host tissues. To circumvent the host immune response further virulence determinants need to be produced.

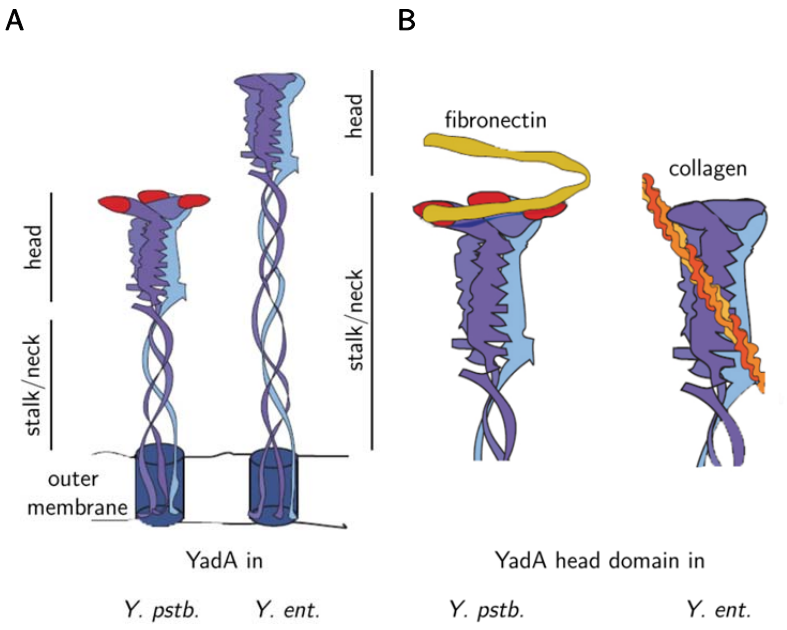

Fig. 3. YadA from *Y. pseudotuberculosis* and *Y. enterocolitica*. A. Domain structures of YadA from *Y. pseudotuberculosis* (*Y. pstb.*) and *Y. enterocolitica* (*Y. ent.*) attached to the bacterial outer membrane. Red domains in YadA (*Y. pstb.*) mediate invasion into host cells. B. Head domain of YadA in *Y. pseudotuberculosis.* binds to fibronectin, whereas YadA from *Y. enterocolitica* interacts with collagen (according to Heise and Dersch 2007).

A **type III secretion system** (T3SS) translocates effector proteins of *Yersinia* from the bacterium to extracellular space or into host cells. It represents a protein delivery machinery which finds its structural counterparts in the flagellum organelle (Journet, *et al.* 2005). The T3SS is synthesized prior to host cell contact by *Yersinia* secretion (Ysc) proteins. First, YscC polymerizes in the outer membrane (Ramamurthi and Schneewind 2002). YscW (VirG) helps to localize YscC at the polymerization site and facilitates oligomerization of YscC (Burghout, *et al.* 2004; Koster, *et al.* 1997). The inner membrane ring consists of polymerized YscD subsequently filled with a 24-subunit ring of the lipoprotein YscJ. The ATPase-C ring complex, consisting of YscN, K, L and Q drives the protein pump and shows activity for recruitment of proteins (Fig. 4). The export apparatus located within the inner membrane pore consists of YscR, S, T, U and V is transcribed in an operon. These integral membrane proteins recognize the Yops which are effector proteins exported by the type III secretion system. The needle, a hollow tube, is formed by polymerization of the 6 kDa protein YscF

(Cornelis 2002a; Cornelis 2002b; Cornelis 2006; Diepold, *et al.* 2010; Silva-Herzog, *et al.* 2008; Spreter, *et al.* 2009).

The T3SS senses the contact to the host cell which is facilitated by the binding of outer membrane proteins like YadA to integrins. Host cell contact or the penetration of the mammalian cell membrane might trigger the translocation of effector proteins.

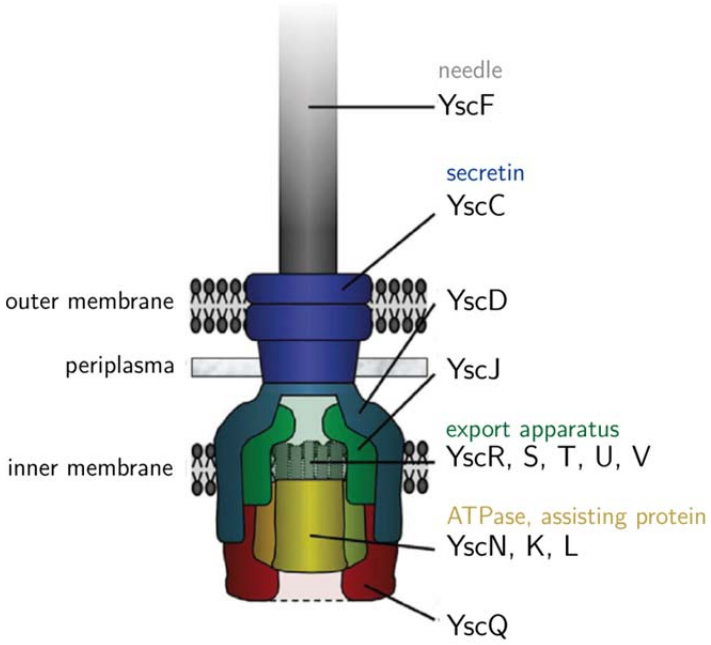

Fig. 4. Model of the *Yersinia* injectisome assembly. The different *Yersinia* secretion (Ysc) components are embedded within the inner membrane, through the periplasm and the outer membrane to the extracellular area (according to Diepold, *et al.* 2010).

Lipopolysaccharides, lipoproteins and lipoteichoic acids exposed on the bacterial cell surface stimulate the innate immunity response of the host. Phagocytes internalize intruding bacteria. This kills the bacteria and induces the production of proinflammatory cytokines such as TNF-α and IL-8 which in turn activate natural killer cells, T-cells and macrophages of the innate immune system. Moreover, cytokines promote formation of T helper 1 cell belonging to the adaptive immune response. The **Yersinia outer proteins**, or Yops, counteract this defence mechanism (Ruckdeschel, *et al.* 2008; Viboud and Bliska 2005).

Some effector molecules assist the translocation of others into the host cell. YopN, TyeA and LcrG function as a secretion channel plug that opens the T3SS needle, when it has pierced the mammalian cell membrane. YopB and YopD show pore forming activity and together with LcrV help to translocate effectors through the needle. In addition, the V-antigen LcrV is secreted to the extracellular milieu where it has shown to inhibit inflammation by binding to Toll-like receptors (Cornelis 2002b; Viboud and Bliska 2005).

Yops, transferred to the eukaryotic cell, interfere with numerous signaling pathways and cell functions. YopH, a protein tyrosine phosphatase, manipulates the signaling cascade of focal adhesion proteins in epithelial cells and macrophages (Aepfelbacher, *et al.* 2007; Trosky, *et al.*

2008). YopE, T and O (YpkA in *Y. enterocolitica*) represent members of the bacterial toxin family which target Rho GTPases of the host cell (Fig. 5). Thereby, reorganization of the cytoskeleton for phagocytosis is impaired (Matsumoto and Young 2009; Trosky, *et al*. 2008). YopJ (YopP in *Y. enterocolitica*) inhibits MAP (mitogen-activated protein) kinases and the NF-κB signaling pathway which leads to a repression of the cytokine production (Ruckdeschel, *et al*. 2008). Furthermore, YopJ is essential for *Yersinia* initiating apoptosis in naïve macrophages. The leucine-rich protein YopM is transported into the nucleus of the host cell by a vesicle-associated pathway (Fig. 5). There, the protein seems to affect transcription of genes which regulate cell growth and -cycle (Aepfelbacher, *et al*. 2007). Functions of the Yops show that yersiniae have developed various ways to inhibit or reprogram the immune response.

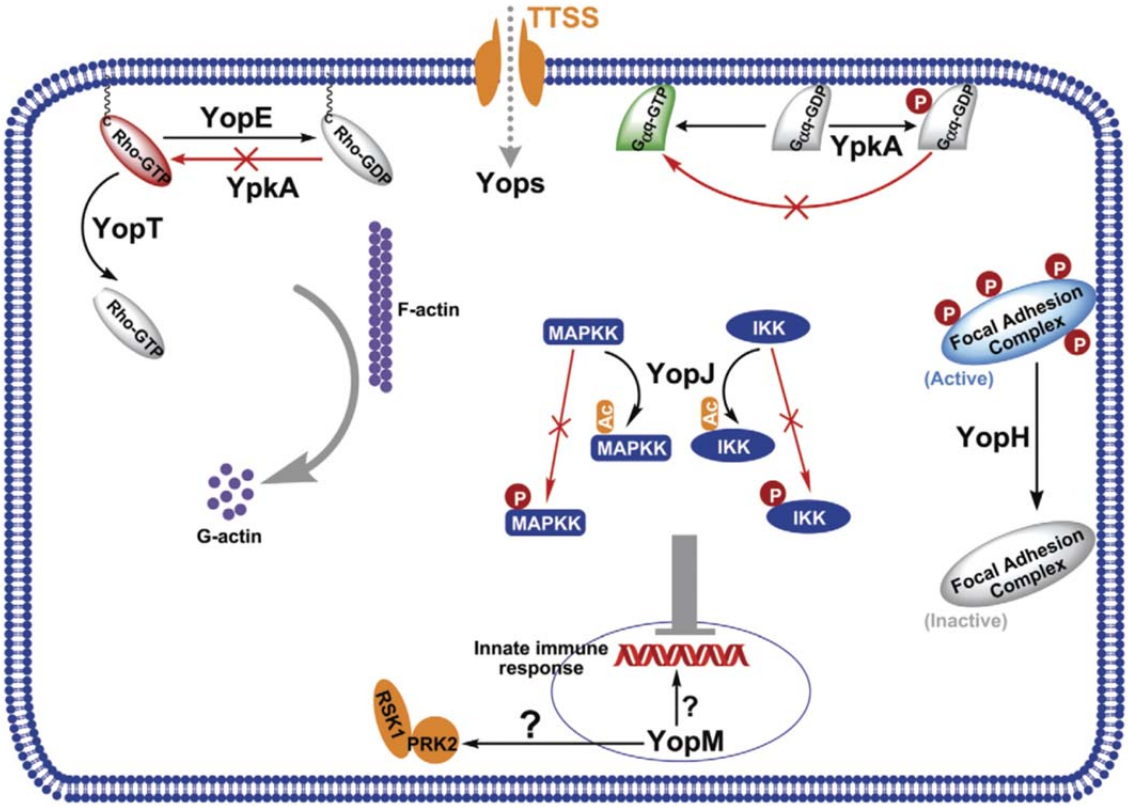

Fig. 5. Targets of the *Yersinia* type III effectors within the host cell. Three effectors including YopE, YopT, and YpkA impair the function of the Rho family small GTPases. YpkA phosphorylates Gaq and stimulates the GTPase. YopH influences components of the focal adhesion complex by dephosphorylation, which interferes with processes of host phagocytosis. Phosphorylation and activation of MAPK kinases is prevented by acetylation of Ser/Thr residues through YopJ. The actin cytoskeleton in the host cell is rearranged and transcription of immune response genes is inhibited (Shao 2008).

To produce early or late phase virulence factors in the target tissues for efficient and long-term infection of the host, *Yersinia* needs to tightly regulate their expression in response to environmental keys. *In vitro*, *Y. pseudotuberculosis* synthesizes early virulence factors only at moderate temperature, during stationary growth phase and nutrient rich environment which resembles external environment or contaminated food conditions. Production of virulence determinants from the late stage is monitored at temperatures above 30°C, during exponential growth and minimal medium (Eitel and Dersch 2002; Heroven, *et al*. 2007; Heroven and

Dersch 2010; Nagel, *et al*. 2001; Pepe, *et al*. 1994). The bacteria sense these triggering signals within the host via a complex regulatory network.

1.2 Environmental control of virulence determinants of the early infection phase

Invasin expression is regulated by specific environmental signals such as temperature, nutrient availability and growth rate. In contrast to *inv* transcription in *Yersinia*, an *inv-phoA* promoter fusion was not activated in *E. coli* under invasin synthesis conditions. Thus, *inv* gene expression seemed to be the result of the induction by a *Yersinia* specific factor. By transposon mutagenesis in *Yersinia* and a complementation strategy in *E. coli*, an *inv* regulatory protein, the regulator of virulence A (RovA), was identified (Nagel, *et al*. 2001; Revell and Miller 2000).

1.2.1 The invasin activator RovA – regulator of virulence A

The RovA protein is highly homology to proteins like Hor or SlyA which represent global transcriptional activators belonging to the MarR family. The crystal structure of the 15 kDa protein revealed a central helix-turn-helix motif which is responsible for DNA binding. It is followed by two β-sheets (N. Quade, unpublished data, Fig. 6A). The RovA protein forms dimers achieved by a dimerization domain consisting of the first N-terminal helix and the last two C-terminal helices. For DNA binding in promoter regions, RovA recognizes non-palindromic target sites with a consensus sequence of $^{A}/_{T}$ ATTAT $^{A}/_{T}$. Two recognitions sites were found within the *inv* promoter 207 nt upstream of the transcriptional start site (Nagel, *et al*. 2001; Tran, *et al*. 2005).

RovA itself is transcribed from two promoters P1 and P2 located 76 nt and 343 nt upstream of the transcription start. The protein binds to its own promoter region and autoregulates its expression. Autoactivation of *rovA* gene transcription is achieved by binding of at least two RovA dimers upstream of promoter P2. High RovA concentrations within the cell, however, induce the binding of the regulator to a low affinity binding site downstream of promoter P1 and abolishes further induction of *rovA* gene expression. This autoregulatory feed back loop represents a mechanism to control RovA levels within the bacterium.

RovA synthesis occurs during stationary growth, in complex medium and at moderate temperatures similar to invasin expression. An *inv* promoter missing the RovA binding site was deregulated in response to temperature (Heroven, *et al*. 2004; Nagel, *et al*. 2001). Temperature-regulation of *inv* transcription through regulation of RovA synthesis is affected by the thermosensing characteristics of the RovA protein. The structure of the RovA protein was found to be thermally instable revealing altered helix and β-sheet arrangements at higher temperatures compared to moderate temperatures. At 37°C, the conformational changes impair the DNA binding affinity of RovA and reduce transcription activation of invasin and *rovA* expression (Fig. 6B). Additionally, partially defolded RovA at 37°C is subject to

degradation by ClpP/Lon proteases, especially during exponential growth phase, which is most probably facilitated by an unknown cofactor (Herbst, *et al*. 2009). Thus, regulation of RovA synthesis mediates invasin expression in response to temperature and growth phase.

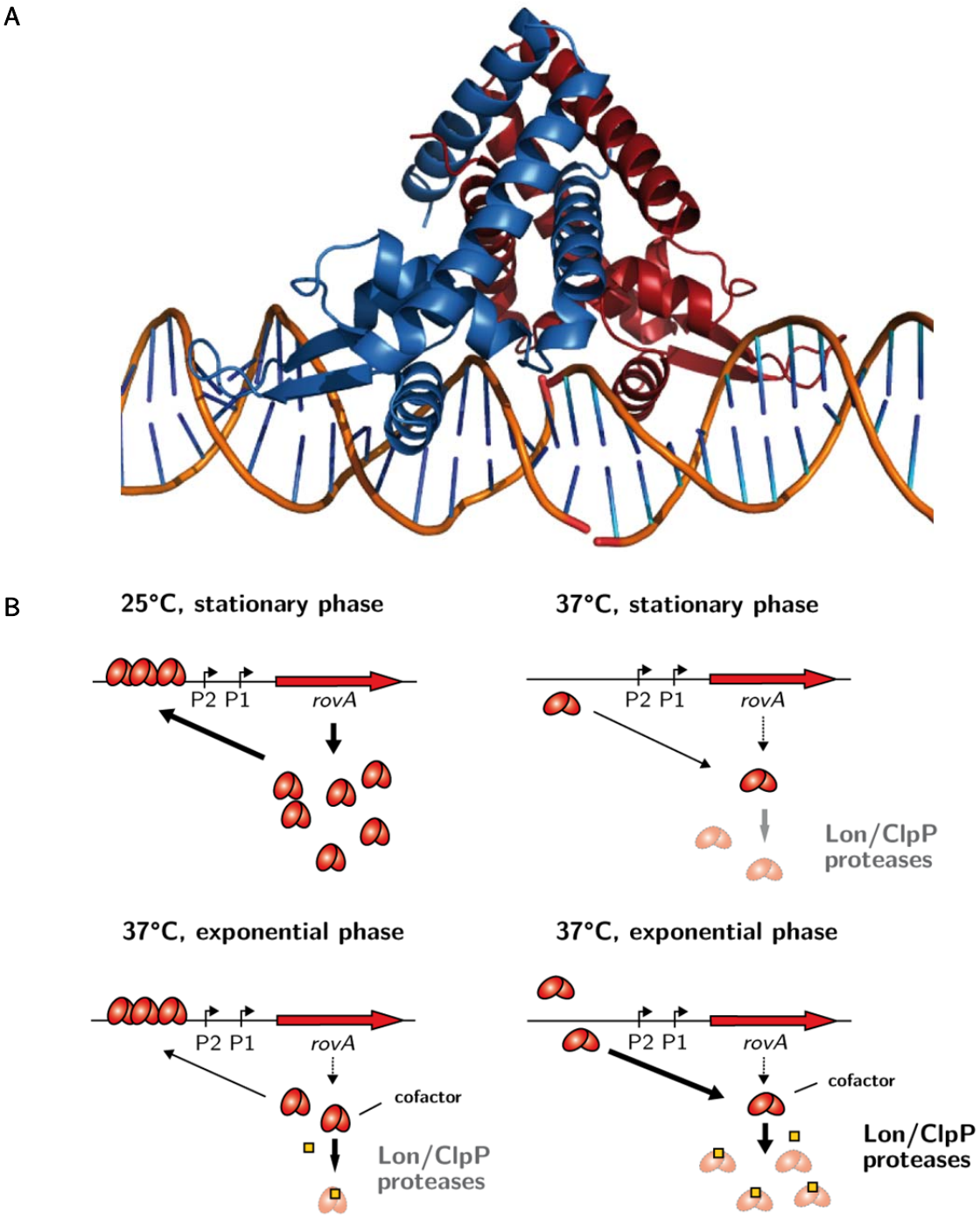

Fig. 6. Structure and thermoregulation of RovA. A. Crystal structure of RovA, which forms homodimers (in red and blue), each containing several α-helices (labeled at the red monomer). The central helix-turn-helix motif is required for binding to the DNA (N. Quade, unpublished data). B. Model of thermo-dependent *rovA* gene expression at 25°C and 37°C during stationary phase and during exponential growth at 37°C (Herbst, *et al*. 2009).

During mouse infection experiments, a *rovA* deletion in *Yersinia* confers lower virulence to the bacteria than deletion of the *inv* gene. *rovA* mutants were severely attenuated in dissemination to deeper tissues. An infection was only established in the Peyer's patches, whereas an *inv* mutant was also isolated from mesenteric lymph nodes and the spleen (Heroven, *et al*. 2007; Nagel, *et al*. 2003; Revell and Miller 2000). Further investigations revealed that a *Y. enterocolitica rovA*-deficient strain resulted in an increased inflammation in the Peyer's patches. In addition, IL-1α expression was not induced. These results and recent microarray data show that the global transcriptional activator RovA does not only activate *inv* expression. It also influences a variety of other genes including virulence determinants such as pH6 antigen and genes involved in metabolism (Tran, Heroven unpublished results; Cathelyn, *et al*. 2006). Virulence of a *Y. pestis rovA* mutant after subcutaneous infection of mice was 80fold attenuated whereas it was only slightly reduced after infection of mice intranasanally or intraperitoneally. This indicated that RovA in *Y. pestis* encounters a more important role during bubonic plaque than during pneumonic plaque.

A genetic search for regulators influencing *rovA* transcription led to the identification of the nucleoid-associated protein H-NS, the LysR-type regulator RovM, the Carbon storage regulator system (Csr) and the nucleoid-associated protein YmoA.

1.2.2 The nucleoid-associated protein H-NS

The nucleoid-associated protein H-NS forms dimers by its N-terminal oligomerization domain, which is connected to the C-terminal DNA-binding domain by a flexible linker peptide (Fig. 7A) (Arold, *et al*. 2010; Fang and Rimsky 2008; Stoebel, *et al*. 2008). In general, H-NS is known to organize chromosomal DNA (Dorman 2004). By DNA-protein-DNA bridges, H-NS binds simultaneously to independent DNA-binding sites and induces loop formation resulting in a higher condensation of chromosomal DNA (Fig. 7B) (Noom, *et al*. 2007; Stoebel, *et al*. 2008). Further, the nucleoid-associated protein influences transcription activity by altering the DNA topology in the promoter regions of target genes. It preferentially binds to AT-rich DNA sequences in promoter regions with intrinsic curvature which leads to an impaired association of the RNA polymerase. Further studies demonstrated a very weak binding of H-NS to unspecific DNA. Binding of H-NS to DNA with high affinity occurs to the consensus sequence 5'-TCGATATATT-3'. This sequence acts as a nucleation site from which H-NS oligomerizes along the DNA (Dame, *et al*. 2001; Prosseda, *et al*. 2004; Tolstorukov, *et al*. 2005). The protein exhibits preference to repress horizontally acquired DNA to protect the recepting bacterium from expression of harmful gene products. H-NS recognizes xenogenic DNA because of its lower GC-content compared to chromosomal DNA (Blot, *et al*. 2006; Lucchini, *et al*. 2006; Navarre, *et al*. 2007; Oshima, *et al*. 2006). H-NS also revealed the ability to bind to RNA molecules and might act as a chaperone (Brescia, *et al*. 2004).

Besides homodimer formation, H-NS has been described to form heterodimers with other nucleoid-associated proteins such as Hha in *E. coli* and *Salmonella* or YmoA in *Yersinia*

(Cordeiro, *et al*. 2008; Fass and Groisman 2009; Madrid, *et al*. 2007). H-NS and Hha of *Salmonella* were reported to repress expression of *hilD, hilC* and *rtsA*, encoding essential cell invasion factors, in response to osmolarity (Olekhnovich and Kadner 2007). In *Salmonella*, a major part of gene transcription was upregulated during a temperature shift from 25°C to 37°C which was attributed to a putative conformational change in the H-NS structure, thus reduced DNA-binding ability (Duong, *et al*. 2007; Ono, *et al*. 2005). In contrast, H-NS oligomerizes at 37°C to a higher extent than at 25°C (Fang and Rimsky 2008).

In *Yersinia, inv* and *rovA* transcription are repressed by the H-NS protein which binds to AT-rich sequences within the *inv* and *rovA* promoter regions (Ellison, *et al*. 2004; Heroven, *et al*. 2007; Heroven and Dersch 2010). To inhibit invasin expression, H-NS interacts with the *inv* promoter from position -31 nt to -207 nt relative to the transcription start. Within the *rovA* promoter H-NS covers a DNA stretch from -429 nt to -547 nt upstream of promoter P2. By that, the *inv* and the *rovA* promoter are repressed at 37°C (Ellison 2006, Heroven 2007). At 25°C, the RovA protein functions as an antagonist of H-NS silencing because of its higher binding affinity to the target promoter sequences (Heroven, *et al*. 2004; Tran, *et al*. 2005). This has also been shown for other proteins such as SlyA in *Salmonella* or the H-NS-type protein Ler from enteropathogenic *E. coli* strains (Fass and Groisman 2009; Stoebel, *et al*. 2008).

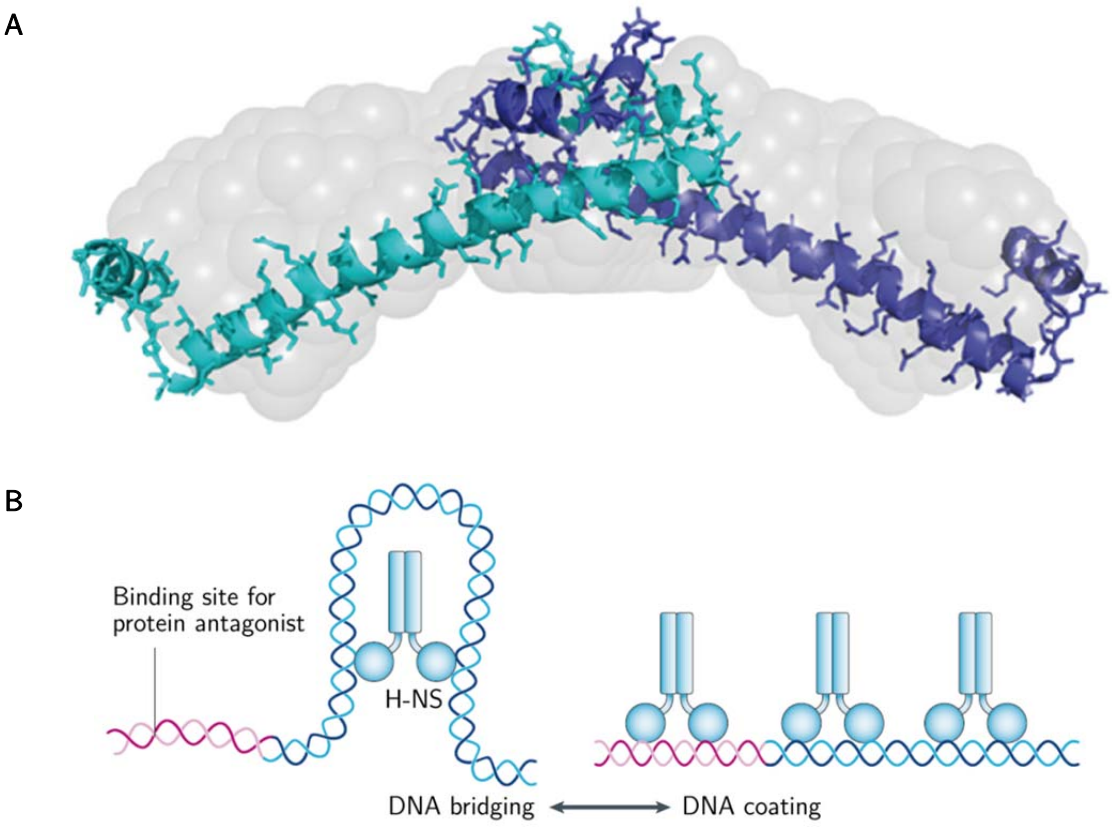

Fig. 7. The nucleoid-associated protein H-NS A. H-NS1-82 dimer (cyan and blue) model (Arold, *et al*. 2010) B. Binding of the nucleoid-associated protein H-NS affects the DNA conformation and leads to DNA bridging or oligomerization along DNA strands. This sterically prevents binding of the RNA polymerase or covers the recognition site of an antagonist (according to Dillon and Dorman 2010).

1.2.3 RovM - the modulator of *rovA* expression

In addition to H-NS, the LysR-type regulator RovM (PecT, HexA, LrhA) inhibits transcription of the *rovA* regulator gene. During growth in nutrient-deprived media, RovM downregulates RovA synthesis (Heroven and Dersch 2006).

In *Y. pseudotuberculosis*, the LysR regulator binds to palindromic sequences of 30 nucleotides with the central motif T-N_{11}-A upstream of *rovA* promoter P1. The association of RovM to the DNA does not interfere with H-NS binding sites (sec. 1.2.2). Still, RovM downregulates *rovA* expression in cooperation with H-NS. The nucleoid-associated protein might induce structural rearrangements of the promoter region, for example curvature, leading to a more efficient RovM-DNA complex formation.

Homologs of RovM have been found in *Erwinia chrysanthemi* where PecT negatively regulates expression of pectate lyases, motility, exopolysaccharides and also virulence of the phytopathogens (Castillo, *et al*. 1998; Condemine, *et al*. 1999; Nasser, *et al*. 2005). LrhA in *E. coli* has shown to repress genes responsible for motility, flagella synthesis, chemotaxis and biofilm formation (Blumer, *et al*. 2005; Lehnen, *et al*. 2002). Higher RovM levels in *Y. pseudotuberculosis* induced flagellar synthesis but showed attenuated dissemination to deeper tissues in the mouse model. *rovM* expression is positively autoregulated and maximal under minimal medium conditions. Heroven and Dersch (2006) further demonstrated that RovM mediates medium-dependent regulation of *rovA* transcription.

1.2.4 The carbon storage regulator system

In *Y. pseudotuberculosis*, medium-dependent control of RovM synthesis is controlled by the activity of the carbon storage regulator (Csr) system (Heroven and Dersch 2010). The Csr system has been identified in other enterobacteria such as *E. coli* and *Salmonella* (Babitzke and Romeo 2007; Papenfort and Vogel 2010; Vogel 2009). In *Pseudomonas* and *Erwinia* the homologous system was named Rsm system for regulator of secondary metabolism (Cui, *et al*. 1995; Cui, *et al*. 1999; Lapouge, *et al*. 2008). In general, the system is composed of the RNA-binding protein CsrA (RsmA/E), and untranslated regulatory Csr or Rsm RNAs. The CsrA protein forms dimers of approx. 18 kDa. A monomer consists of five β-strands β1 to β5 followed by an α-helix H1. Dimerization of CsrA monomers is mediated by the interaction of β-strands β1 and β5 (shown for the crystal structure of RsmE in Fig. 8A) (Gutierrez, *et al*. 2005; Schubert, *et al*. 2007). Mercante et al. (2006) described that these β-strands contain important residues for regulation and RNA-binding. CsrA (RsmA/E) proteins are able to bind to GGA motifs within target mRNAs, overlapping with ribosomal binding sites. This blocks binding of ribosomes and in most cases renders the target mRNAs for RNA degradation, for instance the mRNA of the *glgCAP* operon in *E. coli* (Baker, *et al*. 2002) (Fig.8B). However, it has been reported that binding of CsrA to the mRNA of *flhDC* positively influenced RNA levels (Wei, *et al*. 2001).

The regulatory Csr (Rsm) RNAs form secondary structures with several hairpin-loops of complementary RNA sequences. Single-stranded loop regions within these hairpins contain GGA motifs which bind CsrA dimers and thereby sequester the CsrA (RsmA/E) proteins from regulating other factors in the cell (Babitzke and Romeo 2007; Majdalani, *et al*. 2005; Vogel 2009). Another component of the Csr system, the CsrD protein was found to destabilize CsrB and CsrC RNAs in *E. coli*. The GGDEF and EAL domain containing protein seems to facilitate targeting of the RNAs by RNAse E (Suzuki, *et al*. 2006).

In other pathogens, the Csr (Rsm) system is implicated in the regulation of virulence factors. In *S.* Typhimurium, the Csr system controls gene expression promoting invasion and gene transcription from *Salmonella* pathogenicity island 1 (SPI-1), which encodes a type III secretion system (Altier, *et al*. 2000; Vogel 2009). The *csrA*-deficient strains of enteropathogenic *E. coli* were impaired to form actin pedestals on epithelial cells and were not able to disrupt transepithelial resistance, which is established across polarized epithelial cells. Bhatt and coworkers (2009) demonstrated that the secretion of effectors and translocators was strongly reduced. In *Erwinia*, the RsmA (CsrA) protein is implicated in expression of soft rot disease genes (Cui, *et al*. 1999). RsmA (CsrA) of *Pseudomonas* regulates exoenzyme production and secondary metabolite production (Blumer, *et al*. 1999; Lapouge, *et al*. 2008; Reimmann, *et al*. 2005).

Besides the regulation of virulence, CsrA (RsmA/E) proteins are involved in the control of global gene expression. In *Salmonella*, CsrA affects flagella synthesis and carbon metabolism (Lawhon, *et al*. 2003; Vogel 2009). A *csrA* deletion in *E. coli* leads to attenuated growth. The CsrA protein is essential for the bacterium to grow on synthetic medium containing glycolytic carbon sources (Timmermans and Van Melderen 2009). It activates glycogen biosynthesis and glyconeogenesis and represses glycolysis (Majdalani, *et al*. 2005; Romeo 1998; Timmermans and Van Melderen 2010).

Such a global effect was also observed for a *Y. pseudotuberculosis csrA* mutant strain (Heroven, *et al*. 2008). Loss of the CsrA protein leads to a strong growth defect in the bacteria. Furthermore, transcription of flagella and motility genes is abolished due to reduced levels of the *flhDC* mRNA. CsrA in *Y. pseudotuberculosis* was found to indirectly upregulate RovM synthesis, which in turn inactivates *rovA* expression. Expression of the CsrA-antagonizing regulatory RNAs CsrC and CsrB stimulated transcription of the *rovA* gene by repressing RovM production. As in *E. coli,* CsrC and CsrB RNA levels in *Y. pseudotuberculosis* are counterregulated due to an autoregulatory loop (Heroven, *et al*. 2008; Weilbacher, *et al*. 2003).

Moreover, the Csr system revealed to be responsible for mediating medium-dependent regulation of *rovM* and therefore *rovA* transcription (Heroven, *et al*. 2008). In *E. coli*, both RNAs, CsrC and CsrB, are induced in minimal medium, depending on the addition of certain amino acids (Jonas and Melefors 2009). In contrast, the regulatory RNA CsrC of *Y. pseudotuberculosis* is highly abundant in complex medium in stationary growth, whereas it

is absent in minimal medium. This is similar to the expression of the *rovA* gene in response to environmental conditions. RovA levels were only elevated in minimal medium, when *csrA* was deleted and hence the synthesis of RovM was inhibited. CsrB levels in *Y. pseudotuberculosis* were low under all tested conditions. c*srB* expression was only elevated by overexpression of *uvrY*, which resembles one component of the two-component-system UvrY/BarA (see 1.2.4.1) (Heroven, *et al.* 2008).

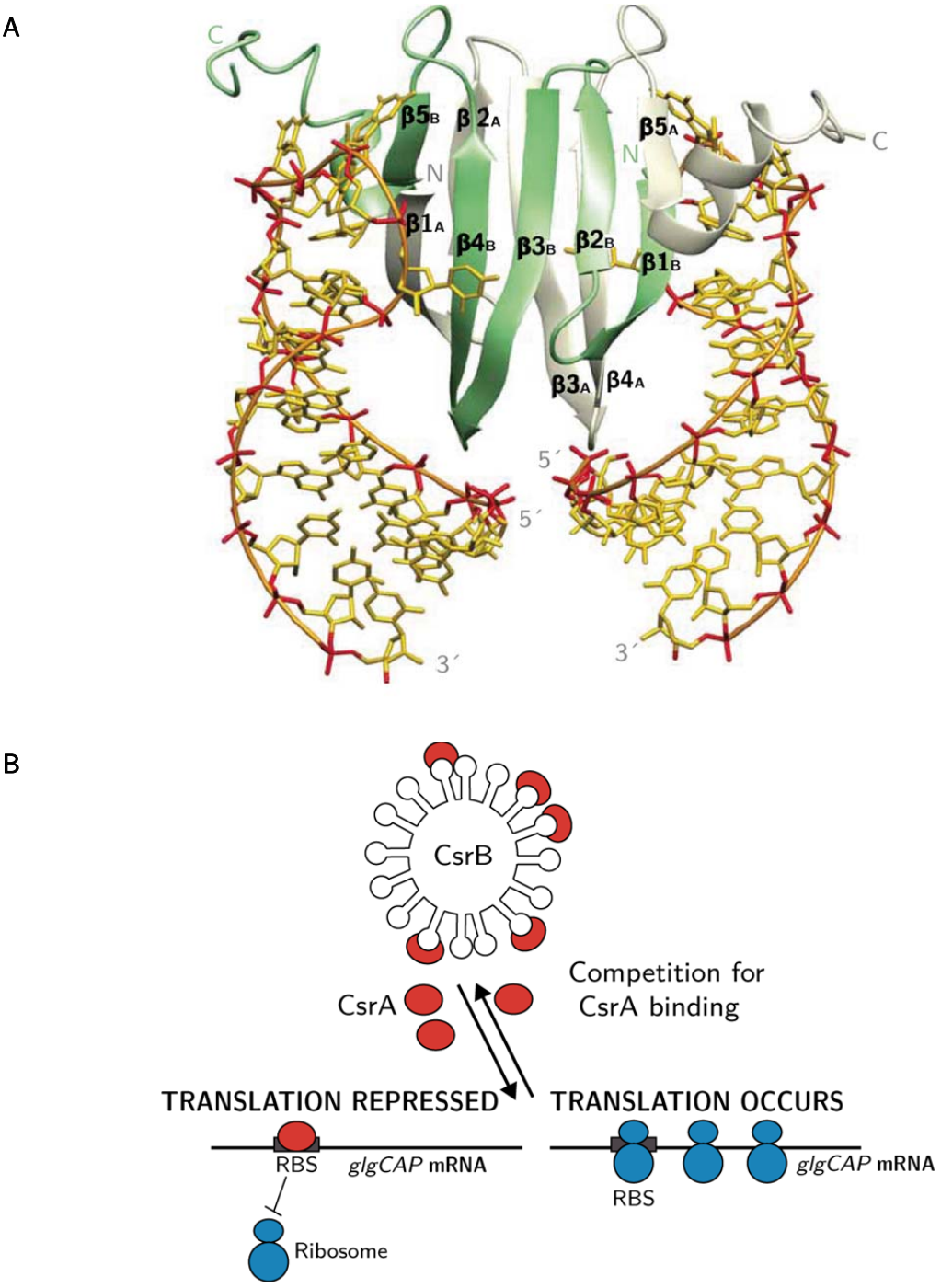

Fig. 8. Structure of the CsrA-like protein RsmE and the function of CsrA within the Carbon storage regulatory system. A. RsmE homodimer interacting with 20 nucleotides of the *hcnA* RNA (Schubert, *et al.* 2007). B. Interplay of the CsrA protein binding either to the CsrB RNA or the Shine-Dalgarno sequence of the *glgCAP* mRNA (Majdalani, *et al.* 2005).

1.2.4.1 Regulators of the Csr system

The **two-component system UvrY/BarA** is composed of the sensor kinase BarA and the response regulator UvrY, also found in *Pseudomonas* (GacS/GacA) and *Vibrio* (VarS/VarA) (Lapouge, *et al*. 2008; Lenz, *et al*. 2005). BarA belongs to a subclass of tripartite sensor kinases, phosphorylating the cognate response regulators via an ATP-His-Asp-His-Asp phosphorelay system. UvrY represents a member of the FixJ family. The regulator is phosphorylated at the N-terminal regulatory domain which activates the DNA-binding domain at the C-terminus (Birck, *et al*. 1999; Pernestig, *et al*. 2001).

The BarA-UvrY system in *E. coli* upregulates expression of both, the CsrB and CsrC RNAs. The sensor kinase was found to be activated by metabolic end products such as formate and acetate whereas low pH values represses *uvrY* transcription. Regulation by the UvrY/BarA system is essential for *E. coli* to trigger the Csr system to switch between glycolytic and gluconeogenic metabolic pathways (Mondragon, *et al*. 2006; Pernestig, *et al*. 2003). Also the induction of Csr or Rsm RNAs in *Pseudomonas* and *Vibrio* is mediated by the UvrY/BarA-like two-component systems. In this case the system is implicated in quorum sensing via secretion and senses an unknown autoinducing signal molecule (Lapouge, *et al*. 2008).

Up to date, the environmental activation signal inducing the BarA/UvrY of *Yersinia* is unknown but overexpression of UvrY under the control of an inducible promoter was found to activate *csrB* expression (Heroven, *et al*. 2008). CsrC synthesis instead is reduced under these conditions due to the negative feedback control between the Csr RNAs.

The ubiquitous **RNA-binding protein Hfq** is a homolog of the eukaryotic Sm or Sm-like proteins, which are involved in splicing and degradation of mRNAs. In general, the chaperone binds to regulatory RNAs involved in RNA metabolism. It was first identified as a host factor in *E. coli* which was essential for *in vitro* replication of RNA phage Qβ (Aiba 2007; Brennan and Link 2007; Chao and Vogel 2010). Hfq is a hexameric protein of 11 kDa subunits which binds to AU rich and polyA sequences (Brennan and Link 2007; Link, *et al*. 2009). Hfq is involved in several RNA-related regulation mechanisms. It facilitates base-pairing of regulatory RNAs to mRNAs. For example it promotes base pairing of the SgrS RNA with the *ptsG* mRNA at its ribosomal binding site, resulting in silencing of *ptsG* translation. In this case, presence of Hfq leads to rapid duplex formation of the RNAs, whereas it is decelerated under Hfq depletion conditions (Kawamoto, *et al*. 2006; Rasmussen, *et al*. 2005).

The binding of Hfq to the *sodB* mRNA in *E. coli* and the subsequent binding of the small iron-responsive regulatory RNA RyhB showed that base-pairing occurs because Hfq-annealing changed RNA structure. The RNA chaperone thereby promotes interaction of the two accessible complementary RNAs *sodB* and RyhB (Geissmann and Touati 2004).

Hfq controls a large number of regulatory RNAs. As a consequence, deletion of *hfq* often results in a strong growth reduction and attenuation of virulence in gram-negative pathogens such *E. coli*, *S. typhimurium*, *V. cholerae* or *Y. pestis* (Chao and Vogel 2010). Also Csr/Rsm

RNAs are often controlled by the RNA-binding protein Hfq. For instance, Hfq and RsmA bind concurrently to the Csr-type RNA *P. aeruginosa*. The chaperone binding site overlaps with the RNAse E recognition sequence. As a result, Hfq prevents degradation of the regulatory RNA (Sorger-Domenigg, *et al.* 2007).

In *Y. pseudotuberculosis*, loss of Hfq had a major negative effect on the bacterial growth and abolished *rovA* expression during stationary growth at 25°C (Heroven, Böhme, unpublished results). This indicates that Hfq might also be important for the Csr-type RNAs in *Y. pseudotuberculosis.*

1.2.5 The nucleoid-associated protein YmoA

Genetic screening for *rovA* transcription regulators in *Y. pseudotuberculosis* revealed *ymoA* as a regulator. An *ymoA*-deficient strain was less invasive into HEp-2 cells in gentamycin protection assays (Böhme, unpublished results). Thus, YmoA seems to play a crucial role in *Y. pseudotuberculosis* virulence factor regulation.

The 8 kDa "*Yersinia* modulator A" (YmoA) belongs to the Hha/YmoA family, which is part of the nucleoid-associated proteins super family. Members of the Hha/YmoA have pleiotropic effects on the bacterial physiology and virulence and are encoded in one or more copies in bacterial genomes. They influence the regulation of gene expression, plasmid supercoiling and frequency of insertion element transposition (Madrid, *et al.* 2007; Madrid, *et al.* 2002).

The homolog of YmoA in *E. coli* and *Salmonella,* the regulator of "High hemolysin activity" (Hha), shares 82% sequence identity with the *Yersinia* protein. Both are able to complement each other. Hha induces transposition events in a *Y. enterocolitica ymoA* mutant. YmoA restores regulation of hemolysin activity in a *hha* mutant in *E. coli* (Balsalobre, *et al.* 1996; de la Cruz, *et al.* 1992; Mikulskis and Cornelis 1994).

Structures of the *E. coli* Hha and the *Yersinia* YmoA protein have been elucidated (Fig. 9). Both form four helices, of which three comprise a helical bundle core structure. Helix four represents the shortest helix and is positioned against the outer face of helix three. Hha and YmoA show a conserved structure with only small difference according to their high sequence identity. Further, their N-termini show a significant similarity to the N-terminal oligomerization domain of the H-NS protein family. This indicated that the members of the YmoA/Hha family interact with H-NS-type proteins. In fact, interaction of YmoA and H-NS as well as Hha and H-NS has been described recently (Nieto, *et al.* 2002). Purification of H-NS by affinity chromatography from *E. coli* cell extracts led to the co-purification of Hha. H-NS-Hha complexes showed stronger binding to DNA than Hha homomers itself. Conformational analysis of YmoA suggests, that YmoA might substitute for an H-NS dimer in a higher order structuring which could lead to altered scaffolding and DNA suprastructuring (McFeeters, *et al.* 2007). Microarray analysis revealed several genes, which are controlled by Hha and H-NS (Madrid, *et al.* 2002). Rodriguez et al. (2005) demonstrated that replacement

of the N-terminal domain of H-NS by Hha complements some of the *hns*-mediated phenotypes in *E. coli*.

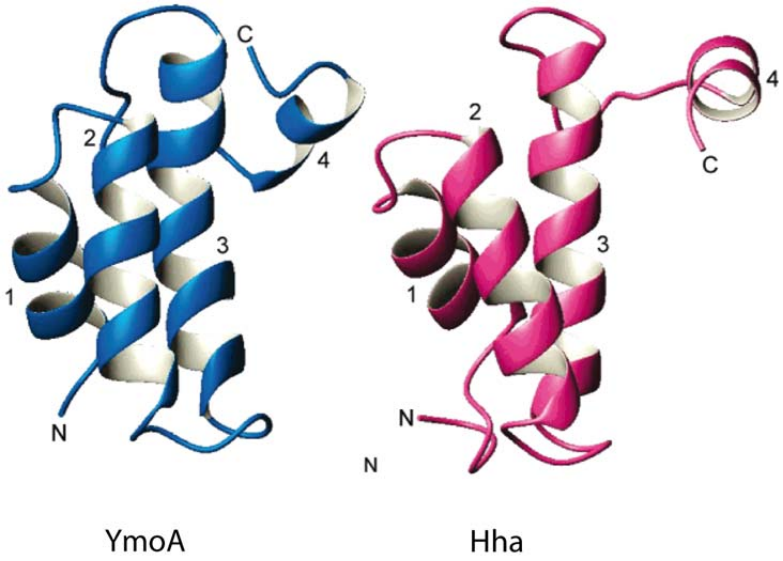

Fig. 9. Protein structures of YmoA and Hha. N and C represent the N and the C terminus. α-helices are indicated by numbers (McFeeters, *et al.* 2007).

In contrast to *Yersinia*, other Enterobacteriaceae genomes encode two or multiple homologs of the Hha/YmoA family. For example, besides Hha, S. *enterica* serovar Typhimurium encodes the Hha-type protein YdgT which regulates effector gene expression of *Salmonella* pathogenicity island 2. Synthesis of YdgT allows survival of *Salmonella* in host cell vacuoles (Coombes, *et al.* 2005; Paytubi, *et al.* 2004; Silphaduang, *et al.* 2007). The Hha-like protein oriC-binding nucleoid-associated protein (Cnu) in *E. coli* interacts with 26 nucleotide sequence called *cnb* within the origin of replication. Elimination of *cnu* and *hha* resulted in reduced origin content (Bae, *et al.* 2008; Kim, *et al.* 2005). No redundant members of the YmoA/Hha family seem to be expressed in *Yersinia*. That might explain that deletion of the *ymoA* gene in *Y. pseudotuberculosis* causes a severe reduction in bacterial growth. Furthermore, *ymoA* mutant strains exhibit a significantly lower stress resistance against temperature, osmotic, ionophoric and pH stress (K. Böhme, unpublished data). Loss of *ymoA* in *Y. enterocolitica* has been observed to be lethal (Ellison, *et al.* 2003).

In enteropathogenic bacteria, proteins of the YmoA/Hha family are often implicated in virulence gene expression. Hha, the regulator of, was named after the regulation of virulence factor synthesis such as pore-forming toxin hemolysin in *E. coli*. There it binds to the promoter region of the *hlyCABD* operon. Moreover, Hha shows impact on the expression of virulence factors from the Vir plasmid. Repression of these virulence factors occurs in response to environmental signals, i.e. low temperature and high osmolarity (Balsalobre, *et al.* 1999; Mourino, *et al.* 1996; Sharma and Zuerner 2004).

In S. *enterica* serovar Typhimurium, Hha downregulates the transcription of two crucial virulence regulator genes, *invF* and *hilA*, that stimulate the expression of virulence genes located in the *Salmonella* pathogenicity island 1. In comparison to Hha in *E. coli*, Hha in

Salmonella inhibits gene expression at low temperature and low osmolarities, which prevents the synthesis of a type III secretion apparatus and production of secreted effector proteins under these conditions (Eichelberg and Galan 1999; Fahlen, *et al.* 2001; Jones 2005).

In *Y. enterocolitica*, a transposon insertion in the *ymoA* gene led to an induced expression of the *yadA* and *yopE* gene at moderate temperatures, which are usually repressed under these conditions. In addition, synthesis of the effector proteins YopB and YopD was further stimulated at 37°C in a *ymoA*-deficient strain compared to the wild type (Cornelis, *et al.* 1991). Mikulskis *et. al.* (1994) demonstrated that YmoA is responsible for temperature and growth phase control of the *Yersinia*-enterotoxin encoding *yst* gene. In a *ymoA*-deficient strain, *yst* was transcribed during the exponential growth phase at 25°C, whereas in the wild type strain *yst* expression occurs mainly at 37°C during stationary growth. Further, Cornelis (1993) described an increased fragility of chromosomal DNA in a *ymoA* mutant in *Y. enterocolitica*. Ellison and Miller (2003) found that YmoA in *Y. enterocolitica* also downregulates transcription of the primary invasion factor invasin. It is proposed that the YmoA protein interacts with H-NS to establish a repression complex binding to the *inv* promoter at moderate temperatures as well as 37°C (Ellison and Miller 2006).

Taken together, YmoA and Hha influence expression of their target genes depending on environmental signal such as temperature or osmolarity. This regulation is due to the environmental control of the YmoA or Hha protein synthesis itself. Hha in *E. coli* is maximally expressed at high osmolarities (Mourino, *et al.* 1998). In contrast to YmoA levels in *Y. enterocolitica*, YmoA protein in *Y. pestis* was found to be degraded at 37°C by ATP-dependent ClpP and Lon proteases (Ellison, *et al.* 2003; Jackson, *et al.* 2004). Deletion of *clpP* and *lon* repressed expression of the *yop* genes at elevated temperatures. Such degradation might also occur in *Y. pseudotuberculosis* where the YmoA protein levels are similarily increased at 25°C compared to higher temperatures (K. Böhme, unpublished data).

Considering the activating effect on *rovA* expression in *Y. pseudotuberculosis* and its negative impact on the expression of genes essential during the ongoing infection, such as *yadA* and the *yop* genes, YmoA might represent an important trigger in *Yersinia* virulence.

1.3 Model of virulence factor regulation in *Y. pseudotuberculosis*

The following model comprises data on the regulatory components affecting important virulence factors during early infection stage of *Y. pseudotuberculosis* in the host (Fig. 10). Synthesis of the primary invasion factor invasin in the initial phases of the infection is activated by RovA in response to conditions such as 25°C, complex medium and stationary growth. RovA is able to displace H-NS from the *inv* and the *rovA* promoter, where the RovM protein can repress *rovA* expression in concert with the nucleoid-associated protein under minimal medium conditions. Synthesis of RovA in complex medium is activated by the presence of the CsrC RNA, which binds and thereby titrates the CsrA protein from inducing RovM synthesis. The CsrB RNA can activate *rovA* expression in the same manner when its

expression is strongly upregulated by the two component system UvrY/BarA. Additionally, Hfq and YmoA induce *rovA* expression and so invasin which leads to adhesion and invasion into the M-cells and translocation to the Peyer's patches.

On the other side, YmoA represses *yadA* and *yop* gene expression as well as the transcription of type III secretion system genes at lower temperatures by preventing the synthesis of the AraC-like regulator LcrF.

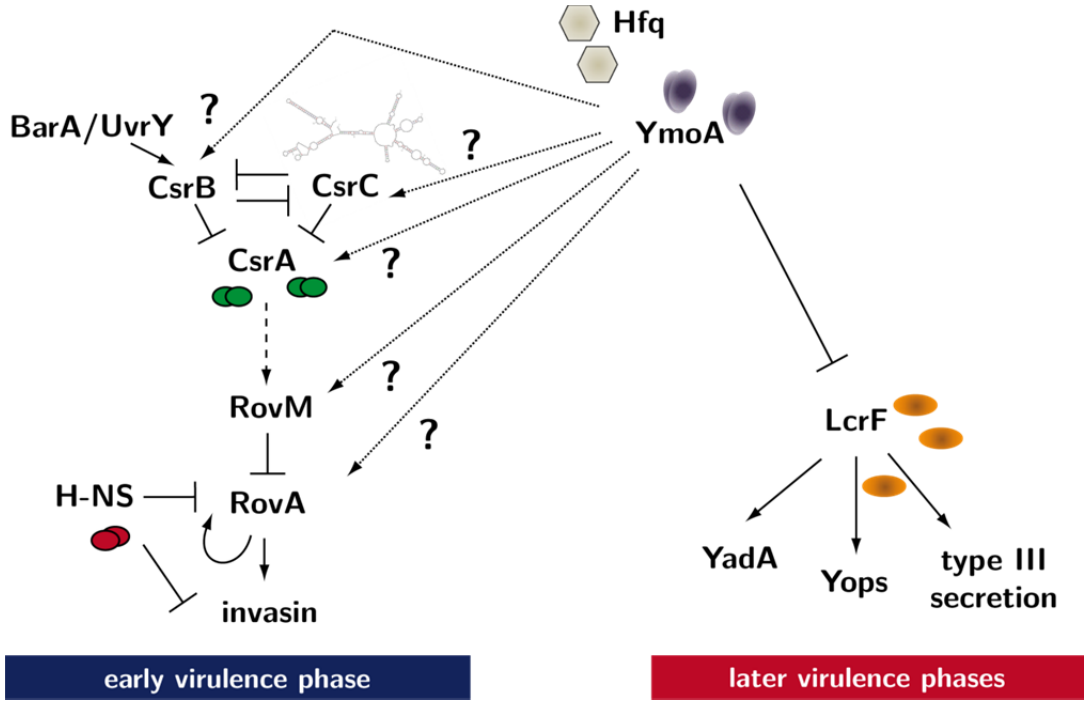

Fig. 10. Working model of virulence factor expression in *Y. pseudotuberculosis*. Arrows display direct activation of the gene expression or protein synthesis, whereas dashed arrows label indirect regulation. Dotted arrows indicate unkown regulation mechanisms. T represents repression or inactivation. Virulence factors expressed during early (blue) and late (red) virulence phases are indicated on the bottom.

1.4 Environmental control of virulence determinants during the later infection phases

When *Y. pseudotuberculosis* enters the later stages of the infection the bacterium is exposed to higher temperatures over a longer period of time. Moreover the pathogen faces dramatic changes in the nutrient availability during the transition from the gut lumen to the environment in the deeper tissues. Especially, temperature and Ca^{2+} concentration are known to trigger production of a whole set of virulence factors encoded by the virulence plasmid pYV. Transcription of *yadA*, the type III secretion system and the *yop* genes is upregulated at elevated temperature above 30°C and under low Ca^{2+} level conditions. *In vitro*, yersiniae show a strong growth restriction in Ca^{2+}-deprived nutrient-rich medium at 37°C, which is caused by a massive secretion of Yop effector proteins (Ramamurthi and Schneewind 2002). This is referred to as the low calcium response (Lcr).

Activation of the *yop* genes occurs in the presence of **the transcriptional activator LcrF** (VirF in *Y. enterocolitica*) also encoded on pYV. The 30 kDa protein is highly homologous to transcriptional activators of the AraC-like protein family. This group of regulators is characterized by a highly conserved C-terminal domain with two helix-turn-helix DNA-binding motifs. The poorly conserved N-terminal domain containing regions for oligomerization is connected to the C-terminus by a flexible linker (Cornelis, *et al*. 1989; Gallegos, *et al*. 1997; Martin and Rosner 2001).

In *Y. enterocolitica*, VirF (LcrF) was found to induce transcription of *yopE*, *yopH*, the *virC* operon, the *lcrGVH-yopBD* operon and *yadA* (Hoe, *et al*. 1992; Lambert de Rouvroit, *et al*. 1992; Skurnik and Toivanen 1992). Alignments of the promoter regions controlled by the AraC-type regulator revealed that VirF dimers bind to isolated sequences or inverted repeats covering a region with a length of about 60 nt. The promoter sequences of VirF-regulated genes *yopE*, *lcrG*, *virC* and *yopH* share a TTTTaGYcTtTat motif (Wattiau and Cornelis 1994). AraC-like transcriptional regulators which influence the expression of type III secretion systems, have also been analyzed in other pathogens (Francis, *et al*. 2002). For example, a homolog of LcrF (VirF) in *Pseudomonas aeruginosa*, ExsA, regulates ten genes of the type III secretion system in response to Ca^{2+} concentrations (Brutinel, *et al*. 2008; Vakulskas, *et al*. 2009; Yahr and Wolfgang 2006).

Production of LcrF (VirF) is controlled by environmental signals and regulatory components. LcrF (VirF) synthesis is strongly dependent on the growth temperature. Higher protein levels of the regulator are only produced at 37°C but not at moderate temperatures. Hoe and Goguen (Hoe and Goguen 1993) hypothesized post-transcriptional regulatory mechanism based on RNA structure rearrangements that induce LcrF translation at higher temperatures in *Y. pestis*. Waldminghaus *et al*. (2007) performed a database screen for RNA thermometers. The search was based on the ability of 5' untranslated regions of protein-coding RNAs to form a secondary structure with imperfect base pairing at the Shine-Dalgarno sequence. The 5' untranslated region of the *Y. pestis* LcrF RNA was predicted to encounter a FourU RNA thermometer (Fig. 11A). These FourU thermometers are characterized by a consecutive stretch of four uracils interacting with the AGGA motif of the Shine-Dalgarno sequence. In their model they propose that, at low temperatures, this base pairing sequesters the ribosomal binding site of the target RNA and inhibits translation into the protein. Elevated temperatures may unfold the RNA secondary structure and thereby permit recognition of the Shine-Dalgarno site by ribosomal subunits, initiating protein synthesis (Fig. 11B) (Narberhaus 2010).

Temperature regulation of LcrF (VirF) synthesis was further found to depend on the presence of the nucleoid-associated protein YmoA. In *Y. enterocolitica,* loss of *ymoA* induced the expression of a *virF* (*lcrF*) reporter gene fusion already at moderate temperature, whereas it is repressed in a wild type strain (Cornelis, *et al*. 1991). The *lcrF* promoter region, which is affected by YmoA, remains to be analyzed.

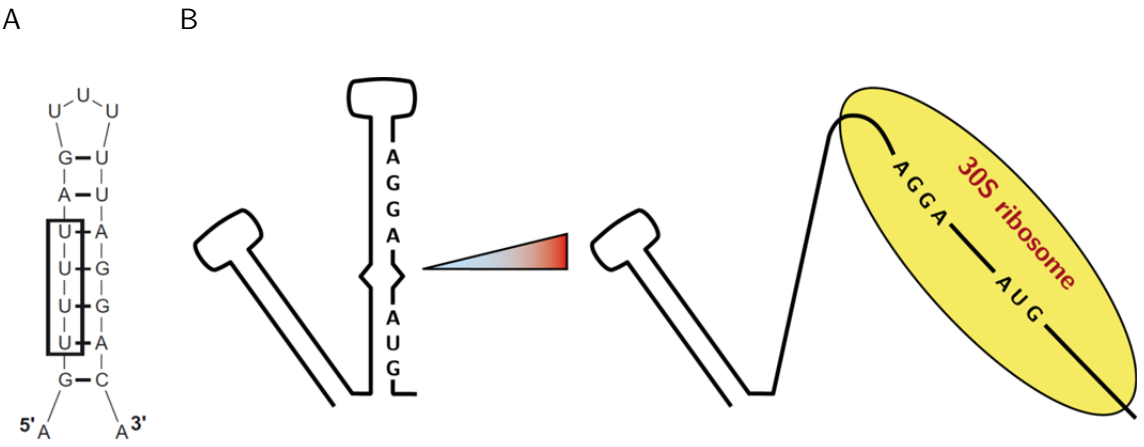

Fig. 11. The FourU RNA thermometer within the 5' untranslated region of LcrF in *Y. pestis*. A. Model of the predicted secondary structure of the FourU RNA thermometer within the 5' untranslated region of *lcrF* in *Y. pestis*. The FourU motif is marked by a rectangle (Waldminghaus, *et al*. 2007). B. Function of a RNA thermometer. Secondary structures form at low temperatures (left) which leads to base pairing of the ribosomal binding site. Increasing temperatures unfold the RNA conformation which liberates the Shine-Dalgarno site (right). Ribosomal subunits bind to the AGGA motif and start translation of the coding RNA (According to Narberhaus 2010).

1.5 Aim of this work

In this study, environmental control of the two major virulence factors invasin and YadA by the nucleoid-associated protein YmoA and regulatory elements should be analyzed. Preliminary experiments revealed that the activator RovA of the primary invasion factor invasin is not synthesized in the absence of YmoA (Heroven, *et al*. 2007). Previous studies demonstrated that *rovA* expression is controlled by the Csr system involving the RNA-binding protein CsrA and two regulatory RNAs CsrC and CsrB. These regulate *rovA* expression through the LysR-type regulator RovM depending on the nutrient-availability and temperature. A major goal of this study was to determine how YmoA exerts its influence on *rovA* expression and what components of the RNA regulatory network contribute or are implicated in the YmoA-mediated control of *rovA*. As nucleoid-associated proteins such as YmoA have been found to form heteromers with H-NS (Nieto, *et al*. 2002) the role of YmoA/H-NS interaction in the control of *rovA* expression in *Y. pseudotuberculosis* should be addressed. In addition, it was studied how the RNA chaperone Hfq is involved in the control of *rovA* expression mediated by the regulatory RNAs CsrC and CsrB.

YmoA represses YadA production and the expression of genes encoding for Yop effector and type III secretion proteins at moderate temperatures. The transcription of these genes is induced by the activity of the LcrF protein which itself underlies YmoA-dependent thermoregulation. The aim in this work was to elucidate the complex control of LcrF synthesis including transcriptional regulation by YmoA or other regulatory components and posttranscriptional mechanisms such as the predicted RNA FourU thermometer.

2 Material and Methods

2.1 Material

2.1.1 Equipment

Equipment used in this study is listed in Table 1.

Table 1. Equipment and material.

equipment	manufacturer
bunsen burner Fireboy Plus	IBS Integra
centrifuge 3-18 K	Sigma
centrifuge RC5C	Sorvall
chromatography columns Poly-Prep	Biorad
Cuvettes	Sarstedt
developing machine, Optimax Typ TR	MS Laborgeräte
electroporation cuvettes	Peqlab
electroporator GenePulser II	Biorad
elisa reader iMark Microplate	BioRad
falcon tubes (15 ml; 50 ml)	Greiner
filter units (0,075 mm)	Nalgene
french press	Aminco
gel documentation system	Biorad
gel system minigel	Peqlab
gel system PerfectBlue Gelsystem Mini L Revolution	Peqlab
glass funnels, bottles, beakers and flasks	Schott
glass pipets	Hirschmann
hybridisation oven OV-2	Biometra
magnetic stirrer MR3001	Heidolph
microcentrifuge 5415 R	Eppendorf
microcentrifuge Mini-Spin	Eppendorf
microtiter plates	Greiner
microwave	Panasonic
petri dishes	Sarstedt
pH meter 827 pH lab	Metrohm
pipet tips	Sarstedt
pipettes	Eppendorf
pipettor Accu-Jet	Brand
power supply high power voltage	Biorad
Power Supply Power Pac Universal	Biorad
precision balance	Sartorius
protein blotting system Mini Trans-Blot cell	Biorad
protein electrophoresis system Mini Protean Tetra cell	Biorad
reaction tubes (1,5 ml; 2 ml)	Sarstedt
shaker Multitron 2	Infors HAT
spectrophotometer UV/VIS Ultrospec 2100 pro	Amersham Biosciences
sterile filters 0,2 µm	Schleicher/Schüll

equipment	manufacturer
sterile plastic pipettes	Greiner
thermocycler T3000	Biometra
thermocycler Mastercycler personal	Eppendorf
Thermomixer comfort	Eppendorf
vacuum pump	VWR
vertical electrophoresis PerfectBlue™ Twin	Peqlab
vortexer	Scientific industries
whatman paper	Schleicher/Schüll

2.1.2 Chemicals

Chemicals used in this study are listed in Table 2.

Table 2. Chemicals.

chemicals	manufacturer
5-bromo-4-chloro-3-indolyl phosphate (BCIP)	Roth
5-bromo-4-chloro-3-indolyl-beta-D-galactopyranoside (X-gal)	Roth
acrylamid/bisacrylamid mix (30)	Roth
acrylamid/bisacrylamid mix (40)	Roth
agar for *E. coli*	Gerbu
agar, noble for *Yersinia*	Difco
agarose	Peqlab
ammoniumpersulfate (APS)	T.H. Geyer
anhydrotetracycline	IBA BioTagnology
Bacto tryptone	Difco
Bacto yeast extract	Difco
blocking reagent	Roche
bromophenol blue	Roth
calcium chloride	Roth
carbenicillin	Merck
chloramphenicol	Merck
chloroform	J.T. Baker
Coomassie Brilliant Blue G250	Roth
D-desthiobiotin	IBA BioTagnology
dimethylformamide (DMF)	Roth
di-potassium hydrogen phosphate (K_2HPO_4)	Roth
dithiothreitol (DTT)	Roth
ECL Western blotting substrate	Thermo Scientific (Pierce)
ethanol absolut	Sigma
ethidium bromide	Roth
formamide	Applichem
glucose	Roth
glycerol	Applichem
glycine	Roth
isopropanol	J.T. Baker

chemicals	manufacturer
isopropyl β-D-1-thiogalactopyranoside (IPTG)	Roth
kanamycin	Merck
L(+)-arabinose	Roth
magnesium chloride	Roth
magnesium sulfate	Merck
methanol	J.T. Baker
Ni-NTA agarose	Qiagen
o-nitrophenyl-β-galactoside (ONPG)	Fluka
p-nitrophenyl phosphate (PNPP)	Sigma
potassium dihydrogen phosphate ($KH_2PO_{4)}$	Roth
sodium carbonate	Roth
sodium chloride	Roth
sodium dodecyl sulfate (SDS)	Applichem
sodium hydroxide	Merck
Strep-Tactin® Superflow® high capacity	IBA BioTagnology

Unless noted otherwise, chemicals, which are not shown, were purchased from Roche Germany GmbH, Difco, Merck, Roth and Sigma.

2.1.3 Enzymes, antibodies and kits

Enzymes used in different experiments of this study are listed in Table 3.

Table 3. Enzyme.

enzyme	manufacturer
benzonase	Merck
Mango *Taq* polymerase	Bioline
Phusion polymerase	Finnzymes
Taq polymerase	NEB
antarctic phosphatase	NEB
T4 DNA ligase	Promega
RNase A	Qiagen
RNase V1	Ambion
RNase T	Ambion
calf intestine phosphatase (CIP)	NEB
T4 polynucleotide kinase (PNK)	Fermentas
Moloney Murine Leukemia Virus (M-MLV) reverse transcriptase	USB

Antibodies used in this study are listed in Table 4. Primary antibodies are polyclonal antibodies produced in rabbits.

Table 4. Used antibodies.

antibody	manufacturer/source	dilution
primary antibodies		
Anti-RovA	Davids Biotechnology	1:3,000
Anti-RovM	Davids Biotechnology	1:5,000
Anti-H-NS	Davids Biotechnology	1:10,000
Anti-YmoA	Davids Biotechnology	1:2,500
Anti-CsrA	Davids Biotechnology	1:10,000
Anti-Hfq	Davids Biotechnology	1:5,000
Anti-LcrF	H. Wolf-Waatz	1:20,000
secondary antibodies		
Anti-rabbit immunoglobulin alkaline phosphatase	Sigma	1:8,000
Anti-rabbit immunoglobulin horse radish peroxidase	NEB	1:6,000

Commercial kits were used for detection or purification of nucleic acids and are listed in Table 5.

Table 5. Kits used in this study.

Kit	Use of kit	manufacturer
Dig luminescent detection	detection of dig-labeled RNA	Roche
QIAquick™PCR Purification	purification of DNA	Qiagen
QIAquick™Plasmid Midiprep	preparation of plasmids	Qiagen
QIAquick™Plasmid Miniprep	preparation of plasmids	Qiagen
SVTotal RNA Isolation	preparation of total RNA	Promega
TranscriptAid™ T7 High Yield Transcription Kit	*in vitro* transcription of template DNA	Fermentas

2.1.4 Media and supplements

LB medium (Luria-Bertani medium): (Sambrook J. 1989)

5	g	Bacto yeast extract
10	g	Bacto tryptone
5	g	NaCl

filled up to 1 L with *aqua bidest*

DYT medium (Double Yeast Trytone medium): (Miller 1992)

10	g	Bacto yeast extract
16	g	Bacto tryptone
5	g	NaCl

filled up to 1 L with *aqua bidest*

BHI medium (Brain heart infusion medium):

37	g	BHI (BD Biosciences, USA)

filled up to 1 L with *aqua bidest*

SOC medium (Super optimal broth):

5	g	Bacto yeast extract
20	g	Bacto tryptone
0.5	g	NaCl
2.5	ml	1 M KCl
10	ml	1 M $MgCl_2$
10	ml	1 M $MgSO_4$

filled up to 1 L with *aqua bidest*

1x minimal medium A: (Sambrook J. 1989)

10.5	g	K2HPO4
4.5	g	KH2PO4
1	g	(NH4)2SO4
0.5	g	sodiumcitrate · 2H2O

filled up to 1 L with *aqua bidest*

After autoclaving other sterile supplements of the following end concentrations were added to minimal medium A:

1	mM	$MgSO_4$
0.1	mM	$CaCl_2$
0.2	%	casamino acids
0.2	%	glucose

For solid media 15 g of agar were added to 1 L of liquid media. Selective medium was prepared by addition of appropriate sterile filtrated antibiotics after autoclaving which are listed in Table 6.

Table 6. Antibiotics and applied concentrations.

antibiotic	concentration of stock solution	final concentration in media
carbenicillin	100 mg/ml H_2O	100 µg/ml
chloramphenicol	30 mg/ml Ethanol	30 µg/ml
kanamycin	50 mg/ml	50 µg/ml
tetracycline	5 mg/ml Ethanol	10 µg/ml

2.1.5 Oligonucleotides

The following oligonucleotides in Table 7 were used for cloning and mutagenesis purposes.

Table 7. Oligonucleotides.

name	sequence	restriction site
primers for plasmid construction		
1	5'- GCG GCG GTC GAC CTC TTG GCG ACA GCC ATC -3'	*Sal*I
2	5'- GGG CGC GGA TCC GCT AAG CAG ACT ATT TCA C -3'	*Bam*HI
3	5'- TTT GCT AGC GTG ATT TAT TAT ATT GGT TTT G -3'	*Nhe*I
4	5'- GTT ATA CTG TCC TAA AAA TCT AAT GAG GTG TAT TGA G -3'	
5	5'- CTC AAT ACA CCT CAT TAG ATT TTT AGG ACA GTA TAA C -3'	
6	5'- TTT GAA TTC GCC ATC TTG TGA ATG CTC AAC -3'	*Eco*RI
7	5'- GCG GCG GCT AGC CTC AAT ACA CCT CAT TAG -3'	*Nhe*I
8	5'- GGG CCG GTC GAC CCA TTA CGT TCC TTA AAC ATA AG -3'	*Sal*I
9	5'- GCG GCG GAA TTC CCT TCA TCC CGT GGT AGG -3'	*Eco*RI
10	5'- GGG CCG GTC GAC CTT GTA TAT CCA TTA CGT TCC TTC CTT GCA TGG TGT ATC CGT ACC -3'	*Sal*I
11	5'- GCG GCT GCA GCC ATC TTG TGA ATG CTC AAC AAC C -3'	*Pst*I
12	5'- GCG GCC TGC AGG GCT GCA ATG TAA CTA GGA ATA TGG -3'	*Pst*I
13	5'- GCG GCC TGC AGG CTA TAA TAC GAC TCA CGC -3'	*Pst*I
14	5'- GCG CGC TGC AGG ACT GGC GTG AGT CGT ATT ATA GC -3'	*Pst*I
15	5'- GCG GCC TGC AGG GGG TGA TTA ACA CCG GC -3'	*Pst*I
16	5'- GCG GCC TGC AGC AGT ATG GTA ATT GTA TTT CTC C -3'	*Pst*I
17	5'- GCG GCC TGC AGC AGT ATT GTC ATT ACT ATT ACA TG -3'	*Pst*I
18	5'- GCG GCC TGC AGG CGC AAG GTG TGA TAT TGC -3'	*Pst*I
19	5'- GCG GCC TGC AGC CAC ATA TTG CGC GAA CTC G -3'	*Pst*I
20	5'- GCG GCG CTG CAG CCT TCA TCC CGT GGT AGG -3'	*Pst*I

name	sequence	restriction site
21	5'- GCG GCG CTG CAG CCA ATA ACA AAT TGA CTA GC -3'	*Pst*I
22	5'- GCG GCG CTG CAG CTT GTA TATCCA TTA CGT TCC -3'	*Pst*I
23	5'- GCG CGG GTC GAC *TCC CTA TCA GTG ATA GAG ATT GAC ATC CCT ATC AGT GAT AGA GAT ACT GAG CAC* TTG GTA CGG ATA CAC CAT -3' [a]	*Sal*I
24	5'- CGG CGC GGA TCC GAA AGA AGA GAA AGA AAA AAG -3'	*Bam*HI
25	5' CTT GTA TAT CCA TTA CGT TCC TTC CTT GCA TGG TGT ATC CGT ACC -3'	
26	5'- GGT ACG GAT ACA CCA TGC AAG GAA GGA ACG TAA TGG ATA TAC AAG -3'	
27	5'- GCG GCG GTC GAC CCT TCA TCC CGT GGT AGG -3'	*Sal*I
28	5'- GGG CGC GGA TCC GAT TGG GCC GGA ATC TAG C -3'	*Bam*HI
29	5'- CGG CGC GGA TCC GGA CAA TGG TCG ATG AC -3'	*Bam*HI
30	5'- GGG GGC GTC GAC GTT ACA CGA GAC GCT GC -3'	*Sal*I
31	5'- GGG CGC CTG CAG GCA ATG AAG CCG GAA CAA ATC -3'	*Pst*I
32	5'- GGG GCC CTG CAG CGA GTC AGA ATA AGC ATT CTT TG -3'	*Pst*I
primers for mutagenesis		
33	5'- C TAC GCG ACG AAA TAC TTT TTT TGT TTT GGC GTT AAA AGG TTT TCT TTA TT*G TGT AGG CTG GAG CTG CTT C* -3' [b]	
34	5'- CGA GCT TGA GAA GCG ACG CCG GAC GCG CCC TAG CAG CGA CAT CCG GCC TCA G*CA TAT GAA TAT CCT CCT TAG T* -3' [b]	
35	5'- GCT CTA TTA TTA CCT CAA CAA ACC ACC CCA ATA TAA GTT TGA GAT TAC TAC *GTG TAG GCT GGA GCT GCT TC* -3' [b]	
36	5'- CAA TAA AAA ATC CCG CCG CTG GCG GGA TTT TAA GCA AGT GCA ATC TAC AAA AG*C ATA TGA ATA TCC TCC TTA GT* -3' [b]	
37	5'- CCT GCG AGT TTA TCT TGT TAG AAT TAT TAC AAC CAT AGG TAG AAG *GTG TAG GCT GGA GCT GCT TC* -3' [b]	
38	5'- GGG TAT GTC TTC ATG GCG AAA AAG TAT AAA ATT CTT AAT AAA CAG CCG GTT ATA GCT CCG AAA GCG *CAT ATG AAT ATC CTC CTT AGT* -3' [b]	
39	5'- GCA AAG CAA AAG TTC AAA ATC ACC -3'	
40	5'- GGT TAA TTG GTT GTA ACA CTG G -3'	
41	5'- CGA TAG ACA GCT GTA TTT ATA TG -3'	
42	5'- *GCA AAG CAA AAG TTC AAA ATC ACC* GGT TTT TCT TCT CGA TAT ACA AAT TAA TAT TGG TGG AAC TAT CCC -3' [c]	
43	5'- *GGT TAA TTG GTT GTA ACA CTG G*CT GCT TAG CGC TGG TTA AGA CAC ACA ACG TTG AGC CGA TAA TCT CTA TCG -3' [c]	
44	5'- CCT GTA TTA TCA CTT TCC TGC -3'	
45	5'- CTT TCA GTG AGC TGA TGA ATC -3'	

name	sequence	restriction site
46	5'- *GCA AAG CAA AAG TTC AAA ATC ACC* CCG TCT CCT AAT AGA ATT TAC TTT GGC GCC ATT CAT AAC CGA TTC TAC TTG -3' [c]	
47	5'- *GGT TAA TTG GTT GTA ACA CTG GGA* CTT ATT TCT GCG AGC CGA TAT ACT ATA GTG TAT GTA AAT AGA AC -3' [c]	
48	5'- GAC GCT TGT AGT GGT TAT AC -3'	

underlined ... restriction sites; [a] *italic* ... tetracycline promoter sequence; [b] *italic* ... homologous to pKD4 kanamycin cassette; [c] *italic* ... homologous to kanamycin cassette from pACYC177

2.1.6 Strains and plasmids

E. coli and *Yersinia* strains which were used in this study are listed in Table 8. Plasmids, which are referred to in this study are listed in Table 9.

Table 8. *E. coli* and *Yersinia* strains.

strains	description	reference/source
E. coli		
CC118 λpir	F$^-$ Δ(*ara-leu*)7697 Δ(*lacZ*)74 Δ(*phoA*)20 a*raD139 galE galK thi rpsE rpoB arfE*^{am} *recA1*, λ*pir*	(Manoil and Beckwith 1986)
BL21 λ DE3	F$^-$ *ompT gal dcm lon hsdSB*(r_B^- m_B^-) λDE3	(Studier, *et al.* 1990)
KB1	BL21λDE3 (Δ*stpA*)	this study
KB2	BL21λDE3 (Δ*hns*)	this study
KB3	KB1 (Δ*hns*)	this study
KB4	KB3 (Δ*hha*)	this study
Y. pseudotuberculosis		
YPIII	pIB1, wild type	(Bolin, *et al.* 1982)
YP3	pIB1, *rovA*::Tn*10*(60)[a]; Cm^R	(Nagel, *et al.* 2001)
YP41	pIB1, Δ*rovM*; Kn^R	(Heroven and Dersch 2006)
YP48	pIB1, Δ*csrC*; Kn^R	(Heroven, *et al.* 2008)
YP50	pIB1, Δ*ymoA*; Kn^R	A.K. Heroven
YP51	pIB1, Δ*csrB*; Ap^R	(Heroven, *et al.* 2008)
YP52	pIB1, Δ*csrB,* Δ*csrC*; Ap^R, Kn^R	(Heroven, *et al.* 2008)
YP53	pIB1, Δ*csrA*; Kn^R	(Heroven, *et al.* 2008)
YP63	pIB1, Δ*clpP*; Kn^R	(Herbst, *et al.* 2009)
YP67	pIB1, Δ*lon*, Ap^R	(Herbst, *et al.* 2009)
YP68	pIB1, Δ*clpP,* Δ*lon*, Kn^R, Ap^R	(Herbst, *et al.* 2009)
YP69	pIB1, Δ*csrB*	(Heroven, *et al.* 2008)
YP72	pIB1, Δ*rovM*	A.K. Heroven

strains	description	reference/source
YP73	pIB1, Δ*rovM*; Δ*ymoA*, Kn^R	this study
YP75	pIB1, Δ*csrB,* Δ*ymoA*; Kn^R	Julia Schaake
YP78	pIB1, Δ*lon*	A.K. Heroven
YP80	pIB1, Δ*hfq*	A.K. Heroven
YP81	pIB1, Δ*lon* Δ*clpP*, Kn^R	this study

^{R} ... antibiotic resistance

Table 9. Plasmids.

plasmid	description	reference
pACYC177	cloning vector, p15A, Ap^R, Kn^R	(Chang and Cohen 1978)
pACYC184	cloning vector, Tet^R, Cm^R, ori p15A	(Chang and Cohen 1978)
pAKH11	pET28a, *hns*$^+$, Kn^R	(Heroven, *et al*. 2004)
pAKH31	pK18, *hns*'; Tet^R	A.K. Heroven
pAKH32	pK18, Tet^R	A.K. Heroven
pAKH42	pACYC184, *rovM*$^+$, Cm^R	(Heroven and Dersch 2006)
pAKH47	pGP20, *rovA'-'lacZ* (17)[a], Tet^R	(Heroven and Dersch 2006)
pAKH56	pACYC184, *csrA*$^+$, Cm^R	(Heroven, *et al*. 2008)
pAKH59	pACYC184, *csrC*$^+$, Cm^R	(Heroven, *et al*. 2008)
pAKH63	pGP20, *rovM'-'lacZ* (41)[a], Tet^R	(Heroven and Dersch 2006)
pAKH71	pACYC184, *ymoA*$^+$, Cm^R	A.K. Heroven
pAKH73	pGP20, *hns'-'lacZ* (24)[a], Tet^R	A.K. Heroven
pAKH74	pACYC184, *hns*$^+$, Cm^R	(Heroven and Dersch 2006)
pAKH76	pHT124, *csrC*'-*lacZ* (-355 to +81)[b], Ap^R	(Heroven, *et al*. 2008)
pAKH77	pASK-IBA5plus, *ymoA*$^+$, Ap^R	A.K. Heroven
pAKH88	pHT124, *csrB*'-*lacZ* (-431 to +45)[b], Ap^R	A.K. Heroven
pAKH97	pHT124, *csrC*'-*lacZ* (-500 to +4)[b], Ap^R	(Heroven, *et al*. 2008)
pAKH103	pHT124, *csrC*'-*lacZ* (-355 to +4)[b], Ap^R	A.K. Heroven
pAKH104	pHT124, *csrC*'-*lacZ* (-355 to +257)[b], Ap^R	A.K. Heroven
pAKH106	pHT124, *csrC*'-*lacZ* (-355 to +31)[b], Ap^R	A.K. Heroven
pAKH107	pHT124, *csrC*'-*lacZ* (-355 to +61)[b], Ap^R	A.K. Heroven
pAKH115	pACYC184, *hfq*$^+$, Cm^R	A.K. Heroven
pAKH119	pHSG575, *hfq*$^+$, Cm^R	A.K. Heroven
pAKH125	pHT124, *csrC*'-*lacZ* (-310 to +4)[b], Ap^R	A.K. Heroven
pAKH126	pHT124, *csrC*'-*lacZ* (-283 to +4)[b], Ap^R	A.K. Heroven
pAKH127	pHT124, *csrC*'-*lacZ* (-204 to +4)[b], Ap^R	A.K. Heroven
pAKH128	pHT124, *csrC*'-*lacZ* (-106 to +4)[b], Ap^R	A.K. Heroven
pBAD18-*lacZ*(481)	translational *lacZ* fusion vector, Ap^R, ori pBR, ori M13	(Waldminghaus, *et al*. 2005)
pBO1817	pUC18, T7-*lcrF*'(-123 to 10)[c], for structure probing, Ap^R	J. Kortmann
pBO1818	pUC18, T7-*lcrF*'(-123 to 63)[c], for toeprint analysis, Ap^R	J. Kortmann
pBO1819	pUC18, T7-*lcrF*'(-51 to 10)[c], for structure probing, Ap^R	J. Kortmann

plasmid	description	reference
pBO1822	pUC18, T7-*lcrF*'(-51 to 63)[c], for toeprint analysis, Ap^R	J. Kortmann
pBO1823	pUC18, T7-*lcrF*'(-123 to 10)[c], for structure probing, Ap^R, (UU-28/-27CC)[c]	J. Kortmann
pBO1824	pUC18, T7-*lcrF*'(-123 to 63)[c], for toeprint analysis, Ap^R, (GUU -30 to -28 AAA)[c]	J. Kortmann
pBO1825	pUC18, T7-*lcrF*'(-51 to 10)[c], for structure probing, Ap^R, (UU-28/-27CC)[c]	J. Kortmann
pBO1832	pUC18, T7-*lcrF*'(-51 to 10)[c], for structure probing, Ap^R, (GUU -30 to -28 AAA)[c]	J. Kortmann
pBO1833	pUC18, T7-*lcrF*'(-123 to 63)[c], for toeprint analysis, Ap^R, (UU-28/-27CC)[c]	J. Kortmann
pBO1855	pUC18, T7-*lcrF*'(-123 to 10)[c], for structure probing, Ap^R, (GUU -30 to -28AAA)[c]	J. Kortmann
pCP20	FLP recombinase expression vector, Ap^R, Cm^R	(Datsenko and Wanner 2000)
pED05	pBAD18-*lacZ*(481), P_{BAD}::*gnd*'-'*lacZ*, Ap^R	E. Dornbusch
pED06	pBAD18-*lacZ*(481), P_{BAD}::*lcrF*(-123; AG -46/-45 CC)[c]-'*lacZ* (25)[a], Ap^R	E. Dornbusch
pED07	pBAD18-*lacZ*(481), P_{BAD}::*lcrF*(-123; GUU -30 to -28 AAA)[c]-'*lacZ* (25)[a], Ap^R	E. Dornbusch
pED08	pBAD18-*lacZ*(481), P_{BAD}::*lcrF*(-123; UU -28/-27 CC)[c]-'*lacZ* (25)[a], Ap^R	E. Dornbusch
pED10	pBAD18-*lacZ*(481), P_{BAD}::*yscW(+5)lcrF*'-'*lacZ* (25)[a], Ap^R	E. Dornbusch
pED13	pBAD18-*lacZ*(481), P_{BAD}::*lcrF*(-123; AUA -36 to -34 CCC)[c]-'*lacZ* (25)[a], Ap^R	E. Dornbusch
pET28a	T7 overexpression vector, Kn^R	Novagen
pGP20	protein fusion vector, *'lacZ*, Tet^R, ori pSC101	P.Gerlach
pHT124	promoter-probe vector, *lacZ*$^+$, Ap^R, ori ColE1	H. Tran-Winkler
pK18	cloning vector, Kn^R, ori pUC18	(Pridmore 1987)
pKB01	pBR322, *ymoA*$^+$, Ap^R, Tet^R	K. Böhme
pKB02	pGP20, *ymoA'-'lacZ* (6)[a], Tet^R	K. Böhme
pKB03	pZA31-*luc*, P_{tet}::*csrB*, Cm^R	(Heroven, *et al.* 2008)
pKB04	pHSG575, *ymoA*$^+$, Cm^R	this study
pKB06	pGP20, *barA*'-'*lacZ* (2)[a], Tet^R	(Heroven, *et al.* 2008)
pKB07	pGP20, *uvrY*'-'*lacZ* (3)[a], Tet^R	(Heroven, *et al.* 2008)
pKB13	pBAD18-*lacZ*(481), *lcrF*'(-127 to 74; Δ-41 to -30)[c], Ap^R	this study
pKB14	pBAD18-*lacZ*(481), *lcrF*'(-127 to 74), Ap^R	this study
pKB17	pHT124, *csrC*'-*lacZ* (81; Δ24 to 57)[b], Ap^R	this study
pKB18	pBAD18-*lacZ*(481), *lcrF*'(-63 to 74), Ap^R	this study
pKB20	pHT124, *csrC*'-*lacZ* (71)[b], Ap^R	this study
pKB34	pTS02, *yscW*(-573)[c]*lcrF*'-'*lacZ* (25)[a], Ap^R	this study
pKB35	pTS02, *yscW*(-573)[c]-'*lacZ* (5)[a], Ap^R	this study

plasmid	description	reference
pKB38	pTS02, *yscW*(-8)[c]*lcrF*'-'*lacZ* (25)[a], Ap^R	this study
pKB39	pTS02, *yscW*(-466)[c]*lcrF*'-'*lacZ* (25)[a], Ap^R	this study
pKB40	pTS02, *yscW*(-368)[c]*lcrF*'-'*lacZ* (25)[a], Ap^R	this study
pKB41	pTS02, *yscW*(-267)[c]*lcrF*'-'*lacZ* (25)[a], Ap^R	this study
pKB42	pTS02, *yscW*(-171)[c]*lcrF*'-'*lacZ* (25)[a], Ap^R	this study
pKB43	pTS02, *yscW*(-73)[c]*lcrF*'-'*lacZ* (25)[a], Ap^R	this study
pKB45	pTS03, *csrC*'-*lacZ* (-355 to +4)[b], Ap^R	this study
pKB46	pTS03, *csrC*'-*lacZ* (-355 to +81)[b], Ap^R	this study
pKB47	pHSG575, P_{tet}::*csrC,* Cm^R	this study
pKB49	pHSG576, P_{csrC}::*csrC* (Δ+24 to +57)[b], Cm^R	this study
pKB59	pHSG576, P_{csrC}::*csrC,* Cm^R	this study
pKB60	pHSG576, *csrA*$^+$, Cm^R	this study
pKB63	pTS02, *csrA*'-'*lacZ* (5)[a], Ap^R	this study
pKD4	kanamycin cassette template, Kn^R	(Datsenko and Wanner 2000)
pKD46	recombination vector, λ*red*$^+$, Ap^R	(Datsenko and Wanner 2000)
pKOBEG-*sacB*	recombination vector, *sacB*$^+$, Cm^R, ori pBAD	(Derbise, *et al.* 2003)
pPD264	pACYC184, *inv::*Tn*phoA*(60), Cm^R, Kn^R	(Nagel, *et al.* 2001)
pSF3	pGP20, *lcrF*(-526)[c]'-'*lacZ* (25)[a], Tet^R	S. Fehse
pSF4	pGP20, *yscW*(-573)[c]*lcrF*'-'*lacZ* (25)[a], Tet^R	S. Fehse
pTS02	pGP20, Ap^R	T. Stolz
pTS03	promoter-probe vector, *lacZ*$^+$, Ap^R, ori pSC101	T. Stolz
pTT01	pTS03, P_{tet}-*lacZ*, Ap^R	T. Thiermann
pUC18	cloning vector, Ap^R, ori pBR322	(Norrander, *et al.* 1983)

a ... amino acids, b ... nucleotides relative to transcription start, c ... nucleotides relative to start codon

2.2 Methods

2.2.1 General microbiological methods

2.2.1.1 Cultivation conditions

E. coli strains used in this study were grown under aerobic conditions at 37°C on solid or in liquid media. All cultures were shaken in a desk shaker. The cultivation of *Y. pseudotuberculosis* strains was mainly carried out at 25°C, for special experiments at 37°C.

2.2.1.2 Sterilisation

All autoclaveable solutions were sterilized for 20 min at 121°C and 1 to 2 bar overpressure in an autoclave. Non-autoclaveable solutions such as antibiotic solutions were sterile filtered (sterile filter, pore diameter 0.2 µm). Pipettes and glass ware were sterilized in a dry heat sterilizer at 180°C.

2.2.1.3 Measurement of cell density

The cell density of a bacterial strain was determined photometrically by measuring the optical density OD_{578} with a spectrophotometer. An OD_{578} of 1 corresponds to about $1 \cdot 10^9$ cells/ml (Sambrook, *et al*. 1989) containing 150 µl of protein (Miller 1992). For reference the identical growth medium was used.

2.2.1.4 Characterization of the bacterial growth

To monitor the growth curve of a bacterial culture an overnight culture was diluted 1:1000 in the appropriate medium. The culture was grown at different conditions and OD_{578} was measured isochronously. The growth rate was calculated by

$$\text{growth rate } [h^{-1}] = \Delta OD_{600}/\Delta \text{time}$$

2.2.2 General genetic and molecular biological methods for DNA

2.2.2.1 DNA marker

To measure the size of DNA fragments after agarose gel electrophoresis GeneRuler™ DNA Ladder Mix (Fermentas, Germany) was used for each run containing the following fragment lengths: 10000, 8000, 6000, 5000, 4000, 3500, 3000, 2500, 2000, 1500, 1200, 1031, 900, 800, 700, 600, 500, 400, 300, 200 and 100 base pairs. A gel pocket was filled with 0.1 to 0.5 µg of the marker.

2.2.2.2 Measurement of DNA concentration and purity

To determine the DNA concentration and the purity of DNA samples, their optical density was measured at 260 nm and 280 nm with the NanoDrop (PEQLAB Biotechnologie GmbH, Germany). DNA absorbs light maximally at a wavelength of 260 nm. One unit OD_{260} corresponds to a concentration of 50 µg/ml for double-stranded DNA. The DNA concentration is the product of the OD_{260} of the sample multiplied with its dilution factor and 50 µg/ml. In contrast to DNA, protein absorbs light optimally at 280 nm. The purity of a DNA sample is calculated by the ratio OD_{260}/OD_{280}. Ratios between 1.7 and 1.9 represent pure DNA.

2.2.2.3 Polymerase chain reaction (PCR)

Polymerase chain reaction was carried out to amplify DNA fragments. For this reaction, a heat stable DNA polymerase (Taq polymerase) elongates two oligonucleotides (see sec. 2.1.5) hybridized to the beginning and the end of the target DNA region.

The Phusion High-Fidelity DNA Polymerase (Finnzymes, USA) with a proof reading activity to reduce the error rate was used for amplification of DNA fragments for cloning. A typical Phusion PCR reaction with a volume of 100 µl contained the following ingredients:

HF buffer (5 x)	20 µl
dNTPs (10 mM)	2 µl
template	1 µl
primer A (10 mM)	3 µl
primer B (10 mM)	3 µl
Phusion polymerase (2 U/µl)	1 µl
H_2O	70 µl

For test-PCR purposes, e.g. to check for positive cloning results, the Mango*Taq* polymerase was used with the following PCR reaction mixture:

Mango buffer (5 x)	20 µl
dNTPs (100 mM)	1 µl
$MgCl_2$ (50 mM)	3 µl
template	1 µl
primer A (10 mM)	3 µl
primer B (10 mM)	3 µl
Mango *Taq* polymerase (1 U/µl)	1 µl
H_2O	69 µl

A PCR cycle begins with the denaturating of the DNA double strand at 95 °C. The next step is performed at temperatures from 50°C to 65°C (depending on the primer sequence) and leads to the annealing of the primers to complementary single strands. The synthesis of the corresponding complementary strand starting at each primer occurs at 72°C (elongation).

The variable parameters during the PCR were calculated as the following:

1. The time of the first elongation step depends on the size of the DNA segment to be amplified and the elongation rate of the Taq polymerase. The Mango*Taq* polymerase as well as the Phusion polymerase synthesizes 1,000 bp per 30 sec.
2. The annealing temperature is determined by the length and the composition of the primers used in the reaction. It is calculated after Suggs *et al.* (1981).

One cycle is repeated 30 to 40 times. A typical program is carried out with the following procedure:

1. Denaturating 5 min at 95°C	
2. Denaturating 30 sec at 95°C	
3. Annealing 30 sec at variable temperature	30-40 cycles
4. Elongation variable at 72°C	
5. Elongation 5 min at 72°C	

The first denaturating step ensures complete denaturation of all DNA double strands and the second elongation step completes synthesis of all PCR products. If necessary, primer sequences included restriction sites for cloning purposes (sec. 2.1.5). PCR products were cleaned from 100 µl reaction volume as described by the manufacturer instructions using the "QIAquick PCR Purification Kit" and were eluted in 30 µl *aqua bidest*.

2.2.2.4 Isolation of DNA

2.2.2.4.1 Plasmid preparation

To isolate plasmid DNA a culture with bacteria harboring the plasmid to be isolated was grown overnight in LB medium supplemented with the appropriate antibiotic. Preparation of the plasmid was carried out according to the alkaline extraction procedure described by Birnboim and Doly (1979) using the "QIAGEN Plasmid Mini Kit" (QIAGEN, Germany). Plasmid-DNA was generally eluted from the columns with 50 µl H_2O.

For large-scale preparation of plasmid DNA "QIAGEN Plasmid Midi Kit" (QIAGEN, Germany) was performed according to the manufacturer's instructions. The DNA was eluted in 50 µl *aqua bidest*.

2.2.2.4.2 DNA agarose gel electrophoresis

Separation of double-stranded DNA fragments according to their size was achieved by agarose gel electrophoresis. This method makes use of the ability of negatively charged DNA to move towards the anode when an electrical field is applied. The DNA moving velocity is determined by the length and the conformation of the DNA as well as the agarose concentration within the gel and the applied voltage. In this study an agarose concentration of 0.8% was usually used for DNA separation. Small DNA fragments were separated in 2% agarose gels. The gel electrophoresis was performed at a voltage of 90 to 120 V in TAE buffer. To facilitate the

application of DNA samples to the gel, loading buffer (1 x) was added. As the reaction buffer of the Mango Taq polymerase already contained loading buffer substances, these PCR reaction samples were directly applied to the gel. To measure the size of the DNA fragments 5 µl marker were used.

For visualization of the DNA the gel was stained in ethidium bromide (1 µg/ml in water), which intercalates within nucleic acids and are fluorescent under UV light. Gels were exposed to UV light at 226 nm and photographed with a CCD (charge-coupled device) camera of the gel documentation system.

TAE buffer (1 x): 40 mM TRIS acetate; 1 mM EDTA pH 8.0
loading buffer (1 x): 50% glycerol; 0.01% bromophenol blue; 0.01% xylene cyanol

2.2.2.4.3 DNA isolation from agarose gels

DNA fragments of interest with a specific size were separated from other fragments via gel electrophoresis, stained and isolated under UV light at a wavelength of 315 nm. The DNA fragment was separated from the agarose using the "QIAquick Gel Extraction Kit" (QIAGEN, Germany) as described by the manufacturer. The DNA was eluted from the column with 30 µl *aqua bidest*.

2.2.2.4.4 DNA extraction with phenol

To remove contaminating proteins from a DNA solution, phenol extraction was used with subsequent precipitation of the DNA with sodium acetate and ethanol. Therefore, one volume of DNA solution was mixed thoroughly with one volume of phenol. The mixture was centrifuged at 13,000 rpm for 3 min in a 5415 R microcentrifuge (Eppendorf, Germany) and the aqueous phase was transferred to a new tube. In the following, one volume of chloroform was added, mixed and centrifuged. After transfer of the aqueous phase to a new tube, the chloroform extraction was repeated. For precipitation of the DNA, 1/10 volume sodium acetate and two volumes ethanol (100%) were added, mixed intensively and incubated for 10 min at -20°C. After centrifugation for 10 min at 4°C, the supernatant was discarded. The DNA pellet was dried and resolved in *aqua bidest*.

2.2.2.4.5 DNA sequencing

The DNA sequencing was performed by GATC (Constance, Germany) or at the Department of Genome Analysis (HZI, Germany).

2.2.2.5 Cloning techniques

2.2.2.5.1 Restriction digests

Restriction analysis was used to insert DNA fragments into vectors during the cloning process or to determine the size of a certain DNA fragment. Therefore, type II restriction enzymes were used which recognize specific palindromic nucleotide sequences of four to eight base

pairs. Within these sequences these enzymes produce overhanging ("sticky") ends or blunt ends. Restrictions enzymes cut optimally at a specific temperature and buffer, which are provided by the manufacturer.

Enzymes and buffers (10 x concentrated) used in this study were purchased by New England Biolabs (USA). Each restriction experiment was carried out for 30 min to four hours at the optimum reaction temperature described by the manufacturer. Inactivation was achieved by heat inactivation for 20 min at 80°C. If the enzymes could not be inactivated by heat, they were removed by purification with the "QIAquick PCR Purification Kit" (QIAGEN, Germany) or by phenol extraction with subsequent sodium acetate and ethanol precipitation (sec. 2.2.2.4.4).

2.2.2.5.2 Preparative digest

To achieve appropriate amounts of a certain DNA fragment for cloning experiments, preparative restriction digests were performed. Therefore, one to two µg of plasmid DNA were digested for 30 min at 37°C. A standard reaction volume of 100 µl consisted of:

aqua bidest	82	µl
plasmid DNA (midi prep.)	5	µl
buffer (10 x)	10	µl
restriction enzyme 1	1.5	µl
restriction enzyme 2	1.5	µl .

2.2.2.5.3 Analytical digest

Analytical digests were used to check the result of a cloning experiment. Prepared plasmid DNA was digested with appropriate restriction enzymes. A 20 µl standard reaction mix contained the following ingredients:

aqua bidest	7.5	µl
plasmid DNA (mini prep.)	10	µl
buffer (10 x)	2	µl
restriction enzyme	0.5	µl

The reaction mixture was incubated generally at 37°C for one hour. DNA fragments were separated by gel electrophoresis to analyze the size of the digested fragments.

2.2.2.5.4 Dephosphorylation of plasmid DNA

To reduce the religation rate of a vector, which was linearized with one restriction enzyme, the digested plasmid was treated with "Antarctic Phosphatase" (NEB, USA). The enzyme catalyzes the removal of phosphate groups at 5'-position from the cleavage site. A standard reaction volume contained:

restriction reaction	100	µl
Antarctic Phosphatase	2	µl
10 x reaction buffer	11	µl

This reaction was carried out for 15 min at 37°C and was inactivated for 5 min at 65°C.

2.2.2.5.5 Ligation

For the construction of plasmids, ligation reactions were carried out. The T4 DNA ligase (Promega) helps to form new phosphodiester bondages between an insert, generated by PCR or by preparative digests, and the linearized vector.

A ligation reaction was generally incubated overnight at 8°C and was composed of:

ligation buffer (10 x)	1.0	µl
vector (0.5-1.0 µg/µl)	0.5	µl
DNA fragment (ca. 0.5-1.0 µg/µl)	8.0	µl
T4 DNA-Ligase (4 U/µl)	0.5	µl

10 x Reaction Buffer: 300 mM TRIS-HCl (pH 7.8 at 25°C), 100 mM $MgCl_2$, 100 mM DTT and 10 mM ATP

Plasmid constructions are described in the supplementary material.

2.2.2.6 Transformation

2.2.2.6.1 Electrocompetent *E. coli* cells

To prepare electrocompetent *E. coli* cells bacteria of a single colony were incubated overnight at 37°C in 5 ml LB medium supplemented with the appropriate antibiotic. This preculture was used to inoculate 200 ml LB or DYT medium 1:100, incubated at 37 °C. At an OD_{600} of 0.5 to 0.8 the culture was cooled on ice for 15 to 30 min. Cells were harvested at 4°C by centrifugation in a Sigma 3-18 K centrifuge using 19776-H rotor at 6,000 rpm for 5 min. The bacterial pellets were washed with 30 ml cold *aqua bidest* and centrifugation was repeated at 6,000 rpm for 8 min and 4°C. In the following, the bacterial pellets were washed with 30 ml 10% glycerol. After the last centrifugation step the pellet was resuspended in 1/1000 volume of 10% glycerol and divided into 40 µl aliquots. These aliquots were used immediately for transformation or stored at -20°C.

Electrocompetent *E. coli* pKD46 cells were cultivated as described for *E. coli* above. At an OD_{600} of 0.2 the culture was induced by arabinose at a final concentration of 0.2% and cultivation was continued. When the culture reached an OD_{600} of 0.8, cells were harvested and washed as described for *E. coli*.

2.2.2.6.2 Electrocompetent *Yersinia* cells

Electrocompetent *Yersinia* cells were produced by inoculation of 200 ml BHI medium 1:50 with a fresh overnight culture. This culture was incubated at 25°C until an OD_{600nm} of approx. 0.8 was reached. The bacteria were prepared and washed as described above for *E. coli* but the last washing step was carried out using 30 ml transformation buffer instead of 10% glycerol. Subsequent to the centrifugation, the pellet was resuspended in 1/500 volume transformation buffer. 40 µl aliquots were directly used for transformation.

For production of electrocompetent Y*ersinia* pKD46, 200 ml of LB medium supplemented with carbenicillin were inoculated 1:50 by an overnight culture and incubated at 25°C. At an OD_{600nm} of 0.2 the culture was induced by arabinose at a final concentration of 0.2%. Cells were harvested at an OD_{600nm} of 0.5 to 0.8 by centrifugation as described above. Washing steps were performed as described for *E. coli* using 10% glycerol. The washed pellet was resuspended 1:500 in 10% glycerol. 40 µl aliquots were prepared and immediately used for transformation.

Transformation buffer for *Yersinia spp.*: 272 mM sucrose; 15% glycerol

2.2.2.6.3 Electroporation

For the efficient transformation of plasmids into electroporation into *E. coli* and *Y. pseudotuberculosis* strains electroporation was performed. Therefore, 1 µl of desalted DNA or 4 µl of a dialyzed ligation reaction were added to a 40 µl aliquot of electrocompetent cells. This mixture was filled into a chilled cuvette harboring an electrode gap of 0.2 mm (Peqlab, Germany). A voltage of 2.2 kV with a capacity of 25 µF and a resistance of 200 Ω was applied.

For RED-recombinase-mediated mutagenesis 6 to 16 µl of the PCR fragment encoding the insertion fragment were transformed into *Yersinia* pKD46 strains. Electroporation was performed as described for *Yersinia* except that cells were incubated in SOC medium for phenotypical expression.

After electroporation *E. coli* cells were resuspended immediately in 1 ml LB, *Yersinia* cells were suspended in DYT medium. For phenotypical expression of the resistance genes, *E. coli* was incubated for one hour at 37°C, whereas *Yersinia* cells were incubated for two hours at 25°C. *E. coli* pKD46 cells were incubated at 25°C since pKD46 carries a temperature-sensitive ori. In the following, cells were plated on the appropriate selective solid medium and incubated overnight at 37°C. Solid media with *Y. pseudotuberculosis* were incubated for two days at 25°C.

2.2.2.7 Mutagenesis of *E. coli* and *Yersinia*

Gene knock-outs in *E. coli* and *Yersinia* were generated using the RED recombinase system as described previously (Datsenko and Wanner 2000; Derbise, *et al.* 2003).

E. coli strain KB1 was generated by introducing a fragment carrying a *stpA* deletion amplified with primers 33 and 34 in strain BL21λDE3. *E. coli* KB1 was used to mutate the *hns* gene with a fragment amplified with primers 35 and 36 leading to strain KB3. *E. coli* strain BL21λDE3 *stpA*$^-$*hns*$^-$*hha*$^-$, described as KB4, was derived from KB3 by transformation of a fragment amplified with primers 37 and 38 encoding a *hha* mutation. These strains were derived by amplifying a kanamycin cassette by PCR. The used primers were homologous to the resistance gene encoded on pKD4 followed by homologous sequences of adjacent regions of the target gene. The PCR fragment was transformed into *E. coli* BL21 pKD46 (sec. 2.2.2.6.1). Chromosomal integration of the fragment was selected by plating on LB supplemented with kanamycin. Subsequently, mutant derivatives were cured of the temperature-sensitive plasmid pKD46 by cultivation at 37°C. To remove the resistance gene at its FLP recognition sites the mutants were transformed with the helper plasmid pCP20 encoding the FLP recombinase. For thermal induction of FLP synthesis and subsequent removal of the temperature-sensitive plasmid pCP20, mutants were incubated at 37°C.

Y. pseudotuberculosis strains YP73 was derived from YP72 (YPIII *rovM*$^-$) by deleting *ymoA*. Further, the *clpP* gene was mutated in YP78 (YPIII *lon*$^-$) generating YP81. To do so, the kanamycin resistance gene was amplified using primer pair 39/40. Next, the *Yersinia* genomic DNA was used as a template to amplify 500-bp regions flanking the target gene. The upstream fragment was amplified with a primer pair of which the reverse primer contained additional 20 nt at the 5'-end which were homologous to the start of the kanamycin resistance gene. The downstream fragment was amplified with a primer pair of which the forward primer contained additional 20 nt at the 5'-end which were homologous to the end of the kanamycin resistance gene. In the next step, a PCR reaction was performed with the forward primer of the upstream fragment and the reverse primer of the downstream fragment using the upstream and downstream PCR products of the target gene and the *kan* PCR fragments as templates. For the deletion of *ymoA*, the upstream fragment was synthesized by using primers 41 and 42. The downstream fragment was amplified with primers 43 and 44. The last PCR step was carried out with primer pair 41/44. To delete the *clpP* gene, an upstream and downstream fragment were generated using primer pairs 45/46 and 47/48. Using primers 45 and 48 the kanamycin cassette was amplified with flanking *clpP* regions. The PCR fragments were transformed into *Y. pseudotuberculosis* YPIII pKOBEG-*sacB* and chromosomal integration of the fragment was selected by plating on LB supplemented with kanamycin. Mutants were subsequently grown on LB agar plates without NaCl plus 10% sucrose, and faster growing colonies without pKOBEG-*sacB* were selected and proven by PCR and DNA sequencing.

2.2.3 Molecular biological methods for RNA

2.2.3.1 RNA isolation

To study influences of gene regulation on RNA levels of the virulence factors in *Y. pseudotuberculosis*, total RNA of the bacteria was isolated. Two to four ml of bacterial culture were withdrawn and mixed with 0.4 volume stop solution. Subsequently, the suspension was snap-frozen in liquid nitrogen. Bacterial cells were pelleted by centrifugation at 13,000 rpm for 5 min at 4°C in a microcentrifuge 5415 R (Eppendorf, Germany) and lysed by resuspension in a lysozyme solution for 5 min at room temperature. RNA isolation was performed using the SV Total RNA purification kit (Promega, USA) according to the manufacturer's description. RNA was eluted with 100 µl RNase-free H_2O (Gibco,USA) and the RNA concentration was determined.

stop solution: 95% ethanol, 5% Aqua phenol
lysozyme solution: 50 mg/ml lysozyme in TE buffer (pH 7.5)
TE buffer (pH 7.5): 100 mM TRIS-HCl pH 7.5, 1 mM EDTA pH 8.0

2.2.3.2 Measurement of RNA concentration

RNA concentration of a RNA isolation experiment was determined with a NanoDrop (Peqlab, Germany). RNA absorbs light at a wavelength of 260 nm. One unit of absorbance at 260 nm corresponds to 40 µg RNA per ml water. RNA purity is measured by the ratio of absorbance at 260 nm to 280 nm.

2.2.3.3 RNA agarose gel electrophoresis

To separate RNAs by size, RNA samples were applied to gel electrophoresis. In an electrical field, negatively charged RNA molecules move towards the anode. RNA size and conformation determine the velocity of the RNA migration through a polymeric agarose matrix. Since RNA forms secondary structures, RNAs samples were denatured prior to gel electrophoresis by the addition of a loading buffer containing formaldehyde and formamide and heating for 10 min at 70°C. To determine the quality of an RNA sample, ethidium bromide was added to the loading buffer.

In general, 10 µg of total RNA were applied to a 1.2% MOPS-agarose gel. Gel electrophoresis was carried out for 90 min at a voltage of 120 V. After gel electrophoresis, the RNA was visualized by exposure to UV light at a wave length of 226 nm and documented by a gel documentation system.

RNA loading buffer (5 x): 0.03% bromophenol blue, 4 mM EDTA, 0.1 mg/ml EtBr, 2.7% formaldehyde, 31% formamide, 20% glycerol in 4 x MOPS buffer
MOPS (20 x): 200 mM MOPS, 50 mM sodium acetate, 10 mM EDTA

2.2.3.4 Northern blot analysis

Northern blotting was used to detect specific RNAs within a RNA population with a hybridization probe complementary to the target RNA. After gel electrophoresis the RNA is transferred onto a positively charged nylon membrane by capillary forces. Therefore, the agarose gel was equilibrated by incubation in 20 x SSC solution for 30 min and then placed upside down onto whatman papers saturated with 2 x SSC, covering whatman paper saturated with 20 x SSC solution. The gel was covered with a nylon membrane Nytran™ N (Whatman, USA), overlayed with dry whatman paper. The blotting was performed for 4.5 hours. Subsequently, the RNA was crosslinked twice to the membrane with a stratalinker UV (Stratagene, USA).

Prehybridization, hybridization to Dig-labeled DNA-probes and membrane washing was carried out using the DIG luminescent Detection kit (Roche, Germany) according to the manufacturer's instructions. Probes were synthesized by PCR (for primers see Table 10) using the *Taq* polymerase (NEB) as followed:

ThermoPol buffer (10 x)	10	µl
DIG DNA labelling Mix (10 x)	10	µl
$MgSO_4$ (25 mM)	10	µl
template	1	µl
primer A (10 µM)	3	µl
primer B (10 µM)	3	µl
Taq polymerase (1 U/µl)	1	µl
H_2O	62	µl

The following primers were used to synthesize Dig-labeled DNA probes from chromosomal DNA of *Y. pseudotuberculosis* strain YPIII.

Table 10. Primer for DNA probes.

name	sequence	
51	5'- GCA ATC AGC TAG TCA ATT TG -3'	*csrC* forward
52	5'- GGG CGC GGA TCC GAT TGG GCC GGA ATC TAG C -3'	*csrC* reverse
53	5'- CGG CGC GGA TCC CTC TCA CAC CAG CTG TG -3'	*csrB* forward
54	5'- GGG GGC GTC GAC GGC AAA CTC AAT ATC CTG -3'	*csrB* reverse

Dig-labeled DNA-RNA hybrids were visualized by chemiluminescence detection using CDP-Star (Roche, Germany). After incubation with the chemiluminescent substrate the membrane was exposed to X-ray films CL-Xposure (Thermo Scientific, USA) and developed by a developing machine Optimax Type TR (MS Laborgeräte, Germany).

20 x SSC: 3 M NaCl, 0.3 M Natriumcitrat, pH 7

2.2.3.5 RNA stability assay

RNA stability assay was used to determine the degradation of the CsrC RNA in different *Yersinia* mutant backgrounds. A *Y. pseudotuberculosis* overnight culture was mixed with Rifampicin at a final concentration of 500 µg/ml to inhibit transcription initiation. Samples were taken simultaneously and centrifuged at 13,000 rpm for 2 min in a 5415 R microcentrifuge. A 0.4 volume stop solution was added. Total RNA was isolated and Northern blotting was performed as described above (sec. 2.2.3.1 to sec. 2.2.3.4).

rifampicin solution: 10 mg/ml rifampicin in methanol

2.2.3.6 *In vitro* transcription

To monitor RNA stability of regulatory RNAs or to analyze the secondary structure and its influences on translational events, RNA needed to be transcribed *in vitro* using PCR product or linearised plasmids as templates.

2.2.3.6.1 *In vitro* transcription with PCR templates

For synthesis of RNA *in vitro,* the template of the target gene was amplified by using a forward primer, carrying a T7 recognition site fused to the 5' end of the gene sequence, and a reverse primer binding to the 3' end. The PCR product was purified by "QIAquick PCR Purification Kit" (Qiagen, Germany)

Primers used to synthesize the template for the reverse transcriptase reaction from chromosomal DNA of *Y. pseudotuberculosis* strain YPIII are listed below (Table 11).

Table 11. Primer for Reverse transcription template.

name	sequence	
55	5'- GGG CGC GTA ATA CGA CTC ACT ATA GTT GGT ACG GAT ACA CCA TGC- 3'	P*tet*::*csrC* forward
56	5'- CCA GTG TCC TAA CAT CCC T- 3'	*csrC* reverse
57	5'- GGG CGC GTA ATA CGA CTC ACT ATA GGC CTG GCG GCC ATA GCG- 3'	P*tet*::5S rRNA forward
58	5'- GCCTGGCAGTGTCCTACTC- 3'	5S rRNA reverse

underlined ... recognition site for T7 polymerase

In vitro transcription was performed using the TranscriptAid™ T7 High Yield Transcription Kit as described by Fermentas (Germany). A typical *in vitro* transcription reaction was prepared as the following:

5 x TranscriptAid™ reaction buffer	4	µl
ATP/CTP/GTP/UTP mix (equal volumes)	8	µl
template DNA	2	µl
DEPC-treated water	4	µl
TranscriptAid™ enzyme mix	2	µl

The reaction mixture was incubated overnight at 37°C.

2.2.3.6.2 Run-off *in vitro* transcription

RNAs synthesized *in vitro* by run-off transcription were used for RNA structure probing and toeprint analysis. Therefore, an insert which carried the T7 polymerase recognition site fused to the 5' end of the DNA sequence encoding the target RNA region was ligated into the vector pUC18 (plasmids see Table 9). Plasmids were linearized by digestion with *Mls*I, extracted by phenol method and precipitated with sodium acetate and ethanol (sec. 2.2.2.4.4).

The purified DNA was used in a reaction mix as described in the following:

5 x transcription buffer	40	µl
dNTP Mix (20 mM)	20	µl
linearized template DNA	4	µg
RiboLock™ RNase inhibitor	5	µl
T7 RNA polymerase	6	µl
triton	2	µl

RNA synthesis was carried out overnight at 37°C. The RNA was purified by phenol extraction and ethanol precipitation as described in sec. 2.2.3.7 and 2.2.3.8.

2.2.3.7 RNA phenol extraction

To remove contaminating proteins from a RNA sample RNA was extracted with phenol. For that, a 200 µl RNA solution was mixed thoroughly with 150 µl Roti-Aqua phenol (Roth, Germany) and centrifuged at 13,000 rpm for 3 min in a 5415 R microcentrifuge. The aqueous phase was transferred to a new tube and mixed with 150 µl chloroform. After mixing, centrifugation was performed as described before. This step was repeated and the aqueous phase transferred to a new vial for precipitation.

2.2.3.8 RNA precipitation

To precipitate RNA, three volumes of ethanol were added to one volume of RNA solution supplemented with 1/10 volume of Na acetate and glycogen. The mixture was incubated at -20 °C for 15 min. In the following, the precipitate was centrifuged at 13,000 rpm for

15 min at 4°C in a 5415 R microcentrifuge. The pellet was washed with 100 µl 70% ethanol and centrifuged again at 13,000 rpm for 5 min at 4°C. The RNA was diluted in RNase-free water.

2.2.3.9 RNA isolation from polyacryamide gels

For purification of RNA after run-off *in vitro* transcription and radioactive-labeling, RNA was separated in 6% polyacrylamide/urea gels with a thickness of 1 mm in TBE buffer. After preparation of the gel at 20 mA, 1,000 V for 30 min, gel run was performed in a gel system S2001 (Life technologies, USA) at 25 mA (ca. 1,200 V) depending on the size of the RNA.

The RNA was visualized under UV-light, the RNA band was cut out and transferred to a clean tube filled with 400 µl RNA elution buffer. The sample was incubated for 1 h at 30°C in a shaking thermomixer (Eppendorf, Germany). 400 µl RNA elution buffer were transferred to a new vial and elution was repeated with additional 400 µl RNA elution buffer. Subsequently, the RNA was precipitated with sodium acetate and ethanol (sec. 2.2.3.8).

TBE buffer (1 x): 89 mM TRIS; 89 mM boric acid; 2 mM EDTA
6% polyacrylamide/urea solution: 6% acrylamide/bisacrylamide (40%, 19:1 stock), 7 M urea in TBE
RNA elution buffer: 10 mM EDTA, 0.5 % SDS, 0.1 M sodium acetate pH 5.6

2.2.3.10 RNA structure probing

To determine the secondary structure of the 5' untranslated region of LcrF, the radioactively labeled RNA was digested with specific RNases and the fragments were separated by polyacrylamide gel electrophoresis.

2.2.3.10.1 Dephosphorylation of RNA

RNA needs to be dephosphorylated at its 5' end to allow radioactive labeling of the molecule. Calf intestine phosphatase (CIP, NEB, USA) catalyses the removal of two phosphate groups at the 5' end, leaving one monophosphate group for the labeling reaction. A typical dephosphorylation reaction contained the following:

in vitro transcribed RNA	3	pmol
10 x CIP buffer	5	µl
CIP	1	µl

The reaction was incubated for 45 at 37°C. Subsequently, 150 µl of RNase-free water were added and the RNA was extracted using phenol (sec. 2.2.3.7). After precipitation with ethanol and sodium acetate (sec. 2.2.3.8) the RNA pellet was dissolved in 7 µl.

2.2.3.10.2 Radioactive labeling of RNA

For radioactive labeling, RNA, desphosphorylated at the 5' end, was phosphorylated with radioactive γ-ATP^{32} (Hartmann, Germany) using T4 polynucleotide kinase (PNK, Fermentas,

Germany) as described by Brantl and Wagner (1994). The enzyme transfers the γ-phosphate from ATP to 5' hydroxyl group of RNA.

The reaction consisted of:

dephosphorylated RNA	15	pmol
PNK buffer	1	µl
PNK	1	µl
Ribolock RNase inhibitor	0.5	µl
γ-ATP^{32}	4	µl

and was incubated for 5 min at 37°C. The reaction was inactivated by the addition of 10 µl formamide stop solution and incubated for 5 min at 95°C. In the following, the reaction was applied to a 6% polyacrylamide/urea gel and the RNA bands were isolated from the gel (sec. 2.2.3.9). After precipitation of the RNA, the pellet was dissolved in 15 µl RNase-free water and radioactive labeling efficiency was measured by a scintillation counter (liquid scintillation analyzer Tri-Carb 2800 TR, Perkin Elmer, USA).

formamide stop solution: 17 mM EDTA, 0.05% bromophenol blue/xylene cyanol in formamide

2.2.3.10.3 Digestion and separation of RNA

The RNA formation of the LcrF untranslated 5' region was analyzed at 25°C and 37°C. Partial digestion of RNA molecules with ribonucleases T1 and V (Ambion, USA) was conducted as described by Waldminghaus *et al.* (2008). Ribonuclease T1 cleaves RNA 3' of single-stranded G residues, whereas RNase V recognizes base-paired nucleotides. A reaction mixture of 4 µl, the RNA (30,000 counts) was first incubated with 1 µl TMN buffer (5 x), 0.4 µl tRNA (Invitrogen, Germany) and RNase-free water for five minutes at 25°C or 37°C. Then, a volume of 1 µl RNase T1 (0.001 U/µl), RNase V (0.0002 U/µl) or RNase-free water (control) were added. After 5 min of incubation at the appropriate temperature, the reaction was stopped by addition of 5 µl formamide stop solution. The samples were incubated on ice for a few minutes and subsequently heated to 95°C for 5 min for denaturation of secondary structures. Alkaline ladders were generated as described previously (Brantl and Wagner 1994). 60,000 counts of LcrF RNA were supplemented with 4 µl tRNA, 1 µl RNA ladder buffer and RNase-free water to a total volume of 10 µl. The ladder reactions were heated for 2 min at 90°C. 10 µl of formamide stop solution were added. After 5 min of incubation on ice, samples were applied to a denaturing 8% polyacrylamide/urea gel to separate RNA fragments. Electrophoresis was carried out in TBE buffer at 2,100 V for 1.5 h. Subsequently, the gel was dried (gel dryer 583, Biorad, USA), RNA fragments were visualized by overnight exposure to an X-ray film and documented by Bioimager FLA-3,000 (Fujifilm, Japan).

TMN buffer (5 x): 100 mM TRIS acetate pH 7.5; 10 mM $MgCl_2$; 500 mM NaCl
RNA ladder buffer (10 x): 1 M Na_2CO_3; 1 M $NaHCO_3$

2.2.3.11 RNA toeprint analysis

RNA toeprinting experiments (Hartz, *et al*. 1989), also known as primer extension inhibition experiments, were used to analyze whether ribosomal binding to the recognition site in the 5' untranslated region of LcrF was impaired by secondary structure formation of the RNA at low temperatures. In general, *in vitro* translated RNA of LcrF, consisting of the 5' untranslated region and the first 63 nucleotides of the coding sequence, was mixed with radioactively labeled primer. After the primer had annealed to the 3' end in the coding region of LcrF, the RNA was incubated with or without 30S ribosomal subunits at 25°C and 37°C and the reverse transcriptase was added. Moloney Murine Leukemia Virus reverse transcriptase (M-MLV, USB, USA) synthesizes cDNA starting at the labeled primer towards the 5' end of the RNA (Roth, *et al*. 1988). In case the RNA forms secondary structures or stable ribosome-RNA complexes, the M-MLV reverse transcriptase stops transcription in this region and falls off the RNA generating small cDNA fragments (toeprint). Full length transcripts are synthesized when the secondary structure of the RNA thermometer is resolved at higher temperatures or ribosomes are not present.

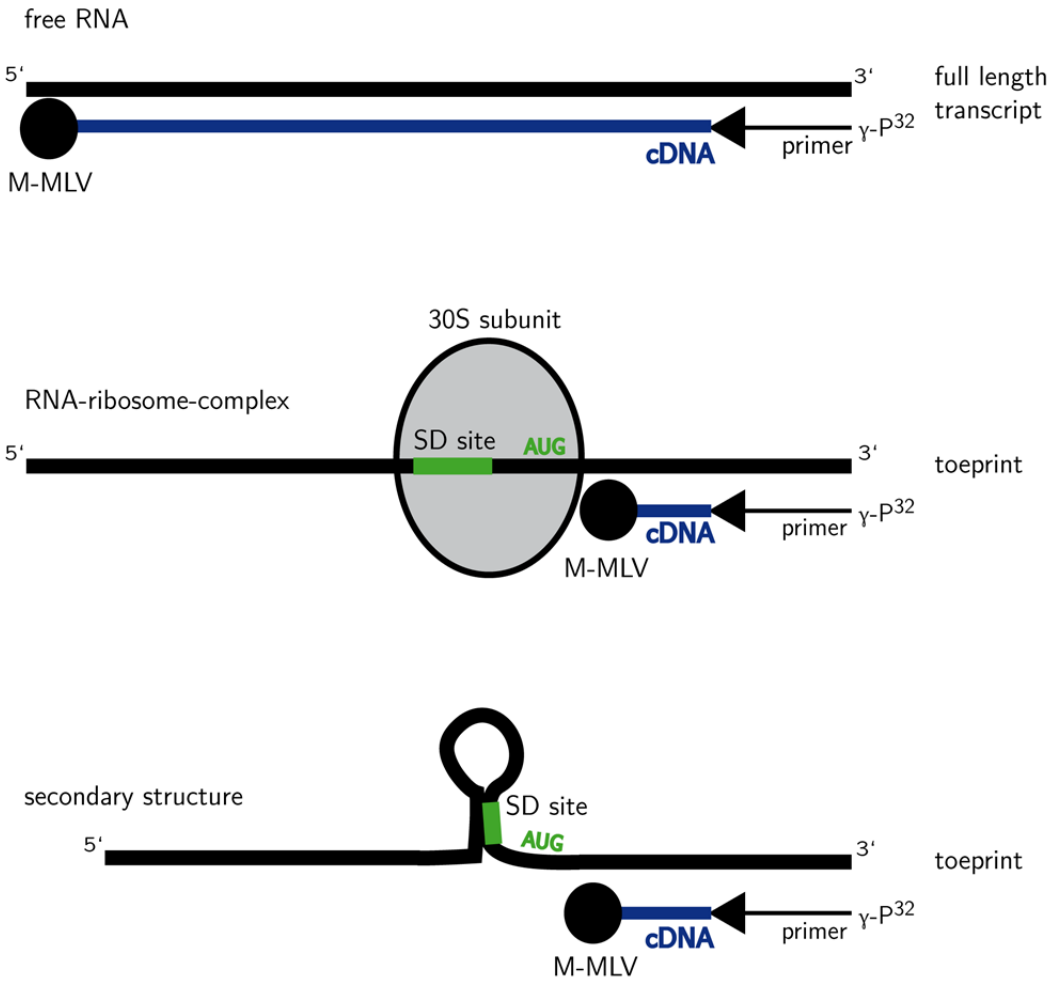

Fig. 12. The principle of primer extension inhibition (toeprint analysis).M-MLV reverse transcriptase synthesizes cDNA from the radioactively-labeled primer at the 3' end of the RNA in 5' direction. Full length transcripts are produced when M-MLV is incubated with linear RNA. Toeprint transcripts are generated when

RNA and 30S ribosomal subunits or secondary RNA structures are formed, since the M-MLV transcription is stopped and the enzyme falls of the RNA template.

2.2.3.11.1 Radioactive labeling of primers

To visualize cDNA fragments of the toeprint experiment, the primer, which anneals to the 3' end of the RNA template, was labeled with γ-ATP^{32} at its 5' end. The reaction mixture was composed of:

primer (10 pmol/µl)	1	pmol
10 x PNK buffer	2	µl
PNK (10 U/µl)	1	µl
γ-ATP^{32}	2	µl
H_2O	14	µl

This mixture was incubated for 60 min at 37°C and inactivated by heating to 65°C for 10 min. Subsequently, the labeled DNA was precipitated as described above (sec. 2.2.3.8). The pellet was resuspended in 20 µl RNase-free water.

2.2.3.11.2 Annealing of primers

Radioactively labeled primers were annealed to the target mRNA for three hours at 80°C in the following reaction:

primer (0.5 pmol/µl)	4	pmol
1 x VD buffer-Mg^{2+}	17	µl
mRNA	0.25	pmol/µl
total	25	µl

Subsequently, the mixture was snap-frozen in liquid nitrogen and thawed on ice for at least 30 min.

5 x VD buffer-Mg^{2+}: 0.05 M TRIS-HCl pH 7.4, 0.3 M NH_4Cl, 30 mM β-mercaptoethanol, 0.05 M MgO acetate

2.2.3.11.3 Extension reaction

For the toeprinting experiment, the 5' untranslated region of LcrF with the annealed primer (annealing mix, sec. 2.2.3.11.2) was incubated with or without 30S ribosomal subunits at two different temperatures, 25°C and 37°C. 30S ribosomal subunits were isolated from *E. coli* as described previously (Hartz, *et al.* 1989). Uncharged tRNA^{tMet} (Sigma-Aldrich, USA) was added to stabilize the ribosomal binding complex. A typical reaction was prepared as described in the following:

Watanabe buffer I	4	µl
tRNA^{tMet} (8 pmol/µl)	17	µl
annealing mix	4	µl

The mixture was incubated for 10 min at 25°C or 37°C. Subsequently, 6 µl 30S ribosomal subunits or TICO buffer were added and incubation was continued for additional 10 min at the appropriate temperatures. To initiate the primer extension, 2 µl M-MLV reaction mix was

added, containing the reverse transcriptase, and the reaction was carried on for 10 min at 25°C.

The MMLV reaction mix was composed of:

5 x VD buffer-Mg^{2+}	0.16 µl
MMLV (200 U/µl)	0.33 µl
BSA (1 mg/ml)	0.50 µl
dNTPs solution	0.50 µl
H_2O	0.50 µl

Watanabe buffer I: 60 mM HEPES-KOH pH 7.5 (0°C), 10.5 mM $Mg(COO)_2$, 690 mM NH_4COO,
12 mM β-mercaptoethanol, 10 mM spermidine, 0.25 mM spermine
dNTPs solution: 4.3 mM 4 x dNTPs, 23% 5 x VD buffer-Mg^{2+} in RNase-free H_2O
Tico buffer: 60 mM HEPES pH 7.4, 10.5 mM $Mg(COO)_2$, 690 mM NH_4COO, 12 mM β-mercaptoethanol

The reaction was stopped by the addition of 20 µl formamide stop solution and heating for 5 min at 95°C to resolve secondary structures. For separation of the cDNA fragments, 6 µl of the samples were applied to an 8% polyacrylamide/urea gel. 4 µl sequencing reaction (sec. 2.2.3.11.4) were applied to obtain a sequence ladder. The gel run was performed for 1.5 hours at 2 kV. In the following the gel was dried and exposed to an X-ray film overnight. The cDNA was visualized by the Bioimager FLA-3,000 (Fujifilm, Japan).

2.2.3.11.4 Sequencing reaction

To synthesize a sequence ladder for toe printing analysis, a sequence reaction was carried out using the Thermo Sequenase cycle Sequencing Kit (USB, USA) according to the manufacturer's instructions. Therefore, a mastermix containing the labeled primer was prepared as the following:

template plasmid (100 ng/µl)	1	µl
γ-P^{32}-primer	6	µl
buffer (1 mg/ml)	2	µl
Sequenase	7	µl
H_2O	2	µl

Four times 4 µl mastermix were added to 4 µl nucleotide termination mix each containing one kind of dideoxy-NTPs. The reaction was performed in a thermocycler (Biometra, Germany) programmed as described below:

denaturating	96°C	60 s	
denaturating	96°C	30 s	
annealing	50°C	30 s	40 cycles
elongation	72°C	2 min	

The reaction was stopped by the addition of 4 µl formamide stop solution and applied to an 8% polyacrylamide/urea gel.

2.2.4 Biochemical methods

2.2.4.1 β-Galactosidase activity assays

To monitor expression activities of genes, the specific β-galactosidase activity of a culture containing the gene's promoter fused to a *lacZ* gene was determined by a modified assay described by Miller (1992).

The OD_{600} of an overnight culture was measured. Directly from the cuvette 200 µl cells were filled into two separate glass tubes for duplicates. Lysis was performed by the addition of one drop 0.1% SDS and two drops chloroform, mixing and incubation for 10 min at room temperature. In the following 1.8 ml Z-buffer were added. The reaction was started with 400 µl ONPG and stopped at an appropriate yellow coloration by 1 ml Na_2CO_3. The reaction samples were centrifuged for 2 min and the supernatant was measured by a microtiter plate reader at an OD of 405 nm.

$$\text{specific activity} = OD_{405} \cdot 6.75 \cdot (OD_{600} \cdot \Delta t \cdot V)^{-1}$$

specific activity	... [µmol cleaved substrate/(min · mg protein)] or [U · mg protein]
OD_{405}	... optical density of stopped reaction
6.75	... extinction coefficient of cleaved ONPG [µmol/(min · mg)]
OD_{600}	... optical density of bacterial culture
V	... used culture volume [ml]
Δt	... period from start (addition of ONPG) to end (addition of Na_2CO_3) of enzyme reaction

Z-buffer (1 x): 100 mM sodium phosphate buffer pH 7.0; 10 mM KCl; 1 mM $MgSO_4$

2.2.4.2 Preparation of whole cell extracts

The optical density of overnight cultures was adjusted and a 300 µl aliquot was withdrawn from each culture. The cells were harvested by centrifugation and resuspended in 150 µl 1 x sample buffer. The samples were incubated for 5 min at 95°C (Sambrook, *et al.* 1989). In case the cell extract showed viscosity, 1.5 µl benzonase (Merck, Germany) were added and the sample was incubated for 1 h at 37°C. Generally, three to five µl whole cell extract were applied on SDS polyacrylamide gels. When the target protein was present in lower amounts, the volume of the loaded sample was increased.

1 x sample buffer: 60 mM TRIS-HCL pH 6.8, 2% SDS; 10% glycerol; 3% DTT; 0.02% bromophenol blue

2.2.4.3 SDS-PAGE analysis

SDS polyacrylamide gel electrophoresis (Laemmli 1970) allows the separation of proteins according to their size in a polyacrylamide gel matrix. The addition of the anionic detergent

SDS denatures proteins and charges them negatively, which allows electrophoretic separation without the influence of protein charge or conformation.

In this study, SDS gel electrophoresis was carried out with vertical electrophoresis chambers Mini-Protean II (BioRad, USA). Gels were composed of a stacking and separating gel, prepared with different polyacrylamide concentrations.

These different concentrations as well as the different pH values of the stacking and the separating gel help to focus the proteins of the samples at the border of the two gels. This allows more efficient protein separation.

A 15% SDS separating gel contained (Sambrook, *et al*. 1989):

separating gel buffer pH 8.8	2.5	ml
acryl/bisacrylamide (30%)	5.0	ml
aqua bidest	2.5	ml
TEMED	50	µl
APS (10%)	50	µl

separating gel buffer (4 x): 1.5 M TRIS-HCl pH 8.8; 4% SDS

After polymerization of the separating gel, the stacking gel was prepared of the following solutions:

stacking gel buffer (4 x)	2.5	ml
acryl/bisacrylamide (30%)	1.1	ml
aqua bidest	6.5	ml
TEMED	40	µl
APS (10%)	80	µl

stacking gel buffer (4 x): 0.5 M TRIS-HCl pH 6.8; 4% SDS

Samples were incubated in 1 x SDS sample buffer for 5 min at 95°C for denaturation and loaded onto the gel. SDS-PAGE was performed at a constant current of 25 mA per gel and maximum voltage.

Subsequently, the gels were either stained in Coomassie™ Brilliant Blue G250 for one hour or prepared for Western blot analysis (sec. 2.2.4.6). Gels stained with Coomassie™ Brilliant Blue were destained by shaking in destaining solution for at least two hours.

To determine the molecular weight of proteins, 5 µl of markers were used as described above (sec. 2.2.4.5).

SDS running buffer: 33 mM TRIS-HCl pH 8.3; 192 mM glycine; 0.1% SDS
destaining solution: 30% methanol; 10% acetic acid

2.2.4.4 TRICINE-PAGE for low molecular weight proteins

To separate proteins of low molecular weight, samples were applied to TRICINE-PAGE as described previously (Schagger 2006). A typical 20% separating gel was prepared as the following:

3 x gel buffer	3.0	ml
glycerol (100%)	1.0	ml
acryl/bisacrylamide (40%)	4.5	ml
aqua bidest	0.5	ml
TEMED	6.0	µl
APS (10%)	60.0	µl

A typical stacking gel was composed of:

3 x gel buffer	1.6	ml
acryl/bisacrylamide (30%)	0.8	ml
aqua bidest	3.8	ml
TEMED	7.5	µl
APS (10%)	75.0	µl

Electrophoresis was carried out using cathode buffer for the cathode chamber and anode buffer filled in the anode chamber. A voltage of 30 mA was applied per gel.

3 x gel buffer: 3 M TRIS base, 1 M HCl, 0.3% SDS
cathode buffer: 0.1 M TRIS base, 0.1 M TRICINE, 0.1% SDS
anode buffer: 0.1 M TRIS base, 0.0225 M HCl

2.2.4.5 Molecular weight marker for SDS polyacrylamide gel electrophoresis (SDS-PAGE)

To measure the molecular weights of proteins separated by SDS-PAGE, "Protein Ladder 10-200 kDa" (Fermentas) marker with the following molecular weights (in kDa) was used: 116, 66.2, 45, 35, 25, 18.4 and 14.4.

If SDS-PAGE was followed by a Western blotting, "PageRuler Prestained Protein Ladder" by Fermentas was applied with molecular weights in kDa as followed: 170, 130, 100, 72, 55, 40, 33, 24, 17 and 11.

2.2.4.6 Western blot analysis

Proteins, which have been separated by SDS-PAGE, can be detected by antibodies and are therefore transferred onto a nitrocellulose membrane (Towbin, *et al*. 1979). Blotting was performed using the "Mini-protean II" Western blot cell (BioRad, USA). The membrane, activated with methanol, was placed face-to-face to the gel. These were then enclosed by whatman paper and fiber pads soaked in transblot buffer in the blotting gasket. The blot cell was placed into the tank filled with transblot buffer, with the membrane facing the anode.

Proteins were transferred for one hour at 100 V while cooling and maximum current was allowed. Subsequently, the membrane was incubated in 5% TBSTM buffer for 2 hours at room temperature or overnight at 4°C to saturate non-specific protein interactions. After removal of TBSTM, the membrane was incubated with the primary polyclonal antibody diluted in 10 ml TBSTM which was performed for one hour at room temperature. Thereafter, the membrane was washed three times with TBST for 10 min and incubated with the secondary antibody for one hour. When using anti-rabbit or anti-mouse alkaline phosphatase (AP) conjugate was used, the blot membrane was washed with TBST and AP buffer, for 10 min after each incubation step. To develop the blot a staining solution based on AP buffer was applied which contained NBT and BCIP. The reaction was stopped by *aqua bidest* and the stained proteins on the membrane was documented by digital photography. The membrane was stored protected from light.

If the membrane was incubated with anti-rabbit horse radish peroxidase (HRP) conjugate, the blot was washed three times with TBST for 10 min. Thereafter, the membrane was incubated with Pierce ECL Western blotting substrate (Thermo Scientific, USA) for 5 min. The substrate was removed and the blot was exposed to X-ray film for 1 to 15 min. The film was developed using a developing machine.

transblot buffer: 25 mM TRIS, 192 mM glycine; 20% methanol (v/v)
TBST: 20 mM TRIS pH 7.5; 150 mM NaCl; 0.05% TWEEN-20
TBSTM: TBST; 5% non-fat dry milk.
AP buffer: 100 mM TRIS pH 9.5; 100 mM NaCl; 5 mM $MgCl_2$
AP staining solution: 10 ml AP buffer; 33 µl NBT (100 mg/ml in 70% DTT); 33 µl BCIP (50 mg/ml in DMF)

2.2.4.7 Protein overexpression and purification

To study the interaction of YmoA, H-NS and the YmoA-H-NS heteromer with DNA or RNA molecules, these proteins were overexpressed and purified.

2.2.4.7.1 Overexpression of YmoA

For overexpression of YmoA, the *E. coli* strain KB4 (BL21 Δ*hns*Δ*stpA*Δ*hha*) was transformed with pAKH77 encoding an N-terminal Strep-tagged YmoA protein. The deletion of *hns*, *stpA* and *hha* in KB4 prevents the heteromerization of YmoA with *E. coli* homologs (Nieto, *et al.* 2002) and allows purification of the homologous *Yersinia* protein. Overexpression was performed as described by the manufacturer (IBA GmbH, Germany)

500 ml LB supplemented with carbenicillin were inoculated 1:50 with an overnight culture of KB4 pAKH77 and incubated at 37°C. To induce P_{tet}::*ymoA* expression, 50 µl of an AHT solution were added at an OD_{578nm} of 0.6. Cultivation was continued for additional four hours. Thereafter, cells were harvested at 6,000 rpm for 5 min in an SLA-3000 rotor using a Sorvall centrifuge.

AHT solution: 2 mg AHT dissolved in 1 ml DMF

2.2.4.7.2 Overexpression of H-NS

To overexpress H-NS, the C-terminal H-NS-His_6 producing strain KB4 pAKH11 was cultivated overnight at 37°C in LB supplied with kanamycin. The next day, 500 ml LB containing kanamycin was inoculated 1:100 with the preculture and incubated at 37°C. At an OD_{578nm} between 0.4 and 0.6, 2 mM IPTG were added to induce protein production. Cells were harvested after an additional cultivation for three hours by centrifugation at 6,000 rpm for 5 min with a SLA-3000 rotor in a Sorvall centrifuge.

2.2.4.7.3 Preparation of cell extracts

For cell disruption, the frozen pellets were thawed and resuspended in the appropriate buffer. To purify Strep-YmoA, pelleted cells of the 500 ml overexpression culture of KB4 pAKH77 were resuspended in 5 ml buffer W. Cells of a 500 ml H-NS-His_6 overexpression culture KB4 pAKH11 were dissolved in 5 ml lysis buffer.

Protein extraction of the cell suspension was performed by mechanical cell lysis using a French press (Aminco, USA) as described by the manufacturer. Cell debris was removed by centrifugation of the cell lysate at 14,000 rpm for 30 min at 4°C in a Sigma 3-18 K (Germany). The centrifugation was repeated with the supernatant.

buffer W (washing buffer): 100 mM TRIS-HCl, 150 mM NaCl, 1 mM EDTA, pH 8
lysis buffer: 50 mM TRIS-HCL pH 8; 300 mM NaCl

2.2.4.7.4 Purification of YmoA protein

Purification of Strep-YmoA was carried out using a PolyPrep column (Biorad, USA) filled with a column volume (CV) of 2 ml Strep-Tactin® Superflow® high capacity (IBA GmbH, Germany). The purification was performed according to the manufacturer's instructions.

After equilibration of the column with 2 CV's buffer W, the supernatant (sec. 2.2.4.7.3) was applied. To remove unspecifically bound protein from the column, it was washed five times with 1 CV buffer W. Elution of Strep-YmoA was performed by applying six times of 0.5 CV elution buffer. Washing and elution fractions were collected in clean tubes and samples were taken for SDS-PAGE analysis.

buffer E: 100 mM TRIS-HCl, 150 mM NaCl; 1 mM EDTA; 2.5 mM desthiobiotin; pH 8

2.2.4.7.5 Purification of the H-NS protein

His-tagged H-NS was purified by applying the supernatant (sec. 2.2.4.7.3) to a PolyPrep column (Biorad, USA), which was filled with a column volume of 2 ml Ni-NTA agarose (Qiagen, Germany) and equilibrated with 5 ml lysis buffer.

Unspecifically bound protein was eluted in two steps. The column was washed twice with 5 ml washing buffer 1 containing 40 mM imidazole. In the following the column was washed three

times with 5 ml washing buffer 2 with an imidazole concentration of 60 mM to achieve more intensive removal of contaminating protein.

His-tagged H-NS was eluted from the column by applying one CV elution buffer for five times. All fractions were collected in clean tubes and samples were taken to analyze the protein content via SDS-PAGE.

washing buffer 1: 50 mM TRIS-HCl pH 8, 300 mM NaCl, 40 mM imidazole
washing buffer 2: 50 mM TRIS-HCl pH 8, 300 mM NaCl, 60 mM imidazole
elution buffer: 50 mM TRIS-HCl pH 8, 300 mM NaCl, 250 mM imidazole

2.2.4.8 Measurement of the protein concentration

The protein concentration of purified proteins was determined using the Protein Assay Kit II (BioRad) or Coomassie™ Protein Assay Reagent (Bradford 1976). The procedure was followed according to the manufacturer's instructions.

2.2.4.9 RNA-Protein electrophoretic mobility shift assay (EMSA)

The interaction of YmoA and H-NS homomers with the CsrC RNA was studied by incubation of *in-vitro* transcribed CsrC RNA with increasing protein amounts. Therefore, the reaction was composed of the following:

ivT CsrC	13.5	pmol
5S RNA (control)	13.5	pmol
10 x RNA binding buffer	0.4	µl
protein	6.0	µl
Ribolock RNase inhibitor	0.1	µl
filled to 10 µl with H_2O		

The mixture was incubated for 30 min at 25°C and subsequently applied to an 8% polyacrylamide gel in PerfectBlue™ Twin chambers (Peqlab, Germany). RNA and RNA-protein complexes were separated for 2.5 hours at 70 V. The gel was stained with SYBR® Green II (Invitrogen, USA) and photographed by a gel documentation system (BioRad, USA).

RNA binding buffer (10 x): 0.1 M TRIS-HCl pH 7.5, 0.1 M $MgCl_2$, 1 M KCl, 75% glycerol, 0.03 M DTT

3 Results

3.1 YmoA activates early infection virulence factor invasin through a complex regulatory network

During the early infection phase, *Yersinia pseudotuberculosis* expresses the outer membrane protein invasin which most efficiently helps the bacterium to invade into M-cells. Production of invasin in response to environmental signals is mediated by the MarR-type regulator RovA. The synthesis of RovA itself is the result of a complex regulatory network comprising the global regulator H-NS, the LysR regulatory protein RovM, the Carbon storage regulator (Csr) system and the two-component system UvrY-BarA. The nucleoid-associated protein YmoA was identified during a gene bank screen to induce expression of a chromosomal *rovA-lacZ* fusion in *Y. pseudotuberculosis* strain YP38. This work analyzes, how YmoA affects RovA production by regulating components of the regulatory cascade of *rovA* transcription, in particular the Csr system.

3.1.1 YmoA activates *rovA* expression by downregulating RovM

Previously, Nieto *et al*. (2002) demonstrated, that the nucleoid-associated proteins YmoA and H-NS are able to form heterodimers. Furthermore, transcription of the *rovA* gene was shown to be regulated by H-NS which binds to an AT-rich stretch upstream of both *rovA* promoters (Heroven, *et al*. 2004). To analyze whether YmoA controls *rovA* expression through YmoA-H-NS complex formation which interferes with H-NS oligomerization, the RovA synthesis was monitored in the presence or absence of functional H-NS in *Y. pseudotuberculosis* wild type strain YPIII and a *ymoA* mutant strain YP50. Since H-NS mutations have been shown to be lethal in *Y. pseudotuberculosis,* a dominant-negative N-terminal H-NS fragment (H-NS') encoded on a plasmid (pAKH31) was overexpressed in the *Y. pseudotuberculosis* wild type strain YPIII and *ymoA*-deficient strain YP50. The N-terminal H-NS fragment (H-NS'), missing the DNA-binding domain of H-NS, dimerizes with functional H-NS monomers. This leads to non-functional H-NS'/H-NS dimers with impaired DNA-binding function that are unable to silence *rovA* expression (Heroven, *et al*. 2004).

Whole cell extracts of the *ymoA* mutant strain YP50 contained lower amounts of the RovA protein compared to samples of wild type strain YPIII. Inactivation of the H-NS-DNA-binding activity by introducing p*hns*' into the wild type strain YPIII resulted in elevated levels of RovA. RovA levels of a *Y. pseudotuberculosis* strain expressing non-functional H-NS' in the absence of *ymoA* (YP50 p*hns*') were significantly reduced in comparison to the parent strain producing inactive H-NS' (YPIII p*hns*') and the *Y. pseudotuberculosis* wild type strain YPIII (Fig. 13).

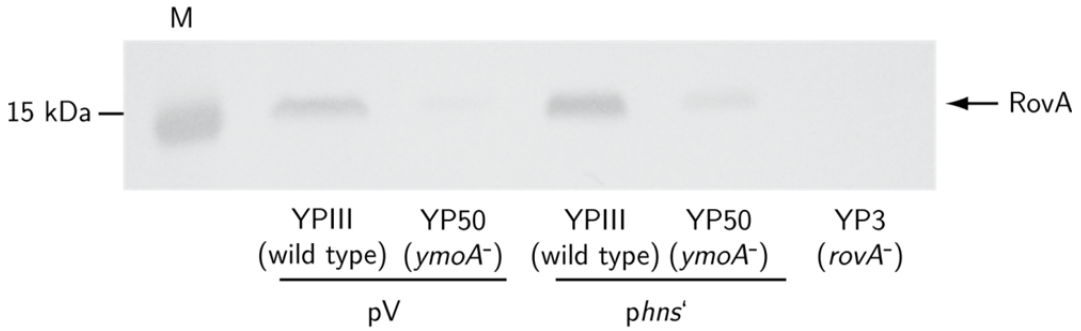

Fig. 13. YmoA and H-NS independently regulate RovA synthesis. Whole cell extracts were prepared from overnight culture samples at 25°C of *Y. pseudotuberculosis* wild type strain YPIII and *ymoA* mutant strain YP50 containing the empty vector pV (pAKH32) or p*hns*' (pAKH31). Proteins were separated by 15% SDS gel electrophoresis and immunoblotted using a polyclonal anti-RovA antibody. For control of unspecific antibody detection whole cell extract of the *rovA* mutant strain YP3 was analyzed. A protein molecular weight marker was loaded on the left. The RovA protein is marked by an arrow.

Deletion of *ymoA* in *Y. pseudotuberculosis* repressed RovA synthesis whereas non-functional H-NS'-dimers induced RovA production. H-NS inactivation in a *Y. pseudotuberculosis ymoA* mutant did not restore wild type levels of RovA protein. This indicates that YmoA regulation of RovA synthesis does not occur through inactivation of H-NS-mediated silencing of *rovA* transcription.

Despite H-NS, also the LysR regulator RovM represses *rovA* transcription. RovM interacts with a short site upstream of the *rovA* promoter P1 (Heroven and Dersch 2006; Lawrenz and Miller 2007). To analyze whether YmoA affects *rovA* gene transcription through RovM, expression of a plasmid-encoded *rovA-lacZ* fusion (pAKH47) was determined in *Y. pseudotuberculosis* wild type (YPIII), *ymoA* mutant (YP50), a *rovM* mutant (YP72) and a *ymoA*/*rovM*-deficient strain (YP73). β-galactosidase activity was monitored from overnight cultures and whole cell extracts were prepared to examine RovA protein levels. β-galactosidase activity of *rovA-lacZ* fusion in a *ymoA* mutant was reduced to about 50% of the wild type expression. In a *rovM* mutant strain, *rovA* expression was about twofold increased compared to the wild type independent whether YmoA was present or not (Fig. 14A).

Immunoblotting with an anti-RovA antibody confirmed this result and showed that RovA protein levels are downregulated in a *ymoA* mutant strain, whereas an increase of RovA production was observed in whole cell extracts of a *rovM* and a *rovM*/*ymoA* mutant strain compared to the wild type strain. (Fig. 14B).

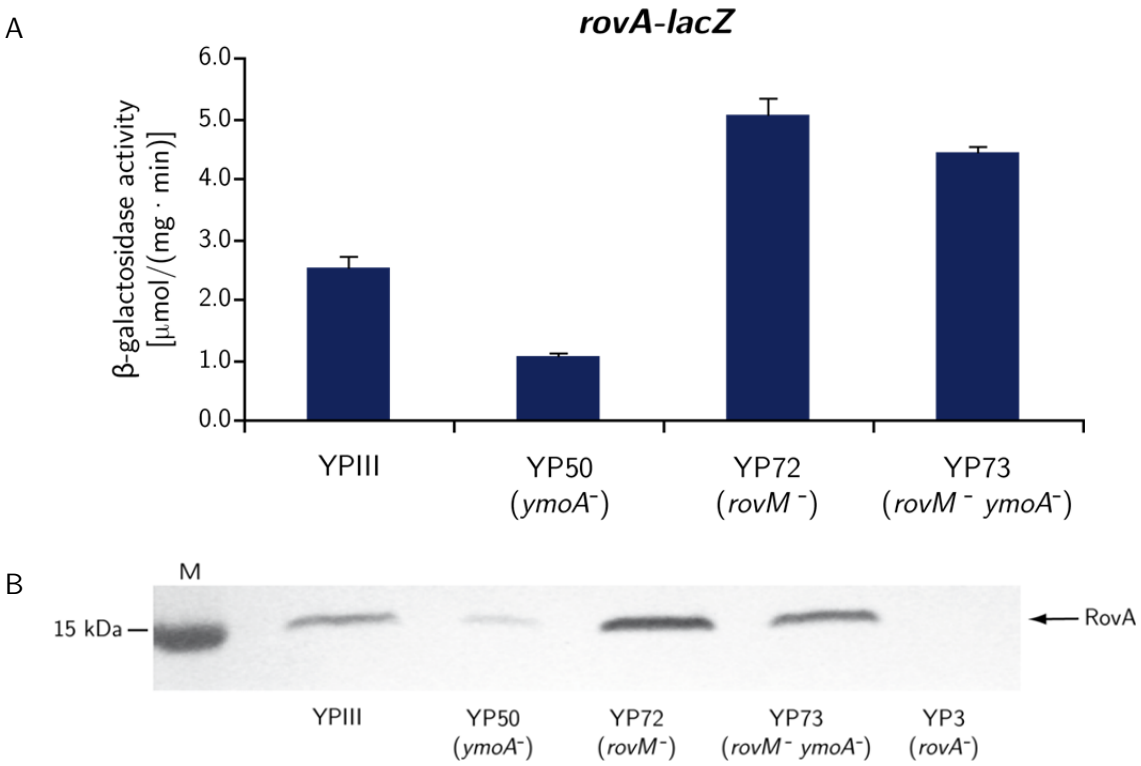

Fig. 14. YmoA activates *rovA* expression indirectly through RovM. A. To monitor *rovA* promoter activity, plasmid pAKH47 encoding a *rovA-lacZ* fusion was introduced into *Y. pseudotuberculosis* wild type strain YPIII, the *ymoA* mutant strain YP50, the *rovM* mutant strain YP72 and the *ymoA*/*rovM* double mutant strain YP73. β-galactosidase activity was measured from overnight cultures in LB medium at 25°C. The enzyme activity is given in µmol/(min · mg). Data show mean values ± standard deviation of three independent experiments, each performed in duplicate. B. Cultures of *Y. pseudotuberculosis* YPIII, YP50 (*ymoA*⁻), YP72 (*rovM*⁻) and YP73 (*ymoA*⁻/*rovM*⁻) were grown overnight at 25°C. Samples were withdrawn, the OD_{600nm} was adjusted and whole cell extracts were prepared. Using 15% SDS gel electrophoresis proteins were separated, transferred onto an Immobilon membrane and RovA was detected by immunoblotting with a polyclonal anti-RovA antibody. The molecular weight marker is loaded on the left and the RovA protein marked by an arrow.

The previous experiments demonstrated that YmoA induces RovA production at the transcriptional level. Absence of RovM derepressed *rovA* transcription in the presence and absence of YmoA indicating that YmoA regulates *rovA* expression upstream of RovM (Fig. 13). In addition, YmoA might affect RovA on the post-transcriptional level, since slightly lower amounts of the RovA protein were detectable in the *ymoA*/*rovM* double mutant compared to a *rovM* mutant although *rovA* transcription remained unaffected.

To determine whether YmoA regulates *rovA* expression by controlling RovM synthesis, the YmoA influence on a *rovM*'-'*lacZ* fusion (pAKH63) and on RovM protein levels was tested. To do so, the *rovM*'-'*lacZ* fusion plasmid was transformed in *Y. pseudotuberculosis* wild type (YPIII) and the *ymoA* mutant strain (YP50). To determine the effect of *ymoA* overexpression and complementation of the *ymoA* mutant, the *ymoA* expression plasmid (pAKH71) was also introduced into the wild type and the *ymoA*-deficient strain. β-galactosidase activity was measured from overnight cultures and samples for whole cell extracts were prepared to monitor the RovM protein amount within the cells. Expression of the *rovM*'-'*lacZ* fusion was

highly induced in a *ymoA* mutant strain in contrast to wild type whereas addition of the *ymoA*$^+$ plasmid fully complemented the *ymoA* deletion (Fig. 15A).

Analysis of RovM protein levels in the wild type and the *ymoA* mutant strain confirmed these data. Significantly higher levels of RovM were observed in the *ymoA* mutant strain and introduction of a *ymoA*$^+$ plasmid reduced RovM to levels found in the wild strain (Fig. 15B).

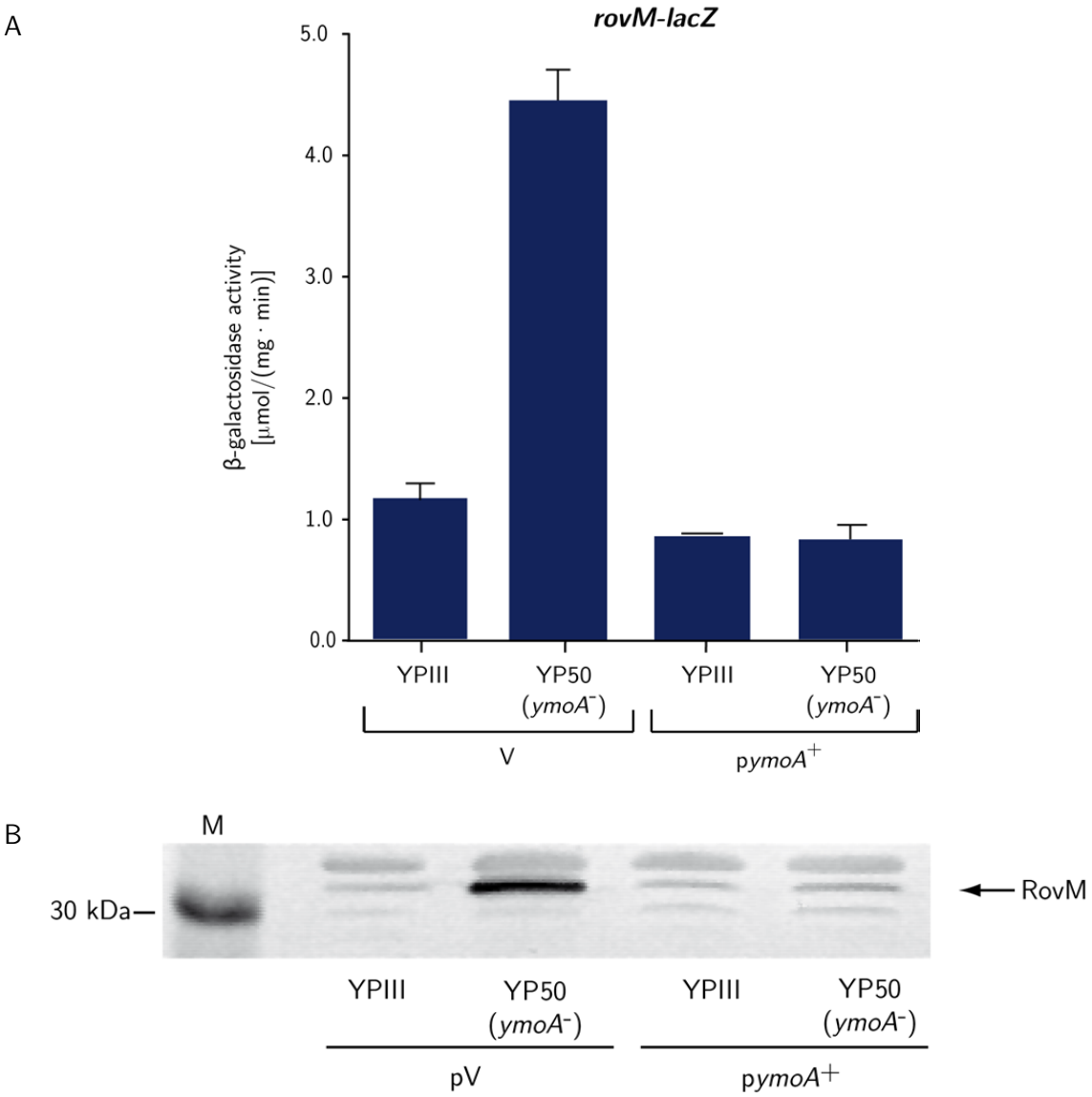

Fig. 15. YmoA represses *rovM*. A. The impact of YmoA on *rovM* gene expression was determined by measuring the β-galactosidase activity of a plasmid-encoded *rovM-lacZ* fusion (pAKH63) in *Y. pseudotuberculosis* YPIII and YP50 (*ymoA*$^-$) transformed with the empty vector pV (pAKH85) or p*ymoA*$^+$ (pAKH71). β-galactosidase activity was examined in overnight cultures in LB medium at 25°C and is given in µmol/(min · mg). The data represents the mean ± standard deviation of three independent experiments, each performed in duplicate. B. To monitor RovM protein levels whole cell extract were prepared from overnight culture samples of strains as described above. Proteins were separated by 12% SDS gel electrophoresis, transferred onto an Immobilon membrane by Western blotting and RovM was detected with polyclonal anti-RovM antibody. A molecular weight marker was loaded on the left and RovM is marked by an arrow.

These results suggest that YmoA negatively controls *rovM* expression in *Y. pseudotuberculosis*. Absence of YmoA results in a strong activation of RovM protein synthesis which in turn represses *rovA* transcription together with H-NS.

3.1.2 YmoA represses *rovM* expression through the Csr system

Synthesis of the LysR regulator RovM of *Y. pseudotuberculosis* is controlled by the Csr system in response to nutrient availability. The RNA-binding protein CsrA stimulates RovM protein production indirectly. This function is inhibited by two untranslated regulatory RNAs, CsrC and CsrB. Synthesis of these RNAs is strongly induced in complex medium but repressed in minimal medium (Heroven, *et al*. 2008).

To determine whether YmoA controls RovM synthesis by controlling *csrA* expression, a *csrA*'-'*lacZ* fusion (pKB63) was introduced into *Y. pseudotuberculosis* YPIII (wild type) and YP50 (*ymoA*$^-$). Complementation of the *ymoA* deletion and overexpression of *ymoA* was tested by introduction of the *ymoA*$^+$ plasmid pAKH71 into the *ymoA* mutant and the wild type strain, respectively. To measure *csrA* promoter activity, β-galactosidase activity of the promoter fusion was monitored and whole cell extracts were prepared to compare protein levels with an anti-CsrA antibody. Expression of the *csrA*'-'*lacZ* fusion was similar in the wild type and the *ymoA* mutant strain in the absence or presence of the *ymoA*$^+$ plasmid *(*Fig. 16A). Furthermore, CsrA levels in a *ymoA* mutant were similar or only slightly reduced relative to the *Y. pseudotuberculosis* wild type strain, and no significant changes were observed in the both strains in the presence of the *ymoA*$^+$ plasmid. (Fig. 16B). As a loss of *ymoA* in *Y. pseudotuberculosis* causes only mild effects on CsrA synthesis, YmoA seems to use a different mechanism to control RovM levels.

A

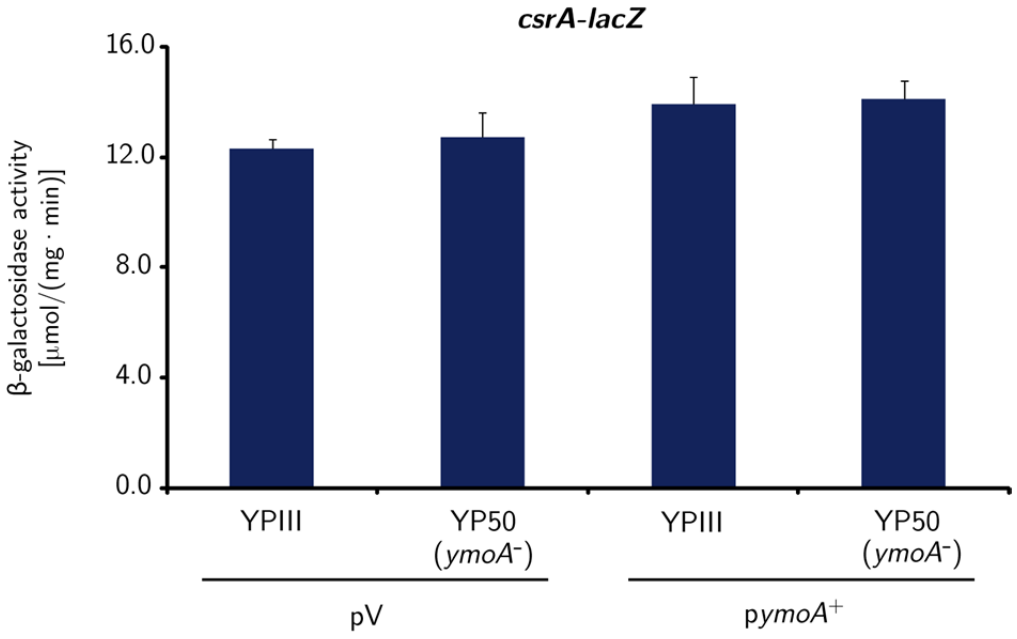

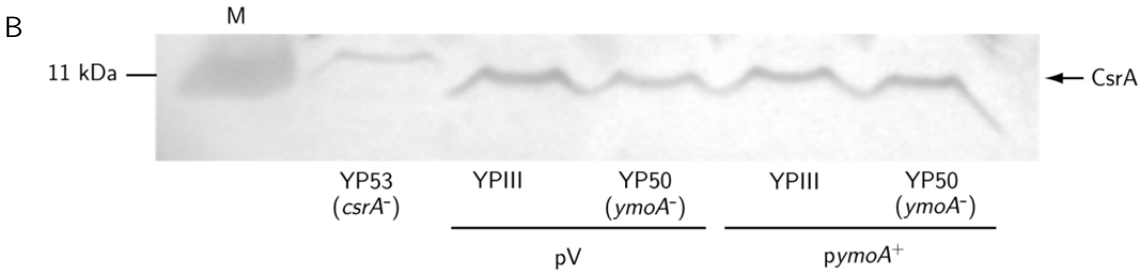

Fig. 16. CsrA synthesis is not influenced by YmoA. A. *csrA* gene expression was monitored by expression of a plasmid-encoded *csrA-lacZ* fusion (pKB63) in *Y. pseudotuberculosis* YPIII and YP50 (*ymoA*$^-$) harboring an empty vector pV (pAKH85) or p*ymoA*$^+$ (pAKH71). β-galactosidase activity was measured from overnight cultures, grown in LB medium at 25°C. The enzyme activity is given in µmol/(min · mg). The data shows the mean ± standard deviation of three independent experiments, each performed in duplicate. B. Cultures of *Y. pseudotuberculosis* YPIII and YP50 (*ymoA*$^-$) harboring the empty vector pV (pAKH85) or p*ymoA*$^+$ (pAKH71) were grown overnight. The OD_{600nm} of the samples withdrawn was adjusted and whole cell extracts were prepared. Using 18% TRICINE gel electrophoresis proteins were separated, transferred onto an Immobilon membrane and CsrA protein was detected by immunoblotting with a polyclonal anti-CsrA antibody. The molecular weight marker is loaded on the left and the CsrA protein is marked by an arrow.

The Csr RNAs CsrC and CsrB downregulate RovM synthesis in *Y. pseudotuberculosis* by binding multiple (9–18) copies of the CsrA protein to their AGGA motifs in the loop structures of the regulated RNAs. Thereby, they sequester CsrA from interacting with their target mRNAs and inhibit CsrA mediated activation of RovM production (Dubey, *et al*. 2005; Heroven, *et al*. 2008). For that reason, it was evaluated whether YmoA influences expression of *csrC* and *csrB*. Expression of transcriptional *csrC-lacZ* (pAKH97) and *csrB-lacZ* (pAKH88) fusions was analyzed in *Y. pseudotuberculosis* YPIII (wild type) and YP50 (*ymoA*$^-$). To complement the loss of *ymoA* in YP50, a plasmid carrying the *ymoA* gene (pAKH71) was introduced. The promoter activity was measured by determining the β-galactosidase activity of the reporter gene fusions in overnight cultures. Additionally, RNA samples were prepared and Northern blotting was performed with anti-CsrC and anti-CsrB probes to visualize the two Csr RNAs in the wild type and the *ymoA* mutant strain. Expression of the *csrC-lacZ* fusion was not significantly altered in the absence of the *ymoA* gene (Fig. 17A). Introduction of a *ymoA*$^+$ plasmid to the *ymoA* mutant had only a small effect (30% reduction) on *csrC* transcription. However, CsrC RNA concentrations were significantly reduced in a *ymoA* mutant strain in contrast to CsrC levels in the wild type strain. Complementation of the *ymoA* deletion led to an increase of CsrC levels, but did not fully restore CsrC concentrations to wild type levels (Fig. 17A).

In contrast, *csrB* transcription was 1.5fold induced in the *ymoA*-deficient strain relative to the wild type strain and *ymoA* was able to complement *csrB* expression although CsrB RNA levels were not fully restored (Fig. 17B).

A

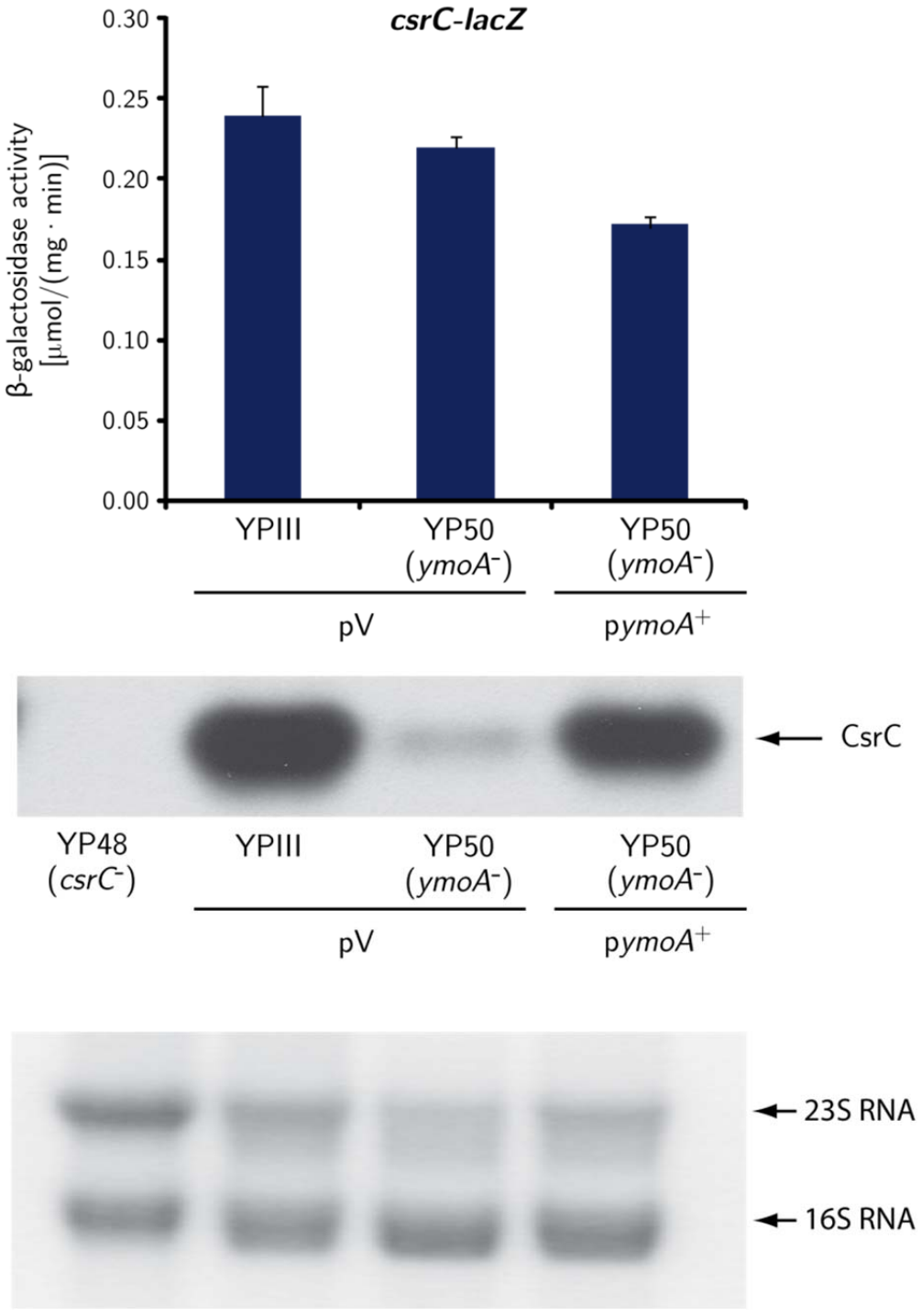
csrC-lacZ
β-galactosidase activity [μmol/(mg · min)]
0.30
0.25
0.20
0.15
0.10
0.05
0.00
YPIII
YP50 (ymoA⁻)
YP50 (ymoA⁻)
pV
pymoA⁺
CsrC
YP48 (csrC⁻)
YPIII
YP50 (ymoA⁻)
YP50 (ymoA⁻)
pV
pymoA⁺
23S RNA
16S RNA

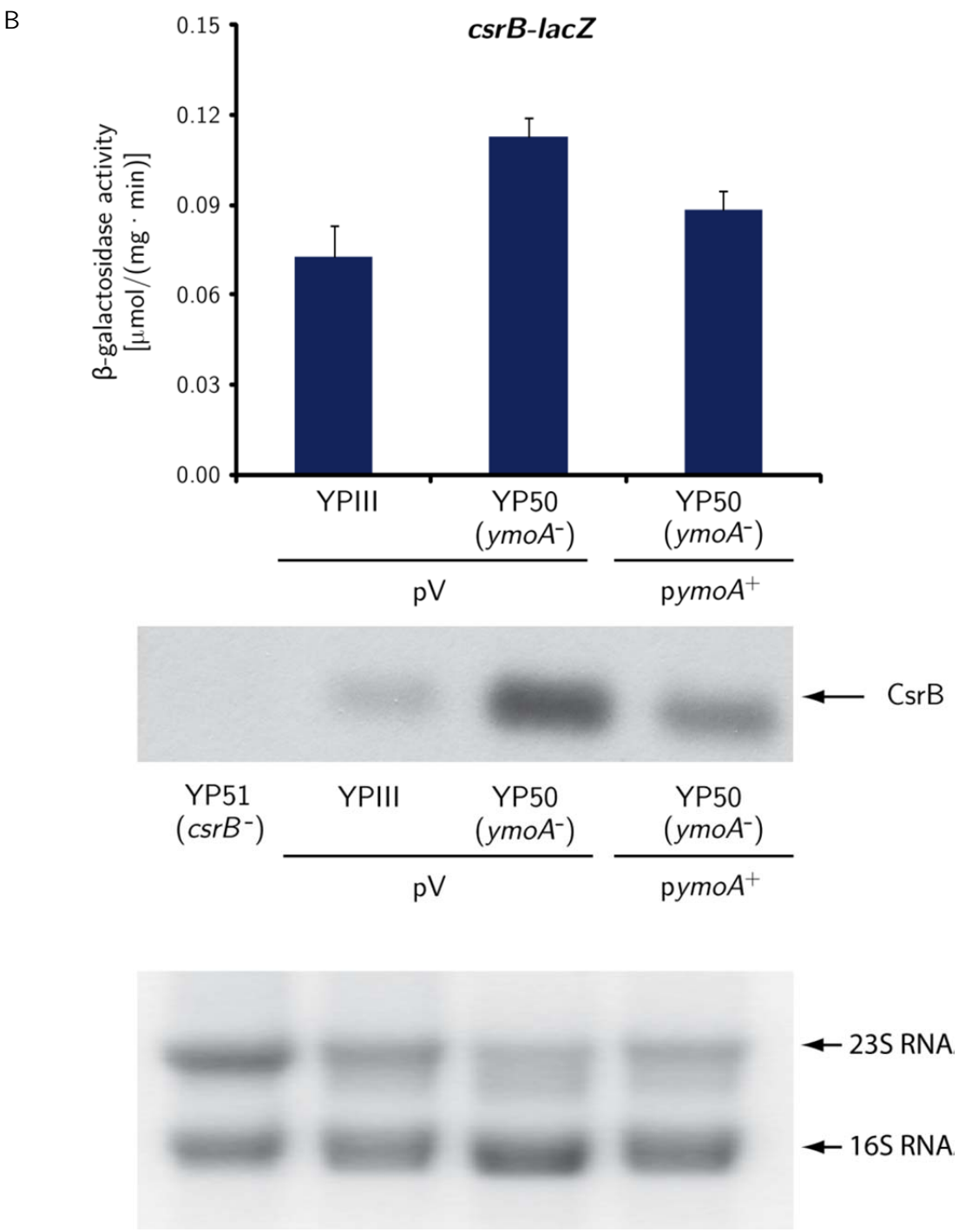

Fig. 17. YmoA activates CsrC synthesis and represses *csrB* expression. A plasmid-encoded *csrC-lacZ* fusion (pAKH97) or *csrB-lacZ* fusion (pAKH88) was used to determine the expression of (A) the *csrC* or (B) *csrB* gene in *Y. pseudotuberculosis* YPIII and YP50 (*ymoA*⁻) carrying an empty vector pV (pAKH85). For complementation plasmid p*ymoA*⁺ (pAKH71) was introduced into the *ymoA* mutant. β-galactosidase activity was examined in overnight cultures grown in LB medium at 25°C and is given in µmol/(min · mg). The data represent the mean ± standard deviation of three independent experiments, each performed in duplicate. Furthermore, overnight cultures of YPIII, YP50 (*ymoA*⁻), YP48 (*csrC*⁻) and YP51 (*csrB*⁻) were grown in LB medium at 25°C. Total RNA was prepared and used for Northern blot analysis. CsrC (A) and CsrB (B) RNAs were detected by hybridization using Dig-labeled specific DNA-probes. 23S and 16S rRNAs were used as loading controls.

Whereas *csrC-lacZ* transcription was independent of *ymoA*, CsrC RNA levels were strongly reduced in the absence of YmoA (Fig. 17A). This suggested that YmoA influences CsrC synthesis on the post-transcriptional level. Furthermore, YmoA affects CsrC and CsrB synthesis in an opposite manner. Most likely, YmoA controls expression of one RNA which in turn leads to counterregulation due to the negative autoregulatory control mechanism of CsrB and CsrC.

3.1.3 YmoA regulates CsrC synthesis independently of CsrB

Heroven *et al.* (2008) found, that CsrB in *Y. pseudotuberculosis* is activated by the UvrY/BarA two-component system in response to an unknown signal. For this reason it was analyzed whether YmoA regulates the expression of *uvrY* and *barA*. A *barA*'-'*lacZ* (pKB06) and a *uvrY*'-'*lacZ* (pKB07) fusion were introduced into *Y. pseudotuberculosis* YPIII (wild type) and YP50 (*ymoA*$^-$) and β-galactosidase activity was measured from overnight cultures. To test the influence of overexpression and complementation of *ymoA* on *uvrY* and *barA* expression, the plasmid p*ymoA*$^+$ (pAKH71) was also introduced into wild type and *ymoA* mutant. As shown in Fig. 18A, *barA-lacZ* expression was not influenced by loss or overexpression of *ymoA*. In contrast, *uvrY-lacZ* expression was stimulated to about 1.5fold of the wild type promoter activity in a *ymoA* mutant strain and expression of *ymoA* reduced *uvrY* transcription to about 60% (Fig. 18B). In summary, YmoA seems to activate transcription of *uvrY*, independently of *barA* expression (Fig. 18).

A

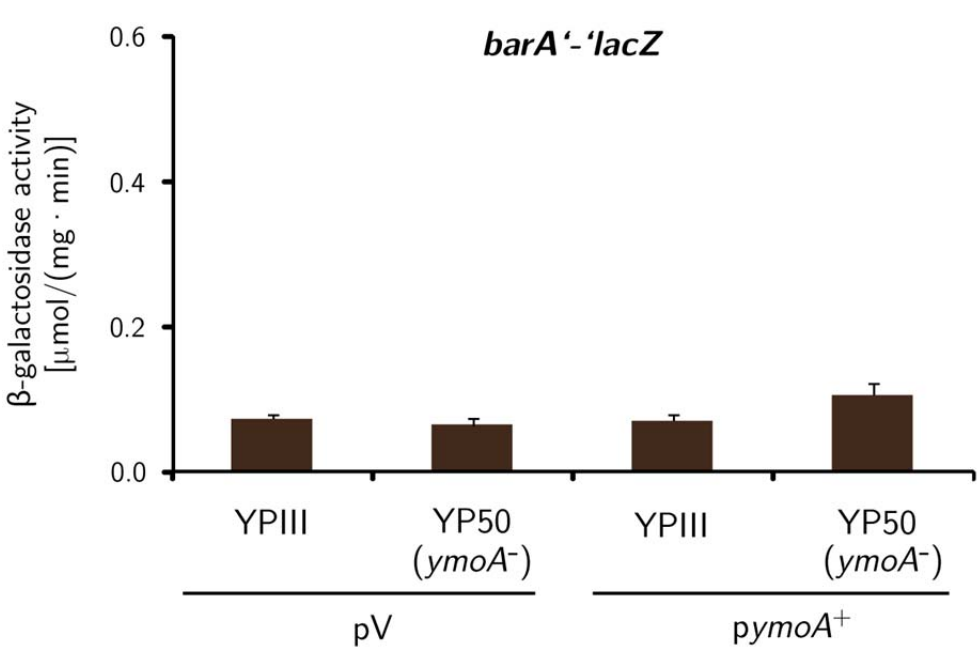

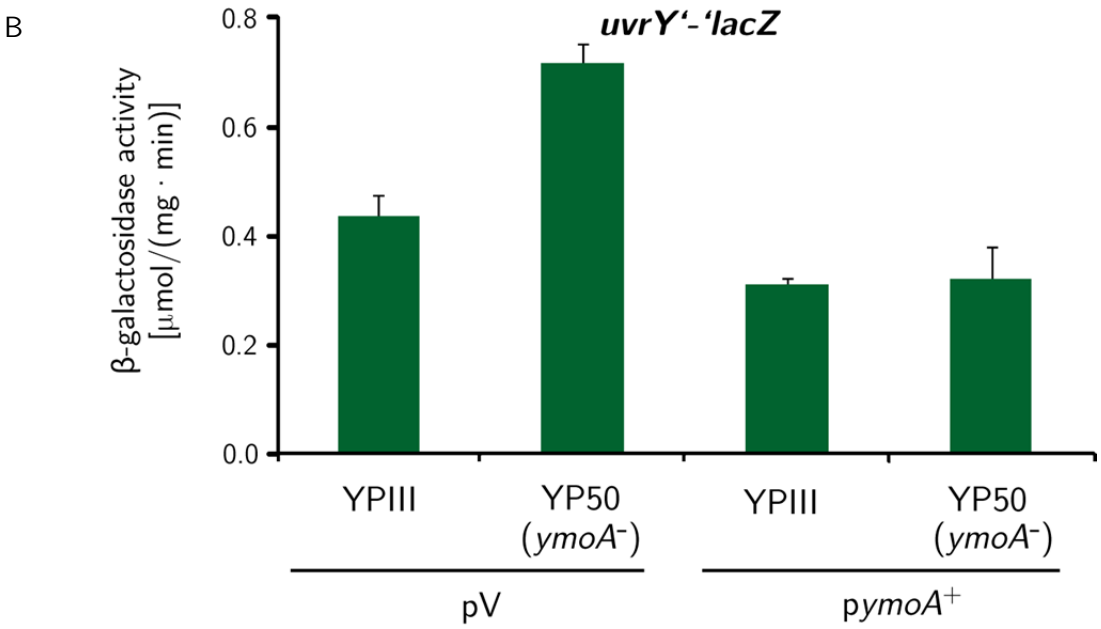

Fig. 18. YmoA represses *uvrY* expression. The β-galactosidase activity of a (A) *barA-lacZ* fusion (pKB06) or (B) *uvrY-lacZ* fusion (pKB07) in *Y. pseudotuberculosis* YPIII and YP50 (*ymoA*$^-$) harboring an empty vector pV (pAKH85) or p*ymoA*$^+$ (pAKH71) was measured from cultures grown overnight in LB medium at 25°C. The β-galactosidase activity is given in µmol/(min · mg). The data represent the mean ± standard deviation of three independent experiments, each performed in duplicate.

Next, it was important to determine whether YmoA-dependent CsrC synthesis occurs through upregulation of CsrB RNA levels, which is compensated by downregulation of *csrC* expression through an unknown negative control mechanism (Heroven, *et al*. 2008). RNA was prepared from *Y. pseudotuberculosis* YPIII (wild type) and YP50 (*ymoA*$^-$), YP69 (*csrB*$^-$) and YP75 (*ymoA*$^-$/*csrB*$^-$). To measure the outcome of the Csr control system the activity of a CsrA-dependent translational *rovM*'-'*lacZ* fusion (pAKH63) was determined in overnight cultures of these strains, and Western blot analysis was performed to detect RovM by immunoblotting.

CsrC RNA levels were reduced significantly in the *ymoA*-deficient strain compared to the wild type. Loss of the *csrB* gene leads to slightly higher CsrC RNA levels whereas CsrC synthesis in a *ymoA*/*csrB* double mutant strain is drastically repressed similar to a *ymoA* mutant strain (Fig. 19A).

In agreement with previous results, *rovM* expression and RovM synthesis are regulated in the opposite manner. Deletion of *ymoA* induces *rovM* transcription, whereas a loss of *csrB* had no effect. Expression of *rovM* in a *ymoA*/*csrB* double mutant was still strongly increased and significantly higher amounts of the RovM protein were detectable, similar to the *ymoA*-deficient strain (Fig. 19B).

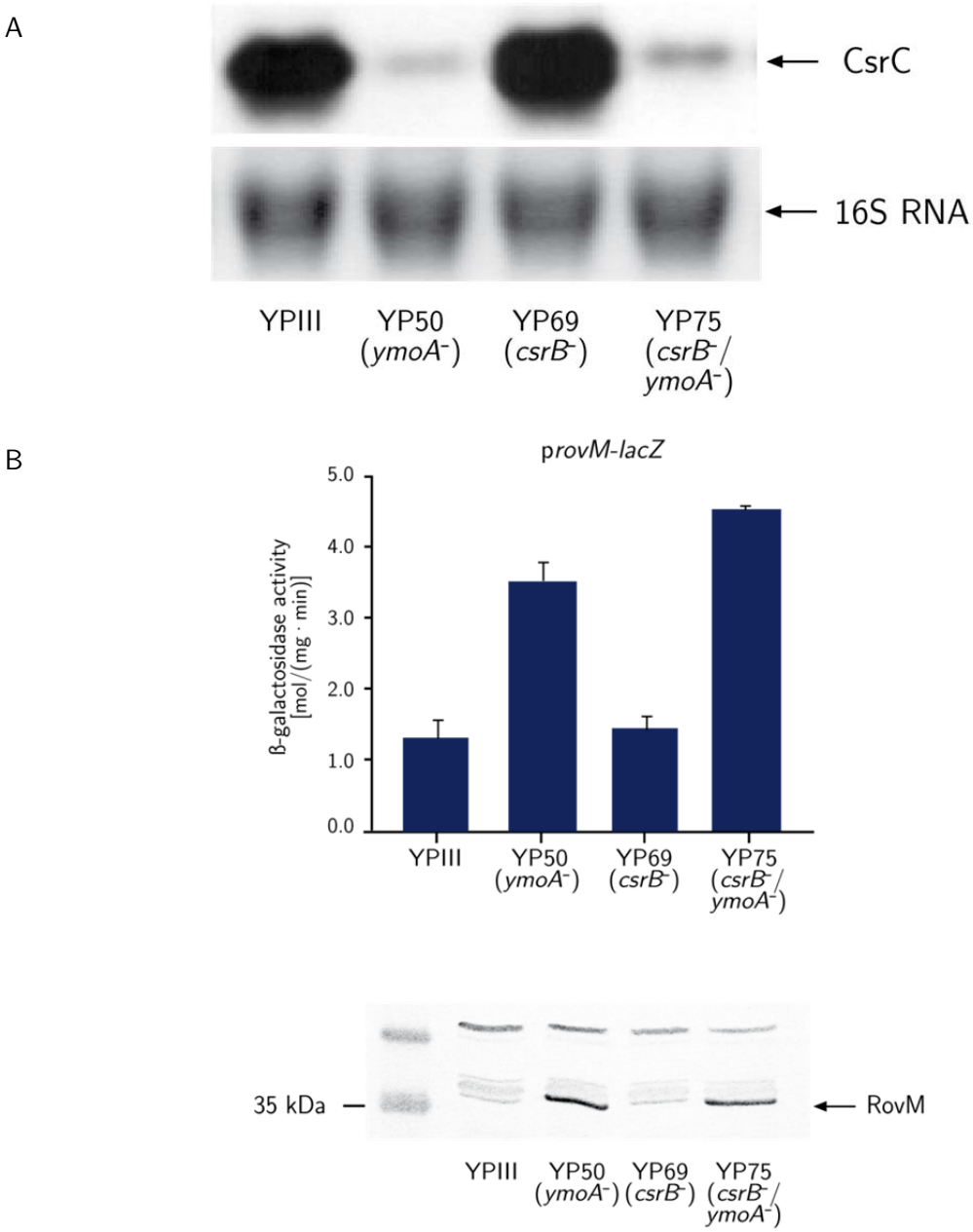

Fig. 19. YmoA regulates CsrC independently of CsrB. A. Total RNA was prepared from overnight cultures of *Y. pseudotuberculosis* YPIII, YP50 (*ymoA*⁻), YP69 (*csrB*⁻) and YP75 (*ymoA*⁻/*csrB*⁻) grown in LB medium at 25°C. The RNA was separated and transferred onto a membrane by Northern blotting. CsrC RNA was detected by a specific Dig-labeled probe. 16S rRNA was visualized as a loading control. B. *rovM-lacZ* expression was measured in YPIII, YP50, YP69 and YP75 harboring pAKH63. β-galactosidase activity was determined from overnight cultures in LB medium at 25°C and is given in µmol/(min · mg). The data represent the mean ± standard deviation of three independent experiments, each performed in duplicate.

Taken together, absence of YmoA led to a strong reduction of CsrC levels in a *csrB*⁺ and *csrB*-deficient strain. This demonstrated that YmoA activates CsrC production independently of *csrB* expression.

3.1.4 YmoA influences CsrC RNA stability

Previous experiments of this study (Fig. 17A) demonstrated that loss of *ymoA* does affect CsrC levels but not expression of a *csrC-lacZ* fusion. To analyze how YmoA influences CsrC RNA post-transcriptionally, a set of transcriptional *csrC-lacZ* fusions was constructed, harboring *csrC* fragments with varying portions of the *csrC* gene, i.e. up to position +4, +39, +61, +71, +81, +254 relative to the transcriptional start point. *Y. pseudotuberculosis* YPIII (wild type) and YP50 (*ymoA*$^-$) were transformed with p*csrC*(+4)-*lacZ* (pAKH103), p*csrC*(+39)-*lacZ* (pAKH106), p*csrC*(+61)-*lacZ* (pAKH107), p*csrC*(+71)-*lacZ* (pKB20), p*csrC*(+81)-*lacZ* (pAKH76) or p*csrC*(+254)-*lacZ* (pAKH104) and β-galactosidase activity was measured from overnight cultures (Fig. 20A). Transcription activity of *csrC* fused to the *lacZ* gene at positions +39, +61, +71, +81 and +254 in the wild type strain YPIII was reduced to circa 60-70% of *csrC*(+4)-*lacZ* with only the first 4 nucleotides of the *csrC* gene. Expression of *csrC* fused to *lacZ* at position +4, +39 and +61 was identical in the wild type and the *ymoA* mutant strain. In contrast, *csrC* expression of *csrC*(+71)-*lacZ*, *csrC*(+81)-*lacZ*, *csrC*(+254)-*lacZ* expression was about 50% lower in the absence of YmoA. (Fig. 20B).

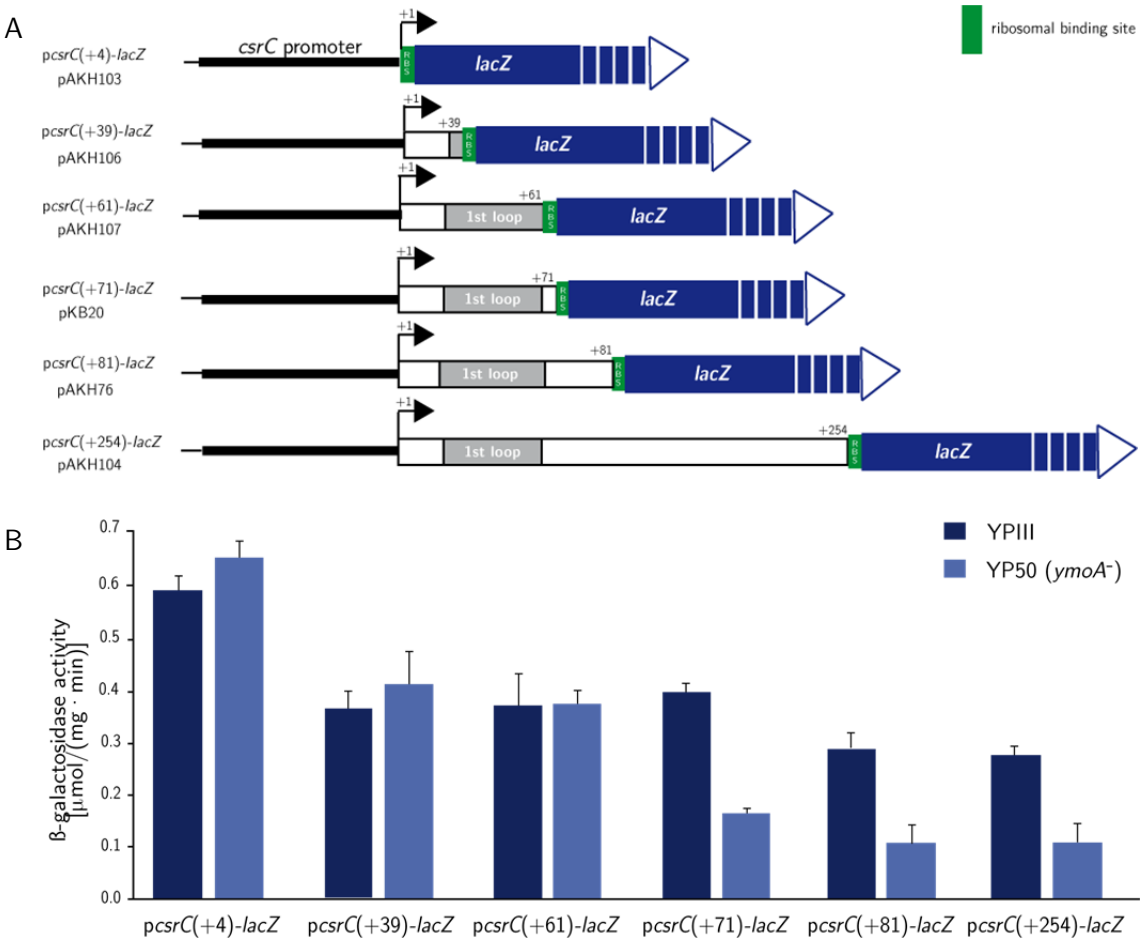

Fig. 20. YmoA activates expression of *csrC* 5' transcripts harboring the first 71 nt of the *csrC* gene. A. Constructed *csrC-lacZ* fusions with varying 3' ends of *csrC*. B. Transcription activity of p*csrC*(+4)-*lacZ* (pAKH103), p*csrC*(+39)-*lacZ* (pAKH106), p*csrC*(+61)-*lacZ* (pAKH107), p*csrC*(+71)-*lacZ* (pKB20), p*csrC*(+81)-*lacZ* (pAKH76) or p*csrC*(+254)-*lacZ* (pAKH104) in *Y. pseudotuberculosis* YPIII and YP50 (*ymoA*$^-$)

was determined by measuring β-galactosidase activity of overnight cultures grown in LB medium at 25°C. β-galactosidase activity is given in µmol/(min · mg). The data represent the mean ± standard deviation of three independent experiments, each performed in duplicate.

Extending 3' portions of the *csrC* gene lead to reduced expression of the *csrC-lacZ* fusions. This indicates that an increasing length of the CsrC transcripts might interfere with the translation of the *lacZ* gene. Transcription of at least 71 nucleotides of the *csrC* gene was required for YmoA-mediated activation of *csrC* expression whereas expression of *csrC-lacZ* fusion with shorter *csrC* portions was independent of YmoA.
Computational analysis of the CsrC RNA structure by Mfold (http://mfold.bioinfo.rpi.edu/cgi-bin/rna-form1.) revealed that the first 61 nucleotides of CsrC form a stem-loop structure (Fig. 21A). To test, whether this loop influences *csrC-lacZ* expression, a sequence from position +24 to +57 (Fig. 20A) relative to the transcription start was deleted from a *csrC*(+81)-*lacZ* fusion (pKB17) and introduced into *Y. pseudotuberculosis* YPIII (wild type) and YP50 (*ymoA*$^-$). Expression of *csrC*(+81)-*lacZ* fusion in a *ymoA* mutant was reduced to about 50% of the wild type level. The deletion of the +24 to +57 region also downregulated *csrC-lacZ* expression to circa 50% regardless of the presence or absence of the *ymoA* gene (Fig. 21B).

To confirm these results and to analyze whether the *csrC* fragment from position +24 to +57 is important for YmoA regulation and CsrC stability, CsrC and CsrC (Δ+24 to +57) RNA levels were monitored in the wild type and the *ymoA* mutant strain. To monitor CsrC RNA levels, plasmids carrying the wild type *csrC* gene (pKB59) or *csrC* with a deletion from positions +24 to +57 (pKB49) were introduced into *Y. pseudotuberculosis* YPIII (wild type) and YP50 (*ymoA*$^-$). In agreement to the *csrC-lacZ* expression data, significantly lower levels of CsrC RNA were found when nucleotides +24 to +57 relative to the transcription start were deleted. In the *ymoA* mutant, the overall concentration of the CsrC and the CsrC (Δ+24 to +57) RNA was significantly reduced, whereby amounts of the CsrC RNA were slightly higher than that of the deletion variant (Fig. 21C).

A

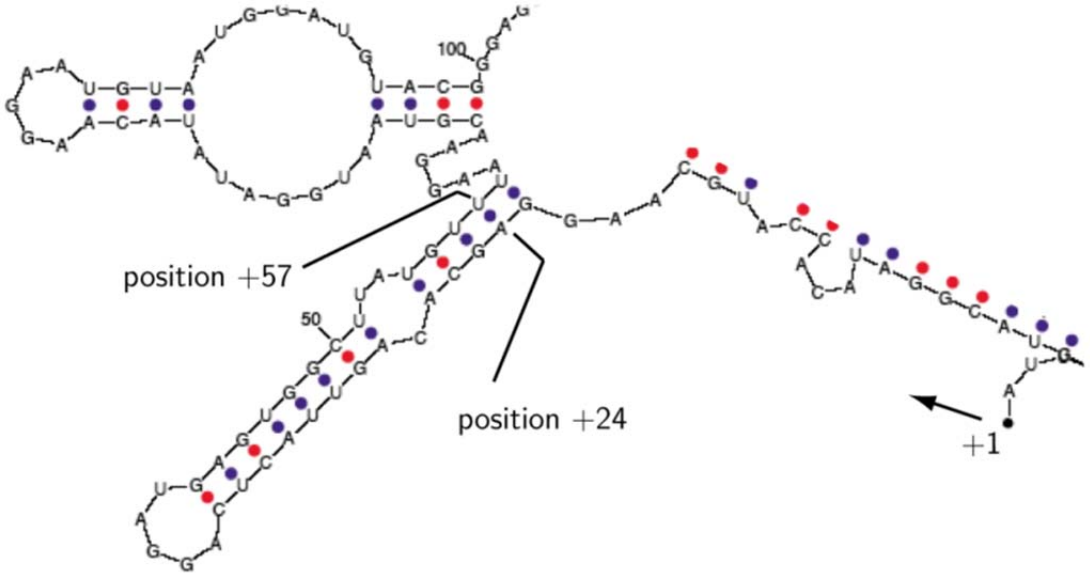
position +57
position +24
+1
50
100

B

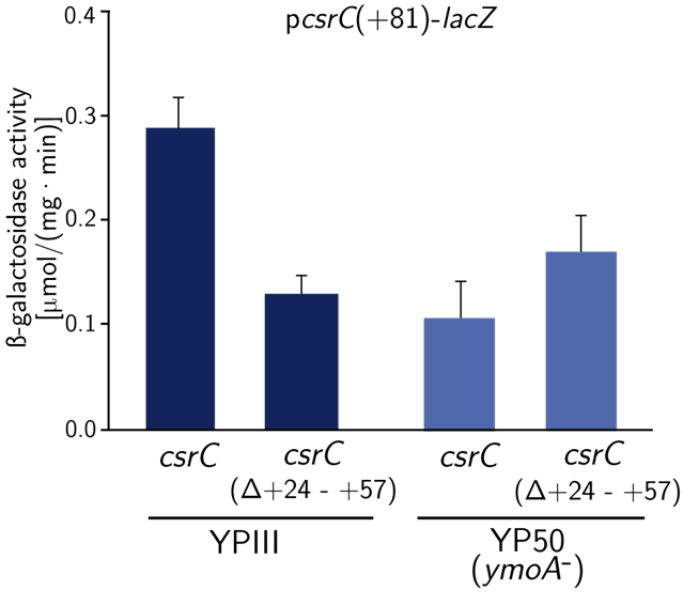
pcsrC(+81)-lacZ
ß-galactosidase activity
[µmol/(mg · min)]
0.4
0.3
0.2
0.1
0.0
csrC
csrC
(Δ+24 - +57)
csrC
csrC
(Δ+24 - +57)
YPIII
YP50
(ymoA-)

C

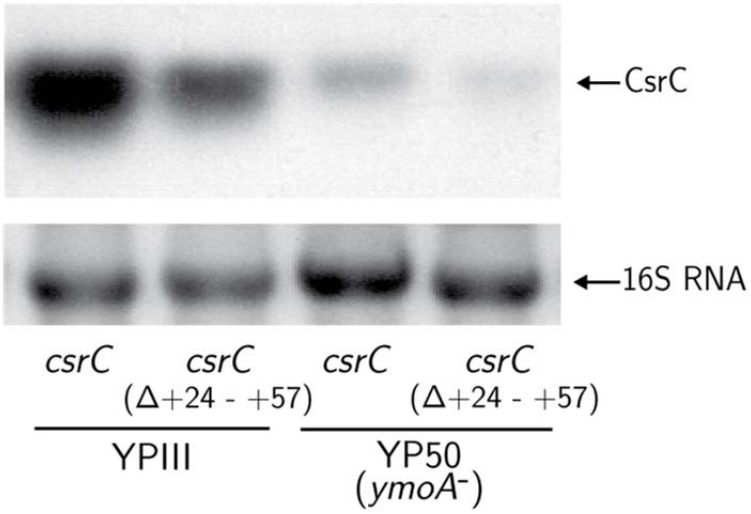
CsrC
16S RNA
csrC
csrC
(Δ+24 - +57)
csrC
csrC
(Δ+24 - +57)
YPIII
YP50
(ymoA-)

Fig. 21. Deletion of the first secondary loop formation in the CsrC RNA destabilizes CsrC synthesis. A. Secondary structure prediction of CsrC from nucleotide +1 to +102 generated by Mfold (http://mfold.bioinfo.rpi.edu/cgi-bin/rna-form1.cgi). The transcription start (+1) and positions 24 and 57, which represent the 5' and 3' end of the deletion, are indicated. B. β-galactosidase activity was measured in overnight cultures at 25°C of *Y. pseudotuberculosis* YPIII and YP50 (*ymoA*$^-$) carrying a *csrC*(+81)-*lacZ* (pAKH76) or *csrC*(+81; Δ +24 - +57)-*lacZ* (pKB17) fusion. Enzyme activity is given in µmol/(min · mg). The data represent mean values ± standard deviation of three independent experiments, each performed in duplicate. C. For Northern blot analysis, total RNA was prepared from overnight cultures of *Y. pseudotuberculosis* YPIII and YP50 (*ymoA*$^-$) harboring *csrC*$^+$ (pKB59) and *csrC*(Δ+24 - +57) (pKB49) plasmids. Total RNA was separated and transferred onto a Nytran membrane. CsrC was detected with specific Dig-labeled DNA probe.

This demonstrated that formation of the first stem loop of CsrC RNA enhance RNA synthesis, most likely by promoting a stable RNA structure. Although expression of the CsrC (Δ+24 to +57) RNA is identical in the wild type and the *ymoA* mutant, intracellular RNA concentrations are still somewhat reduced in the absence of YmoA. This implies that in addition to the 5' hairpin structure also other portions of the CsrC RNA are stabilized by YmoA.

To further proof that YmoA regulates CsrC on the post-transcriptional level, the *csrC* promoter was exchanged by an inducible promoter, to exclude YmoA influence on *csrC* transcription. First, a P_{tet}-*lacZ* (pTT01) fusion was transformed into wild type strain and the *ymoA* mutant to determine, whether YmoA affects transcription of the P_{tet} promoter. No difference of the P_{tet}-*lacZ* expression was detectable between the wild type and the *ymoA* mutant demonstrating that P_{tet} expression is independent of *ymoA* (Fig. 22A).

In the following, a plasmid encoding *csrC* transcribed from the P_{tet} promoter (pKB47) was introduced into wild type strain YPIII and the *ymoA* mutant YP50. The strains were cultivated in minimal medium overnight to prevent expression of the chromosomal *csrC* gene, which was previously shown to be repressed under these conditions (Heroven, *et al*. 2008).

In fact, synthesis of CsrC from the chromosome in the wild type and the *ymoA* mutant strain was abolished under these cultivation conditions. Strikingly, high CsrC levels were found in the wild type strain expressing *csrC* from the P_{tet} promoter, whereas the amount of CsrC was strongly reduced in the *ymoA* mutant (Fig. 22B). These results support the hypothesis, that YmoA is responsible for post-transcriptional activation of CsrC synthesis, most likely by regulation of the CsrC RNA stability.

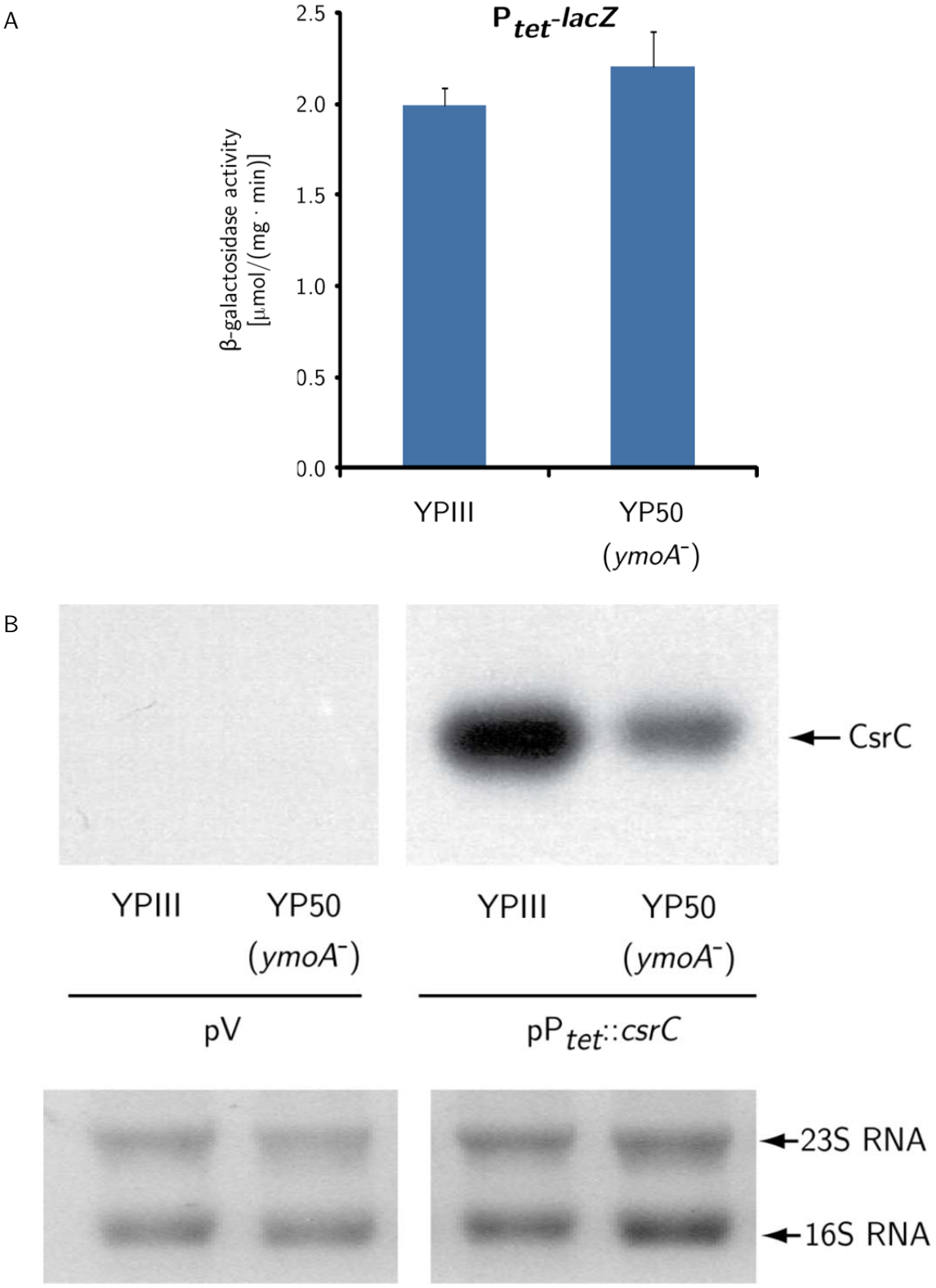

Fig. 22. YmoA-mediated activation of CsrC synthesis occurs on the post-transcriptional level. A. *Y. pseudotuberculosis* YPIII and YP50 (*ymoA*⁻) harboring the P_{tet}-*lacZ* plasmid (pTT01) were grown overnight in MMA medium at 25°C. β-galactosidase activity is given in in µmol/(min · mg). The data represent mean values ± standard deviation of three independent experiments, each performed in duplicate. B. Total RNA was prepared from samples of *Y. pseudotuberculosis* YPIII and YP50 (*ymoA*⁻) carrying an empty vector pV (pHSG575) or P*tet::csrC* (pKB47). Strains were cultivated overnight in minimal medium at 25°C. Total RNA was prepared for

Nothern blot analysis and CsrC was detected by a specific Dig-labeled probe. The 16S and 23S rRNAs served as loading controls.

3.1.5 CsrC RNA stability in *Y. pseudotuberculosis* is affected by YmoA in a CsrA-independent manner

In *Y. pseudotuberculosis*, the CsrC RNA is not detectable, when CsrA is absent (Heroven, *et al.* 2008). In order to test, whether CsrA affects synthesis of CsrC on the post-transcriptional level, *csrC-lacZ* fusions with varying *csrC* gene lengths to position +4 (pAKH103), +39 (pAKH106), +61 (pAKH107), +71 (pKB20), +81 (pAKH76) and +254 (pAKH104) were expressed in *Y. pseudotuberculosis* YPIII and the isogenic *csrA* mutant strain YP53. β-galactosidase activity was measured from overnight cultures.

In contrast to the *ymoA* mutant background, expression analysis of the different *csrC-lacZ* fusions revealed similar or only slightly different expression levels in the wild type and the *csrA* mutant. This indicates that CsrA influence on CsrC might be independent of YmoA and vice versa (Fig. 23).

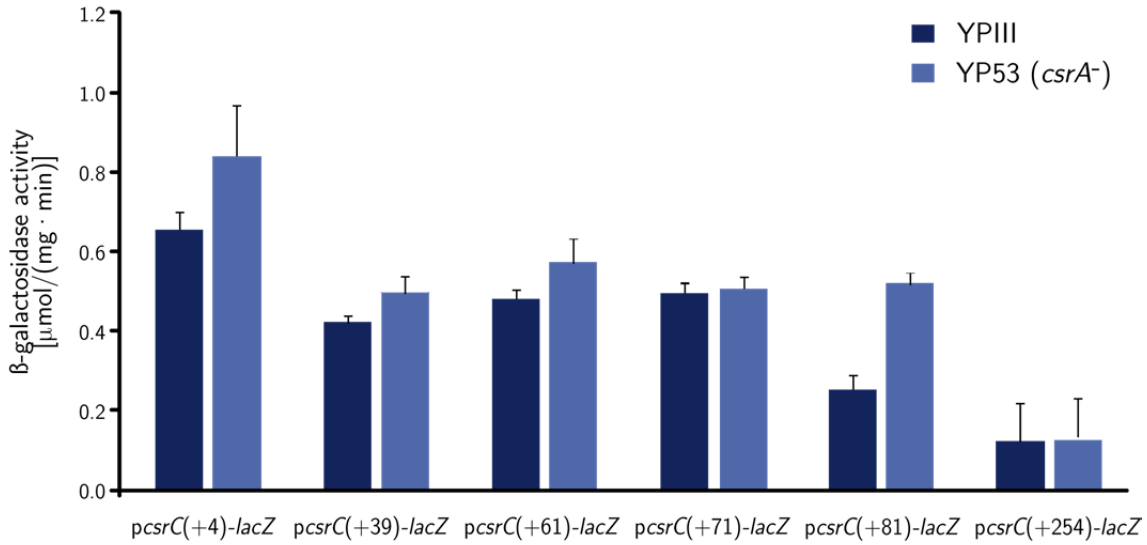

Fig. 23. CsrA has no influence on *csrC-lacZ* expression. Transcription activity of p*csrC*(+4)-*lacZ* (pAKH103), p*csrC*(+39)-*lacZ* (pAKH106), p*csrC*(+61)-*lacZ* (pAKH107), p*csrC*(+71)-*lacZ* (pKB20), p*csrC*(+81)-*lacZ* (pAKH76) or p*csrC*(+254)-*lacZ* (pAKH104) transformed into *Y. pseudotuberculosis* YPIII and YP53 (*csrA*$^-$) was determined by measuring the β-galactosidase activity in overnight cultures in LB medium at 25°C. β-galactosidase activity is given in µmol/(min · mg). The data represent mean values ± standard deviation of three independent experiments, each performed in duplicate.

Fortune *et al.* (2006) found, that the Csr-type RNAs in *Salmonella* were stabilized by the presence of CsrA. To address whether CsrA is also required for CsrC stability, *csrC* was expressed under the control of the *tet* promoter (P_{tet}) and CsrC levels were monitored in *Y. pseudotuberculosis* YPIII (wild type) and YP53 (*csrA*$^-$) grown overnight in minimal medium at 25°C. Although activity of P_{tet} was *per se* not reduced in a *csrA* mutant (Fig. 24A), CsrC RNA transcribed from P_{tet} was only detectable in the wild type and not in the *csrA*-deficient strain (Fig. 24B). This indicates that CsrA influences CsrC on the post-transcriptional level.

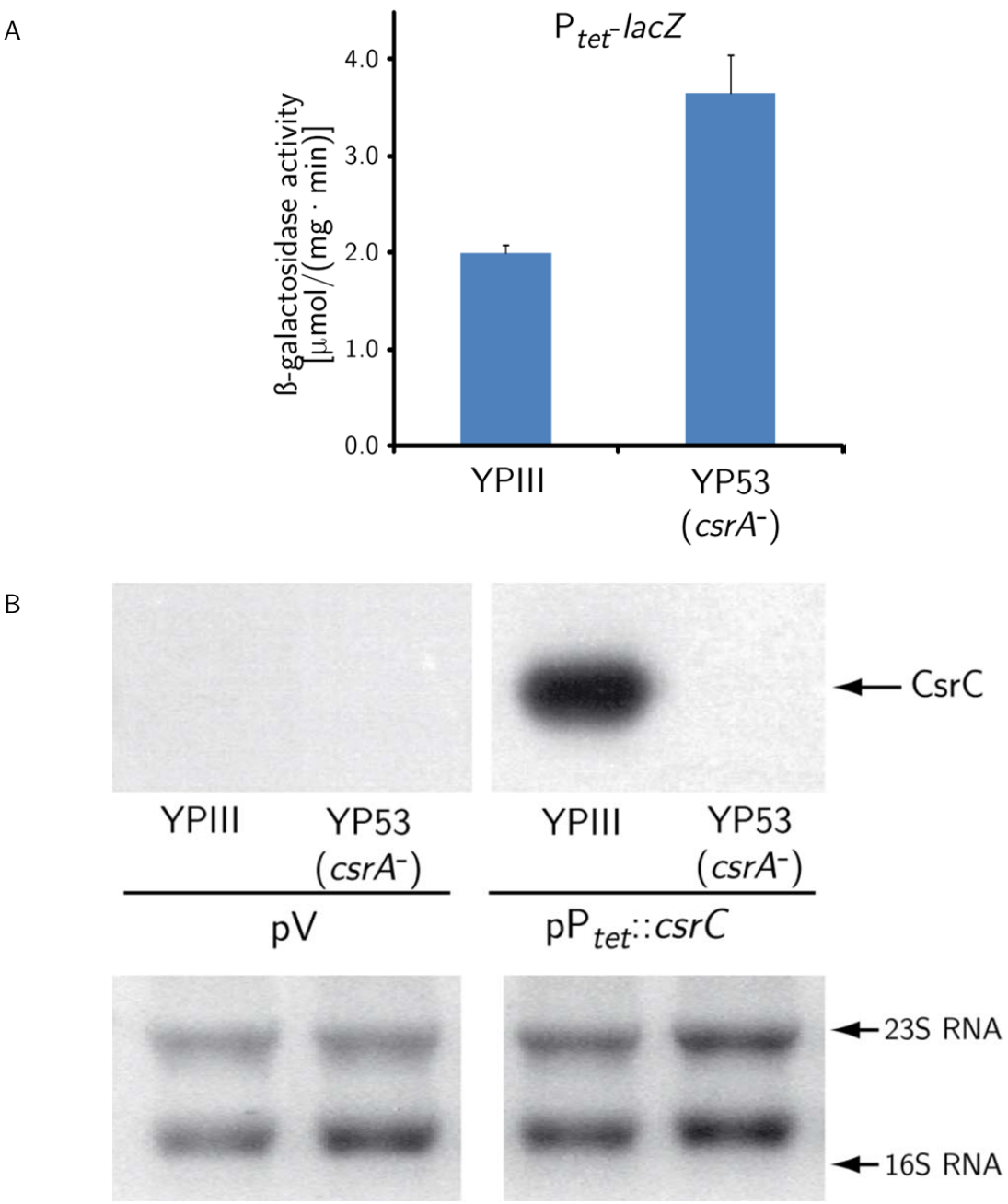

Fig. 24. CsrA is required for the presence of CsrC. The β-galactosidase activity of a P_{tet}-*lacZ* fusion encoded on pTT01 introduced into *Y. pseudotuberculosis* YPIII and YP53 (*csrA*⁻) was measured from overnight cultures in MMA medium at 25°C. The enzyme activity is given in µmol/(min · mg). The data represent mean values ± standard deviation of three independent experiments, each performed in duplicate. B. CsrC was detected by Northern blot analysis with specific Dig-labeled probes using total RNA prepared from samples of YPIII and YP53 (*csrA*⁻) harboring an empty control vector pV (pHSG575) or pP_{tet}::*csrC* (pKB47). Strains were cultivated in MMA medium overnight at 25°C. The 16S and 23S rRNAs served as loading controls.

Previous experiments demonstrated that YmoA and CsrA have a positive influence on the CsrC RNA and exert their influence on the post-transcriptional level. Most likely, they affect the decay of the CsrC RNA. In order to analyze the impact of YmoA and CsrA on CsrC stability in *Y. pseudotuberculosis,* RNA stability assays were performed. CsrC was not detectable in a *csrA* mutant when expressed from its own promoter or P_{tet} under non-inducing conditions (Heroven, *et al.* 2008; Fig. 24B). To allow higher CsrC expression in the absence of

csrA, the *csrA* mutant strain YP53 carrying pP$_{tet}$::*csrC* (pKB47) was grown in the presence of 0.1, 0.25, 0.5 and 1 nM anhydrotetracycline to induce the P$_{tet}$ promoter. As shown in Fig. 25, increasing CsrC RNA levels were detected at AHT concentration from 0.1 to 1 nM, but the overall concentration was still very low in comparison to CsrC production in the wild type strain.

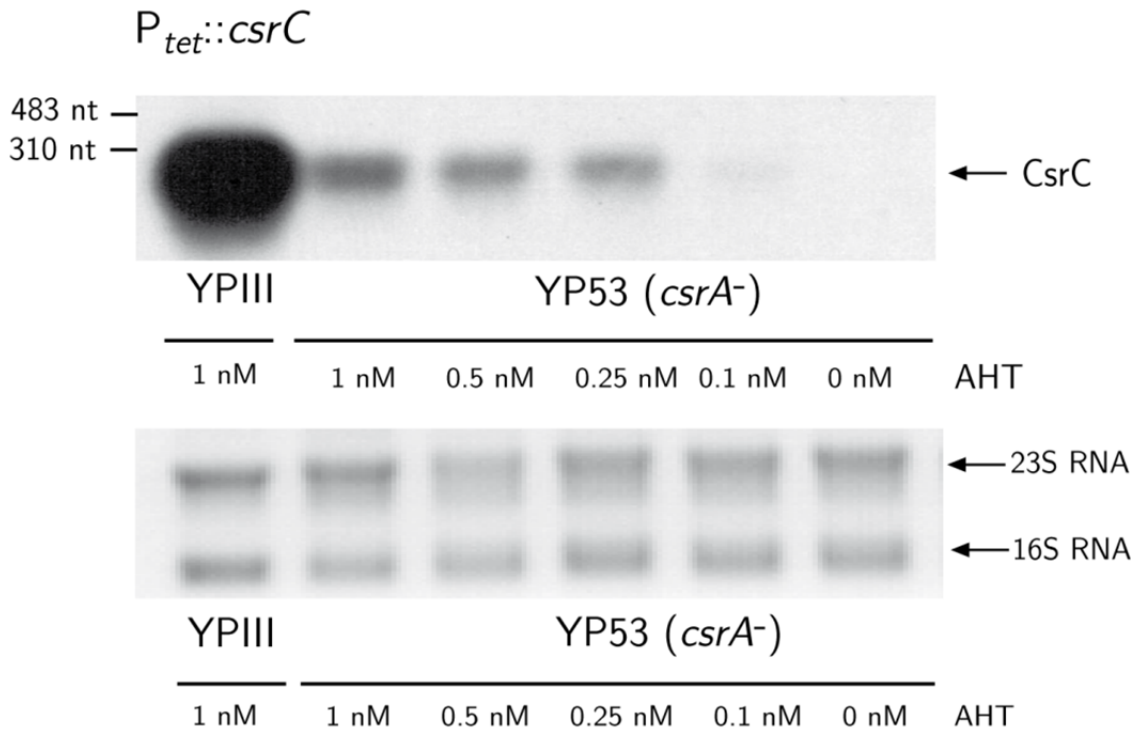

Fig. 25. P$_{tet}$::*csrC* induction analysis in a *csrA* mutant. A plasmid encoding the *csrC* gene under the control of the *tet* promoter was introduced into *Y. pseudotuberculosis* YPIII and YP53 (*csrA*$^-$) and cultivated overnight in MMA medium at 25°C. Subsequently, 0.1, 0.25, 0.5 and 1 nM AHT were added to the *csrA*-deficient strain and 1 nM to the wild type culture. Total RNA was isolated from samples withdrawn after growth for two hours, separated and CsrC was detected by Northern blotting using a specific Dig-labeled probe.

To further analyze the influence of CsrA on CsrC stability, *Y. pseudotuberculosis* YPIII (wild type), YP50 (*ymoA*$^-$) and YP53 (*csrA*$^-$) expressing P$_{tet}$::*csrC* from plasmid pKB47 were cultivated in minimal medium to early stationary phase. To allow CsrC production in the *csrA* mutant background 0.5 nM of the inducer AHT was added. Subsequently, transcription was inhibited by the addition of rifampicin to a final concentration of 500 µg/ml. Samples were withdrawn at indicated time points and CsrC was detected by Northern blot analysis using CsrC-specific probes. The intensities were calculated relative to CsrC amount at the starting point (Fig. 26A/B "0 min.") of the experiment.

CsrC was only slowly degraded with a half-life of about 116 min in *Y. pseudotuberculosis* wild type. In contrast, a significantly faster degradation of CsrC was observed in *ymoA*$^-$ and *csrA*$^-$ mutants. In the *csrA* mutant, the CsrC RNA was rapidly degraded with a half-life of circa 11 min (Fig. 26A). CsrC RNA concentrations in a *ymoA* mutant decreased steadily with a half-life of approx. 46 min (Fig. 26B).

A

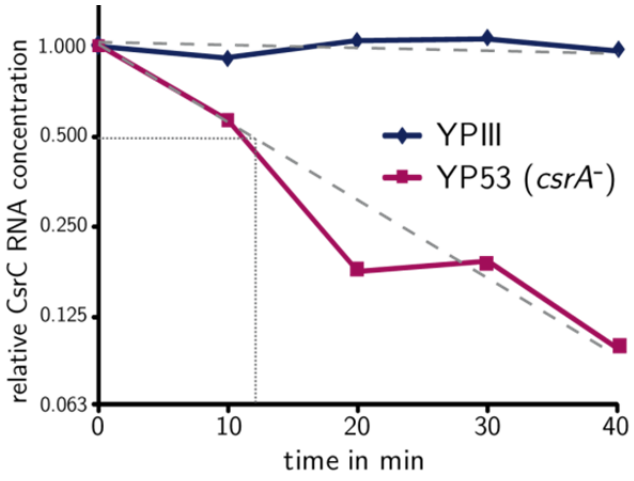
relative CsrC RNA concentration
1.000
0.500
0.250
0.125
0.063
0
10
20
30
40
time in min
YPIII
YP53 (csrA⁻)

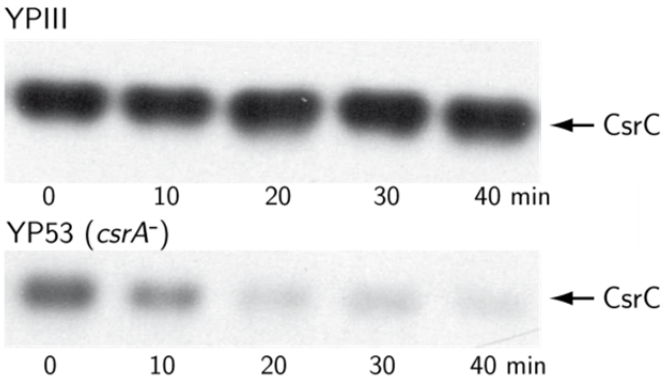
YPIII
CsrC
0
10
20
30
40 min
YP53 (csrA⁻)
CsrC
0
10
20
30
40 min

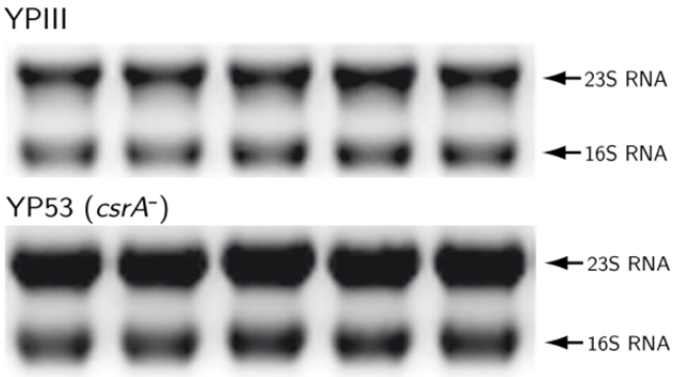
YPIII
23S RNA
16S RNA
YP53 (csrA⁻)
23S RNA
16S RNA

B

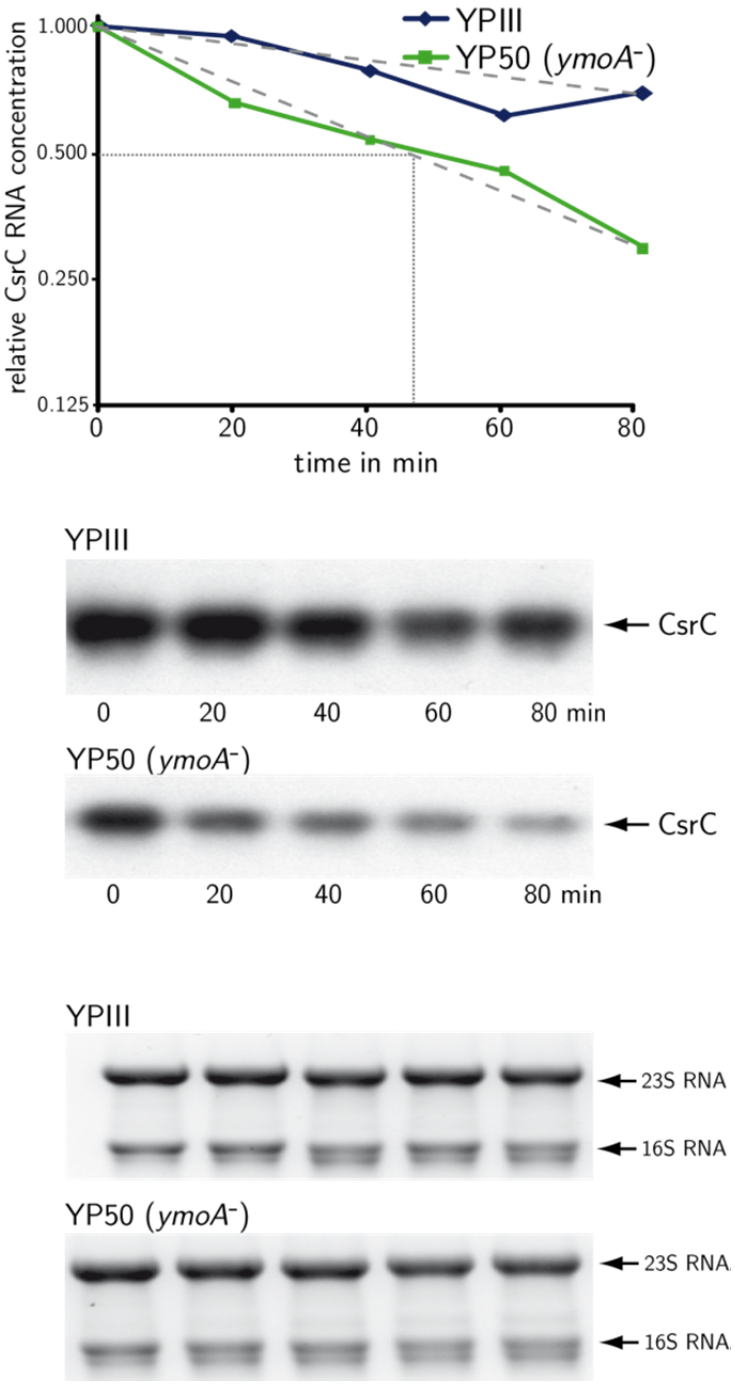

Fig. 26. YmoA and CsrA stabilize the CsrC RNA. CsrC RNA stability was determined in *Y. pseudotuberculosis* YPIII in comparison to YP53 (*csrA*$^-$) (A) and YP50 (*ymoA*$^-$) (B). All strains harboring pP_{tet}::*csrC* (pKB47) were cultivated in MMA medium overnight at 25°C. *csrC* expression in *csrA* mutant was induced by addition of 0.5 nM AHT and cultured for two additional hours at 25°C. Transcription was inhibited by the addition of rifampicin at a final concentration of 500 µg/ml. Samples were taken every 10 minutes to investigate stability in the *csrA* mutant (red line) (A) or 20 minutes to study CsrC stability in the *ymoA* mutant (green line) (B). The total RNA was prepared, separated and CsrC was detected by Northern blotting using a CsrC-specific DNA-probe. 16S and 23S rRNAs served as loading controls. Northern blots were documented by a gel doc system (Biorad) and analyzed by Biorad Image Lab™ Software. Data are presented in relative CsrC RNA concentration units plotted against the time (min). Dotted lines mark time points when half of the RNA amount was degraded. Dashed lines represent the line of best fit.

Taken together, CsrC is less stable in both, a *csrA* and *ymoA* mutant. RNA amounts decline much faster in a *Y. pseudotuberculosis csrA* mutant than in a *ymoA*-deficient strain, which suggests that binding of CsrA to CsrC might stabilize RNA and prevent degradation by RNases. YmoA affects the RNA stability to a smaller extent. Taking into account, that YmoA does not influence CsrA synthesis, the nucleoid-associated protein might promote proper folding of the CsrC RNA, which facilitates CsrA binding and might thus have an indirect influence on CsrC RNA stability.

Furthermore, it was tested whether overexpression of *ymoA* can complement the loss of *csrA* and vice versa. Therefore, low copy plasmids carrying *ymoA* (pKB4) or *csrA* (pKB60) were introduced into *Y. pseudotuberculosis* YPIII (wild type), YP50 (*ymoA*$^-$) and YP53 (*csrA*$^-$). Total RNA was prepared from overnight cultures and CsrC was detected by Northern blotting using a CsrC-specific probe. In comparison to *Y. pseudotuberculosis* wild type CsrC synthesis, no RNA was detected in the *ymoA* and the *csrA* mutants. Overexpression of *ymoA* or *csrA* led to higher CsrC amounts in the wild type strain. Furthermore, CsrC synthesis in the *csrA*- and *ymoA*-deficient strains was fully restored by addition of the *csrA*$^+$ plasmid. Strikingly, no CsrC RNA was detectable in a *csrA* mutant expressing *ymoA*, whereas wild type levels of CsrC were observed in a *ymoA* mutant in the presence of the *ymoA*$^+$ plasmid (Fig. 27).

This clearly showed that loss of CsrC in a *ymoA* mutant strain can be complemented by *csrA* overexpression. In contrast, the YmoA protein is not able to restore the function of the CsrA protein on CsrC stability.

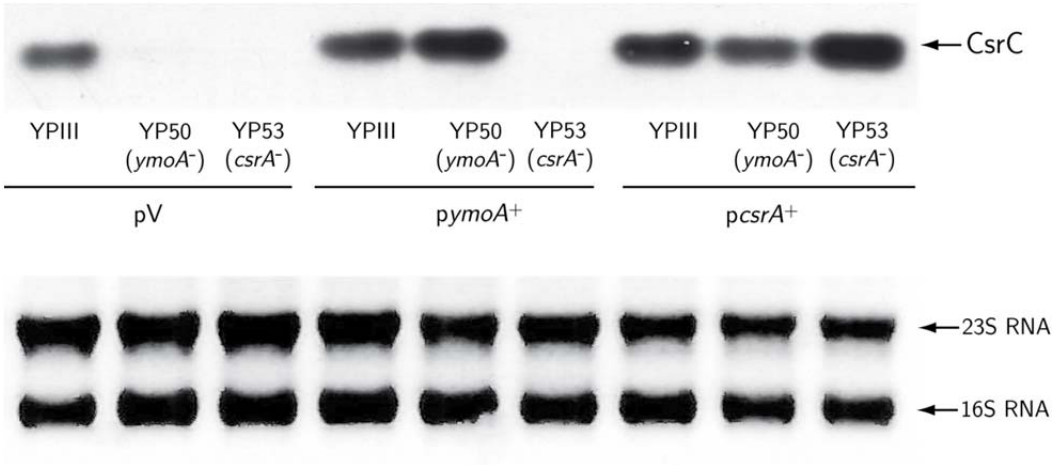

Fig. 27. YmoA and CsrA do not fully complement CsrC synthesis. To monitor CsrC synthesis by Northern blot analysis, *Y. pseudotuberculosis* YPIII and YP53 (*csrA*$^-$) and YP50 (*ymoA*$^-$) were transformed with an empty vector pV (pHSG576), p*ymoA*$^+$ (pKB4) or p*csrA*$^+$ (pKB60) and cultivated in LB medium overnight at 25°C. Total RNA was prepared, separated and the CsrC RNA was visualized after transfer to a Nytran membrane by hybridization with a specific Dig-labeled DNA probe.

These results suggest that influence of CsrA and YmoA on CsrC RNA stability is different. CsrA seems to be far more essential for CsrC stability than the nucleoid-associated protein YmoA. It is possible, that YmoA supports CsrA-mediated stabilization of the CsrC transcript.

In fact, another nucleoid-associated protein, StpA of the H-NS family, has been demonstrated to bind RNA and act as a chaperone facilitating RNA folding and base pairing (Mayer, *et al*. 2007). For this reason, it should be determined whether YmoA is also able to bind to the CsrC RNA and thereby enhances CsrA-mediated CsrC stability. To do so, N-terminal Strep-tagged YmoA protein (pAKH77) was purified from an *E. coli* strain (KB4) which is deficient in *hns*, *stpA* and *hha,* e.g. all *E. coli* homologs of the YmoA and H-NS families. Subsequently, RNA-bandshift experiments were performed with CsrC and the 5S rRNA as a negative control using increasing amounts of YmoA protein.

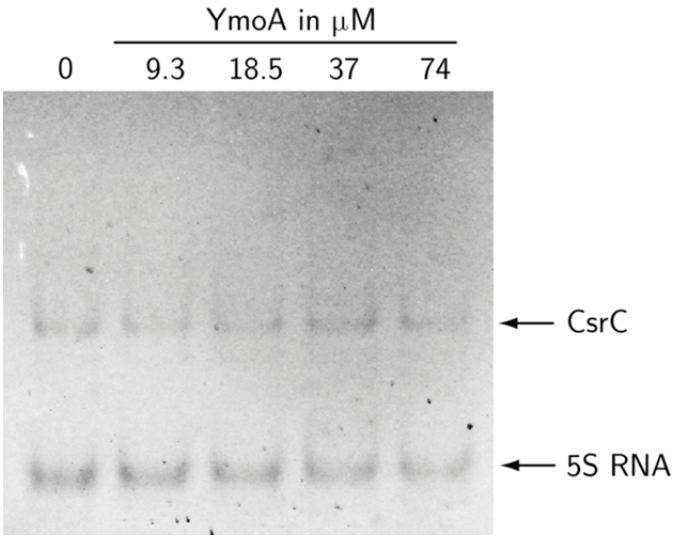

Fig. 28. YmoA does not interact with the CsrC RNA. *In vitro* transcribed CsrC RNA and 5S rRNA were incubated for 30 min at room temperature with purified 9.3, 18.5, 37 and 74 μM of N-terminal Strep-tagged YmoA (lane 2 to 5, respectively). As a control CsrC and 5S rRNA were incubated with 1 x RNA-bandshift buffer (lane 1). Samples were separated in an 8% non-denaturing polyacrylamide gel and visualized by SybrGreen staining under UV light.

As shown in Fig. 27, Strep-tagged YmoA did not interact with CsrC RNA even at higher protein concentrations, indicating that the influence of the nucleoid-associated protein on CsrC stability in *Y. pseudotuberculosis* is indirect and occurs via another regulatory factor.

3.1.6 Control of YmoA and CsrA synthesis influences CsrC levels in response to environmental signals

Production of RovA and RovA-dependent invasin synthesis are regulated by specific environmental conditions. Their expression is induced in complex medium, during stationary growth and at moderate temperatures. Furthermore, CsrA has been shown to be responsible for medium-dependent activation of RovM production, which abolished *rovA* expression (Heroven, *et al*. 2008). To further characterize how the regulatory network of *rovA* reponses to environmental signals, YmoA and CsrA synthesis conditions were addressed in detail. Since

CsrC of *Y. pseudotuberculosis* has been reported to be synthesized only in nutrient-rich, but not under minimal medium conditions, CsrA and YmoA protein levels of *Y. pseudotuberculosis* wild type strain YPIII were monitored in minimal medium MMA and complex medium LB at 25°C and 37°C in exponential and stationary phase (Fig. 29). Expression of the *csrA* gene was subjected to growth phase control. Significantly higher amounts where found during the stationary phase. In contrast, temperature and growth media had no considerable effect on CsrA synthesis (Fig. 29A). In contrast, YmoA protein levels were observed to be strongly dependent on media, temperature and growth phase. Maximal expression was observed at moderate temperature, in complex medium and during exponential growth whereas lowest expression was seen at 37°C in minimal medium during stationary phase (Fig. 29B).

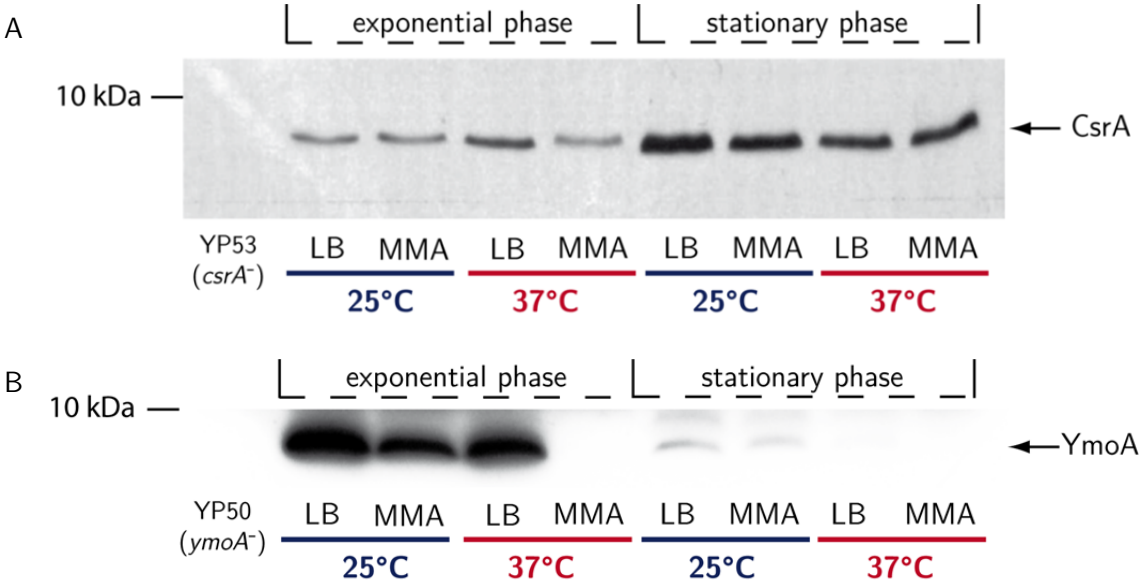

Fig. 29. CsrA and YmoA protein synthesis is regulated by environmental parameters. To monitor CsrA and YmoA levels during stationary growth, *Y. pseudotuberculosis* wild type strain YPIII was cultivated overnight in LB and minimal medium MMA at 25°C and 37°C. For exponential growth, overnight culture were diluted 1:50 in LB or minimal medium MMA and cultivated at 25°C and 37°C until cultures reached an OD_{600nm} of about 0.8. Samples were withdrawn, the OD_{600nm} was adjusted and whole cell extracts were prepared. Proteins were separated by 18%-20%TRICINE-PAGE and transferred onto an Immobilon membrane. A. CsrA was detected with a polyclonal anti-CsrA antibody. Cell extract from a *csrA* mutant strain YP53 culture was used as a control. B. YmoA protein was detected with a polyclonal anti-YmoA antibody. Cell extract from a *ymoA* mutant strain YP50 culture was used as a control. Molecular weight ladder was applied on the left. CsrA and YmoA protein bands were marked by arrows.

Absence of YmoA and the reduced levels of CsrA protein at 37°C in minimal medium during exponential growth could explain the reduced stability of CsrC under these conditions. Otherwise, both proteins are present at 25°C. This could lead to higher CsrC levels, in particular during exponential phase.

To analyze temperature and growth phase regulation and its influence on CsrC synthesis, in more detail, CsrA and YmoA protein levels as well as CsrC RNA amounts were detected along the growth curve of *Y. pseudotuberculosis* wild type strain YPIII grown in LB medium at 25°C and 37°C. Whole cell extracts and total RNA were prepared from samples withdrawn every

two hours from an over-day culture. At 25°C, CsrC levels were found to be low during early exponential phases but increased significantly during the transition from exponential to stationary growth with maximal amounts of CsrC during stationary phase (OD_{600nm}=4.0). At 37°C, CsrC amounts were found to be highest at an OD_{600nm} of about 2.7, when *Y. pseudotuberculosis* entered early stationary growth phase, but CsrC levels decreased again during stationary phase (Fig. 30). Different CsrC concentration patterns seem to be the result of different CsrA and YmoA levels. Whereas the concentration of the CsrA protein increased during stationary growth phase at 25°C as well as 37°C, overall CsrA levels were significantly higher at moderate temperatures. In contrast, high levels of YmoA were only detectable during exponential growth (OD_{600nm}=3.0), but the amounts of YmoA decreased strongly during stationary growth. Overall, significantly higher YmoA concentrations were detectable in *Y. pseudotuberculosis* at moderate temperature, e.g. no protein was observed during stationary growth at 37°C (Fig. 30).

In summary, highest CsrC levels were detected in *Y. pseudotuberculosis* when CsrA reached intermediate levels and YmoA is still present. This indicates that CsrC stability is the result of balanced YmoA and CsrA levels under specific environmental conditions, especially at low temperatures, high cell density and in nutrient-rich medium.

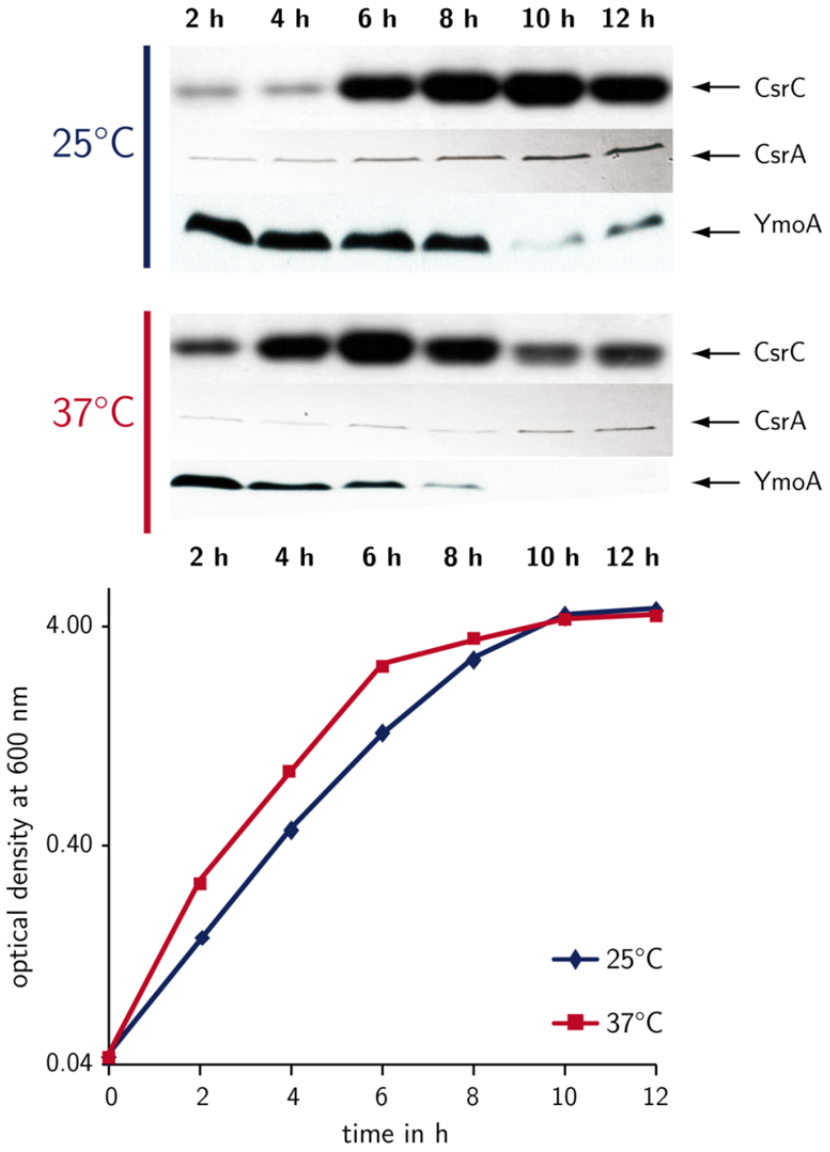

Fig. 30. CsrC, YmoA and CsrA levels are regulated by growth phase and temperature in *Y. pseudotuberculosis*. *Y. pseudotuberculosis* wild type strain YPIII was diluted 1:100 from an overnight culture and grown in LB medium at 25°C (blue) and 37°C (red). Samples were taken simultaneously every two hours and the OD_{600nm} to monitor growth. For CsrC detection, total RNA was prepared from the samples, separated and CsrC was detected by Northern blot analysis using a CsrC-specific Dig-labeled DNA probe. To detect YmoA and CsrA by specific polyclonal antibodies, the cell density of the samples was adjusted and whole cell extracts were prepared. Proteins were separated on 18% (CsrA) and 20% (YmoA) TRICINE gels and visualized by immunoblotting.

YmoA levels seem to be strongly dependent on temperature. Jackson *et al.* (2004) observed that YmoA in *Y. pestis* is rapidly degraded at 37°C by ATP-dependent ClpXP and Lon proteases. To study whether also YmoA of *Y. pseudotuberculosis* was subjected to temperature-regulated proteolysis, YmoA protein levels were analyzed in overnight cultures of *Y. pseudotuberculosis* wild type (YPIII), and isogenic *clpP* (YP63), *lon* (YP67) and *clpP*/*lon* double (YP68) mutant strains.

Whereas YmoA protein was present in *Y. pseudotuberculosis* wild type at 25°C, it was not detectable at 37°C. Absence of *clpP* resulted in elevated YmoA amounts at both temperatures compared to the wild type, although significantly lower protein levels were observed at 37°C.

In a *lon* mutant, YmoA degradation was significantly reduced at 37°C and no temperature-dependent proteolysis of YmoA was observed in the *clpP*/*lon* double mutant (Fig. 31). These results suggest that YmoA in *Y. pseudotuberculosis* is degraded by the ATP-dependent ClpP and the Lon protease in a temperature-dependent manner, i.e. degradation at 37°C.

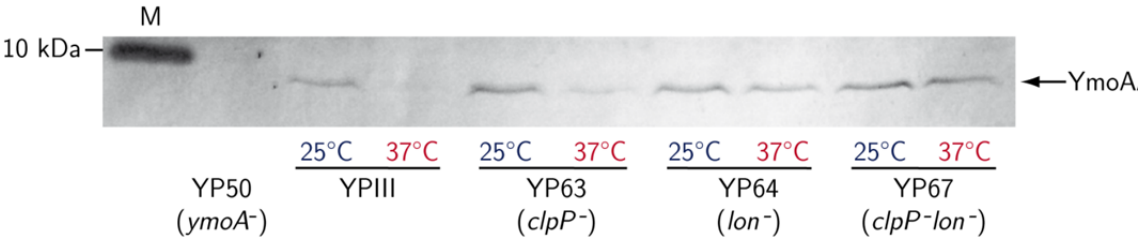

Fig. 31. YmoA is degraded by ATP-dependent Clp/Lon proteases in response to temperature. Whole cell extracts were prepared from overnight culture samples of *Y. pseudotuberculosis* YPIII, YP63 (*clpP*-), YP64 (*lon*-) and YP67 (*clpP*/*lon*-) grown at 25°C and 37°C. Whole cell extract of YP50 (*ymoA*-) was used as negative control. Proteins were separated by 20% TRICINE-PAGE, followed by immunoblotting. YmoA was visualized by a polyclonal anti-YmoA antibody. A molecular weight ladder is loaded on the left. YmoA protein is marked by an arrow.

3.1.7 The chaperone Hfq induces CsrC and CsrB synthesis and activates *rovA* expression

The RNA chaperone Hfq has previously been shown to increase the stability of Rsm (Csr) RNAs whereby it enhances the sequestration of the CsrA-like protein RsmA in *P. aeruginosa* (Sorger-Domenigg, *et al.* 2007). As Hfq has also been found to influence *rovA* expression in *Y. pseudotuberculosis* (A. K. Heroven, unpublished data), the influence of Hfq on the regulatory cascade (e.g. RovM and the Csr-system) was analyzed.

Western blot analysis were performed using whole cell extracts of YPIII and the isogenic *hfq* mutant strain YP80 with or without the *hfq*+ plasmid pAKH115 to visualize RovA and RovM regulator proteins (Fig. 32). In an *hfq* mutant, RovA levels were significantly reduced compared to the wild type. Overexpression of *hfq* restored RovA levels in an *hfq* mutant and resulted in slightly higher amounts of RovA in the wild type strain. Opposite expression levels were observed for the RovM protein. Significantly higher RovM levels were detected in the *hfq*-deficient strain whereas slightly lower amounts of RovM were detected in the presence of the *hfq*+ plasmid in both, the wild type and the *hfq* mutant. Hence, Hfq activates *rovA* expression by downregulation of RovM synthesis.

Because RovM synthesis is controlled by the Csr system, influence of the RNA chaperone Hfq on the presence of the CsrC and CsrB RNA was evaluated. To do so, total RNA was prepared from YPIII (wild type) and YP80 (*hfq*-) with the empty vector or the *hfq*+ plasmid. CsrB and CsrC were visualized by Northern blotting using CsrB- and CsrC-specific probes. In addition, whole cell extracts were prepared of these strains. CsrA was detected by immunoblotting. CsrA levels remained identical in all strains, demonstrating that CsrA production is independent of *hfq*. In contrast, the CsrC RNA was observed in *Y. pseudotuberculosis* wild

type but not in an *hfq* mutant and overexpression of *hfq* resulted in significantly higher amounts in the wild type and the *hfq* mutant strain

CsrB levels were very low in the wild type and could not be detected in the *hfq*-deficient strain. In contrast, *hfq* overexpression from a plasmid resulted in slightly higher amounts of CsrB in the wild type or the *hfq* mutant (Fig. 32B).

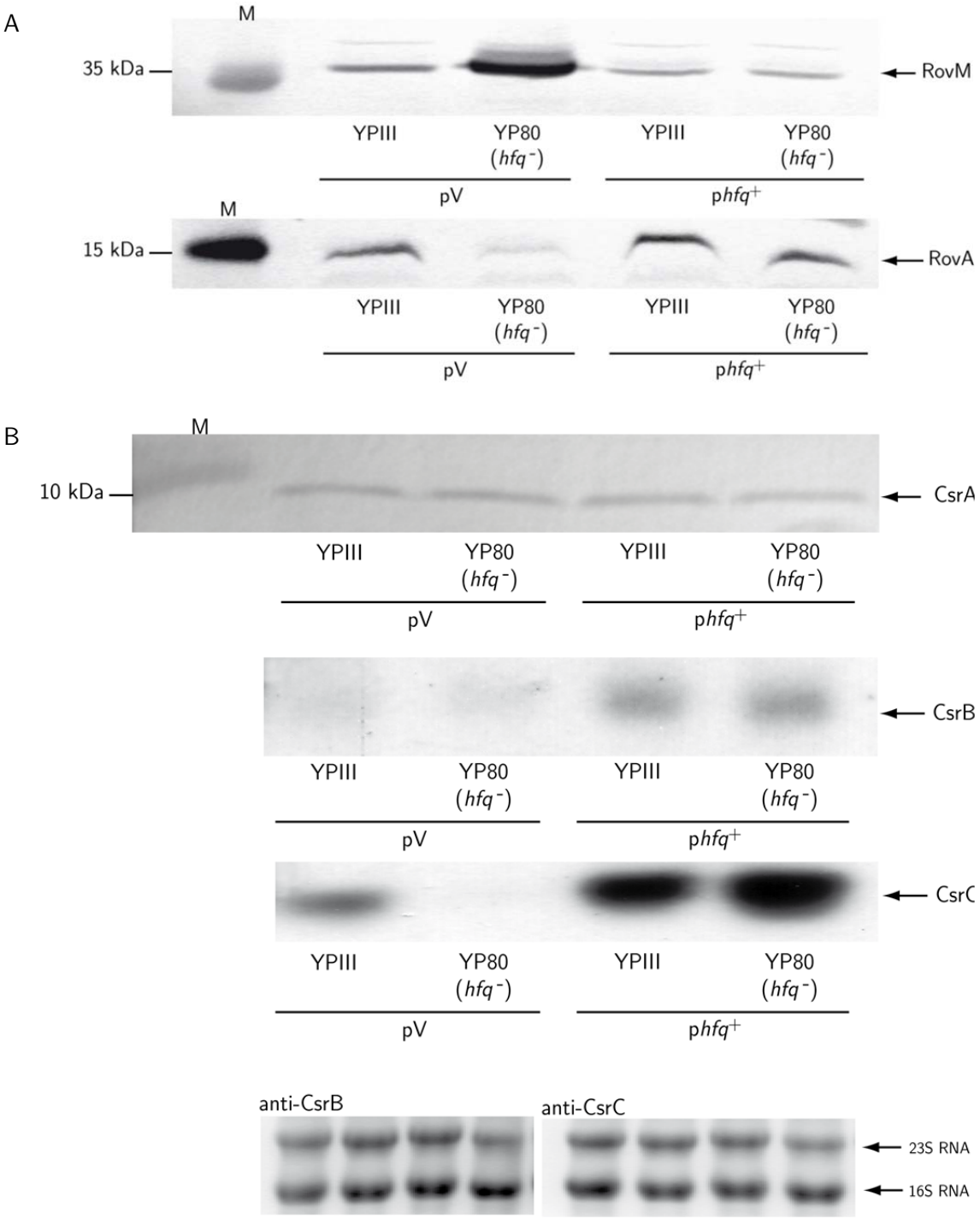

Fig. 32. Hfq activates RovA synthesis by downregulation of RovM synthesis through upregulation of the Csr RNAs. *Y. pseudotuberculosis* YPIII and YP80 (*hfq*⁻) carrying an empty vector pV (pAKH85) or *hfq*⁺ plasmid (pAKH115) were cultivated overnight in LB medium at 25°C. A. For detection of RovA and RovM protein, whole cell extracts were prepared, separated by 15% (RovA) or 12% (RovM) SDS-PAGE and transferred onto an

Immobilon membrane. RovM and RovA were visualized by specific polyclonal antibodies. A molecular weight ladder is loaded on the left and RovM or RovA are marked by arrows. B. CsrA protein levels were determined by Western blotting. Whole cell extracts from strains described above were prepared, separated by 18% TRICINE-PAGE and CsrA was detected after immunoblotting with an anti-CsrA polyclonal antibody. A molecular weight marker is loaded on the left. CsrA is indicated by an arrow. Additionally, total RNA was prepared from samples of overnight cultures and analyzed via Northern blotting using specific anti-CsrC and anti-CsrB Dig-labeled DNA probes. 16S and 23S rRNA was visualized as loading controls.

These results indicate that Hfq is essential for the synthesis of the Csr RNAs in *Y. pseudotuberculosis*. In the presence of Hfq, CsrB and CsrC production is upregulated. This allows the sequestration of CsrA which results in the reduction of RovM levels under these conditions.

As Hfq acts as a chaperone, it was assumed that Hfq might be implicated in YmoA-dependent stabilization of CsrC. To prove this hypothesis, influence of Hfq on CsrC stability was tested. For this purpose, *csrC* was expressed under the control of the *tet* promoter to exclude influence on transcription. Expression analysis of P_{tet}-*lacZ* fusion (pTT01) in YPIII (wild type) and YP80 (*hfq*$^-$) demonstrated that loss of *hfq* has no effect (Fig. 33A). This allowed us to compare CsrC stability in YPIII (wild type) and YP80 (*hfq*$^-$) harboring a plasmid-encoded P_{tet}::*csrC* (pKB47) expression construct. CsrC levels were low in *Y. pseudotuberculosis* grown in minimal media and CsrC was detectable in the *hfq* mutant. However, expression of *csrC* from the P_{tet} promoter resulted in similar CsrC concentrations in the wild type and the *hfq* mutant. This indicated that Hfq did not affect CsrC stability (Fig. 33B).

A

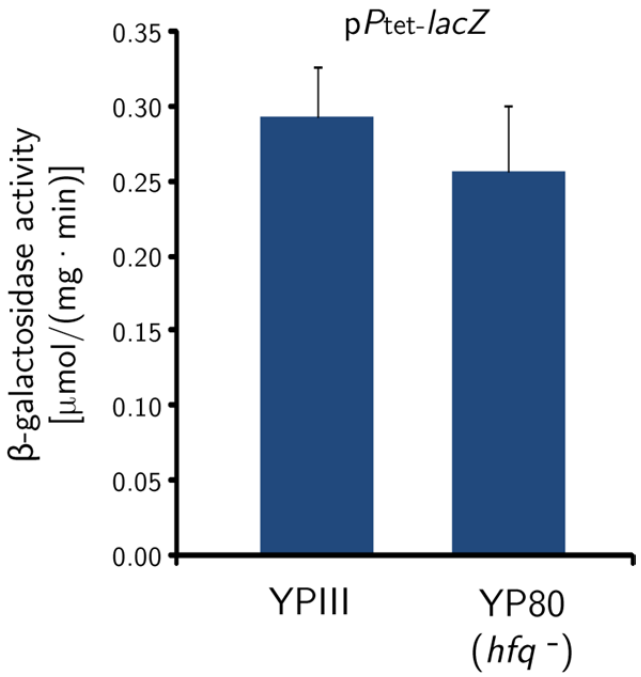

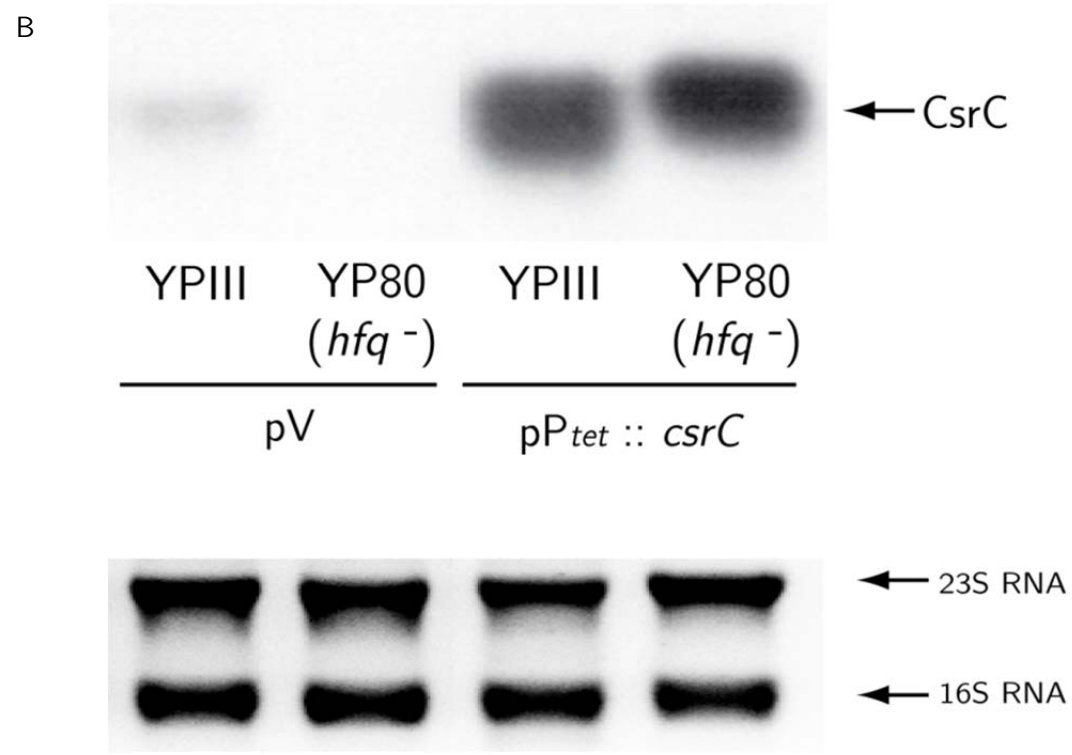

Fig. 33. Hfq does not affect CsrC stability. A. P_{tet}-*lacZ* activity was analyzed in *Y. pseudotuberculosis* YPIII and YP80 (*hfq*$^-$) haboring pP_{tet}::*csrC* (pKB47) after overnight cultivation in minimal medium MMA at 25°C. β-galactosidase activity is given in µmol/(min · mg). The data represent the mean ± standard deviation of three independent experiments, each performed in duplicate. B. CsrC was detected by Northern blot analysis with CsrC-specific Dig-labeled probes using total RNA prepared YPIII and YP80 (*hfq*$^-$) harboring the empty vector pV (pHSG575) or pP_{tet}::*csrC* (pKB47). Strains were cultivated in MMA medium overnight at 25°C. 16S and 23S rRNA served as loading controls.

Next, it was tested whether *ymoA* and *hfq* deletions could be complemented by *ymoA* or *hfq* overexpression to analyze whether the regulators act in a hierarchical manner. Therefore, pKB4 (*ymoA*$^+$) or pAKH119 (*hfq*$^+$) were transformed into YPIII (wild type), YP50 (*ymoA*$^-$) and YP80 (*hfq*$^-$). CsrC levels in the strains were determined by Northern blot analysis. In contrast to the wild type, very low amounts of CsrC were found in the *ymoA* and the *hfq* mutant. Overexpression of *hfq* or *ymoA* resulted in increased CsrC synthesis in the wild type, but neither overexpression of *ymoA* could restore CsrC production in the *hfq* mutant nor could Hfq overproduction induce an increase of CsrC in a *ymoA* mutant (Fig. 34).

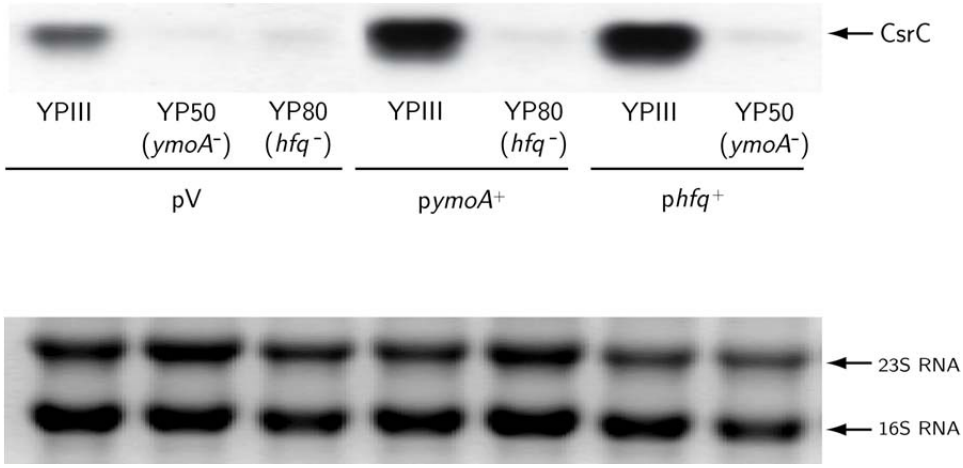

Fig. 34. YmoA and Hfq act independently on CsrC. *Y. pseudotuberculosis* YPIII, YP50 (*ymoA*-) and YP80 (*hfq*-) harboring the empty vector pV (pHSG575), p*ymoA*+ (pKB4) or p*hfq*+ (pAKH119) were cultivated overnight in LB medium at 25°C. Total RNA was prepared, separated and analyzed by Northern blotting using a CsrC-specific Dig-labeled DNA probe. CsrC is marked by an arrow. 16S and 23S rRNA served as loading controls.

This demonstrated that YmoA and Hfq cannot complement each other suggesting that both factors influence CsrC synthesis independently. In fact, YmoA was shown to act on the post-transcriptional level (e.g. CsrC stability) whereas Hfq does not affect CsrC stability. To further address the mechanism how Hfq affects CsrC levels the *csrC*(+4)-*lacZ* (pAKH103) and a *csrC*(+81)-*lacZ* (pAKH76) fusion plasmids were introduced into YPIII (wild type) and YP80 (*hfq*-) to analyze the impact of Hfq on *csrC* transcription. In order to study the complementation and *hfq* overexpression on *csrC* transcription, activities of the fusions were also measured in the wild type and the *hfq* mutant harboring the *hfq*+ plasmid pAKH115.

Expression of both *csrC-lacZ* fusions was significantly reduced (50%-75%) in an *hfq*-deficient strain, and overproduction of Hfq restored *csrC* transcription levels in an *hfq* mutant to wild type levels (Fig. 35). This strongly indicated that Hfq activates *csrC* transcription.

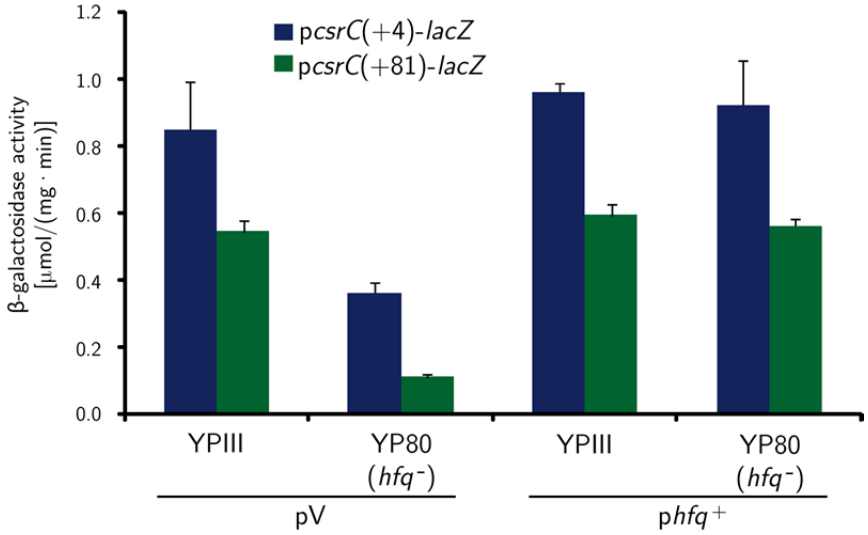

Fig. 35. Hfq activates *csrC* gene expression. β-galactosidase activity of the plasmid-encoded *csrC*(+4)-*lacZ* (pAKH103) and *csrC*(+81)-*lacZ* (pAKH76) fusions was determined in *Y. pseudotuberculosis* strain YPIII and the YP80 (*hfq*-) carrying an empty vector pV (pAKH85) or an *hfq*+ plasmid (pAKH115) cultivated overnight in LB medium at 25°C. Enzyme activity is given in µmol/(min · mg). The data represent the mean ± standard deviation of three independent experiments, each performed in duplicate.

3.1.8 Analysis of the *csrC* promoter region

To determine the promoter region of *csrC*, which might be important for Hfq-mediated activation, transcriptional reporter gene fusions with varying *csrC* promoter lengths were constructed (*csrC*(-355)-*lacZ* (pAKH103), *csrC*(-310)-*lacZ* (pAKH125), *csrC*(-283)-*lacZ* (pAKH126), *csrC*(-204)-*lacZ* (pAKH127) and *csrC*(-106)-*lacZ* (pAKH128) fusions) and their activity was tested in *Y. pseudotuberculosis* YPIII (wild type) grown overnight at 25°C.

The *csrC-lacZ* fusions harboring promoter regions to positions -355, -310, -283 and -204 with respect to the transcription start of *csrC* showed no significant difference in their transcription rate. However, expression of a *csrC-lacZ* fusion encoding only 106 nucleotides of the 5' upstream region was found to be significantly reduced to approx. 14% of the activity of the other fusion constructs (Fig. 36).

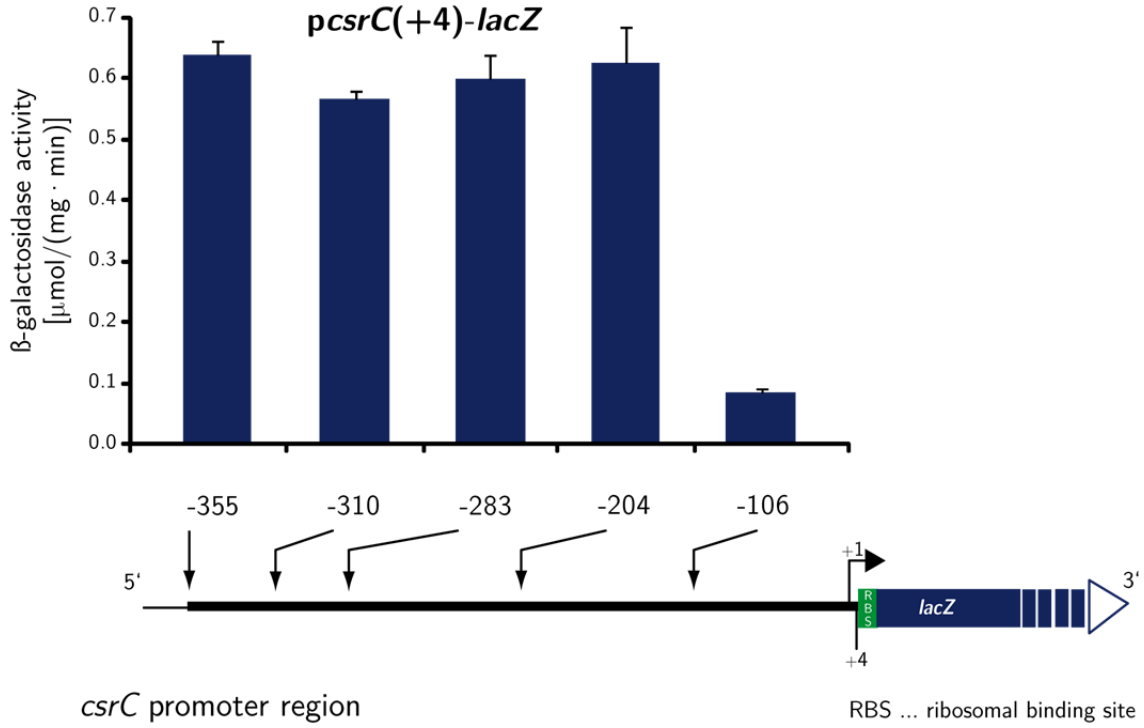

Fig. 36. Promoter deletion studies of the *csrC* regulatory region. Analysis of the *csrC* promoter region was performed by introducing *csrC*(-355)-*lacZ* (pAKH103), *csrC*(-310)-*lacZ* (pAKH125), *csrC*(-283)-*lacZ* (pAKH126), *csrC*(-204)-*lacZ* (pAKH127) and *csrC*(-106)-*lacZ* (pAKH128) fusion plasmids into *Y. pseudotuberculosis* YPIII (wild type). Samples of overnight cultures grown in LB medium at 25°C were taken to measure the β-galactosidase activity. Enzyme activity is given in µmol/(min · mg). The data represent the mean ± standard deviation of three independent experiments, each performed in duplicate.

According to these results, promoter regions of *csrC* transcription located upstream of position -106 relative to the transcription start are required for maximal *csrC* transcription. They might be targeted by activating regulators. This suggests that Hfq stimulates *csrC* transcription through a promoter element located upstream of position -204. Since Hfq is an RNA chaperone, it is most likely, that it stimulates *csrC* transcription indirectly, e.g. by controlling a regulatory RNA element influencing a *csrC* transcription factor.

3.1.9 The nucleoid-associated protein H-NS activates CsrC synthesis

H-NS regulates *inv* and *rovA* expression by binding to the promoter regions of these genes. Lawrenz and Miller (2007) described that, in *Y. enterocolitica*, H-NS binds to its homolog YmoA which in turn prevents repression of *inv* transcription under certain conditions. Furthermore, association of the YmoA homolog Hha and H-NS has been shown to regulate gene expression in *Salmonella* (Olekhnovich and Kadner 2007). This indicated that YmoA might influence CsrC RNA stability through or in association with H-NS.

To address this question, influence of H-NS on *csrC* expression and RNA synthesis was evaluated in the presence and absence of YmoA. Expression of the *csrC*(+4)-*lacZ* (pKB45) and *csrC*(+81)-*lacZ* (pKB46) fusions were analyzed in *Y. pseudotuberculosis* YPIII and the isogenic *ymoA* mutant (YP50) expressing a dominant-negative variant of the *hns* gene encoded on the *hns*' plasmid pAKH31. To test the influence of *hns* overexpression activity, both *csrC*-*lacZ* fusions were also determined in YPIII (wild type) and YP50 (*ymoA*$^-$) carrying the *hns*$^+$ plasmid pAKH74.

Expression of the *csrC*(+4)-*lacZ* fusion in the wild type strain and the *ymoA* mutant was not strongly affected by the production of unfunctional H-NS (H-NS') or H-NS overexpression.

In consistency with previous results, expression of the *csrC*(+81)-*lacZ* fusion was strongly reduced to about 30% in a *ymoA* mutant (Fig. 20, Fig. 37A). Expression of the dominant-negative *hns*' fragment had also no considerable effect on the *csrC* transcription of this fusion but *hns* overexpression restored transcription activity of the *csrC*(+81)-*lacZ* fusion to wild type levels (Fig. 37A).

To confirm this result, Northern blot analysis was performed to determine CsrB and CsrC RNA concentrations in the different strains. As shown in Fig. 37B, CsrC RNA levels in *Y. pseudotuberculosis* wild type were significantly reduced when H-NS protein was inactivated by a non-functional H-NS' fragment. In contrast, overexpression of *hns* stimulated CsrC synthesis. The CsrC RNA was hardly detectable in a *ymoA* mutant carrying an empty vector and was even less expressed when the non-functional N-terminal H-NS' fragment was produced. However, high CsrC concentrations were found in a *ymoA* mutant overexpressing the *hns* gene, indicating that H-NS can complement a *ymoA* mutation when present in high concentrations.

Synthesis of the CsrB RNA was regulated in the opposite manner. Inactive H-NS led to a mild increase of CsrB amounts in the wild type, and overexpression of *hns*' repressed CsrB synthesis. In a *ymoA* mutant CsrB concentrations were strongly elevated compared to the wild type. Further, increase of CsrB levels was detectable in the dominant-negative *hns*'/*ymoA* mutant. In contrast, *hns* overexpression reduced CsrB levels significantly, i.e. to amounts that are even lower than CsrB levels in the wild type (Fig. 37B).

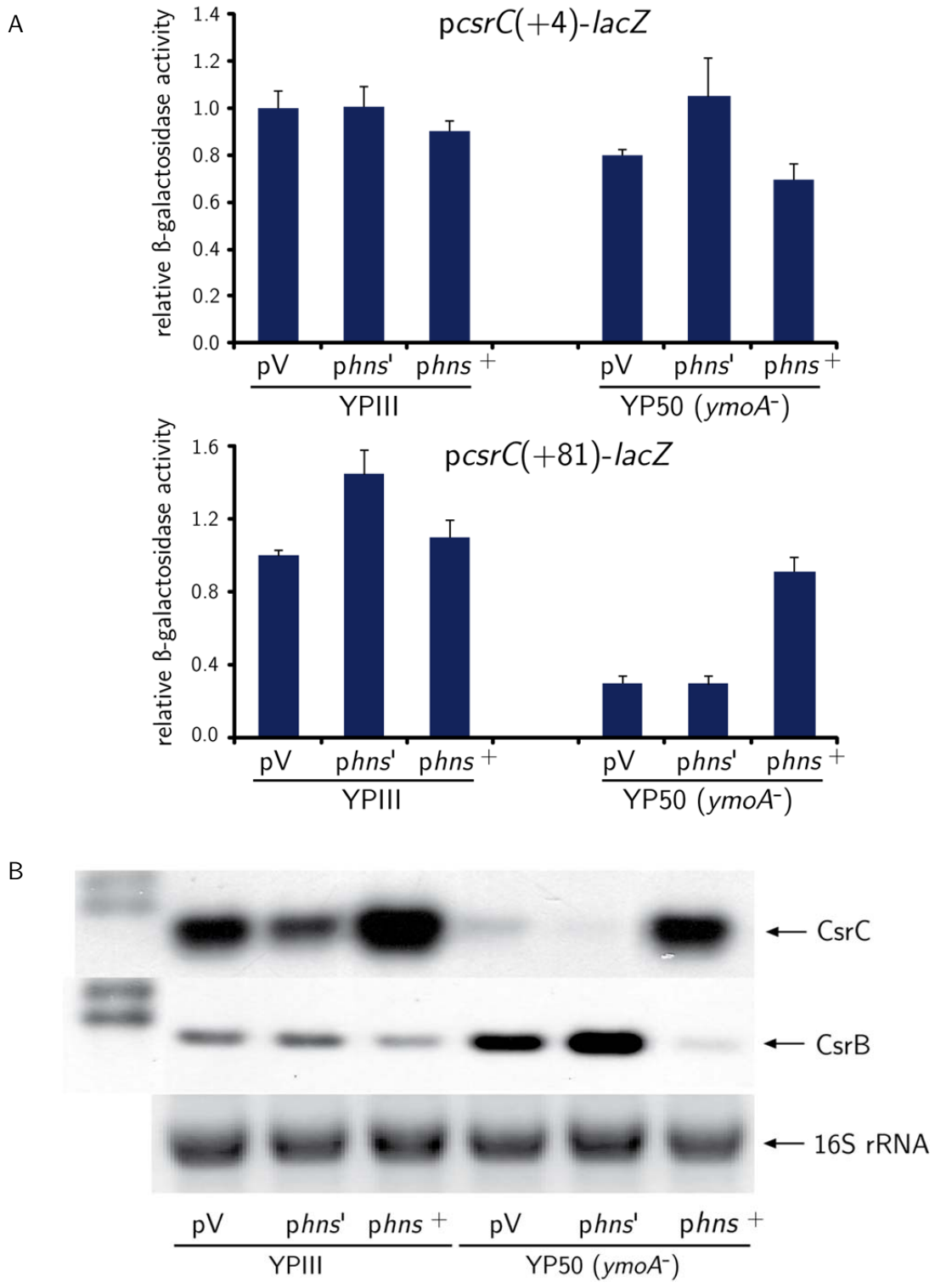

Fig. 37. H-NS upregulates CsrC synthesis post-transcriptionally. A. *Y. pseudotuberculosis* YPIII and YP50 (*ymoA*$^-$) expressing the *csrC*(+4)-*lacZ* (pAKH103) or *csrC*(+81)-*lacZ* (pAKH76) fusion also carrying an empty vector pV (pAKH85), a *hns*' (pAKH31) or *hns*$^+$ (pAKH74) overexpression plasmid were cultivated overnight in LB medium at 25°C. β-galactosidase activity was determined and normalized relative to YPIII with pV. The data represents the value ± standard deviation of three independent experiments, each performed in duplicate. B. Total RNA of the cultures was prepared, RNA was separated and analyzed by Northern blotting. CsrC and CsrB were detected by specific Dig-labeled DNA probes. 16S rRNA was visualized for loading controls.

In summary, H-NS does not seem to influence *csrC* promoter activity but seems to be important for post-transcriptional regulation of CsrC synthesis as shown for YmoA. Still, in the absence of YmoA, only *hns* overexpression led to an increase of *csrC*(+81)-*lacZ* expression to wild type levels and fully complemented the effect of YmoA on CsrC synthesis. CsrB levels are reversely affected by H-NS which might be due to negative regulation by the CsrC RNA in *Y. pseudotuberculosis* (Heroven, *et al*. 2008; Fig. 37B).

Expression of truncated H-NS from *E. coli* strain EPEC activated *ymoA* transcription in *Y. enterocolitica* (Banos, *et al*. 2008). To test whether H-NS regulates CsrC synthesis by altering YmoA protein levels, the dominant-negative H-NS' protein was overproduced in *Y. pseudotuberculosis* wild type (YPIII p*hns*') and YmoA protein levels in this strain were compared to the wildtype (YPIII) or an H-NS overexpressing strain (YPIII p*hns*$^+$). As shown in Fig. 38, YmoA protein levels were strongly increased in the presence of dominant-negative H-NS' protein whereas overexpression of *hns* completely abolished YmoA synthesis. These data suggest that YmoA protein levels are negatively regulated by H-NS. Therefore, this influence of H-NS on *ymoA* expression does not explain CsrC levels in a *ymoA* mutant when overexpressed (Fig. 38).

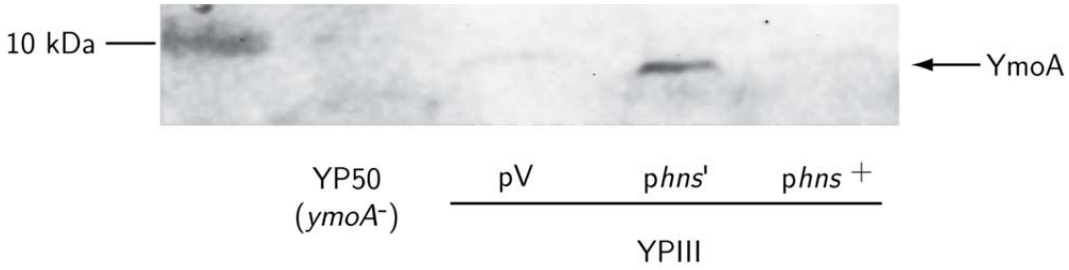

Fig. 38. H-NS represses YmoA synthesis. *Y. pseudotuberculosis* YPIII and YP50 (*ymoA*$^-$) harboring an empty vector pV (pAKH85), p*hns*' (pAKH31) or p*hns*$^+$ (pAKH74) were cultivated overnight in LB medium at 25°C. Samples were withdrawn, the OD_{600nm} was adjusted and whole cell extracts were prepared. Proteins were separated by 20% TRICINE gel electrophoresis and YmoA was visualized by immunoblotting using a specific polyclonal anti-YmoA antibody. A molecular weight ladder was loaded on the left. The YmoA protein is marked by an arrow.

H-NS has previously been shown to bind to the *rpoS* mRNA and the DsrA regulatory RNA in *E. coli* (Brescia, *et al*. 2004). In order to clarify whether a direct interaction of H-NS with the CsrC RNA is responsible for the activation of CsrC synthesis, purified CsrC RNA transcript was incubated with increasing concentrations of C-terminally His-tagged H-NS (pAKH11) purified from *E. coli* strain KB4 Δ*hns*Δ*stpA*Δ*hha* deficient of all *E. coli* H-NS and YmoA homologous proteins. 5S RNA was included in the binding assay as a negative control.

Although high concentrations of H-NS were applied (8.4 to 33.2 µM) no CsrC-H-NS complexes could be detected. At 66.4 µM of His-tagged H-NS protein, CsrC as well as the control 5S RNA were shifted. This suggested, that H-NS binds unspecifically to CsrC and the 5S RNA at high H-NS concentrations. No defined RNA-protein complexes could be observed because of H-NS oligomerization to the RNAs seemed to occur at different degrees resulting in multiple complexes of varying sizes in low concentrations. These cannot be easily detected

in the RNA band shift assay. As a result, H-NS action on CsrC in a *ymoA* mutant appears to be indirect (Fig. 39).

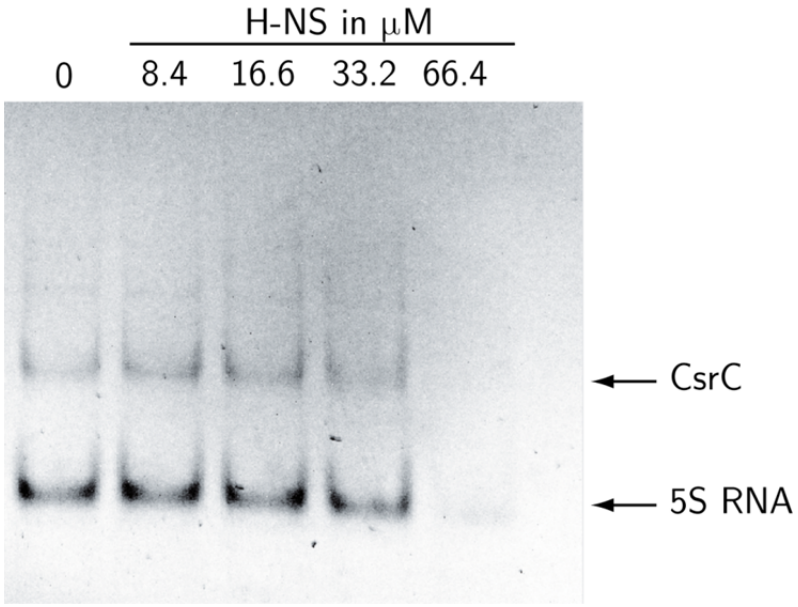

Fig. 39. H-NS binds unspecifically to the CsrC RNA. *In vitro* transcribed CsrC RNA and 5S rRNA were incubated with purified C-terminal His-tagged H-NS protein in increasing concentrations of 8.4, 16.6, 33.2 and 66.4 μM for 30 min at room temperature (lane 2 to 5). As a control, CsrC and 5S rRNA were incubated with 1 x RNA-bandshift buffer (lane 1). Samples were separated by 8% non-denaturing polyacrylamide electrophoresis and visualized by SybrGreen staining under UV light.

To summarize, the synthesis of the regulatory RNA CsrC in *Y. pseudotuberculosis* underlies transcriptional and post-transcriptional control by at least four regulators. The RNA chaperone Hfq upregulates *csrC* gene expression. By binding to the CsrC RNA, CsrA prevents its degradation and is further sequestered from stimulating RovM production. H-NS can indirectly activate CsrC synthesis. The nucleoid-associated protein YmoA is stable at moderate temperatures due to reduced degradation by ATP-dependent ClpP/Lon proteases. YmoA supports production of the major early virulence factor invasin by impairing degradation of CsrC via an unknown pathway. Thereby *rovA* expression is activated and expression of early virulence factors is established at low temperatures.

Tight temperature and growth phase regulation of YmoA lead to the hypothesis that high YmoA levels during exponential growth phase in nutrient-rich medium at 25°C are also important to repress expression of later-stage virulence functions, which are not synthesized under these conditions, for example those expressed from the *Yersinia* virulence plasmid pYV.

3.2 Virulence factor expression during late phase of infection

After penetration of the M-cells and attachment to the underlying Peyer's patches, Y. *pseudotuberculosis* switches its virulence factor expression. The synthesis of invasin is turned off. Instead, the nonfimbrial *Yersinia* adhesin A, YadA, is produced to enable host cell adhesion. Furthermore, a type III secretion system and Yersinia outer proteins (Yops) are synthesized, secreted by this system and injected into professional phagocytes of the host. These factors enable the bacterium to circumvent the host immune system and ensure dissemination into other organs like liver, spleen and kidney. Expression of the virulence factors encoded by the *Yersinia* virulence plasmid pYV occurs under the control of the AraC-like transcriptional activator LcrF (VirF) mainly during exponential growth in minimal medium and at higher temperatures when YmoA production is repressed. The following experiments were performed to address whether LcrF synthesis is controlled by YmoA in response to environmental signal.

3.2.1 The nucleoid-associated protein YmoA represses *lcrF* expression from a promoter upstream of *yscW*

In *Y. enterocolitica*, expression of the late virulence factors YadA, the *Yersinia* enterotoxin Yst, several Yops and their transcriptional activator LcrF were induced in a *ymoA* mutant (Cornelis, *et al*. 1991). In *Y. pseudotuberculosis*, *yadA* expression was shown to be activated during exponential growth, in minimal medium and at 37°C, conditions under which YmoA synthesis is repressed (Fig. 29). Gene transcription of *yadA* occurs only in the presence of LcrF (W. Opitz, unpublished data). To check, whether YmoA influences LcrF synthesis in *Y. pseudotuberculosis* at 25°C and 37°C, expression of a plasmid-encoded translational *lcrF*'-'*lacZ* fusion (pSF3), encoding 526 bp upstream of the *lcrF* gene and 74 bp of the *lcrF* coding sequence, was analyzed in *Y. pseudotuberculosis* wild type (YPIII) and the *ymoA* mutant strain (YP50). To overexpress *ymoA* and to complement the mutation in a *ymoA*-deficient strain, the *ymoA*$^+$ plasmid (pAKH71) was introduced into strains YPIII and YP50. β-galactosidase activity was measured from overnight cultures at 25°C and 37°C. Furthermore, whole cell extracts were prepared from *Y. pseudotuberculosis* YPIII (wild type) and YP50 (*ymoA*$^-$)to detect LcrF protein levels.

As shown in Fig. 40A, *lcrF*'-'*lacZ* was not expressed in the wild type and *ymoA* mutant strains at 25°C or 37°C. In contrast, the LcrF protein could be clearly detected in whole cell extracts of a *ymoA* mutant at 25°C while LcrF was absent in the wild type strain. At 37°C, LcrF production was significantly increased in the wild type and the *ymoA* mutant whereby overall levels of LcrF protein were higher in the *ymoA*-deficient strain (Fig. 40B).

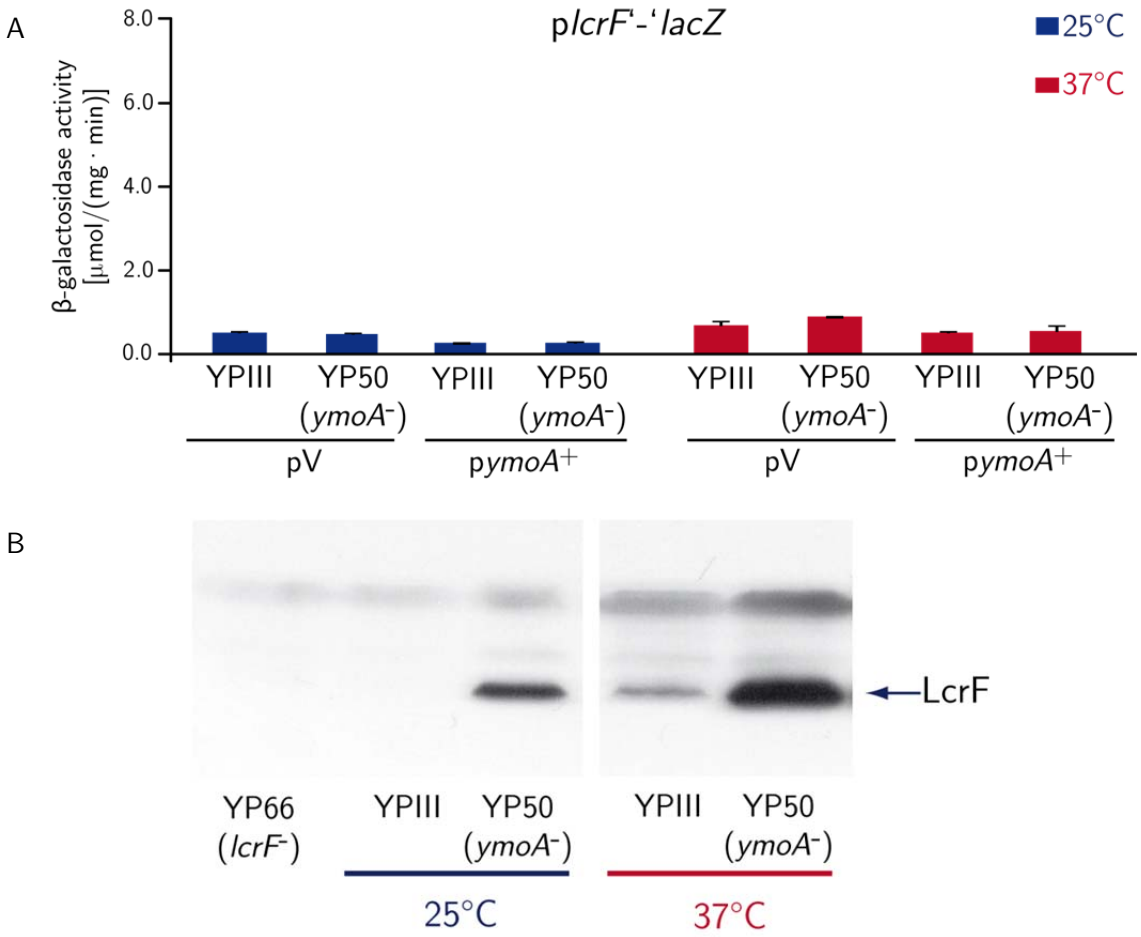

Fig. 40. LcrF synthesis is repressed by YmoA. A. *Y. pseudotuberculosis* YPIII and YP50 (*ymoA*⁻) which express a translational *lcrF*'-'*lacZ* fusion (pSF3) and carry an empty vector pV (pAKH85) or p*ymoA*⁺ (pAKH71) were grown overnight at 25°C and 37°C. β-galactosidase activity was measured and is given in µmol/(min · mg). The data represent the mean ± standard deviation of three independent experiments, each performed in duplicate. B. Whole cell extracts from overnight cultures at 25°C and 37°C of *Y. pseudotuberculosis* YPIII (wild type) and YP50 (*ymoA*⁻) and YP66 (*lcrF*⁻) were prepared and proteins were separated by 12% SDS gel electrophoresis. Immunoblotting was performed using a specific anti-LcrF polyclonal antibody. The LcrF protein is marked by an arrow.

These data suggest that LcrF production is repressed in the presence of YmoA at 25°C. Due to rapid degradation of YmoA at 37°C, *lcrF* expression is increased at higher temperatures. Interestingly, a temperature-induced expression of *lcrF* also occurs in the absence of YmoA, indicating an additional mechanism of LcrF synthesis control. Low expression of a *lcrF*'-'*lacZ* fusion at both temperatures further indicates that the upstream fragment of *lcrF* used for the construction of the *lcrF*'-'*lacZ* fusion might miss the promoter region. Analysis of the 526 bp region upstream of the *lcrF* gene revealed an open reading frame starting at position -499 to position -124 relative to the *lcrF* start codon. The gene product of the upstream gene which has been described as *yscW* (*virG*) is implicated in the localization and oligomerization of the type III secretion component YscC in the outer membrane. The *yscC* gene is transcribed in the same direction as *lcrF* (Allaoui, *et al*. 1995a; Burghout, *et al*. 2004) indicating that both genes might form an operon. In fact, in *P. aeruginosa*, homologs of *yscW* and *lcrF* called *exsB* and *exsA* have shown to be expressed in an operon (Yahr and Frank 1994). For this reason, a

translational *lacZ* fusion was constructed encoding 573 bp upstream of the *yscW* gene, *yscW*, the intergenic region between *yscW* and *lcrF* as well as 74 bp of the *lcrF* 5' end to determine whether *lcrF* was transcribed under the control of the *yscW* promoter region (Fig. 41A). A plasmid-encoded copy of the *yscWlcrF*'-'*lacZ* fusion (pSF4) was introduced into the YPIII (wild type) and also into YP50 (*ymoA*$^-$) in order to analyze the influence of YmoA on *yscW* expression. In addition, *ymoA* was expressed in trans (pAKH71) in both strains to test *yscWlcrF*'-'*lacZ* expression at high YmoA levels. At 25°C, *yscWlcrF*'-'*lacZ* expression was 3fold induced in the *ymoA* mutant compared to the wild type whereas overexpression of *ymoA* led to a complete repression of the fusion construct. Furthermore, a ten times higher activity of the *yscWlcrF*'-'*lacZ* fusion was observed in the wild type at 37°C. Loss of *ymoA* stimulated activity additionally by about 2.5fold whereas overexpression of *ymoA* led to a strong reduction of the promoter activity down to about 5% in both (Fig. 41B). The overall activity of the *yscWlcrF*'-'*lacZ* fusion was significantly increased.

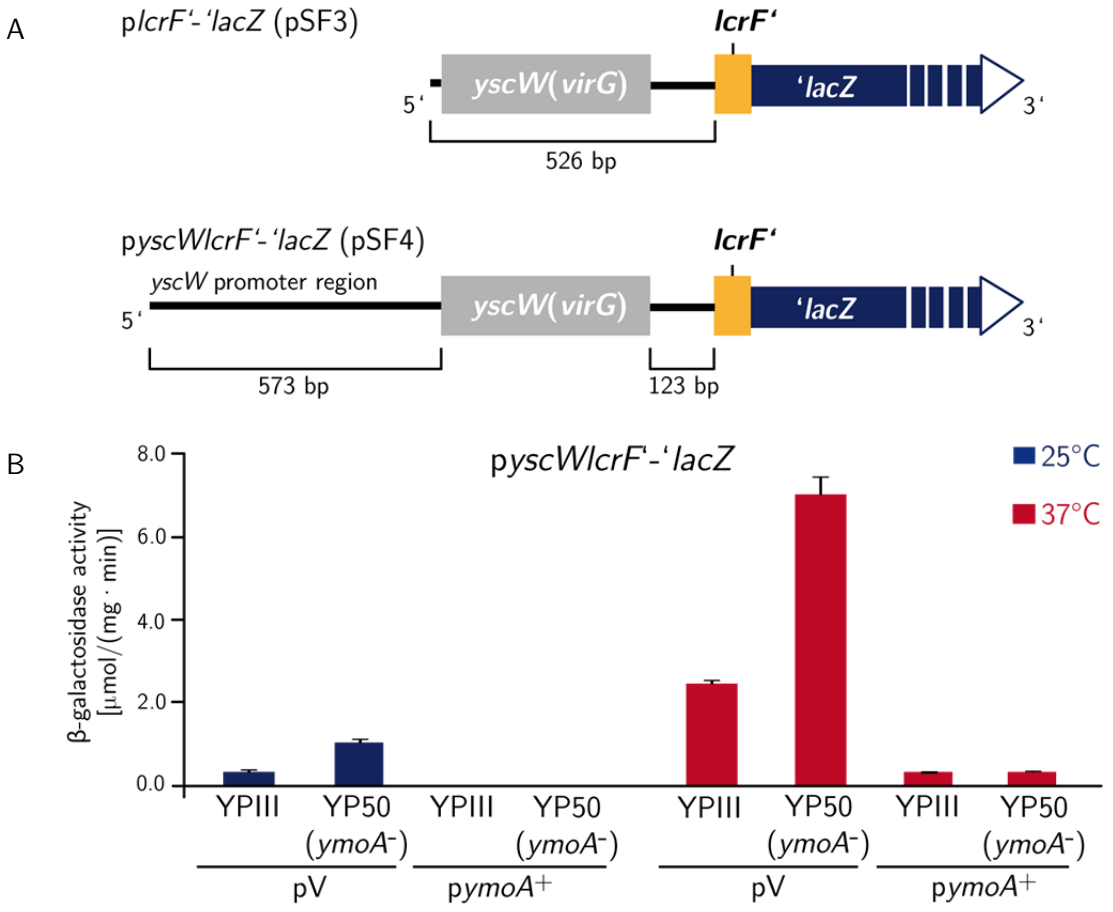

Fig. 41. YmoA represses transcription of the *yscWlcrF* operon. A. Translational *lcrF*'-'*lacZ* and *yscWlcrF*'-'*lacZ* fusions constructed to determine the influence of YmoA on *lcrF* expression. B. Plasmids encoding the *lcrF*'-'*lacZ* (pSF3) and *yscWlcrF*'-'*lacZ* (pSF4) were introduced into *Y. pseudotuberculosis* YPIII and YP50 (*ymoA*$^-$) carrying an empty vector pV (pAKH85) or p*ymoA*$^+$ (pAKH71). Samples were from overnight cultures at 25°C and 37°C and β-galactosidase activity was measured. The enzyme activity is given in µmol/(min · mg). The data represent the mean ± standard deviation of three independent experiments, each performed in duplicate.

This experiment demonstrated that expression of *lcrF* occurs from a promoter region upstream of the *yscW* gene, and YmoA represses the transcription of the putative *yscWlcrF* operon.

To analyze in more detail how YmoA represses *yscWlcrF* transcription, *yscWlcrF*'-'*lacZ* fusions with varying promoter lengths were constructed and introduced into *Y. pseudotuberculosis* YPIII (wild type) and the YP50 (*ymoA*$^-$). The reporter gene fusion contained inserts starting at position -573 (pKB34), -466 (pKB39), -368 (pKB40), -267 (pKB41), -171 (pKB42), -73 (pKB43) and -8 (pKB38) relative to the start codon of the *yscW* gene, followed by the *yscW* gene, the intergenic region and 74 bp of the 5' end of *lcrF*. Strains were cultivated overnight at 25°C, and β-galactosidase activity was monitored. The activity of the *yscW* promoter was maximal when the promoter region encompasses 368 bp of the upstream region of the *yscW* gene (Fig. 42). In comparison, fusions harboring 573 bp or 466 bp upstream of the *yscW* gene exhibited a lower activity of about 50% indicating that a negative regulator might interact upstream of position -368. This component does not seem to be YmoA as all fusions harboring regulatory sequences to position -368, -466 and -573 are 2 to 3fold higher expressed in the *ymoA* mutant background. Thus, YmoA must repress *yscWlcrF* expression through a DNA segment located further upstream of position -573. Transcription of fusions with promoter fragments of only 267 bp or less were not or only very weakly expressed independent whether YmoA was present or not. This indicated that either the promoter is located upstream of position -267 or that a positive regulator is required to induce *yscWlcrF* expression (Fig. 42).

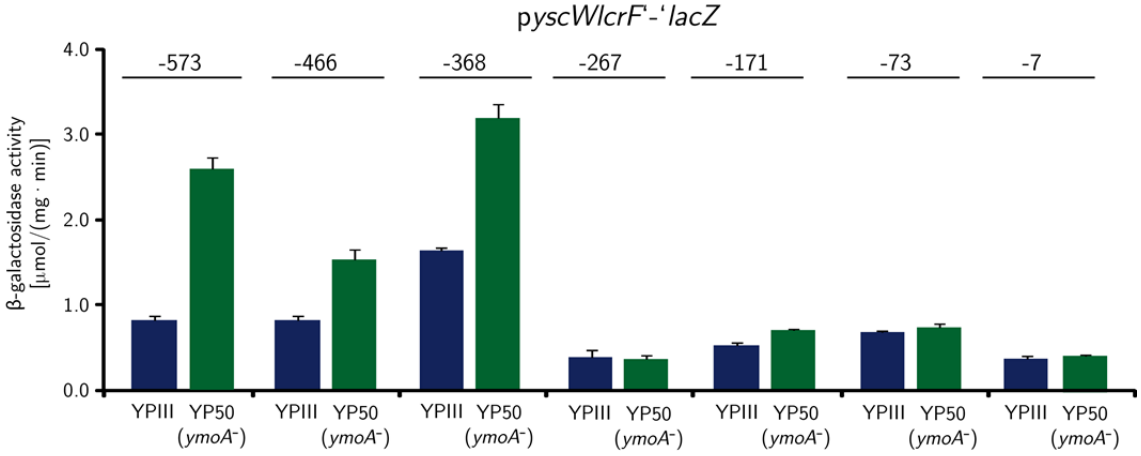

Fig. 42. Expression of the *yscWlcrF* operon is regulated by YmoA. *Y. pseudotuberculosis* YPIII and *ymoA* mutant strain YP50 haboring *yscW*(-573)*lcrF*'-'*lacZ* (pKB34), *yscW*(-466)*lcrF*'-'*lacZ* (pKB39), *yscW*(-368)*lcrF*'-'*lacZ* (pKB40), *yscW*(-267)*lcrF*'-'*lacZ* (pKB41), *yscW*(-171)*lcrF*'-'*lacZ* (pKB42), *yscW*(-73)*lcrF*'-'*lacZ* (pKB43) and *yscW*(-8)*lcrF*'-'*lacZ* (pKB38) fusion plasmids were cultivated overnight in LB medium at 25°C. β-galactosidase activity is given in µmol/(min · mg). The data represent the mean ± standard deviation of three independent experiments, each performed in duplicate.

Taken together, expression studies indicated, that the 5' end of the *yscWlcrF* transcript is located relatively far, between 267 and 367 bp, upstream of the *yscW* start codon. The nucleoid-associated protein YmoA still represses transcription of *yscWlcrF* harboring regulatory sequences up to position -573 upstream of the *yscW* gene. This suggested that a

YmoA-responsible site is located upstream of position -573. Interestingly, deletion of a promoter region upstream of position -466 relative to the *yscW* start codon resulted in lower levels of *yscWlcrF* transcription, indicating the influence of an additional repressing factor.

3.2.2 *yscWlcrF* transcription is influenced by a *Yersinia*-specific regulator

To analyze whether *yscWlcrF* transcription is regulated by a *Yersinia*-specific factor, the *yscW*(-573)*lcrF*'-'*lacZ* fusion (pSF4) was introduced into *E. coli* K12 strain MC4100 and its expression was compared to *Y. pseudotuberculosis* YPIII (wild type) at 25°C and 37°C.
The *yscWlcrF*'-'*lacZ* expression levels were strongly reduced in *E. coli* strain MC4100 relative to the expression in *Y. pseudotuberculosis* wild type at 25°C and 37°C, but a 2 to 3fold increase of the activity of the fusion was observed when the environmental temperature was increased (37°C)(Fig. 43).

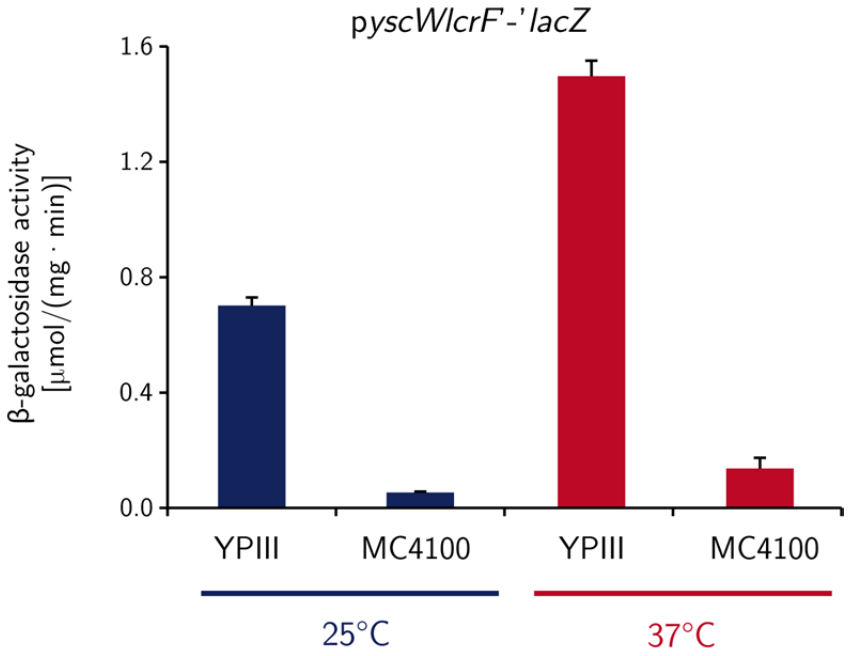

Fig. 43. Expression of *yscWlcrF* is strongly repressed in *E. coli*. *Y. pseudotuberculosis* YPIII and *E. coli* K12 strain MC4100 harboring the plasmid-encoded *yscWlcrF*'-'*lacZ* fusion (pSF4) were cultivated overnight in LB medium at 25°C and 37°C. The β-galactosidase activity was determined and is given in µmol/(min · mg). The data represent the means ± standard deviation of three independent experiments, each performed in duplicate.

Low expression of the *yscWlcrF*'-'*lacZ* fusion in *E. coli* indicates that a *Yersinia*-specific factor is essential for *yscWlcrF* transcription. As some temperature induction of *yscWlcrF* could still be detected in *E. coli*, a control mechanism might be present which is conserved in *Yersinia* and *E. coli*.

Further, it was investigated, whether LcrF is autoregulated. AraC-type proteins were often found to negatively regulate their expression by binding to the RNA polymerase interaction site within their own promoter region (Lee, *et al*. 1981). An *yscWlcrF*'-'*lacZ* encoding plasmid (pSF4) was transformed into the *Y. pseudotuberculosis* YPIII (wild type) and YP66 (*lcrF*$^-$). Expression of the *yscWlcrF*'-'*lacZ* fusion was identical in the wild type and the *lcrF* mutant, which indicates that LcrF does not autoregulate its transcription (Fig. 44A).

In the next step, influence of the *Yersinia* virulence plasmid pYV on *yscWlcrF* expression was tested, which might harbor regulatory components controlling the major transcriptional activator of virulence plasmid-encoded pathogenesis genes. *Y. pseudotuberculosis* YPIII (wild type) and the wild type strain YP12 cured of pYV were transformed with the *yscWlcrF*'-'*lacZ* fusion plasmid (pSF4) and expression of *yscWlcrF*'-'*lacZ* fusion was measured in overnight cultures grown at 37°C.

In the absence of pYV, transcription levels of *yscWlcrF*'-'*lacZ* were reduced to about 50% compared to YPIII harboring pYV. This suggests that a regulator is encoded by pYV which activates gene expression of *yscWlcrF* (Fig. 44B).

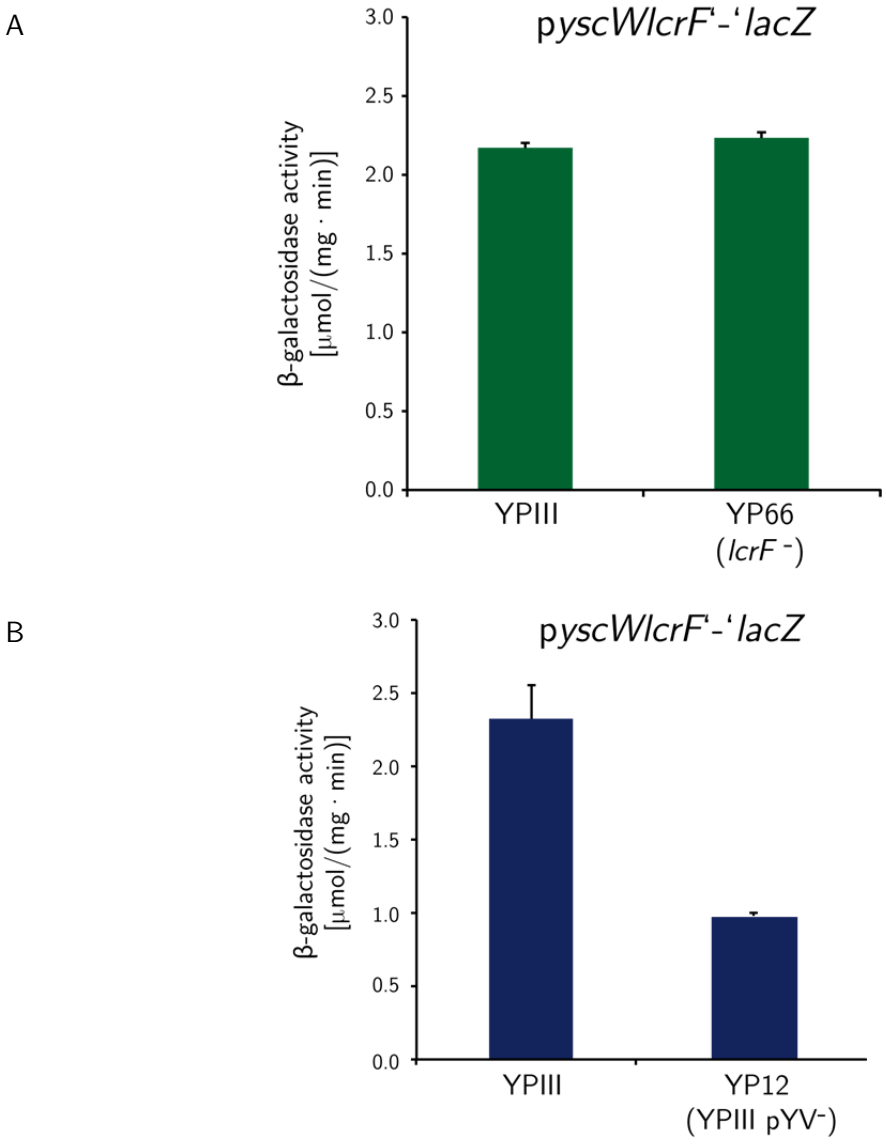

Fig. 44. *lcrF* expression is not autoregulated but activated by a factor encoded on the virulence plasmid. (A) *Y. pseudotuberculosis* YPIII and YP66 (*lcrF*⁻) or (B) YPIII and YP12 (YPIII pYV⁻) haboring an *yscWlcrF*'-'*lacZ* (pSF4) fusion were cultivated in LB medium overnight at 37°C. The β-galactosidase activity was determined and is given in µmol/(min · mg). The data represent the mean ± standard deviation of three independent experiments, each performed in duplicate.

3.2.3 LcrF translation is thermoregulated

Thermoregulation of *yscWlcrF* expression was still observed in *E. coli* or in a *ymoA* mutant strain of *Yersinia* (Fig. 43, Fig. 41). This indicated that besides regulation by YmoA another temperature-dependent control mechanism must affect *lcrF* expression. To test whether this control system affects *yscWlcrF* on the transcriptional or post-transcriptional level, the promoter region upstream of *yscW* was exchanged by a thermo-independent P_{BAD} promoter (Fig. 45A). The P_{BAD}::*yscWlcrF*'-'*lacZ* fusion encoded on pED10 was transformed into *Y. pseudotuberculosis* YPIII (wild type) and the *E. coli* K12 strain MC4100 and β-galactosidase activity was determined from overnight cultures at 25°C and 37°C. Transcription from the P_{BAD} promoter was induced with 0.2% arabinose.

Expression of P_{BAD}::*yscWlcrF*'-'*lacZ* in *Y. pseudotuberculosis* was induced 5fold at 37°C compared to 25°C. In *E. coli*, the overall expression level was reduced, but the activity of the fusion was also increased about 4fold at 37°C (Fig. 45B).

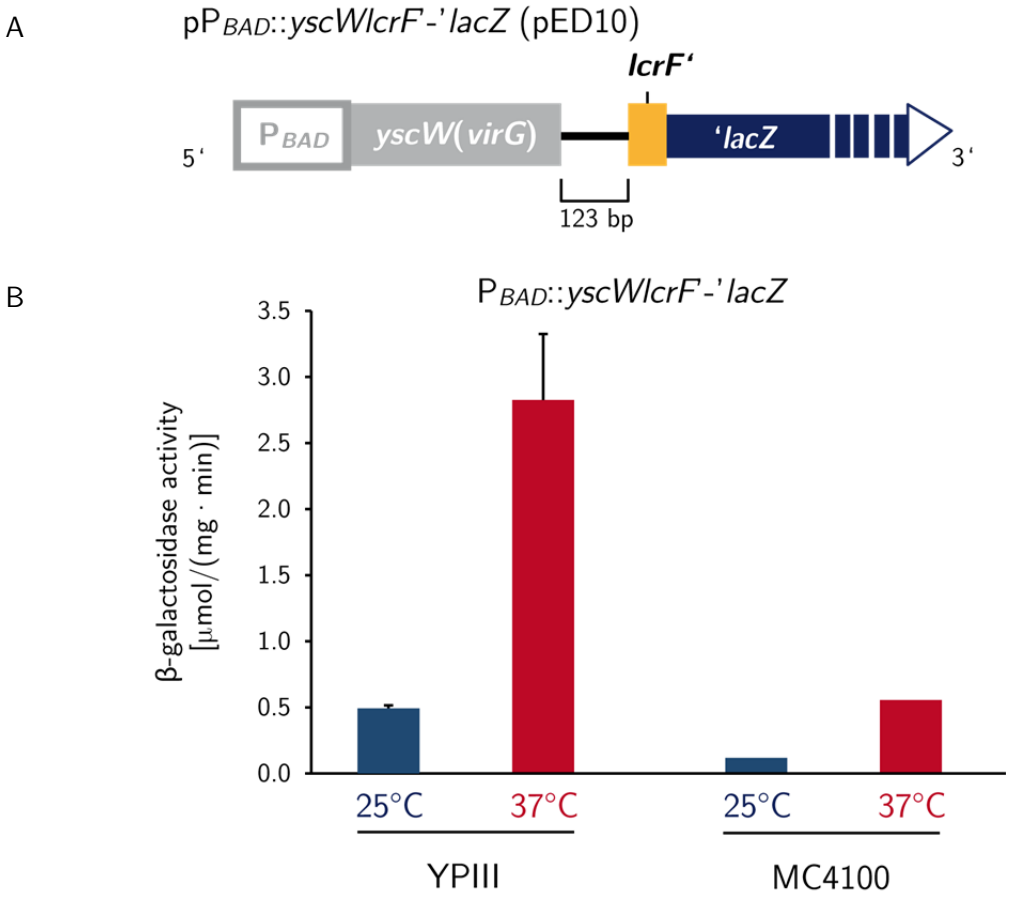

Fig. 45. *lcrF* expression is temperature-regulated independent of the *yscW* promoter. A. Schematic representation of pED10 harboring the *yscWlcrF*'-'*lacZ* expression under the control of the inducible P_{BAD} promoter. B. To measure P_{BAD}::*yscWlcrF*'-'*lacZ* expression, pED10 was introduced into *Y. pseudotuberculosis* YPIII and the *E. coli* K12 MC4100 and grown overnight in LB medium with 0.2% arabinose at 25°C and 37°C. The β-galactosidase activity was determined and is given in µmol/(min · mg). The data represent mean values ± standard deviation of three independent experiments, each performed in duplicate.

Despite of the use of a different promoter, *yscWlcrF*'-'*lacZ* was still controlled by temperature, in *Y. pseudotuberculosis* and *E. coli* K12 (Fig. 45). This suggests that thermodependency is not controlled on the transcriptional level but is regulated post-transcriptionally by a different unknown mechanism. To more elucidate the region which might be responsible for thermoregulation of *yscWlcrF*'-'*lacZ* expression, the intergenic region between *yscW* and *lcrF* with additional 74 nt of the *lcrF* 5' end was fused to the *lacZ* reporter gene and transcribed from the P_{BAD} promoter (pKB14). Expression of the fusion was determined at 25°C and 37°C in LB medium supplemented with 0.2% arabinose to induce P_{BAD} expression. Furthermore, a P_{BAD}::*gnd*'-'*lacZ* fusion (pED05) encoding the 5' untranslated region (UTR) of the thermo-independently expressed gluconate-phosphate dehydrogenase was transformed to proof that the inducible promoter P_{BAD} is independent of the growth temperature when used in wild type strain YPIII (Fig. 46A). Expression of P_{BAD}::*gnd*'-'*lacZ* at 25°C and at 37°C was identical, demonstrating that transcription from P_{BAD} is not affected by temperature. In contrast, expression of P_{BAD}::*lcrF*(-123)'-'*lacZ* was about 5fold induced at 37°C compared to 25°C (Fig. 46B).

This strongly suggests that temperature-regulation of *lcrF*'-'*lacZ* is independent of the *yscWlcrF* promoter and occurs on the post-transcriptional level implicating elements of the intergenic region between *yscW* and *lcrF* or the *lcrF* 5' untranslated region (UTR).

A

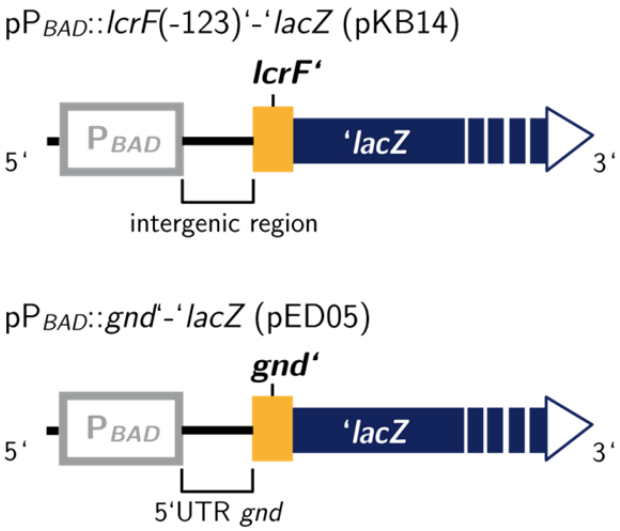

B

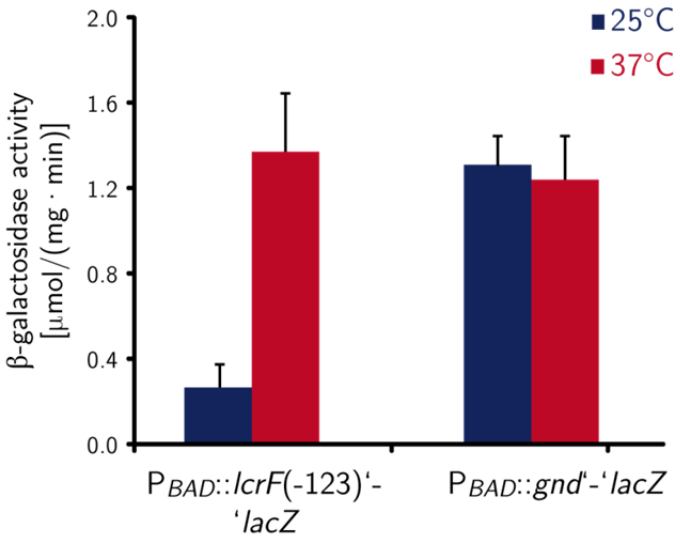

Fig. 46. Thermoregulation of LcrF synthesis involves a mechanism located in the *lcrF* 5' untranslated region. A. pP$_{BAD}$::*lcrF*(-123)'-'*lacZ* (pKB14) and pP$_{BAD}$::*gnd*'-'*lacZ* (pED05) constructs used to determine the temperature-dependent expression of the *lcrF* 5' UTR. B. *Y. pseudotuberculosis* YPIII was transformed with pKB14 and pED05 and cultivated overnight in LB medium with 0.2% arabinose at 25°C and 37°C. The β-galactosidase activity was determined and is given in µmol/(min · mg). The data represent mean values ± standard deviation of three independent experiments, each performed in duplicate.

3.2.4 Secondary structure analysis of the *Y. pseudotuberculosis* LcrF RNA reveals a FourU motif

Hoe and Goguen (1993) hypothesized that LcrF translation in *Y. pestis* is controlled by a secondary structure formation in the 5' untranslated region (UTR) of the *lcrF* RNA. The secondary structure of the *Y. pseudotuberculosis lcrF* RNA transcribed from the 123 nt intergenic region between *yscW* and *lcrF* elongated by 10 nt of the *lcrF* coding sequence was analyzed by the RNA structure prediction tool Mfold (Zuker 2003; http://mfold.bioinfo.rpi.edu/). The most probable secondary structure revealed that the RNA of the intergenic region forms two major hairpins. The first hairpin comprises 57 nucleotides, which show three base pairing regions, interrupted by three single-stranded loop sections consisting of six to nine nucleotides and a bulged uracil 61 bases upstream of the start codon. From the first hairpin a long stretch of 11 unpaired nucleotides leads to hairpin II, which comprises nucleotides -44 to +2 relative to the *lcrF* start codon. This second hairpin contains AU-rich sequences, which undergo base pair formation in three sections. Base pairing regions are connected by single or double unpaired nucleotides forming only small loops in the predicted secondary structure. The start codon itself is partially involved in the formation of the stem. Cornelis (1989) proposed a putative Shine-Dalgarno sequence for the *lcrF* homologous gene *virF* in *Y. enterocolitica* where an AGGA motif is located 14 to 17 nucleotides upstream of the *virF* start codon. A similar ribosomal binding site was also found in the *lcrF* RNA at the same distance. This AGGA motif was included in the stem formation of hairpin II and was predicted to interact with a sequence of four uracils (Fig. 47).

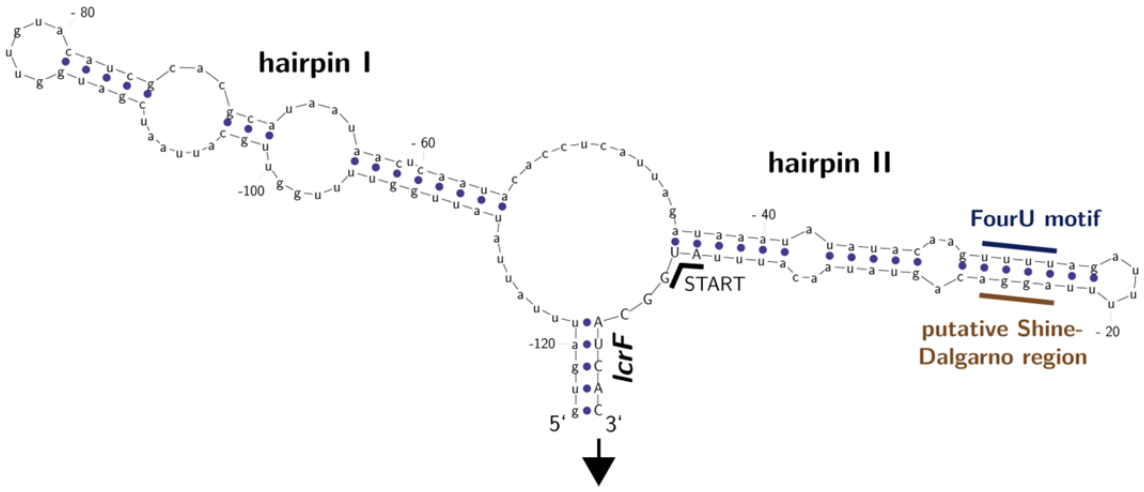

Fig. 47. The 123 nt *lcrF* 5' UTR is predicted to form two hairpin structures. The secondary structure of the *lcrF* 5' UTR was generated using Mfold which applies a free energy minimization algorithm to RNA sequences (Zuker *et al.*, 1999; http://bioweb.pasteur.fr/seqanal/interfaces/mfold-simple.html). For the prediction, parameters were set to default. The most probable prediction with the lowest free energy is shown. Blue circles represent base pairing. START indicates the start codon of the *lcrF* coding region. The putative Shine-Dalgarno (SD) sequence is given in brown. The FourU motif (blue) comprises the AGGA motif of the SD sequence paired with four uracils. Numbers indicate nucleotides relative to the *lcrF* start codon.

3.2.5 The FourU motif within the LcrF 5' UTR functions as an RNA thermometer

Interaction of four uracils with Shine-Dalgarno sequences in a stem-loop-like RNA structure has been described as a so-called FourU thermometer and was found to regulate translation of the *agsA* RNA in response to temperature (Waldminghaus, *et al*. 2007). Formation of the secondary structure and thereby sequestration of the Shine-Dalgarno sequence through imperfect base pairing to the FourU motif at low temperatures impaired translation initiation. High temperatures eliminated the base pairing and, as a result, liberated the ribosomal binding site. This allows translation initiation by ribosome-RNA-interaction.

To test whether elements of the *lcrF* 5' UTR are essential for the temperature regulation of LcrF synthesis, a sequence of hairpin II predicted to base pair with the start codon and the Shine-Dalgarno sequence (Δ-44 to -25) was deleted from P_{BAD}::*lcrF*(-123)'-'*lacZ*. In addition, a *lcrF-lacZ* fusion derivative was constructed in which sequences from -13 to -64 implicated in hairpin I formation were eliminated. The resulting fusion constructs (pP_{BAD}::*lcrF*(-123)'-'*lacZ*(Δ-44 to -25) (pKB13) and pP_{BAD}::*lcrF*(-63)'-'*lacZ* (pKB18)) were introduced into *E. coli* K12 strain DH5αZ1 and cultivated overnight at 25°C and 37°C. The P_{BAD} promoter was induced by 0.2% arabinose and β-galactosidase activity was measured. While expression of the intact *lcrF* 5' UTR was five times induced at 37°C compared to 25°C, deletion of the region from -44 to -25 upstream of the *lcrF* gene led to a significant change of *lcrF* expression. Expression of the fusion was strongly induced at 25°C whereas expression was slightly reduced by about 30% at 37°C. The activity of the *lcrF-lacZ* fusion missing the first hairpin was found to be 2fold upregulated at 25°C. At 37°C, *lcrF-lacZ* expression was still

increased compared to 25°C but the overall expression was somewhat lower in comparison to the intact *lcrF-lacZ* fusion construct (Fig. 48).

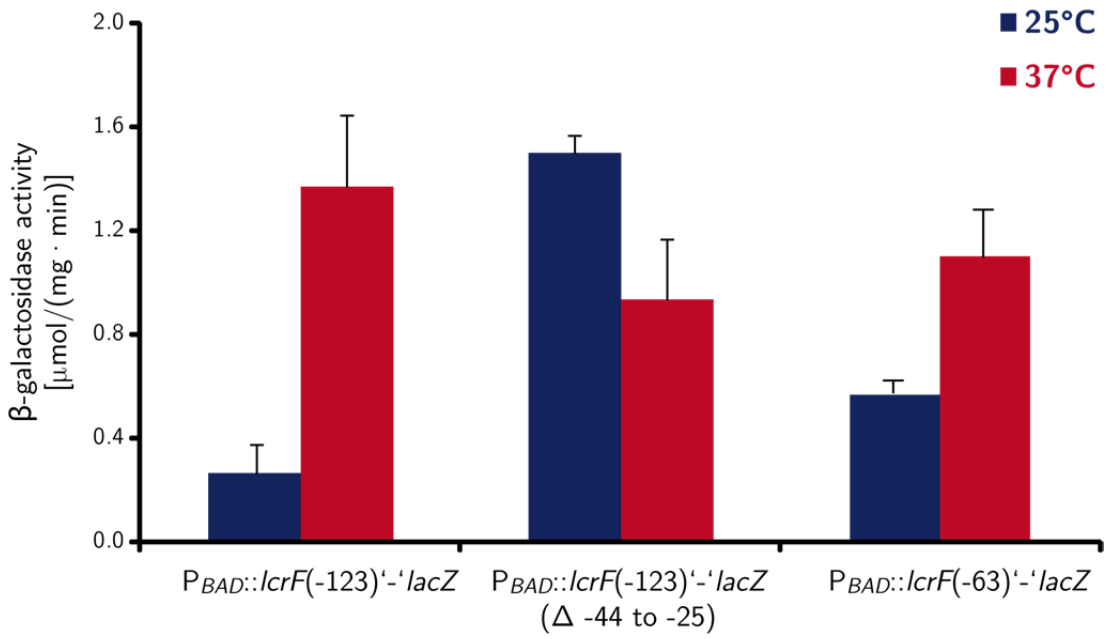

Fig. 48. Deletions of hairpin I or II in the 5' UTR of *lcrF* cause changes in the thermoregulation. *E. coli* K12 strain DH5αZ1 was transformed with pP$_{BAD}$::*lcrF*(-123)'-'*lacZ* (pKB14), pP$_{BAD}$::*lcrF*(-123)'-'*lacZ*(Δ-44 to -25) (pKB13) or pP$_{BAD}$::*lcrF*(-63)'-'*lacZ* (pKB18). Strains were grown overnight at 25°C and 37°C in LB medium supplemented with 0.2% arabinose. The β-galactosidase activity was determined and is given in µmol/(min · mg). The data represent the mean ± standard deviation of three independent experiments, each performed in duplicate.

A deletion of sequences implicated in the formation of the stem structure in hairpin II which undergoes base pair interaction with the start codon and the Shine-Dalgarno sequence resulted in derepression and a temperature-independent translation of *lcrF.* Ribosomes seem to have full access to their target site. Loss of hairpin I still allowed thermo-dependent *lcrF* expression, but expression levels were significantly increased at 25°C and the ratio between expression at 25°C and 37°C was reduced. This indicates that not only hairpin II containing the FourU motif but the entire secondary structure formed by the 123 nt *lcrF* 5' UTR is responsible for tight *lcrF* thermoregulation.

To further analyze the importance of single and double-stranded RNA regions within the second stem-loop structure of the *lcrF* 5' UTR for thermoregulation, different nucleotide exchanges were introduced into the P$_{BAD}$::*lcrF*(-123)'-'*lacZ* fusion construct. According to the secondary structure prediction, an exchange of GUU at position -30 to -28 to AAA (pED07) and of AUA at position -36 to -34 to CCC (pED13) should reduce complementarity and abolish stem formation. In contrast, perfect base pairs were introduced by changing AG to CC at position -46 and -45 (pED06) and UU to CC at position -28 and 27 (pED08) (Fig. 49A). These modified and an unmodified P$_{BAD}$::*lcrF*(-123)'-'*lacZ* fusions were introduced into *E. coli* K12 DH5αZ1 and β-galactosidase activity was determined from overnight cultures induced with 0.2% arabinose at 25°C and 37°C.

An exchange of GUU (-30 to -28) to AAA completely abolished temperature regulation and led to identical expression rates at 25°C and 37°C which were slightly lower than expression of

the intact *lcrF-lacZ* fusion at 37°C. The AUA to CCC substitution at positions -36 to -34 resulted in a high expression of *lcrF-lacZ* at 25°C. The overall expression was identical to the unmodified *lcrF-lacZ* fusion at inducing temperature of 37°C. AUA-GGG exchange led to a reduction of the expression at 37°C (Fig. 49B).

In contrast, *lcrF-lacZ* expression was completely impaired at all temperatures when complementarity of the sequence of hairpin II was increased by exchanging AG (-46/-45) with CC and UU (-28/-27) with CC (Fig. 49C).

A

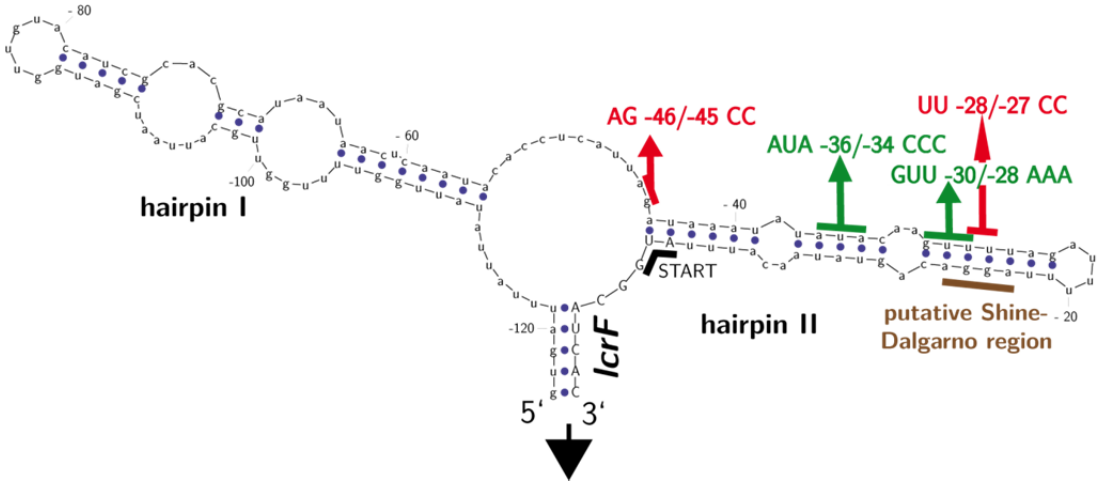

B

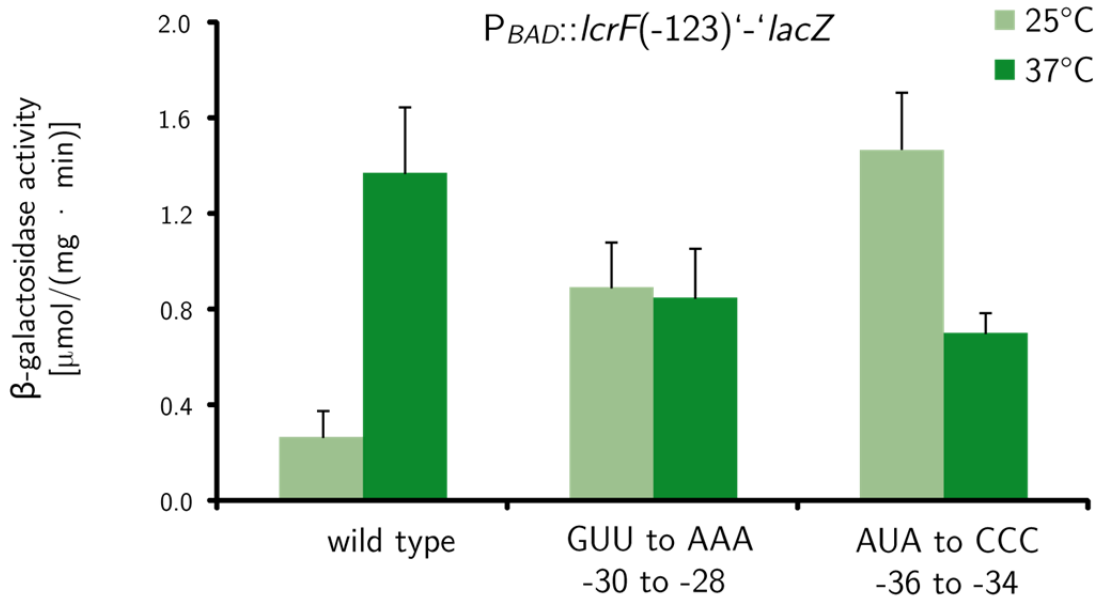

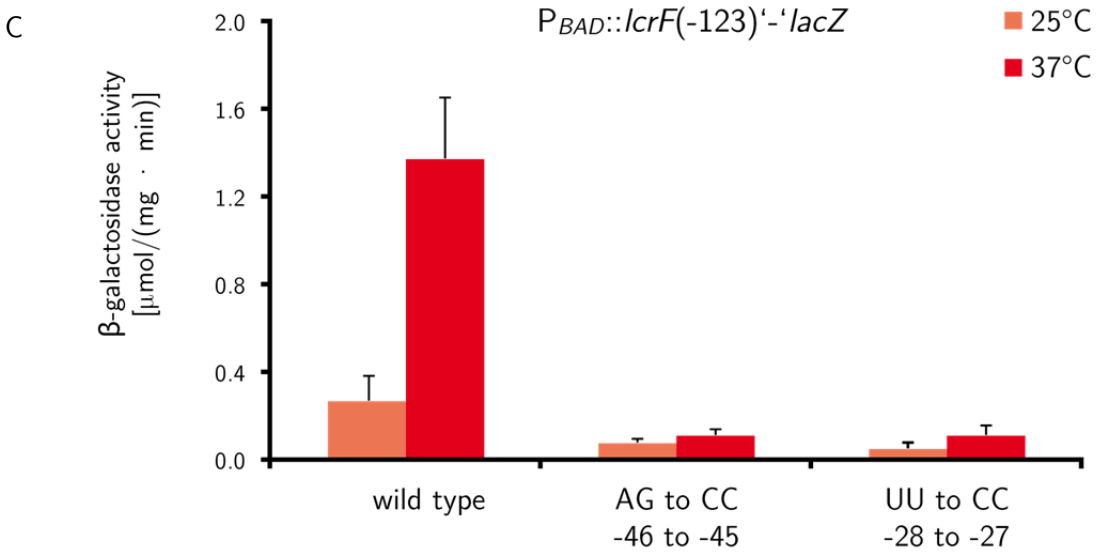

Fig. 49. Mutations within the 5' UTR of *lcrF* change thermoregulation of LcrF synthesis. (A) Base exchanges leading to increased complementarity are marked in red, whereas mutations impairing base pair formation are indicated in green. Blue circles represent base pairing. START indicates the start codon of the *lcrF* coding region. The putative Shine-Dalgarno sequence is marked in brown. The FourU motif is labeled in blue. Numbers indicate nucleotides relative to the *lcrF* start codon. (B) P$_{BAD}$::*lcrF*(-123; GUU -30/-28 AAA)'-'*lacZ* (pED07) and P$_{BAD}$::*lcrF*(-123; AUA -36/-24 CCC)'-'*lacZ* (pED13) or (C) P$_{BAD}$::*lcrF*(-123; AG -46/-45 CC)'-'*lacZ* (pED06) and P$_{BAD}$::*lcrF*(-123; UU -28/-27 CC)'-'*lacZ* (pED08) fusion plasmids were transformed into *E. coli* K12 strain DH5αZ1. Strains were cultivated overnight in LB medium with 0.2% arabinose at 25°C and 37°C. β-galactosidase activity was determined and is given in µmol/(min · mg). The data represents the mean ± standard deviation of three independent experiments, each performed in duplicate.

As a conclusion, mutations which were introduced to destabilize the secondary structure formation of hairpin II of the *lcrF* 5' UTR showed a significant loss of temperature-dependent expression of *lcrF*. Base pair substitutions at these positions seem to resolve the stem formation of hairpin II at or close to the ribosomal binding site which induce *lcrF* expression at low temperatures. On the other hand, nucleotide substitutions in predicted single-stranded regions designed to allow perfect base pairing abolished *lcrF* expression. This indicates that a stable double-stranded RNA structure is formed even at 37°C. Thus, perfect complementarity within the FourU motif towards perfect base pairing with the Shine-Dalgarno sequence completely prevented *lcrF* expression. This suggests that imperfect UG base pairs formed by the FourU motif are essential for proper temperature regulation. These results needs to be further studied by *in vitro* assays.

3.2.6 *In vitro* analysis of the *lcrF* 5' UTR

To proof the predicted secondary structure of the *lcrF* 5' UTR, RNA structure probing was performed. To do so, the 123 bp 5' UTR plus ten nucleotides of the *lcrF* coding region were transcribed *in vitro*, radioactively labeled and incubated at 25°C and 37°C. RNA samples were probed using RNase V1, which cleaves double-stranded RNA regions, and RNase T1 cleaving RNA at the 5' end of single-stranded guanines (G).

The 5' UTR of *lcrF* revealed many cleavage sites of RNase V1. Sites of about one to three nucleotides protected against RNase V1 digestion are located at positions -109, -102

to -100, -93 to -92, -73 to -72, -57 to -56 and -46 to -45 relative to the *lcrF* start codon. Larger sites of about nine to ten nucleotides not influenced by this RNase were found at about -86 to -78 and -19 to -9. These double-stranded regions were not affected by temperature changes, since a temperature shift from 25°C to 37°C did not significantly change the cutting pattern of RNase V1. RNase T1 cut single-stranded Gs at positions -102, -101, -85, -82, -45, -24 and -11. RNase T1 cleavage at other positions was due to unspecific digestion with preference for adjacent single-stranded adenines (A). At 25°C, accessibility of single-stranded Gs was significantly reduced compared to 37°C resulting in lower amounts of RNase T1 cleavage products. In particular, G-16 and G-15 showed partial protection to RNase T1 cleavage at 25°C, whereas they were greatly accessible at 37°C (Fig. 50).

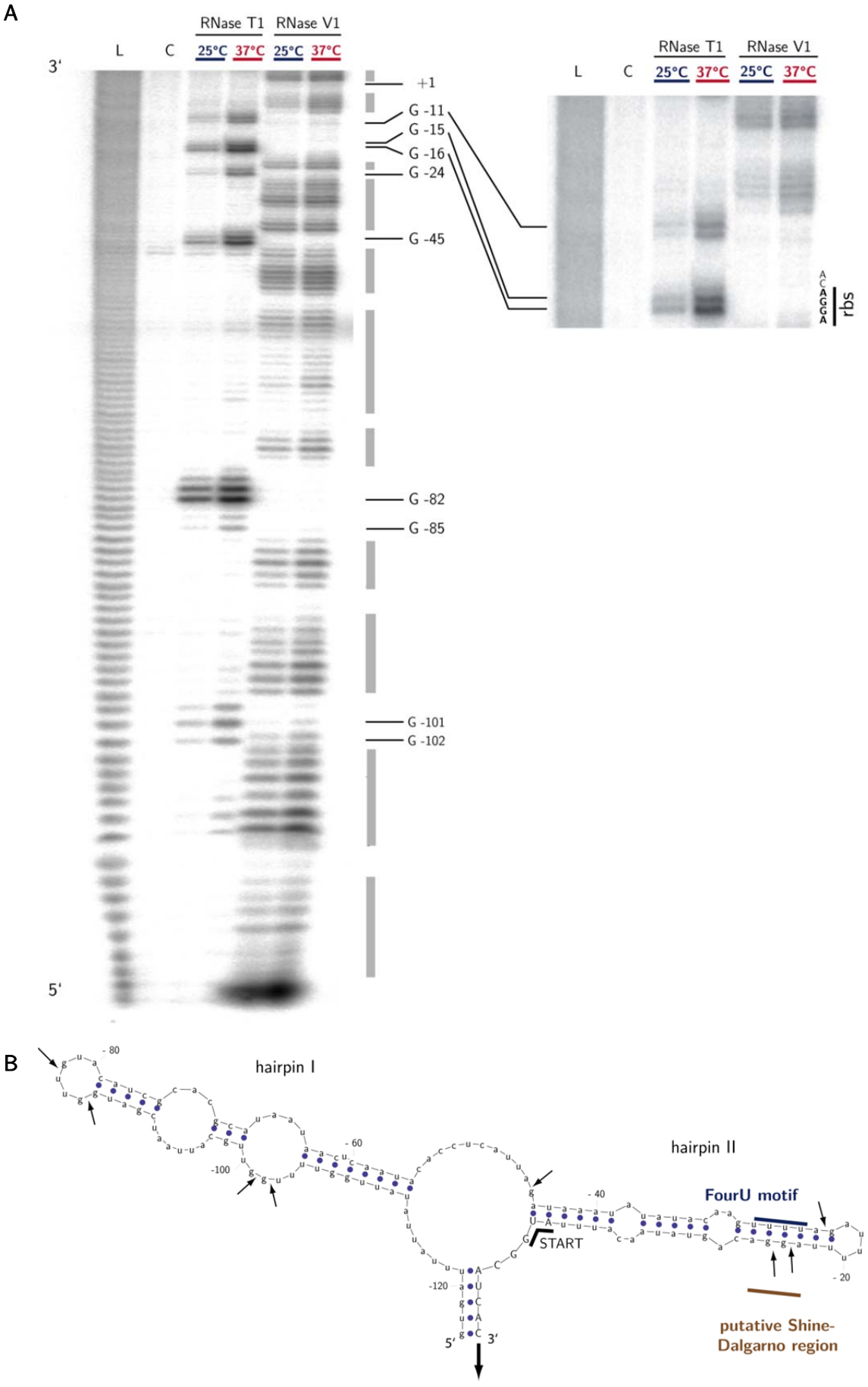
A
RNase T1
RNase V1
L
C
25°C
37°C
25°C
37°C
3'
5'
+1
G -11
G -15
G -16
G -24
G -45
G -82
G -85
G -101
G -102
rbs
B
hairpin I
hairpin II
- 80
- 60
-100
- 40
-120
- 20
START
FourU motif
putative Shine-
Dalgarno region
5'
3'

Fig. 50. The 5' UTR of *lcrF in vitro* exhibits minor structural changes upon temperature shift from 25°C to 37°C. A. The *lcrF* 5' UTR (-123 to +10 relative to the *lcrF* start codon) was enzymatically probed at 25°C and 37°C using RNase T1 (ss G, 0.001 U/µl) and RNase V1 (ds RNA, 0.0002 U/µl). RNA fragments were separated by 8% polyacrylamide gel electrophoresis. Lane C contains the incubation control without RNase. The alkaline reference ladder is loaded in Lane L. Selected nucleotides represent RNase T1 cleavage sites and are marked with arrows. Grey bars label RNase V1 cleavage sites. On the right, the 3' end is magnified. The ribosomal binding site is indicated by "rbs". B. Secondary structure of the *lcrF* 5' UTR predicted by Mfold. Arrows indicate 5' ends of guanines cleaved by RNase T1. Blue circles represent base pairing. START indicates the start codon of the *lcrF* coding region. The putative Shine-Dalgarno sequence is marked in brown. The FourU motif is labeled in blue. Numbers indicate nucleotides relative to the *lcrF* start codon.

Long stretches of RNase V1 cleavage products indicate that large parts of the 5' UTR represent base paired regions, interrupted by only small bulges and loops. Interestingly, RNA structure probing of the *lcrF* 5' UTR exhibited only small structural rearrangements within a very limited region during the temperature shift from 25°C to 37°C (Fig. 50). These mainly occur within the Shine-Dalgarno sequence. At 37°C, the two Gs of the ribosomal binding site were found to be single-stranded to a higher degree than at moderate temperatures which indicates an opening of the region and better accessibility for ribosomes.

3.2.7 Translation initiation at the *lcrF* 5' UTR is thermo-dependent *in vitro*

RNA structure probing revealed only minor rearrangements in the *lcrF* 5' UTR structure upon a temperatures increase from 25°C to 37°C. In order to determine whether these are sufficient for ribosomal binding and translation initiation, toe printing experiments were performed. An RNA sequence comprising the *lcrF* 5' UTR and 63 nucleotides of the coding region was synthesized *in vitro* and a primer complementary to the 3' end was annealed. The subsequent primer extension inhibition reaction, using initiator $tRNA_f^{Met}$ in the presence or absence of 30S ribosomal subunits isolated from *E. coli*, was carried out at 25°C and 37°C.

At 25°C, full length transcript of the *lcrF* 5' UTR was observed at high concentrations in the presence or absence of 30S ribosomal subunits. In addition, some termination products were generated during the primer extension when no ribosomes were added at 25°C, suggesting that the reverse transcriptase might have fallen of the RNA because of a strong RNA secondary structure. In contrast to 25°C, the amount of full length transcript was considerably reduced at 37°C. Addition of ribosomes at 37°C led to an even stronger decrease, but instead additional transcripts were detected at positions corresponding to +18 to +14, representing a typical toe print (Fig. 51).

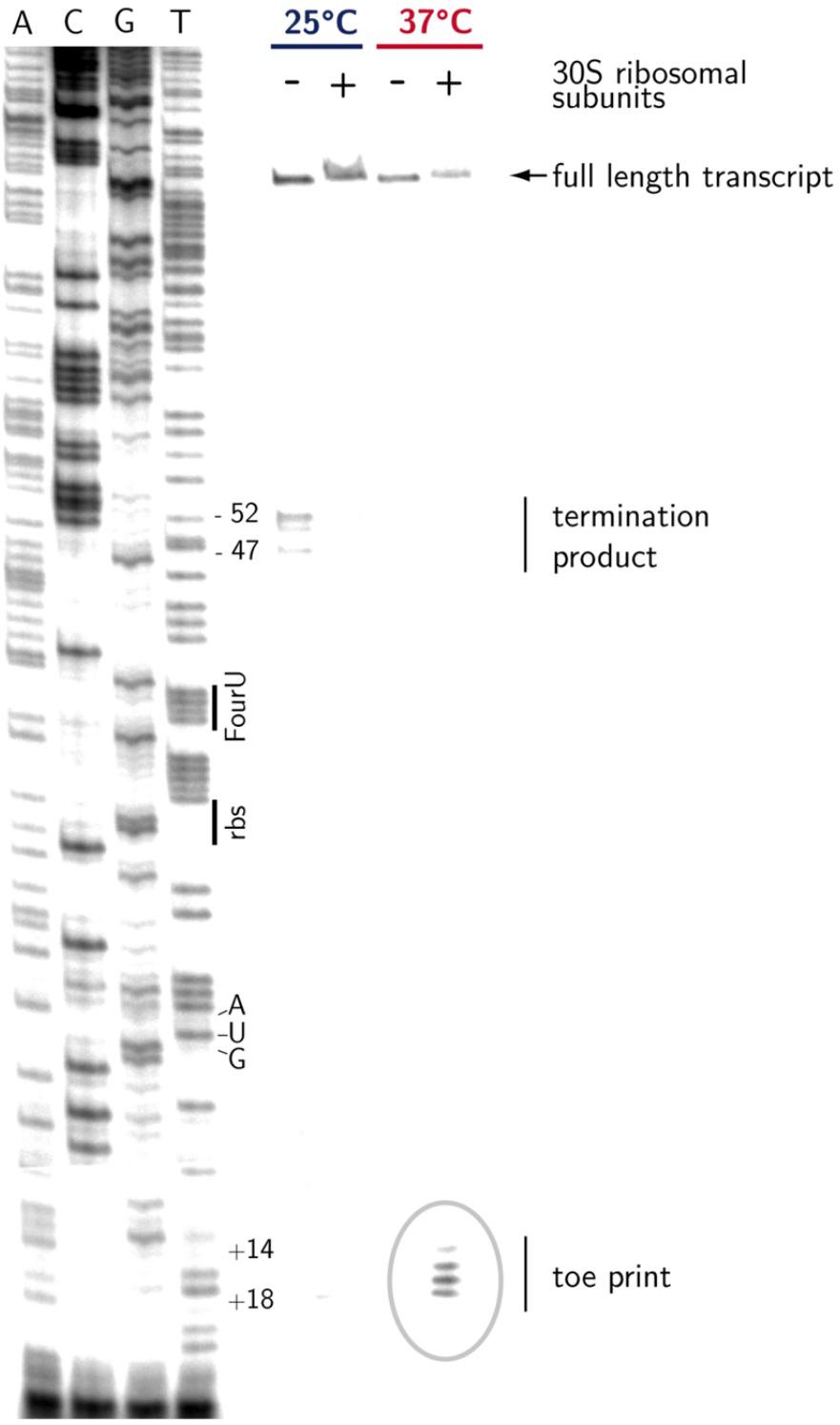

Fig. 51. 30S ribosomal subunits bind to the 5' UTR of *lcrF* at 37°C. *In vitro* transcribed RNA including the 5' UTR of *lcrF* (-123 to +63 relative to the *lcrF* start codon) was incubated with or without 30S ribosomal subunits (indicated above the gel) at 25°C and 37°C. Full length product, termination products and the "toe print" (encircled) of the primer extension inhibition experiment are indicated. The sequencing reaction (ACGT) was carried out with the same labeled primer used for the toe print experiment. The *lcrF* start codon AUG, the ribosomal binding site (rbs) and the FourU motif in the corresponding RNA sequence are marked. Numbers correspond to nucleotides relative to the start codon of *lcrF*.

In summary, addition of 30S ribosomal subunits to the *lcrF* 5' UTR resulted in the formation of an mRNA-ribosome-$tRNA_f^{Met}$ ternary complex which inhibited the primer extension at 37°C. At 25°C, only full length transcript was observed indicating that the binding site for the

ribosomes along the RNA was not accessible. In conclusion, access of the ribosomal binding site and so *lcrF* translation initiation is temperature-controlled. Even small temperature-induced changes within the secondary structure are sufficient to allow ribosome access and interaction with the Shine-Dalgarno sequence in the 5' UTR of *Y. pseudotuberculosis lcrF*.

3.2.8 Mutations in the FourU motif alter temperature-controlled accessibility of the Shine-Dalgarno sequence

The FourU motif and adjacent bases in the *lcrF* 5' UTR were mutated to determine whether the binding of ribosomes to the Shine-Dalgarno sequence at 25°C and 37°C was altered by nucleotide exchanges. Complementarity of the base pairing between the ribosomal binding site and the FourU region was increased by exchanging UU at positions -28 to -27 into CC (UU-28/-27CC). Furthermore, destabilizing mutations were introduced at positions -30 to -28, changing GUU into AAA (GUU-30/-28AAA). RNA structure probing with RNases V1 and T1 were performed at 25°C and 37°C with these variants which comprised the 5' UTR of *lcrF* and the following first ten bases of the 5' coding region (Fig. 49A).

Enzymatic probing within the region from +10 to -34 of the UU-28/-27CC RNA with improved base pairing displayed similar cleavage patterns at 25°C and 37°C. Strikingly, cleavage products of the RNase T1 at G-15 and G-16 were barely detectable and no differences were observed in the intensity of the products at 25°C and 37°C. RNase V1 cleavage in the region adjacent to the Shine-Dalgarno region was observed approx. at positions -34 to -33, -29 to -22, -20 to -19, -8 to -6 and upstream of +1 (Fig. 52A). In summary, strongly improving the complementarity of the FourU motif to the Shine-Dalgarno sequence reduced the ability of the two Gs within in the ribosomal binding site to become single-stranded at both, low and higher temperatures. In fact, melting and cleavage of the RNA at these two nucleotides was still strongly reduced at 37°C, suggesting that the complete secondary structure remained stable with increasing temperatures.

RNase V1 digestion of the *lcrF* 5' UTR with mutations GUU-30/-28AAA revealed many cleavage sites over longer regions but the concentration of the cleavage products due to the cleavage at positions -37 to -27, -18 to -17 and -13 to -10 was significantly reduced compared to the wild type. Positions -21 and -20 as well as position -6 to -1 exhibited a stronger accessibility to RNase V1 at 37°C than at 25°C. Cleavage of RNase T1 at single-stranded Gs or As was also observed in regions from -37 to -34, -18 to -15 and -12 to -7. Furthermore, position G-15 and G-16 displayed reduced protection against the digest by RNase T1 at 37°C as the intensity increased strongly compared to 25°C. Defined signals of the GUU-30/-28AAA RNA under control conditions were also detected at positions -37 to -34, -18 to -17 and -13 to -12 in the absence of RNases indicating that the secondary structure is generally less stable (Fig. 52B).

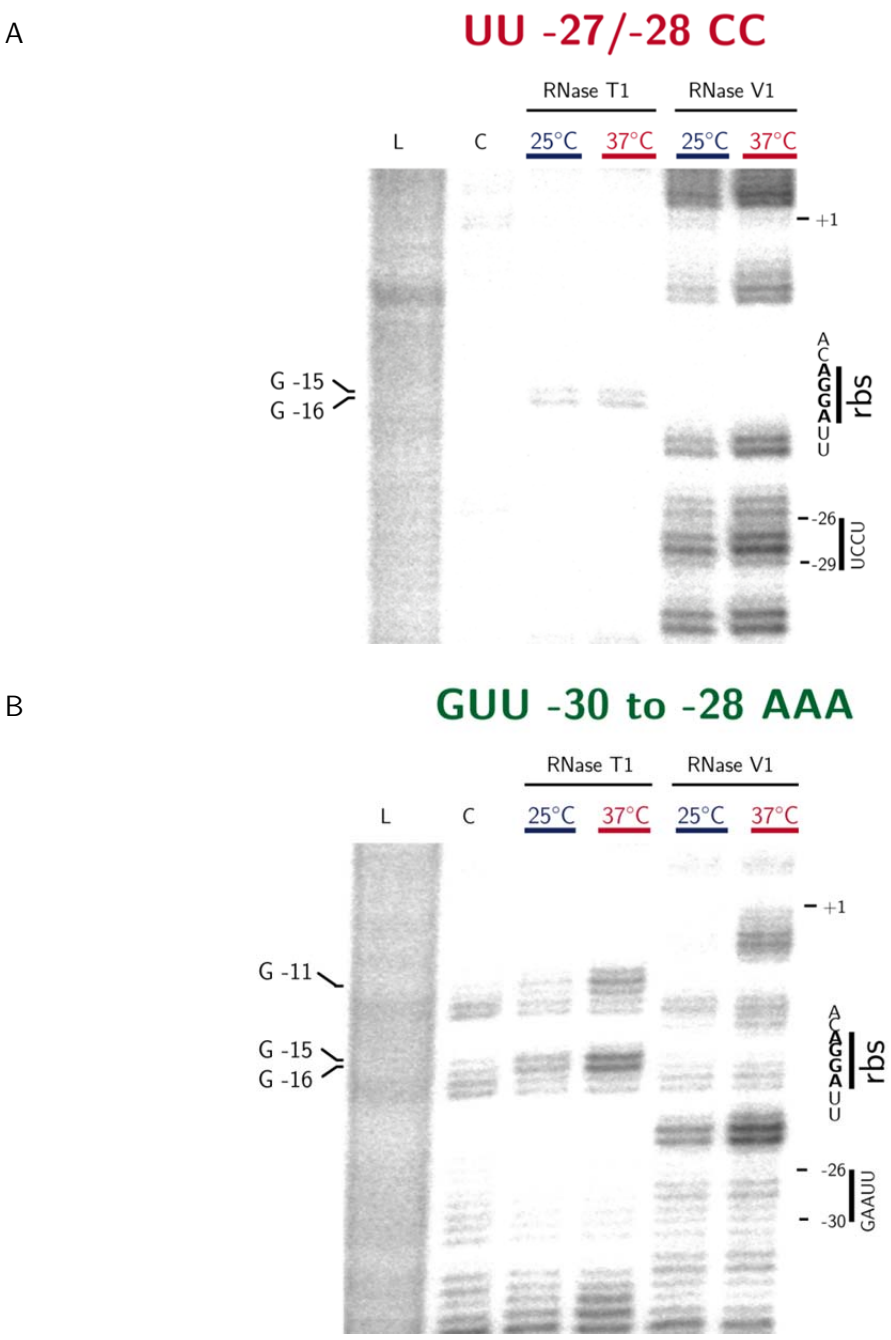

Fig. 52. Mutations within the FourU motif alter temperature-dependent structural rearrangements of the *lcrF* 5' UTR. RNA structure probing of the *lcrF* 5' UTR with nucleotide exchanges either at (A) UU-28/-27CC or (B) GUU-30/-28AAA were applied to enzymatic cleavage at 25°C and 37°C using RNase T1 (cuts ss G, 0.001 U/µl) and RNase V1 (cuts ds RNA, 0.0002 U/µl). RNA fragments were separated by 8% polyacrylamide gel electrophoresis. Cleavage products of the 3' end are shown. Lane C contains the RNA without addition of RNases. The alkaline reference ladder is loaded in lane L. Selected nucleotides represent RNaseT1 cleavage sites and are marked with arrows. Numbers indicate nucleotides relative to the *lcrF* start codon. The ribosomal binding site is indicated by "rbs" and partial sequences were applied to the gel.

Although the 5' UTR of *lcrF* with an exchange at GUU-30/-28AAA seems less stable, a different cleavage pattern with a shorter double-stranded region adjacent to the Shine-Dalgarno sequence was observed in the mutant compared to the wild type RNA. Reduced complementarity resulted in decreased stem structure formation within this region. This is

supported by the detection of single-stranded Gs in the ribosomal binding site, which occur at low and even more intense at 37°C. In contrast, two small regions upstream of the AGGA motif and a second further downstream towards the start codon revealed increased formation of double strands at 37°C which implies strong tension and topological rearrangements within the RNA molecule (Fig. 51).

In order to monitor the effect of structural changes of the *lcrF* 5' UTR caused by the stabilizing or destabilizing mutations on the formation of ribosome-RNA complexes, toe printing experiments were performed. To do so, primers were annealed to an *in vitro* transcript including the *lcrF* 5' UTR plus 63 nucleotides of the coding region with UU-28/-27CC or GUU-30/-28AAA mutations. 30S ribosomal subunits from *E. coli* and $tRNA_f^{Met}$ were added and the primer extensions were carried out at 25°C or 37°C. Primer extension of the UU-28/-27CC RNA at 25°C resulted in full length transcript as well as termination signals corresponding to positions from -12 to -14 and -50 to -51. This indicates the formation of a stable double-stranded region, which interferes with the primer extension reaction. Addition of ribosomes to the reaction reduced the amount of termination product but increased the concentration of full length transcript in comparison to the reaction without ribosomal subunits. At 37°C, mainly full length product was synthesized in the absence of ribosomes, although the overall amount of the transcript was generally low. Primer extension of UU-28/-27CC RNA at 37°C with ribosomes led to high concentrations of full length product, with similar termination products observed at 25°C. A very light toe print was only observed from incubation at 37°C with ribosomes, indicating that the Shine-Dalgarno sequence is weakly accessible to the ribosomes (Fig. 53).

Exchange of GUU (-30/-28) against AAA within the *lcrF* 5' UTR led to full length transcripts in the presence or absence of ribosomal subunits at 25°C. Primer extension of GUU-30/-28AAA RNA without ribosomes produced some transcripts terminating at positions -50 to -51 relative to the start codon. Strikingly, a weak toe print result was already observed at 25°C when the reaction was supplemented with ribosomes. The amount of toe print transcript increased strongly when primer extension was performed at 37°C in the presence of ribosomes. In this reaction, levels of full length transcript were reduced compared to that at 37°C without ribosomal subunits (Fig. 53).

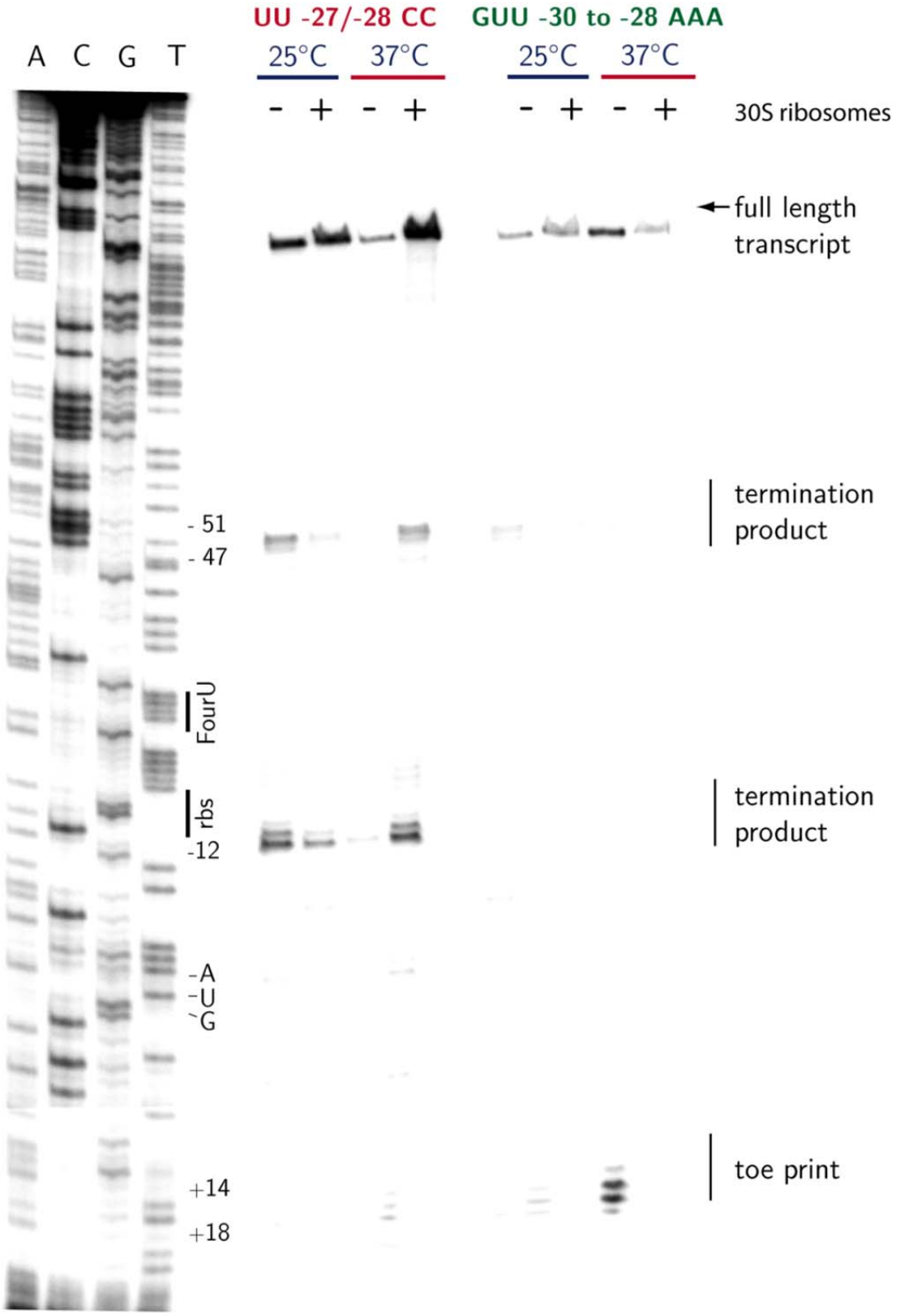

Fig. 53. Mutations within the 5' UTR of LcrF alter access of ribosomes to the Shine-Dalgarno sequence. *In vitro* transcribed 5' UTR of *lcrF* (-123 to +63 relative to the *lcrF* start codon) with mutations UU-28/-27CC (red) or GUU-30/-28AAA (green) were incubated with or without 30S ribosomal subunits (indicated above the gel) at 25°C and 37°C. Full length product, termination products and toe print signals of the primer inhibition experiment are indicated. The sequencing reaction (ACGT) was performed with the same labeled primer as for the toe print experiment. The *lcrF* start codon AUG, the ribosomal binding site (rbs) and the FourU motif in the corresponding RNA sequence are marked. Numbers correspond to nucleotides relative to the start codon of *lcrF*.

Introducing perfect base pairing between the FourU motif and the Shine-Dalgarno sequence in the *lcrF* 5' UTR led to a significant inhibition of primer extension at elevated temperatures. Formation of the mRNA-ribosome-$tRNA_f^{Met}$ ternary complex is impaired by the higher complementarity. The high amount of early termination transcripts further indicated a tight secondary RNA structure which interferes with the activity of the reverse transcriptase.
In contrast, imperfect base pairing by mutating GUU (-30/-28) to AAA within the FourU motif improved toe print formation. RNA-ribosome interaction and blockage of the extension reaction occurred already at moderate temperature and was considerably increased at 37°C. Ribosomes showed to have elevated access to the Shine-Dalgarno sequence, which is exposed due to inefficient base pairing already at 25°C.
In conclusion, *in vivo* expression as well as structural and mutational analysis of the *yscW-lcrF* intergenic region demonstrated that LcrF synthesis is temperature-regulated at two levels. YmoA controls transcription of the *yscWlcrF* operon in response to temperature changes. In addition, LcrF production is controlled by temperature on the post-transcriptional level by a FourU thermometer. At low temperatures, ribosomal access to the Shine-Dalgarno sequence is blocked by base pairing to a FourU motif. Increasing the temperature induces liberation of the ribosomal binding site by conformational alterations mainly within this region and allows access of the ribosomes. These small changes are sufficient to enable translation initiation for protein synthesis, although the entire structure is essential to allow optimal control of the *lcrF* 5' UTR.

3.2.9 The RNA chaperone Hfq activates LcrF synthesis in *Y. pseudotuberculosis*

In *Y. pestis*, the RNA chaperone Hfq was found to repress the expression of components of the type III secretion system, the Yop effector genes and their activator LcrF (Geng, *et al.* 2009). In contrast to *Y. pestis*, Hfq of *Y. pseudotuberculosis* strain IP32953 was shown to stimulate gene expression of these virulence factors (Schiano, *et al.* 2010). In order to determine the influence of Hfq on LcrF synthesis in *Y. pseudotuberculosis* YPIII, an *yscW*'-'*lacZ* fusion (pKB35) was introduced into wild type strain and the *hfq* mutant strain YP80 to monitor the Hfq effect on transcription of the *yscWlcrF* operon. For overexpression and complementation of *hfq*, an hfq^+ plasmid (pAKH115) was transformed into both strains and expression of the *yscWlcrF* fusion was determined in overnight cultures of the strains grown at 25°C and 37°C. Furthermore, whole cell extracts were prepared to determine LcrF protein production. At 25°C, *yscW-lacZ* expression in an *hfq* mutant was about 50% reduced compared to wild type, whereas *hfq* overexpression resulted in 1.3fold increase of transcription. Activity of the *yscW*'-'*lacZ* construct was slightly increased at 37°C independent of the amount of Hfq, indicating that Hfq has no major effect on the *yscW* promoter at this temperature (Fig. 54A). In contrast, LcrF protein synthesis was strongly activated in the absence of *hfq*, whereas overproduction of Hfq completely abolished LcrF synthesis (Fig. 54B).

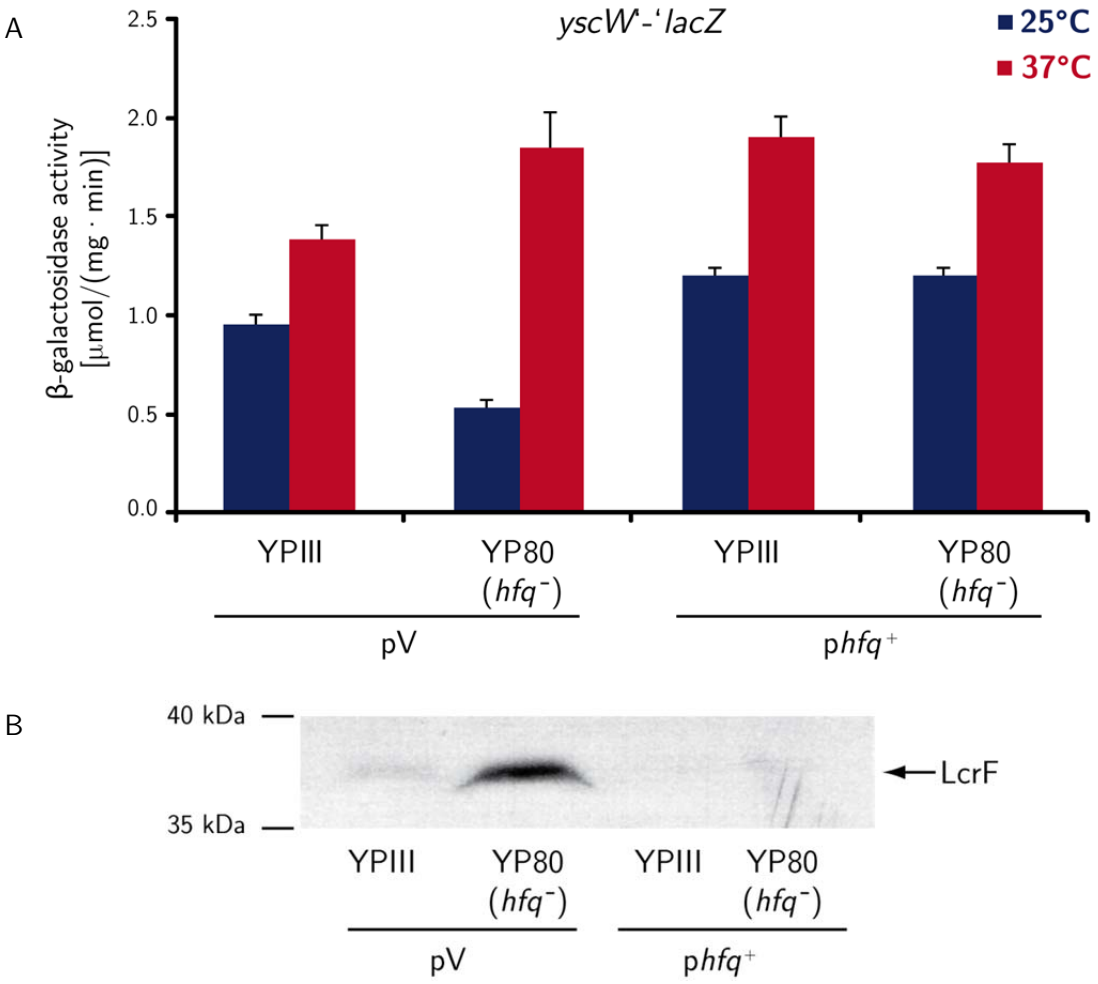

Fig. 54. Hfq activates expression of *yscW* at 25°C, but represses LcrF synthesis at 37°C. A. *Y. pseudotuberculosis* YPIII and YP80 (*hfq*⁻) harboring an *yscW*'-'*lacZ* fusion (pKB35) and an empty vector pV (pAKH85) or the *hfq*⁺ plasmid (pAKH115) were cultivated overnight in LB medium at 25°C and 37°C. β-galactosidase activity was measured and is given in µmol/(min · mg). The data represent the mean ± standard deviation of three independent experiments, each performed in duplicate. B. LcrF protein levels were monitored in *Y. pseudotuberculosis* YPIII and YP80 (*hfq*⁻) carrying an empty vector pV (pAKH85) or the *hfq*⁺ plasmid (pAKH115) grown overnight in LB medium at 37°C. Whole cell extracts were prepared and separated by 12% SDS gel electrophoresis. LcrF was detected by immunoblotting using a specific polyclonal antibody. A molecular weight marker was loaded and LcrF protein is labeled by an arrow.

Hfq seems to control LcrF production in *Y. pseudotuberculosis* YPIII at both, transcriptional and post-transcriptional level, in response to temperature. At 25°C, Hfq activates transcription of the *yscWlcrF* operon whereas no major influence of Hfq was observed at 37°C. In contrast, LcrF protein synthesis was strongly repressed by Hfq. This suggested a post-transcriptional mechanism of Hfq-mediated inactivation of LcrF synthesis. To further analyze this hypothesis, expression of a translational *yscWlcrF*'-'*lacZ* fusion (pKB34) including the 5' UTR of *lcrF* was studied in *Y. pseudotuberculosis* YPIII and YP80 (*hfq*⁻). To complement the *hfq* deletion, *hfq* was overexpressed from a plasmid (pAKH115). β-galactosidase activity was measured from overnight cultures at 25°C and 37°C. Transcription of the *yscWlcrF*'-'*lacZ* fusion was slightly reduced in an *hfq* mutant strain and somewhat higher expressed upon Hfq overexpression at

25°C very similar to the *yscW*'-'*lacZ* fusion at the same temperature (Fig. 54). Additional *hfq* expression enhanced *yscWlcrF*'-'*lacZ* expression approx. 1.7fold relative to wild type activity. However, this *yscWlcrF*'-'*lacZ* expression pattern was significantly different at 37°C. Loss of *hfq* led to a 2.5fold increase of *yscWlcrF*'-'*lacZ* expression and this phenotype could be complemented by overexpression of *hfq* (Fig. 55).

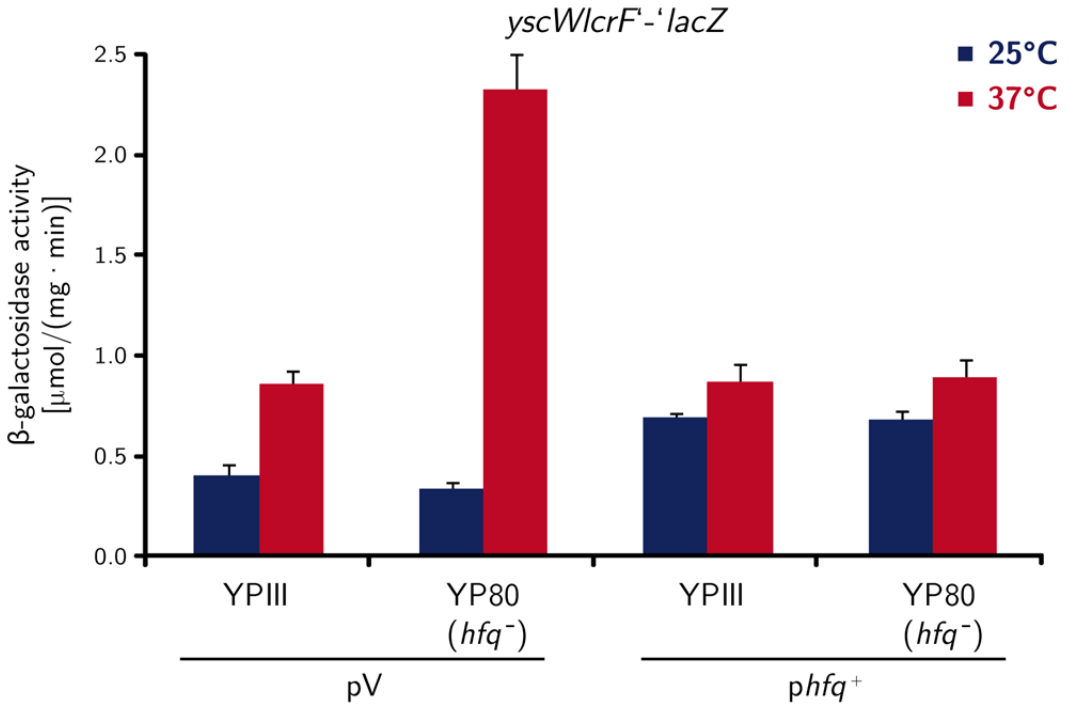

Fig. 55. Hfq represses LcrF synthesis at 37°C. Expression of an *yscWlcrF*'-'*lacZ* fusion (pKB34) in *Y. pseudotuberculosis* YPIII and YP80 (*hfq*⁻) carrying an empty vector pV (pAKH85) or the *hfq*⁺ plasmid (pAKH115) grown overnight in LB medium at 25°C and 37°C was determined by analysis of the β-galactosidase activity. Enzyme activity is given in µmol/(min · mg). The data represent the mean ± standard deviation of three independent experiments, each performed in duplicate.

In summary, Hfq seems to activate transcription of the *yscWlcrF* operon at moderate temperatures. At 37°C, however, Hfq was found to repress LcrF production on the post-transcriptional level. In particular, the region upstream of the *lcrF* coding region appears to be implicated in this control process.

LcrF synthesis in *Y. pseudotuberculosis* and activation of LcrF-controlled late virulence factors underlies a complex regulation in response to temperature. The nucleoid-structuring protein YmoA represses transcription of the *yscWlcrF* operon. Furthermore, a thermoswitch structure controls LcrF protein synthesis post-transcriptionally in response to temperature and the RNA chaperone Hfq affects LcrF production on both levels. This chromosomal factor upregulates *lcrF* gene transcription at 25°C but reversely represses LcrF synthesis, most probably by affecting the 5' untranslated region of *lcrF* at 37°C.

4 Discussion

4.1 YmoA activates *rovA* expression by stabilizing the CsrC RNA

An infection with *Y. pseudotuberculosis* depends on the efficient transition of the bacterium from the gut lumen through the epithelial cell layer to the underlying lymphatic tissues. To attach and invade into the M-cells within the gut epithelium, the pathogen expresses the outer membrane protein invasin (Inv) (Dersch and Isberg 1999; Dersch and Isberg 2000). Its production is activated by the global transcriptional activator RovA which is synthesized during growth in nutrient rich medium when the amount of the LysR-like repressor RovM is reduced (Heroven and Dersch 2006; Heroven, *et al*. 2004; Nagel, *et al*. 2003; Revell and Miller 2000). Under these conditions the regulatory RNA CsrC of the carbon storage regulator system is highly expressed and binds the RNA-binding protein CsrA, resulting in an inactivation of RovM synthesis (Heroven, *et al*. 2008). In a gene bank screen for additional *rovA* regulators, the nucleoid-associated protein YmoA, a member of the Hha-family, was also found to control *rovA* expression.

This study showed that YmoA in *Y. pseudotuberculosis* activates *rovA* indirectly and leads to upregulation of the RovA-dependent *inv* gene. Downregulation of *rovA* expression occured by stimulating the production of the LysR-type regulator RovM (Fig. 14 and Fig. 15). However, a previous study reported that YmoA represses *inv* expression in *Y. enterocolitica*, whereas *rovA* remained unaffected (Ellison and Miller 2006; Ellison, *et al*. 2003). In this study, a different strategy was used to eliminate YmoA function. An insertion was introduced into the open reading frame upstream of *ymoA*, designated "*ymoB"* in order to cause a polar effect on *ymoA* expression. Furthermore, a negative effect of YmoA on *Y. enterocolitica inv* expression was only observed when *ymoA* was overexpressed from a plasmid. In an earlier study, we could also show that overexpression of *ymoA* from a plasmid downregulated transcription from the *Y. pseudotuberculosis inv* promoter but not *rovA* expression (K. Böhme, unpublished data). These results are explained by unspecific effect accompanying overexpression of members of this protein family. For instance, in an *hha* mutant, YmoA was also able to repress transcription of *hlyCABD* when expressed from a midi-copy vector but not from a low-copy vector (Balsalobre, *et al*. 1996). This and other observations in our group indicate that multiple copies of the *ymoA* gene alter regulation patterns of multiple genes unspecifically. High YmoA concentrations were found to result in unspecific binding of YmoA to normally non-regulated promoters. Thus, balanced YmoA protein levels seem to be crucial for proper gene regulation in *Yersinia*.

Experiments in this work clearly demonstrated that YmoA-mediated activation of *rovA* expression is the result of YmoA-mediated repression of RovM production by upregulation of CsrC RNA levels (Fig. 17). Experimental data in this work demonstrated that YmoA stabilizes the CsrC RNA by an indirect mechanism, since direct RNA-protein interaction was not

observed (Fig. 26 and Fig. 28). Turnover of regulatory RNAs such as CsrC is usually subject to degradation by RNases, stabilization by RNA-binding proteins and chaperones or base pairing with other regulatory RNAs. In *P. aeruginoasa*, levels of the Csr-like RNAs RsmY and RsmZ are preferentially degraded by RNase G, which itself is controlled by a two-component system (Petrova and Sauer 2010). In fact, microarray analysis of an *ymoA* mutant versus *Y. pseudotuberculosis* wild type indicated that *ymoA* represses transcription of components of several RNases such as endoribonuclease L-PSP or RNase P (A. K. Heroven, K. Böhme, unpublished data). Little is known about the function of endoribonuclease L-PSP, also referred to as rat liver perchloric acid-soluble protein. L-PSP was found to cleave RNA molecules primarily at single-stranded regions producing 3' monophosphate ends (Morishita, *et al*. 1999). RNase P is a highly conserved ribonuclease found in all eu- and prokaryotes where it was first described to mainly cleave 5' ends of pre-tRNAs (Guerrier-Takada, *et al*. 1983). More recently, RNase P was shown to be implicated in the regulation of metabolic processes. RNase P in *E. coli* was found to cleave intergenic regions within mRNA operons, including that of *tna* (tryptophane biosynthesis), *his* (histidine synthesis), *rbs* (ribose transport) and *sec* operons (protein secretion system) (Li and Altman 2003). Furthermore, ribonuclease P is responsible for the cleavage of some metabolite-binding regulatory RNAs so-called riboswitches. For instance, RNase P affects the stability of coenzyme B_{12} riboswitch of *E. coli* as well as of *Bacillus subtilis* (Altman, *et al*. 2005). Seif and Altman (2008) demonstrated an RNase P-dependent cleavage of an adenine riboswitch of the *pbuE* gene, encoding a purine efflux pump in *B. subtilis*. Thus, RNase P seems to preferentially cleave RNAs with secondary structures, and might be a likely candidate implicating the control of CsrC RNA stability.

In fact, a *ymoA* deletion of *Y. pseudotuberculosis* only affected expression of a *csrC-lacZ* fusion when sequences forming such a secondary structure were present in the fusion construct (Fig. 20). The stem-loop structure could serve as a potential RNase target site. Whether the RNases such as RNase P or L-PSP affect CsrC levels in *Y. pseudotuberculosis* still needs to be determined.

It was also shown that, in the absence of *ymoA*, transcription of the second Csr RNA gene, *csrB,* was slightly induced. This might be due to counterregulation of the Csr RNAs in *Y. pseudotuberculosis*, by which downregulation of one Csr RNA induces the expression of the other (Heroven, *et al*. 2008). Overexpression of the response regulator UvrY has been shown to be the only known stimulating signal for CsrB production, and YmoA was found to induce the transcription of the *uvrY* gene (Fig. 18). Interestingly, other members of the YmoA family were also shown to control two component systems. For instance, Hha in *Salmonella* affects intracellular growth of the pathogen during host infection by blocking the transcription of *ssrB* and *ssrA* (Silphaduang, *et al*. 2007), essential for the expression of type III secretion system genes from SPI-2 (Cirillo, *et al*. 1998; Tomljenovic-Berube, *et al*. 2010). However, YmoA-mediated activation of *uvrY* was rather small and indirect, and does not explain strong YmoA-mediated increase of CsrC levels. In fact, elimination of *csrB* did not abolish YmoA

influence on CsrC levels (Fig. 19). This indicates that the influence on CsrC stability is much more dominant than the YmoA effect on UvrY and CsrB which reduce CsrC expression.

Interestingly, it was found that YmoA does not only regulate *rovA* expression by activating the synthesis of CsrC but might influence RovA synthesis by a different mechanism. A *ymoA* deletion in *Y. pseudotuberculosis* revealed a stronger impact on RovA protein levels than a *csrC* deletion mutant investigated by Heroven *et al.* (2008). Furthermore, in a *rovM* mutant, YmoA did not significantly alter gene expression of *rovA* but protein production (Fig. 14). Herbst and coworkers (2009) analyzed that RovA represents a substrate for the ATP-dependent Lon protease. Microarray analysis in our laboratory revealed increased *lon* transcription in a *ymoA* mutant (A. K. Heroven, K. Böhme, unpublished data). This indicates that YmoA might not only control *rovA* expression but also RovA protein degradation to ensure a tightly regulated invasin synthesis. The presence of the nucleoid-associated protein is essential for early virulence factor expression.

4.1.1 CsrA acts as a chaperone for CsrC stabilization

Besides YmoA, also the RNA-binding protein CsrA was shown to strongly influence CsrC stability. Interestingly, CsrA in *Y. pseudotuberculosis* did not influence expression of *csrC-lacZ fusions* with varying 3' portions of the *csrC* gene (Fig. 23). This indicated that CsrA mediates stabilization of CsrC and/or proper folding of the regulatory RNA. CsrA interaction with a Csr RNA to prevent degradation of the non-coding RNA has also been shown for other Csr-like systems. In *E. carotovora* subsp. carotovora the CsrA homolog RsmA increases the half-life of the non-coding RNA RsmB (Chatterjee, *et al.* 2002). Similarly, RsmA and its homolog RsmE in *P. fluorescens* stabilize the RsmY and RsmZ (Reimmann, *et al.* 2005). CsrB in *E. coli*, however, showed no dependency on CsrA (Gudapaty, *et al.* 2001).

One reason why CsrA-binding to Csr-type RNAs such as CsrC might lead to stabilization of the RNA could be the protection of RNase recognition sites. Csr RNAs have been observed to be degraded by RNase E, for example CsrC and CsrB in *Salmonella* (Viegas, *et al.* 2007). In *P. aeruginosa*, RsmY is subject to degradation by RNase E. RsmA covers one cleavage site of RNase E within RsmY which might contribute to the stabilization of the RNA (Sorger-Domenigg, *et al.* 2007). Similarly, Suzuki *et al.* (2006) found that CsrC as well as CsrB were stabilized in an RNase E mutant in *E. coli*. RNase E is a single-strand specific endo-ribonuclease which recognizes AU-rich regions whose substrate binding is enhanced by the interaction with monophosphorylate 5' ends (Mackie 1998). Moreover structural analysis revealed that RNase E might interact with structured RNA substrates, which was observed for interaction with its own 5' untranslated region forming a stem-loop (Koslover, *et al.* 2008; Schuck, *et al.* 2009). In *E. coli*, a fourth component of the Csr system was found to influence stability of the Csr RNAs CsrC and CsrB. The specificity factor CsrD was found to bind to CsrB and CsrC, which targeted these RNAs for RNase E degradation (Suzuki, *et al.* 2006). CsrD in *Y. pseudotuberculosis* was not found to influence RovA synthesis and thereby unlikely

encounters a significant role in the regulation of RovA production mediated by CsrC (A. K. Heroven, unpublished results).

This work demonstrated, that deletion of *csrA* results in a more rapid degradation of the CsrC RNA than a deletion of *ymoA*. Moreover, overexpression of CsrA stabilizes the CsrC RNA also in the absence of YmoA, whereas YmoA overexpression could not restore CsrC levels in a *csrA* mutant (Fig. 26 and Fig. 27). This suggests that CsrA-binding to CsrC is essential for the abundance of the RNA within *Y. pseudotuberculosis*. YmoA might promote interaction of CsrA and CsrC or might be involved in the regulation of an RNase that controls CsrC stability.

4.1.2 Environmental control of CsrC levels by YmoA and CsrA

Experimental data in this study revealed that YmoA protein synthesis is strongly regulated by environmental parameters such as temperature, growth and medium components. High YmoA protein concentrations occur mainly during the exponential phase in complex medium at 25°C. YmoA was observed throughout the entire growth of *Yersinia* with low protein levels during the stationary phase at moderate temperatures but the nucleoid-associated protein was completely absent during exponential growth in minimal medium at 37°C (Fig. 29, Fig. 30 and Fig. 56).

YmoA concentrations decreased rapidly at 37°C due to the activity of ATP-dependent ClpP/Lon proteases (Fig. 31). This is in full agreement with data obtained for YmoA stability in *Y. pestis* at higher growth temperatures (Jackson, *et al*. 2004). Ellison *et al*. (2006), however, reported that YmoA in *Y. enterocolitica* was found to be synthesized at 26°C as well as 37°C.

The RovA protein represents another regulatory factor of *Y. pseudotuberculosis* within the invasin expression cascade that is rapidly degraded at higher temperatures by the Lon protease (Herbst, *et al*. 2009). YmoA is most prominent during the exponential growth, whereas RovA is predominantly proteolysed during log phase at 37°C, perhaps due to the absence of a stabilizing cofactor. This indicates that degradation of YmoA by Clp and Lon proteases is controlled by a different mechanism. Enhanced degradation of YmoA might be the result of an upregulated *lon* expression during stationary phase (Herbst, *et al*. 2009). Interestingly, *lon* expression was also found to be stimulated in the absence of *ymoA*, indicating a negative autoregulatory circuit for YmoA (A. K. Heroven, K. Böhme unpublished results). Decreasing YmoA levels induce the expression of the *lon* gene which in turn leads to further proteolysis of the regulator. This shows that controlled proteolysis of the crucial virulence regulators such as YmoA is very important for pathogenesis in *Y. pseudotuberculosis*. In fact, Clp/Lon proteases have shown to be implicated in virulence in other pathogens. Expression of virulence factors from SPI-1 in *S.* Typhimurium was induced in *clpXP* mutants causing enhanced macrophage apoptosis. Transcription of the activatory factors *hilC* and *hilD* was elevated under these conditions (Kage, *et al*. 2008). Moreover, Lon

protease activity was found to decrease survival of *Salmonella* in HEp-2 cell cultures (Boddicker and Jones 2004). In *Campylobacter*, inactivation of protease encoding genes *lon*, *clpP* and *clpX* resulted in less viability of the bacterium at 42°C due to accumulation of misfolded proteins within the cell (Cohn, *et al.* 2007). The ClpXP protease was also observed to regulate virulence in *Streptococcus mutans* by cleaving the global regulator Spx (Kajfasz, *et al.* 2009).

Thermodependent proteolysis and regulation of gene transcription is known also for other YmoA homologous members of the related H-NS family. Deletion of the *hns* and *hha* genes in *E. coli* leads to transcription of the *hlyCABD* operon at moderate temperatures (Nieto, *et al.* 2000). An *hha hns* double mutant also allowed synthesis of virulence factors from SPI-1 of *S.* Typhimurium at low temperature (Olekhnovich and Kadner 2006; Olekhnovich and Kadner 2007). In *E. coli*, the nucleoid-associated protein StpA, homologous to H-NS is as well subject to proteolysis by Lon. Johannson and Uhlin (1999) described that StpA is degraded in the absence of H-NS, which stabilizes the protein in heteromeric H-NS-StpA dimers (Johansson, *et al.* 2001).

In contrast to YmoA, CsrA synthesis increased continuously during the growth of *Y. pseudotuberculosis* with a maximum in late stationary phase in complex medium. In general, expression of *csrA* was lower at 37°C compared to growth at moderate temperatures (Fig. 29, Fig. 30 and Fig. 56). This is different to other CsrA-type proteins such as RsmA of *Erwinia*, which was upregulated in minimal medium at 37°C (Hasegawa, *et al.* 2005) or CsrA in *E. coli* which was found to be synthesized predominantly in minimal medium though at low levels (Jonas and Melefors 2009).

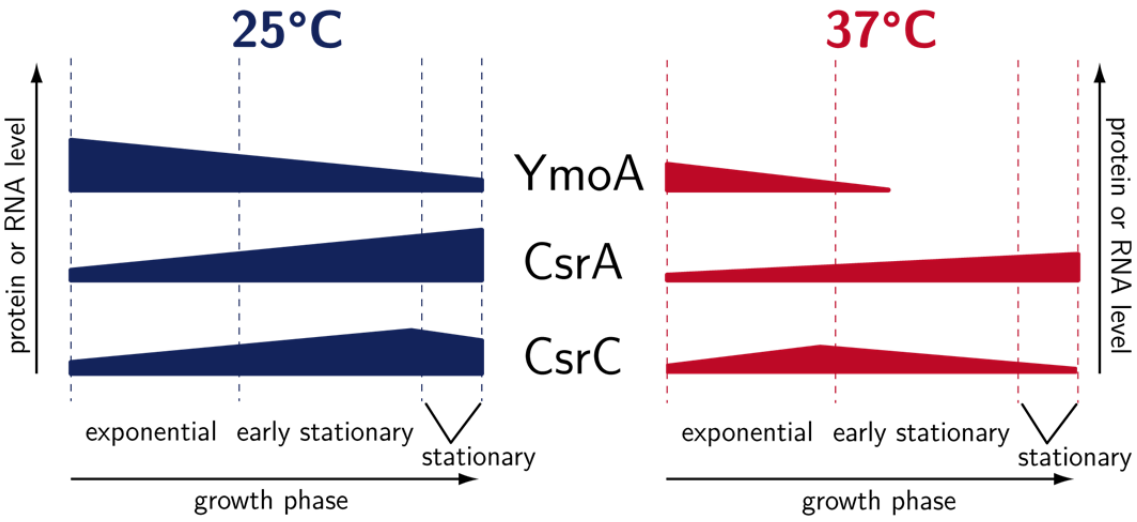

Fig. 56. Levels of YmoA, CsrA and CsrC during growth at 25°C and 37°C in nutrient-rich medium. Model of protein (YmoA and CsrA) or RNA (CsrC) levels at 25°C (blue) and 37°C (red). Qualitative amounts are displayed during the exponential, early stationary and stationary growth. Increasing levels are marked by an arrow.

Both, YmoA and CsrA determine the stability and intracellular concentrations of CsrC which increased during stationary growth at 25°C. At 37°C, CsrC level reached a maximum during the late exponential growth but decreased again during stationary phase, most likely due to

YmoA degradation (Fig. 30 and Fig. 56) (Heroven, *et al*. 2008). A similar temperature regulation was observed for the expression of the Csr-like RNAs RsmX, RsmY and RsmZ in *P. fluorescens* where transcription of the RNAs' encoding genes was more induced at 30°C than at 35°C (Humair, *et al*. 2009).

In summary, CsrC is mainly present during stationary growth, complex medium and moderate temperatures, i.e. *rovA* inducing conditions (Nagel, *et al*. 2001). This strongly suggests that CsrA, which is maximally expressed under these environmental signals, contributes dominantly to the stability of the CsrC RNA. On the other hand, *Yersinia* produces low amounts of YmoA under these conditions and this concentration is still sufficient and important to promote CsrC stability. High YmoA protein concentrations during the exponential phase indicate that the nucleoid-associated protein might be involved in the regulation of additional genes important for growth and survival.

4.1.3 Hfq activates *csrC* gene expression

Besides YmoA, the RNA chaperone Hfq was shown to be important for *csrC* expression and CsrC-dependent *rovA* transcription. Hfq activates the transcription of the *csrC* gene, whereas no influence of Hfq was observed on CsrC RNA stability (Fig. 32 and Fig. 33). In contrast to *Y. pseudotuberculosis*, it was found that loss of *hfq* in *Y. pestis* led to 6.5fold increased transcript expression of *rovA* (Geng, *et al*. 2009). However, this was shown in microarray analysis, with RNA of bacteria grown at 37°C, conditions under which RovA is rapidly degraded (Herbst, *et al*. 2009). As RovA of *Y. pestis* is not required to activate *inv* expression because this gene is not expressed due to a transposon insertion, it is also possible that the RovA protein encounters a different role in *Y. pestis* and is differently regulated (Simonet, *et al*. 1996). In fact, RovA regulons were observed to be distinct between *Y. enterocolitica* and *Y. pestis* suggesting that RovA-regulated genes have evolved in *Y. pestis* more recently (Cathelyn, *et al*. 2007). Deletion of *hfq* in *Y. pestis* did not significantly change cell adhesion of bacteria to macrophages but phagocytosis by macrophages was increased (Geng, *et al*. 2009). This indicates that Hfq is important for *Y. pestis* defense against the host immune response. In agreement with these results, virulence of an *hfq*-deficient *Y. pestis* strain was strongly reduced in mouse experiments, indicating that Hfq is responsible for the regulation of other important virulence determinants (Geng, *et al*. 2009).

Virulence of other pathogens has also been shown to be dependent on the RNA chaperone Hfq. In enterohemorrhagic *E. coli*, EHEC, regulation of factors expressed from the locus of enterocyte effacement (LEE) is affected by the RNA chaperone. Hfq influences the mRNAs of these virulence determinants controlling the formation of attaching and effacing lesions especially during the exponential phase of growth (Hansen and Kaper 2009). Additionally, Hfq is involved in quorum sensing regulation in *V. cholerae*, where it destabilizes the mRNA of the master regulator HapR, which activates expression of *tcpA* encoding a main part of the toxin-coregulated pilus (Lenz, *et al*. 2004). On the other hand, Hfq is reported to repress *ompT* synthesis in this pathogen (Song, *et al*. 2010). Deletion of *hfq* reduced virulence of

N. meningitidis (Fantappie, *et al.* 2009). Virulence of an *hfq* mutant in *S.* Typhimurium was attenuated in mice infection experiments (Sittka *et al.*, 2007). Loss of the RNA chaperone induced drastic effects on the invasiveness of *Salmonella* into epithelial cells. Survival of the bacteria in epithelial cells and macrophages was also reduced. InvR, a non-coding RNA expressed from SPI-1 was found to downregulate the synthesis of the outer membrane protein D (OmpD) in presence of Hfq. Further, the chaperone is essential for the production of the sigma factor RpoS, which implicated control of SPI-1 through the regulation of HilA (Pfeiffer, *et al.* 2007; Sittka, *et al.* 2007).

In *Y. pseudotuberculosis*, Hfq positively affects both Csr RNAs CsrC and CsrB (Fig. 32). However, Hfq stimulates *csrC* on the transcriptional level (Fig. 35), whereas the second known RNA of the Csr system, CsrB, was influenced on the post-transcriptional level (A. K. Heroven, J. Viereck, unpublished data). CsrB was found to be degraded more rapidly in an *hfq* mutant than in the wild type strain. Hfq in *P. aeruginosa* is also responsible for stabilization of the Csr-like RNA RsmY. The RNA chaperone binds to RsmY at single-stranded RNA regions adjacent to stem-loop formations. The Hfq-binding sites overlap with recognitions sites of RNase E and might stabilize the Csr-like RNA post-transcriptionally by preventing RNase activity (Sorger-Domenigg, *et al.* 2007). In contrast to *Y. pseudotuberculosis*, CsrC and CsrB in *Salmonella*, which induce expression of genes from SPI-1, were not influenced by Hfq (Viegas, *et al.* 2007). Stability of CsrC and CsrB from *E. coli* was also independent of the RNA chaperone, since half-life of the RNAs did not change significantly in comparison to the wild type.

Promoter deletion analysis performed in this study to characterize *csrC* transcription demonstrated that 200 nucleotides upstream of the *csrC* transcription start are essential for *csrC* expression. Furthermore, a *Yersinia*-specific positive regulator is required for maximal *csrC* expression (Fig. 36). As Hfq acts mainly as an RNA chaperone, it is unlikely that Hfq activates *csrC* directly. Up to now, only expression of *rpsO* in *E. coli*, which encodes for the ribosomal protein S15, was observed to underlie transcriptional activation by Hfq. The chaperone protein induced the transcription of *rpsO in vivo* and *in vitro*. Le Derout *et al.* (2010) hypothesized that Hfq prevents the arrest of the transcription complex within a secondary structure by unfolding the nascent mRNA. In *Y. pseudotuberculosis*, interaction of an activatory component with the *csrC* promoter region occurs in position -204 and -106 upstream of the transcriptional start site (Fig. 36), but for an *rpsO*-like activation mechanism Hfq might need to interact more closely to the RNA polymerase binding site. Alternatively, Hfq might influence synthesis of a *csrC* activator protein through the control of other regulatory RNAs.

Up to date, little is known about how *csrC* gene expression is regulated in *Y. pseudotuberculosis*. Latest results in our laboratory showed that *csrC* promoter activity depends on the access to iron. Further, the cyclic AMP receptor protein was found to be essential for *csrC* transcription activation in *Y. pseudotuberculosis*. However, both positive regulation

mechanisms seem to be independent of Hfq function (A. K. Heroven, S. Nordlohne, M. Scheb-Wetzel, unpublished results).

In summary, the Hfq protein is essential for the expression of *rovA* and RovA-dependent invasin expression in *Y. pseudotuberculosis*, although its effect on virulence still needs to be investigated in strain YPIII. Its differential influence on CsrC and CsrB points out, that these RNAs might not only represent redundant RNA molecules to induce *rovA* expression but encounter distinct functions within the pathogen.

4.1.4 H-NS stimulates CsrC synthesis

The H-NS protein of *Y. pseudotuberculosis*, another related member of the nucleoid-structuring protein family, was also shown to positively influence CsrC synthesis post-transcriptionally in this study (Fig. 37). It seemed possible that H-NS exerts its influence on CsrC stability by binding to the RNA. Interaction of H-NS with RNAs has previously been shown. For instance, Park *et al.* (2010) analyzed that H-NS stimulates translation of the mRNA into the transcriptional activator MalT of the maltose regulon in *E. coli*. In this case, H-NS interacts with the mRNA, which repositions the 30S ribosomal subunit within the pre-initiation complex and facilitates its binding to suboptimal Shine-Dalgarno sequences. Furthermore, H-NS binds to the mRNA of the sigma factor RpoS (Brescia, *et al.* 2004). Interaction with the nucleoid-associated protein at single-stranded regions destabilized the RNA. In contrast, *rpoS* mRNA of *V. cholerae* is destabilized in the absence of *hns* and allows synthesis of the cholera toxin under non-permissive conditions (Silva, *et al.* 2008). Brescia *et al.* (2004) as well elucidated that H-NS binds to the non-coding RNA DsrA in *E. coli*, which enhanced RNA decay. However, RNA binding assays in this study did not reveal preferential binding of H-NS to the CsrC transcript (Fig. 39). Moreover, another protein of the nucleoid-associated protein family, StpA was also found to act as a RNA chaperone. This regulator is able to facilitate the loosening of the td pre-mRNA three-dimensional structure which leads to a refolding of the RNA (Mayer, *et al.* 2002). StpA preferentially binds to unstructured RNA induced by electrostatic interactions resulting from the negatively charged backbone of the RNA molecule. Strikingly, when StpA-binding affinity to RNA was reduced by mutations in its RNA-binding domain, its RNA chaperone activity is enhanced. One reason for the RNA-binding and chaperone properties of StpA is its disordered protein structure (Mayer, *et al.* 2007). Since StpA and H-NS share structural features, it is also possible that H-NS has an RNA chaperone function. This facilitates CsrC loop formation and CsrA-binding which needs to be further analyzed.

H-NS influence on CsrC through a post-transcriptional mechanism is rather unusual as H-NS has been mainly found to reduce expression of virulence factors in *Yersinia* by inhibiting transcription. For instance, H-NS was identified to downregulate *rovA* and *inv* transcription, whereby RovM levels remain unaffected in *Y. pseudotuberculosis* (Heroven, *et al.* 2008; Heroven and Dersch 2006). A similar mechanism is described for the H-NS-mediated regulation of invasin synthesis in *Y. enterocolitica* (Ellison and Miller 2006). In pathogenic

E. coli, H-NS is responsible for the downregulation of virulence factor synthesis such as fimbriae or capsular polysaccharides (Muller, *et al*. 2010). Deletion of *hns* derepressed the transcription of the long polar fimbriae (*lpf*) leading to enhanced adherence of *E. coli* O157:H7 to tissue-cultured cells (Torres, *et al*. 2007; Torres, *et al*. 2008). Rogers and coworkers (2009) analyzed that H-NS downregulates the expression of the *ehx* operon located in the LEE pathogenicity island. This operon encodes the enterohemolysin EhxA. An *hns*-deficient strain was impaired to bind to human colonic epithelial cells. H-NS also reduces the expression of *acrEF*, *mdtEF* and *emrKY*, operons harboring drug transporter systems (Nishino and Yamaguchi 2004) and H-NS-dependency was shown for multidrug resistance in *S.* Typhimurium (Nishino, *et al*. 2009). Due to its dominant influence on gene transcription it is most likely that H-NS controls transcription of a regulatory component that affects CsrC stability.

Several studies demonstrated that H-NS is also able form heteromers with YmoA (Nieto, *et al*. 2002). YmoA from *Y. enterocolitica* was found to associate with H-NS protein purified from *Yersinia* as well as from *E. coli*. H-NS heteromerization with the YmoA homolog Hha modified the DNA-binding affinity of the complex, whereas Hha homomers interacted with promoter regions unspecifically (Nieto, *et al*. 2000). In *Salmonella*, Hha-mediated suppression of gene expression from SPI-1 and the type III secretion system encoded by SPI-2 occurs also in cooperation with H-NS (Duong, *et al*. 2007; Olekhnovich and Kadner 2007). Interaction of H-NS with StpA in uropathogenic *E. coli* causes the reduction of S fimbriae synthesis because expression of the major subunit expressing gene *sfaA* is abolished (Morschhauser, *et al*. 1993).

Based on these results it seems also possible that YmoA and H-NS act on CsrC stability in a cooperative manner. For example, YmoA-binding to H-NS might enhance the RNA chaperone-like function. In fact, H-NS was able to restore CsrC synthesis in the absence of YmoA, which indicates an independent mechanism of regulation by H-NS. However, very high concentrations were necessary to complement YmoA function. Moreover, findings in this work show that H-NS represses YmoA protein levels (Fig. 38). H-NS-dependent *ymoA* regulation in *Y. enterocolitica* confirms this observation (Banos, *et al*. 2008). Thus, the influence of H-NS on CsrC can occur by different molecular mechanisms which will be addressed in future experiments.

4.2 The complex control of LcrF synthesis – Activator of late stage virulence factors

For survival and dissemination in the deeper tissues like mesenteric lymph nodes, liver, spleen or kidney, *Y. pseudotuberculosis* produces the outer membrane adhesin YadA and a type III secretion system which translocates effector molecules, the *Yersinia* outer proteins (Yops), into host cells (Allaoui, *et al*. 1995b; Eitel and Dersch 2002; Heise and Dersch 2006; Rosqvist, *et al*. 1995). These virulence determinants are encoded on the *Yersinia* virulence plasmid pYV and their expression is induced by the AraC-like activator LcrF (VirF in *Y. enterocolitica*) in response to higher temperature (37°C) (Cornelis, *et al*. 1987; Lambert de Rouvroit, *et al*. 1992; Simonet, *et al*. 1990; Skurnik and Toivanen 1992).

4.2.1 The nucleoid-associated protein YmoA represses expression of the *yscWlcrF* operon

Analysis of reporter gene fusions in *Y. pseudotuberculosis* revealed that *lcrF* forms an operon with *yscW* and that the transcription start site of the *lcrF* gene is located about 260 bp upstream of *yscW* (Fig. 41 and Fig. 42). Indication supporting an expression of *lcrF* from an operon with *yscW* was also obtained in *Y. pestis*. Hoe and coworkers (1992) showed that *lcrF* transcription is only temperature-regulated when two kb of the 5' region of *lcrF* was present in *Y. pestis* strains KIM5 and KIM6.

Homologs of the *yscWlcrF* operon were also found in *P. aeruginosa* and *Vibrio harveyi*. The activator gene *exsA* of the type III secretion system in *P. aeruginosa* is encoded downstream of *exsB*. Alike LcrF, ExsA is a member of the AraC family and is expressed in response to the Ca^{2+} concentration (Hovey and Frank 1995; Vallis, *et al*. 1999). The function of ExsB is still unknown and an *exsB* transcription product could not yet be detected (Goranson, *et al*. 1997). Interestingly, expression analysis revealed an antisense product called *exsB*', with unknown function. Recent experiments in our group showed also the production of an YscW' antisense RNA which stabilized the *yscWlcrF* transcript when overexpressed (R. Steinmann, unpublished data). ExsB exhibits 26% identity to the amino acid sequence of YscW whereas ExsA and LcrF of *Y. enterocolitica* share 56% identity (Allaoui, *et al*. 1995a). In V. harveyi, exsBA expression results in activation of type III secretion genes dependent on quorum sensing signals (Waters, *et al*. 2010). The transcriptional start site of this operon is located 38 nt upstream of the *exsB* start codon. Despite of the homology of the operons, they seem to show very distinct properties. In contrast to *exsB*, the *yscW* gene in *Yersinia* was found to encode a lipoprotein, which assists a component of the type III secretion system, YscC, to localize within the outer membrane (Allaoui, *et al*. 1995a; Koster, *et al*. 1997). Furthermore, the transcript of *yscWlcrF* in *Y. pseudotuberculosis* harbors a long 5' untranslated region upstream of the *yscW* start codon that is subject to intensive processing (K. Böhme, R. Steinmann, unpublished data).

In this study, it was demonstrated that the nucleoid-structuring protein YmoA affects *lcrF* transcription negatively at moderate temperatures and that a region comprising 360 bp upstream of the *yscW* start codon is important for the YmoA-mediated repression of the *yscWlcrF* operon (Fig. 42). Also in *E. coli*, the homolog of YmoA, Hha, was shown to repress expression of genes encoded by the virulence plasmid pCD1 (homolog of pYV) of *Y. pestis* (Bartra, *et al*. 2006). Besides control by low calcium concentrations, LcrF (VirF) production in *Y. enterocolitica* has been described to be regulated by temperature-dependent alterations in the DNA supercoiling of the promoter region. With increasing temperature the regulatory region of *lcrF* (*virF*) was found to partially linearize and so induce *lcrF* (*virF*) expression. The nucleoid-associated protein YmoA was observed to assist structural rearrangements at moderate temperatures (Cornelis, *et al*. 1991; Rohde, *et al*. 1994; Rohde, *et al*. 1999). However, up to date, YmoA has not been found to bind to DNA by itself, only in association with H-NS but reduction of the H-NS function did not influence *yscWlcrF* expression (K. Böhme, S. Sievers, unpublished data). YmoA might regulate expression of the *yscWlcrF* operon by interaction with another regulatory protein.

In *Y. pestis,* regulation of *lcrF* expression in response to temperature occurs due to the thermoregulated proteolysis of YmoA by ATP-dependent Clp/Lon proteases. Activity of ClpP and Lon proteases was found to stimulate expression of several *yop* genes and *ysc* genes encoding the type III secretion system by degrading YmoA at 37°C (Jackson, *et al*. 2004). Similar protease-dependent degradation of YmoA was also observed in *Y. pseudotuberculosis* in this study (Fig. 31). Considering, that YmoA upregulates expression of the early invasion factor invasin at moderate temperatures but represses transcription of the main regulator of late virulence factors *lcrF*, this nucleoid-associated protein seems to function as a molecular switch controlling virulence gene expression during different stages of the infection. Immediately after oral uptake from the environment with moderate temperatures, YmoA is present and induces expression of invasin through the CsrC-CsrA-RovM-RovA regulatory cascade which enables the bacteria to invade into M-cells. Higher temperature within the host environment leads to a rapid degradation of the YmoA protein, resulting in LcrF production and synthesis of YadA, the Yop effector proteins and the type III secretion system.

Besides YmoA, other regulatory factors seem to influence transcription of the *yscWlcrF* operon. Promoter deletion experiments indicated that a *Yersinia*-specific factor stimulates *yscW* transcription through a regulatory segment located about 570 bp upstream of the *yscW* start codon. Data in this study further suggests that this activator might be encoded on pYV in *Y. pseudotuberculosis* (Fig. 42 to Fig. 44). Furthermore, host cell contact was found to activate expression of a *yscWlcrF*'-'*gfp* fusion (W. Opitz, S. Fehse, unpublished results), indicating that a regulatory component might sense the attachment of the bacterium to mammalian cells and transduce this signal to activate the *yscWlcrF* gene. Whether the virulence-encoded activator of *yscWlcrF* expression is also implicated in host cell contact is unclear and will be subject of further studies.

Induction of virulence factors by host cell contact of the pathogenic bacteria has also been observed in *Shigella*, *Salmonella* and *P. aeruginosa* (Ginocchio, *et al*. 1994; Vallis, *et al*. 1999; Watarai, *et al*. 1995). *P. aeruginosa* expresses components of the type III secretion system in the presence of the LcrF homolog ExsA, and Urbanowski *et al.* (2007) found that attachment of *Pseudomonas* to mammalian cells induced ExsA-mediated gene expression of the type III secretion machinery or effector proteins. PsrA, a regulator of the fatty acid degradation operon, was found to activate the expression of the *exsCEBA* operon in *P. aeruginosa.* (Kang, *et al*. 2009).

4.2.2 A FourU thermometer regulates LcrF translation

LcrF protein synthesis in *Y. pseudotuberculosis* is also subject to post-transcriptional temperature regulation by formation of a secondary structure in the 5' untranslated region (UTR) of the *lcrF* mRNA (Fig. 46). Such a mechanism was first suggested for the thermo-dependent LcrF production in *Y. pestis* (Hoe and Goguen 1993). Recently, Waldminghaus *et al.* (2007) predicted a FourU thermometer in the 5' UTR *lcrF* which might be responsible for translation regulation at moderate or elevated temperatures. Structural mapping, computational and toe print analysis in this study demonstrate that within this secondary structure the Shine-Dalgarno sequence interacts with a FourU motif at 25°C which masks the ribosomal recognition site for translation initiation. At 37°C, conformational changes liberate the Shine-Dalgarno sequence and allow access to binding of 30S ribosomal subunits which induces LcrF synthesis. Mutagenesis at the FourU sequence, leading to an increased or reduced complementarity of the FourU motif to the ribosomal binding site, validated these results (sec. 3.2.6 to sec. 3.2.8).

RNA thermometers are often involved in the synthesis of chaperones essential for the bacteria to adapt to higher temperatures. The sigma factor RpoH acts on transcription of target genes under various stress conditions. Its translation occurs at elevated temperatures due to conformational changes of in the 5' UTR of the *rpoH* mRNA in *E. coli* (Morita, *et al*. 1999a; Morita, *et al*. 1999b). RpoH induces the transcription of another heat shock protein, the inclusion body binding protein IbpA. The translation of this protein is activated by increasing temperatures which depends on the structure of its 5' UTR comprising three different hairpins. In this case, the Shine-Dalgarno site forms base pair interactions with a sequence with high complementarity containing a bulged G. Only the third stem-loop of this so-called ROSE (repression of heat shock gene expression) element is instabilized (e.g. melted) by elevated temperatures, whereas the first two do not change their conformation. They might facilitate and stabilize an optimal folding of the *ibpA* RNA structure (Waldminghaus, *et al*. 2009). This is similar to structural alteration of the *lcrF* RNA thermometer. In *Y. pseudo-tuberculosis*, secondary structure changes in response to temperature were only observed within hairpin II (Fig. 50 and Fig. 57), whereas the first hairpin remained unchanged. In contrast, deletion of hairpin I resulted in efficient translation of a *lcrF*'-'*lacZ* fusion and significantly higher LcrF production at 25°C which is confirmed by LcrF protein levels

(R. Steinmann, unpublished results). RNA structure mapping of the hairpin I deletion mutant also showed that it is an unstable RNA molecule (K. Böhme, data not shown). Thus, functionality of the LcrF RNA thermometer is not only dependent on the FourU motif itself but also requires a correct overall conformation of the complete 5' UTR.

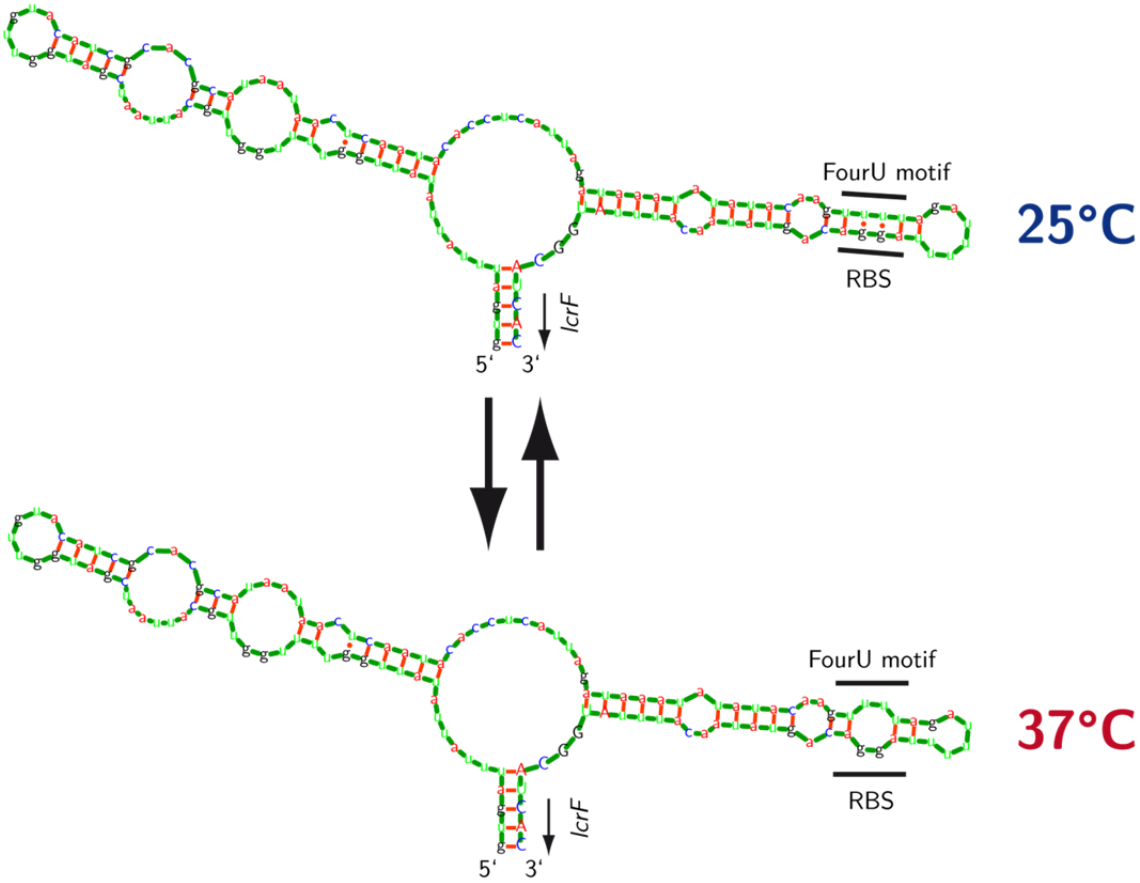

Fig. 57. Small temperature-induced changes of the *lcrF* 5' UTR secondary structure. RNA secondary structure examples predicted by RNAshapes for the *lcrF* 5' UTR (Steffen, *et al.* 2006, http://bibiserv.techfak.uni-bielefeld.de/rnashapes/) at 25°C and 37°C. RBS marks the ribosomal binding site. The FourU motif is indicated.

5' UTR structure probing of *lcrF* further demonstrated that an increase in temperature leads to relatively small changes of the second hairpin conformation. Only the FourU motif, the ribosomal binding site and some adjacent nucleotides underwent conformational changes upon a temperature shift from 25°C to 37°C. However, these small changes at 37°C were sufficient to allow *in vitro* binding of the small ribosomal subunit to the ribosomal binding site and promote efficient translation initiation of a *lcrF-lacZ* fusion *in vivo*. Other RNAs sensing environmental cues have shown to induce more global alterations within their secondary structure. For example, Kulshina and coworkers (2009) observed massive structural rearrangements of the *tfoX* 5' UTR in response to c-di-GMP ligand binding in *V. cholerae*. In the 5' UTR of a putative virulence gene in *Clostridium difficile*, C-di-GMP-binding leads to conformational changes resulting in the formation of alternative splicing sites. Depending on the secondary structure of the RNA, processing occurs either upstream or downstream of the Shine-Dalgarno sequence which regulates translation of the putative virulence determinant (Lee, *et al.* 2010).

A FourU thermometer was also identified in *S. enterica* where it influences synthesis of the small heat shock protein AgsA. Similar to *lcrF*, the Shine-Dalgarno sequence of the *agsA* mRNA interacts with four Uracils within a RNA stem-loop structure (Waldminghaus, *et al.* 2007). NMR spectroscopic analysis revealed that the secondary structure of the *agsA* 5' UTR is unfolded in a zipper-type mechanism which shows high cooperativity. This cooperative behavior was based on the small number of mismatches and bulges within the FourU thermometer in *Salmonella* (Rinnenthal, *et al.* 2010). In contrast to *agsA*, computational analysis and RNA structure probing of the *lcrF* 5' UTR demonstrated that the adjacent region to the FourU/ribosomal binding site contains several mismatches and especially bulges which may lead to the only limited structural alterations in response to higher temperatures (Fig. 57). Interestingly, even more distanced mutations such as AUA -36 to -34 CCC or AG -46/-45 CC within the *lcrF* 5' UTR have a strong impact on the activity of a translational *lcrF*'-'*lacZ* fusion (Fig. 49). In general, Rinnenthal and coworkers (2010) explained such influences by remote effects on the hydration shell surrounding the RNA molecule.

Besides riboswitches, other thermosensory mRNA structures of regulatory genes also undergo conformational alterations upon temperature changes. For instance, synthesis of the cold shock protein CspA in *E. coli* is affected due to the formation of different secondary structures of the *cspA* mRNA at 10°C and 37°C. At low temperatures, the conformation of the mRNA leads to a single-stranded Shine-Dalgarno sequence and AUG start codon. The *cspA* mRNA refolds at higher temperatures. This leads to incooperation of the translation initiation site and the first codon into double-stranded regions, which inhibits translation of the cold shock protein (Giuliodori, *et al.* 2010)

Only few thermosensors have been found to regulate virulence of a pathogen. Besides LcrF, the 5' region of *prfA* mRNA in *Listeria monocytogenes* was shown to be important for pathogenesis. The *prfA* gene encodes a crucial transcriptional activator (PrfA) which stimulates expression of virulence factors for host cell invasion. Its 5' UTR forms a secondary structure at 30 °C which resolves at 35°C and enables access of the ribosomes to the Shine-Dalgarno sequence (Johansson, *et al.* 2002). Interestingly, *prfA* translation is not only temperature-dependent but underlies a more complex regulation. PrfA production is also influenced by the presence of a trans-acting riboswitch, called SreA (Loh, *et al.* 2009) which strongly depends on the nutrient availability. Also LcrF synthesis of *Yersinia* is subject to multiple control systems, e.g. the transcriptional regulation by YmoA and the post-transcriptional control by the FourU thermometer and Hfq. This complex regulatory network ensures that important virulence regulators are only expressed under specific of environmental conditions, e.g. during certain stages during host infection.

4.2.3 Hfq ambivalently regulates *yscWlcrF* expression dependent on the temperature

Studies of this work further revealed that LcrF production is strongly affected by the RNA chaperone Hfq. At 25°C, Hfq of *Y. pseudotuberculosis* YPIII activates transcription of *yscWlcrF* operon, while LcrF production was strongly repressed at 37°C (Fig. 54 and Fig. 55). In *Y. pestis*, loss of *hfq* also induced transcript synthesis of many genes encoded by pCD1. For instance, expression of *lcrF*, *yscW* (*virG*), several *yop* and *ysc* genes were strongly stimulated (Geng, *et al.* 2009). Virulence of an *hfq* mutant in *Y. pestis* was strongly attenuated. The authors explained this by the higher sensitivity of an *hfq* mutant to stress signals from the environment. Furthermore, *in vitro* studies also showed that a *Y. pestis hfq*-deficient strain exhibits a strong growth defect, which may also explain why *Y. pestis* is less virulent when *hfq* was deleted. Results obtained in this study with *Y. pseudotuberculosis* YPIII, however, are different from what has been described for an *hfq* mutant in *Y. pseudotuberculosis* strain IP32953. Loss of *hfq* in this strain led to decreased expression of the type III secretion genes and reduced virulence, although *lcrF* expression levels were significantly induced in an *hfq* mutant (Schiano, *et al.* 2010). Ysc and Yop synthesis and secretion might still be reduced to a contrary Hfq-dependent effect on type III secretion. However, it is more likely that decreased *ysc-yop* expression is the result of loss of the virulence plasmid in the bacterial population. In fact, high overexpression of the LcrF production in a *Y. pseudotuberculosis* YPIII strain deficient in *hfq* or *ymoA* frequently results in the loss of pYV in the culture, due to massive deleterious *yop*/*ysc* overexpression (K. Böhme, A. K. Heroven, unpublished results). Alternatively, it is possible that the pYV-encoded genes are differentially regulated in different *Y. pseudotuberculosis* strains that might be due to differences in the genetic information. This has already been shown for the formation of biofilms on *Caenorhabditis elegans* by Sun and coworkers (2009). In contrast to *Y. pseudotuberculosis* strain IP2666c, strain YPIII carries insertions in the *phoP* gene, encoding the response regulator of the PhoP/Q two component system. This mutation inactivates the expression of *phoP* and induces biofilm formation similar to *Y. pestis*, but does not allow colonization of *C. elegans* in form of biofilms by the *phoP*$^{+}$ *Y. pseudotuberculosis* strain IP2666c. Furthermore, *hfq* deletions lead to different growth behavior in *Y. pseudotuberculosis* strain YPIII and IP32953. Schiano *et al.* (2010) demonstrated that an *hfq* mutant in strain IP32953 was not or slightly attenuated during growth in BHI medium at 37°C. We observed that loss of *hfq* reduced the growth rates of *Y. pseudotuberculosis* strain YPIII significantly under these growth conditions and curing an *hfq* mutant of the virulence plasmid pYV restored wild type growth at this temperature (K. Böhme, unpublished results). This indicates that, during growth of *Y. pseudotuberculosis* strain YPIII in BHI medium at 37°C, Hfq-induced LcrF synthesis and thereby stimulated expression of *yop* genes might lead to toxic effects on *Yersinia* cells and growth arrest. At 25°C, *hfq* deletions in *Y. pestis* KIM6+ and *Y. pseudotuberculosis* strain YPIII also attenuated growth of both strains, but to a lower extent than at 37°C (Bai, *et al.*

2010, Böhme unpublished data). These results suggest a different role of the RNA chaperone in different *Yersinia* species and strain variants.

Involvement of Hfq in the regulation of type III secretion systems and their effectors has also been found in several pathogens. For instance, *invE* in *Shigella sonnei* is upregulated in an *hfq*-deficient strain at low osmolarity, which in turn activates a type III secretion system (Mitobe, *et al*. 2009). Hfq of EHEC represses expression of genes from the pathogenicity island LEE and non-LEE-dependent effectors such as *espFu*, *espJ* or *espK*. The chaperone downregulates synthesis of the major regulator Ler (Shakhnovich, *et al*. 2009).

Hfq implication in the environmental control of different crucial virulence genes expressed during different phases of the infection underlines the importance of this global regulator for pathogenesis. Variation of Hfq function between related species and strain isolates requires a more detailed analysis of the effects in future studies to fully understand its role in virulence.

4.3 Working model for regulation of virulence factor expression in *Y. pseudotuberculosis*

Analysis of environmental control of early and later stage virulence factors of *Y. pseudotuberculosis* in this study revealed a complex regulatory network coregulating and adapting virulence gene expression in *Y. pseudotuberculosis* in response to different environmental conditions. At moderate temperatures, during stationary growth and in complex medium, conditions resembling an environment outside of the host or in contaminated food, the nucleoid-associated protein YmoA and the RNA-binding protein CsrA are present. Hfq activates transcription of the regulatory RNA *csrC* gene indirectly, which is stabilized by an interaction with CsrA. The YmoA protein also reduces the degradation of CsrC, most likely by downregulation of the expression of RNases. Binding of CsrA to the regulatory RNA prevents synthesis of the LysR-type regulator RovM. RovM no longer represses production of RovA in association with H-NS, which leads to invasin expression. Furthermore, YmoA-mediated repression of proteases production reduces rapid degradation of RovA and supports upregulation of RovA and RovA-dependent virulence genes under these conditions. In parallel, YmoA abolishes the expression of the *yscWlcrF* operon, encoding the major activator of late virulence factors, LcrF. Moreover, translation initiation of *lcrF* mRNA is inhibited by the formation of a FourU RNA thermoswitch in the 5' UTR. During the early phase of infection, *Y. pseudotuberculosis* thereby ensures an efficient uptake by the M-cells and translocation through the gut epithelium shortly after ingestion.

After attachment to the gut and colonization of the Peyer's patches, the RovA and YmoA proteins are degraded by ATP-dependent Clp and Lon proteases due to increased temperature and a reduced growth rate. Reduced or changing nutrient availability also influences expression of *rovA* and *ymoA* negatively. Furthermore, lower amounts of CsrA and the YmoA proteins lead to a strong degradation of the CsrC RNA under these conditions. Liberated unbound CsrA molecules lead to enhanced RovM synthesis and prevent *rovA* expression in

cooperation with H-NS. Additionally, RovA proteolysis is even further increased due to a higher production of Clp and Lon proteases caused by the loss of YmoA. Invasin synthesis is prevented because RovA no longer antagonizes the binding of H-NS to the *inv* promoter. Moreover, degradation of the nucleoid-associated protein YmoA and activity of an unknown *Yersinia*-specific regulator induces transcription of the *yscWlcrF* operon. Increased temperatures also lead to structural alterations and melting of the FourU RNA thermometer which results in a higher accessibility and binding of the Shine-Dalgarno sequence by ribosomal subunits. LcrF protein synthesis activates gene expression of several *yops*, the type III secretion system genes and *yadA*. These virulence determinants mediate the defense of *Y. pseudotuberculosis* against immune system attacks, allow proliferation in the mesenteric lymph nodes and dissemination to kidney, spleen or liver (Fig. 58).

In this regulatory network, the nucleoid-associated protein YmoA has a crucial function as it acts as a temperature-sensitive switch controlling the overall change of virulence factor expression in *Y. pseudotuberculosis* from early to ongoing phases of infection. Temperature-dependent proteolysis of RovA, the main regulator of early virulence genes and the FourU thermoswitch affecting *lcrF* translation act as a second gateway of control to limit expression of the virulence factors to the right time and place during infection.

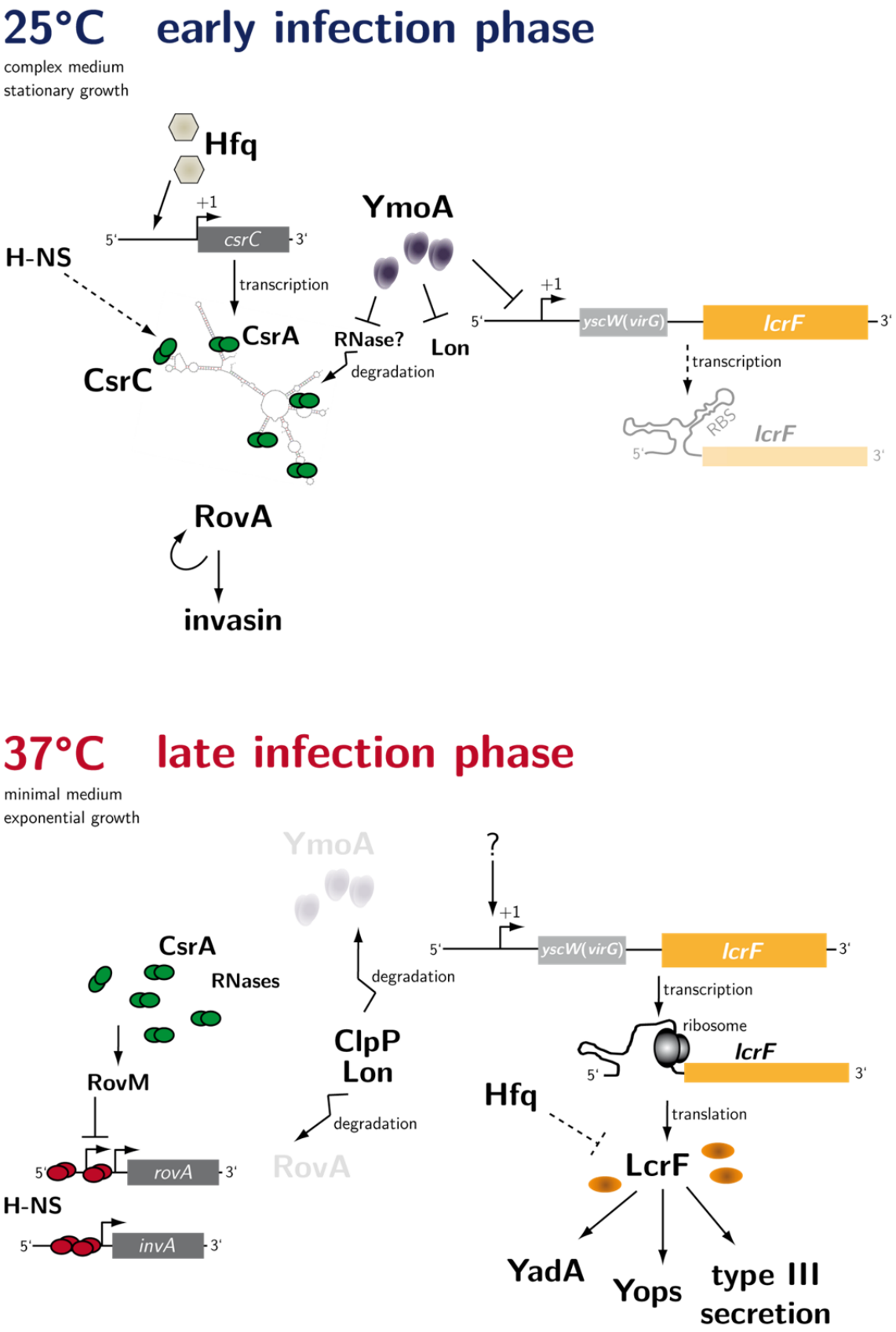

Fig. 58. Regulatory factors YmoA and Hfq as well as a FourU thermometer in the lcrF 5' UTR are essential for tight control of virulence factor expression in *Y. pseudotuberculosis*. Model of virulence factor expression derived from experimental data of this work. Arrows indicate direct activation of the gene expression or protein synthesis, whereas dashed arrows suggest indirect regulation. T represents repression or inactivation.

5 Outlook

This work defined the nucleoid-associated protein YmoA as an activator of early phase virulence factor expression where it stabilizes the CsrC RNA. The mechanism of stabilization needs to be further analyzed, in particular the role of YmoA to regulate the expression of RNases. In general, it is still unclear how YmoA affects gene expression or protein synthesis, since DNA-binding ability could only be observed in association with H-NS (K. Böhme, S. Sievers, unpublished data). Additional gene expression and EMSA studies with or without H-NS will help to elucidate this question.

Furthermore, it needs to be analyzed how and which RNases degrade the CsrC or CsrB RNA in yersiniae. Major influence of YmoA on the control of the carbon storage regulatory system and severe growth defects of a *ymoA* mutant indicate a major role of YmoA in the control of the bacterial metabolism. Influence of the nucleoid-associated protein on the *Yersinia* metabolism is currently studied using microarray, metabolomics and Biolog analysis. Interplay of the regulatory components of *Yersinia* virulence regulators YmoA, CsrA and CsrC were examined *in vitro* but nothing is known about expression of these important regulators in the mouse model during different stages of the infection as invasin expression in *Y. pseudotubrculosis* occurs only in the ileum and in the beginning of the infection (J. Eitel, unpublished data). This would be accomplished, for example, by *in vivo* imaging or histological experiments using reporter gene fusions encoding flourescent proteins.

The RNA chaperone protein Hfq was shown to influence *csrC* transcription, but this seems to occur indirectly by another regulatory protein. In future experiments, it needs to be analyzed whether Hfq controls other regulatory RNA that affect csrC expression directly or through other regulatory components.

Interestingly, Hfq was not only observed to activate invasin expression but also represses LcrF synthesis in *Y. pseudotuberculosis* strain YPIII. This influence occurs mainly on the post-transcriptional level, but the mechanism is not yet clear. Future experiments will address implications of Hfq on the RNA thermometer formation. Therefore, transcription-independent fusion containing the 5' UTR of *lcrF* in the presence and absence of Hfq will be monitored. Furthermore, other regulatory factors and influence of host cell contact on the function of the RNA thermometer will be tested. The importance of the FourU RNA thermometer on LcrF protein production and virulence of *Y. pseudotuberculosis* in the mouse model will be analyzed in more detail. Mouse survival experiments and organ burden of mice infected with mutants harboring mutations to stabilize or destabilize the FourU secondary structure will confirm the significance of such a thermoelement in virulence factor expression of enterobacteria.

Furthermore, involvement of an untranslated antisense RNA in Hfq/YmoA-mediated regulation of LcrF production within similar to *exsB*' in *Pseudomonas aeruginosa* will be addressed.

Expression data in this study showed that *lcrF* is organized in an operon with *yscW*. The existence of the polycistronic RNA will be verified by primer extension analysis, 5' RACE (rapid amplification of cDNA-ends) or Northern blotting. These experiments would also elucidate the transcription start of the *yscWlcrF* operon which seems to be located at least 260 nt upstream of the *yscW* gene. Transcription of the *yscWlcrF* operon was also found to be regulated by other regulatory proteins, e.g. a *Yersinia* specific activator which appears to be encoded by the *Yersinia* virulence plasmid pYV. Genetic screening and mutational analysis will help to identify this regulator and address its role in host cell contact-dependent expression of *lcrF* (W. Opitz, S. Fehse, unpublished data).

6 Summary

The enteric pathogen *Y. pseudotuberculosis* causes gut-associated diseases by ingestion of contaminated food. The bacterium passes the intestinal tract until it reaches the ileum at the end of the small intestine. During the infection process, the bacterium uses two primary invasion factors, invasin and YadA. Invasin synthesis occurs only in the beginning of the infection process, whereas YadA expressed during later stages of the infection helps *Y. pseudotuberculosis* to colonize and disseminate in the host. Expression of invasin is tightly regulated in response to environmental parameters by the MarR-type regulator RovA, which is negatively controlled by the nucleoid-associated protein H-NS and the LysR regulator RovM. The carbon storage regulator system influences *rovA* expression by regulating the synthesis of RovM. Under conditions which suppress expression of invasin, e.g. during later infection phases, production of YadA is induced by the AraC-like regulator LcrF. During genetic screenings, the nucleoid-associated protein YmoA and the RNA chaperone Hfq were found to influence expression of invasin or YadA.

Early phase of infection

Expression studies in this work revealed that YmoA activates the expression of *rovA* in *Y. pseudotuberculosis* by inhibiting the synthesis of the *rovA* repressor RovM. Deletion of *ymoA* in a *rovM* mutant also showed, that the YmoA protein activates RovA synthesis in a post-transcriptional manner most likely by repression of the Lon protease which was previously shown to degrade RovA at 37°C. More importantly, Northern blot analysis demonstrated that YmoA stimulates the synthesis of the *rovA* activating regulatory RNA CsrC, independent of the expression of the second regulatory RNA CsrB known to suppress CsrC synthesis. Regulatory studies and stability assays revealed that YmoA influences the CsrC RNA on the post-transcriptional level by preventing CsrC degradation. Similar experiments using a *csrA*-deficient strain demonstrated that also the RNA-binding protein CsrA inhibits CsrC decay. CsrA-mediated stabilization of CsrC seems to be independent of YmoA and was much more pronounced than YmoA-promoted stability. RNA-binding studies using purified YmoA protein and *in vitro* transcribed CsrC RNA demonstrated that YmoA influence on CsrC stability seems to be indirect and appears to involve additional regulatory components such as H-NS and RNases.

Expression analysis of CsrA and YmoA further showed that synthesis of both regulators is downregulated in minimal medium and at 37°C, which results in reduced CsrC levels under these growth conditions. At 37°C, the YmoA protein is rapidly degraded by ATP-dependent ClpP/Lon proteases. Surprisingly, although high levels of YmoA were produced during the exponential growth in complex medium, CsrC levels were still reduced due to low amounts of CsrA. As presence of CsrA was more important for CsrC than the presence of YmoA, CsrC levels were maximal at high levels of CsrA and moderate YmoA concentrations.

In the present work it was also shown that Hfq influences *rovA* expression through the Csr system. Reporter gene fusion studies revealed that Hfq affects transcription of the *csrC* gene. Promoter deletion analysis further indicated that *csrC* expression is controlled by an additional positive regulator which seems to interact with sequences located 200 to 350 nucleotides upstream of the *csrC* transcription start.

Finally, the nucleoid-associated protein H-NS was found to be implicated in the regulation of CsrC. H-NS was shown to upregulates CsrC levels post-transcriptionally. Induction of CsrC by H-NS was also observed in the absence of *ymoA* indicating that H-NS can partially complement the YmoA function when it is overexpressed. YmoA-mediated activation of H-NS expression was excluded but in this context it was also shown that H-NS is able to repress YmoA protein synthesis in *Y. pseudotuberculosis*.

Later phases of infection

YmoA was also found to inhibit the synthesis of the activator of late stage virulence factors LcrF at moderate temperatures. The *lcrF* gene was shown to be organized in an operon with the *yscW* gene which was regulated by YmoA from a region 300 bp upstream of the *yscW* gene. Promoter deletion studies of *yscWlcrF-lacZ* fusions as well as expression of an *yscWlcrF* fusion in *E. coli* revealed that an additional *Yersinia*-specific activator influences expression of the operon. This regulator seems to be encoded by the *Yersinia* virulence plasmid (pYV), since promoter activities were reduced in a strain cured of pYV. Autoregulation of *lcrF* expression could be excluded. Expression of the operon from a thermo-independent promoter showed that translation of the *lcrF* mRNA is still regulated in response to temperature. Studies using a translational *lcrF*'-'*lacZ* fusion under the control of a thermo-independent promoter demonstrated that an element located within the intergenic region between *yscW* and *lcrF* is responsible for this phenomenon.

Computational predictions indicated that this 5' untranslated region of *lcrF* forms a secondary structure containing two hairpins forming a FourU thermometer. Partial deletions of these hairpins confirmed that the entire structure is essential for a precise thermocontrol of *lcrF* translation. Mutational studies demonstrated that altering the complementarity of the base pairing at the FourU motif changed temperature-dependence of LcrF production drastically. Destabilizing mutations allow LcrF synthesis already at 25°C, whereas stabilizing exchanges abolished LcrF synthesis at 25°C and 37°C. RNA structure mapping of *in vitro* synthesized RNA of the *lcrF* 5' UTR at 25°C and 37°C confirmed structural predictions and revealed enhanced single-stranded regions at the Shine-Dalgarno sequence at 37°C compared to moderate temperatures. Toe print analysis confirmed that these structural rearrangements at high temperatures allow the binding of ribosomal subunits to their recognition site. Experiments using RNAs mutated at the FourU motif confirmed these observations.

In addition, the RNA chaperone Hfq was shown to be implicated in the control of LcrF protein synthesis. Deletion of *hfq* elevates LcrF protein production at 37°C; and expression

analysis showed that Hfq-mediated expression seems to occur on the post-transcriptional level, e.g. via an RNA that affects the stability of the *lcrF* mRNA.

All these results point out that both, the RNA chaperone Hfq and the nucleoid-associated protein YmoA, represent crucial regulators of early and late phase virulence genes in *Y. pseudotuberculosis* (virulence). In particular, YmoA seems to function as a molecular switch which activates expression of virulence genes needed in the initial part of the infection in response to low temperature, whereas factors produced for the survival in the deeper tissues are repressed. At body temperature of 37°C, YmoA is rapidly degraded and allows transcription of the *yscWlcrF* operon. Furthermore, formation of the inhibitory secondary structure of the FourU RNA thermometer is prevented at 37°C and permits efficient translation of the RNA. This sophisticated control system of the *Yersinia* virulence genes demonstrates how synthesis of virulence regulators is finely adjusted in pathogenic bacteria to trigger virulence factor production in response to environmental signals throughout the different stages of an infection.

References

Aepfelbacher, M., C. Trasak, and K. Ruckdeschel. 2007. Effector functions of pathogenic *Yersinia* species. Thromb Haemost 98(3):521-9.

Aiba, H. 2007. Mechanism of RNA silencing by Hfq-binding small RNAs. Curr Opin Microbiol 10(2):134-9.

Allaoui, A., R. Scheen, C. Lambert de Rouvroit, and G. R. Cornelis. 1995a. VirG, a *Yersinia enterocolitica* lipoprotein involved in Ca^{2+} dependency, is related to *exsB* of *Pseudomonas aeruginosa*. J Bacteriol 177(15):4230-7.

Allaoui, A., R. Schulte, and G. R. Cornelis. 1995b. Mutational analysis of the *Yersinia enterocolitica virC* operon: characterization of *yscE, F, G, I, J, K* required for Yop secretion and *yscH* encoding YopR. Mol Microbiol 18(2):343-55.

Altier, C., M. Suyemoto, and S. D. Lawhon. 2000. Regulation of *Salmonella enterica serovar* typhimurium invasion genes by *csrA*. Infect Immun 68(12):6790-7.

Altman, S., D. Wesolowski, C. Guerrier-Takada, and Y. Li. 2005. RNase P cleaves transient structures in some riboswitches. Proc Natl Acad Sci U S A 102(32):11284-9.

Arold, S. T., P. G. Leonard, G. N. Parkinson, and J. E. Ladbury. 2010. H-NS forms a superhelical protein scaffold for DNA condensation. Proc Natl Acad Sci U S A 107(36):15728-32.

Autenrieth, I. B., U. Vogel, S. Preger, B. Heymer, and J. Heesemann. 1993. Experimental *Yersinia enterocolitica* infection in euthymic and T-cell-deficient athymic nude C57BL/6 mice: comparison of time course, histomorphology, and immune response. Infect Immun 61(6):2585-95.

Babitzke, P., and T. Romeo. 2007. CsrB sRNA family: sequestration of RNA-binding regulatory proteins. Curr Opin Microbiol 10(2):156-63.

Bae, S. H., D. Liu, H. M. Lim, Y. Lee, and B. S. Choi. 2008. Structure of the nucleoid-associated protein Cnu reveals common binding sites for H-NS in Cnu and Hha. Biochemistry 47(7):1993-2001.

Bai, G., A. Golubov, E. A. Smith, and K. A. McDonough. 2010. The importance of the small RNA chaperone Hfq for growth of epidemic *Yersinia pestis*, but not *Yersinia pseudotuberculosis*, with implications for plague biology. J Bacteriol 192(16):4239-45.

Baker, C. S., I. Morozov, K. Suzuki, T. Romeo, and P. Babitzke. 2002. CsrA regulates glycogen biosynthesis by preventing translation of *glgC* in *Escherichia coli*. Mol Microbiol 44(6):1599-610.

Balsalobre, C., J. Johansson, B. E. Uhlin, A. Juarez, and F. J. Munoa. 1999. Alterations in protein expression caused by the *hha* mutation in *Escherichia coli*: influence of growth medium osmolarity. J Bacteriol 181(10):3018-24.

Balsalobre, C., A. Juarez, C. Madrid, M. Mourino, A. Prenafeta, and F. J. Munoa. 1996. Complementation of the *hha* mutation in *Escherichia coli* by the *ymoA* gene from *Yersinia enterocolitica*: dependence on the gene dosage. Microbiology 142 (Pt 7):1841-6.

Banos, R. C., J. I. Pons, C. Madrid, and A. Juarez. 2008. A global modulatory role for the *Yersinia enterocolitica* H-NS protein. Microbiology 154(Pt 5):1281-9.

Bartra, S. S., M. W. Jackson, J. A. Ross, and G. V. Plano. 2006. Calcium-regulated type III secretion of Yop proteins by an *Escherichia coli hha* mutant carrying a *Yersinia pestis* pCD1 virulence plasmid. Infect Immun 74(2):1381-6.

Bergsbaken, T., and B. T. Cookson. 2009. Innate immune response during *Yersinia* infection: critical modulation of cell death mechanisms through phagocyte activation. J Leukoc Biol 86(5):1153-8.

Bhatt, S., A. N. Edwards, H. T. Nguyen, D. Merlin, T. Romeo, and D. Kalman. 2009. The RNA binding protein CsrA is a pleiotropic regulator of the locus of enterocyte effacement pathogenicity island of enteropathogenic *Escherichia coli*. Infect Immun 77(9):3552-68.

Birck, C., L. Mourey, P. Gouet, B. Fabry, J. Schumacher, P. Rousseau, D. Kahn, and J. P. Samama. 1999. Conformational changes induced by phosphorylation of the FixJ receiver domain. Structure 7(12):1505-15.

Birnboim, H. C., and J. Doly. 1979. A rapid alkaline extraction procedure for screening recombinant plasmid DNA. Nucleic Acids Res 7(6):1513-23.

Blot, N., R. Mavathur, M. Geertz, A. Travers, and G. Muskhelishvili. 2006. Homeostatic regulation of supercoiling sensitivity coordinates transcription of the bacterial genome. EMBO Rep 7(7):710-5.

Blumer, C., S. Heeb, G. Pessi, and D. Haas. 1999. Global GacA-steered control of cyanide and exoprotease production in *Pseudomonas fluorescens* involves specific ribosome binding sites. Proc Natl Acad Sci U S A 96(24):14073-8.

Blumer, C., A. Kleefeld, D. Lehnen, M. Heintz, U. Dobrindt, G. Nagy, K. Michaelis, L. Emody, T. Polen, R. Rachel, V. F. Wendisch, and G. Unden. 2005. Regulation of type 1 fimbriae synthesis and biofilm formation by the transcriptional regulator LrhA of *Escherichia coli*. Microbiology 151(Pt 10):3287-98.

Boddicker, J. D., and B. D. Jones. 2004. Lon protease activity causes down-regulation of *Salmonella* pathogenicity island 1 invasion gene expression after infection of epithelial cells. Infect Immun 72(4):2002-13.

Bolin, I., L. Norlander, and H. Wolf-Watz. 1982. Temperature-inducible outer membrane protein of *Yersinia pseudotuberculosis* and *Yersinia enterocolitica* is associated with the virulence plasmid. Infect Immun 37(2):506-12.

Bottone, E. J. 1997. *Yersinia enterocolitica*: the charisma continues. Clin Microbiol Rev 10(2):257-76.

Bottone, E. J. 1999. *Yersinia enterocolitica*: overview and epidemiologic correlates. Microbes Infect 1(4):323-33.

Bradford, M. M. 1976. A rapid and sensitive method for the quantitation of microgram quantities of protein utilizing the principle of protein-dye binding. Anal Biochem 72:248-54.

Brantl, S., and E. G. Wagner. 1994. Antisense RNA-mediated transcriptional attenuation occurs faster than stable antisense/target RNA pairing: an *in vitro* study of plasmid pIP501. EMBO J 13(15):3599-607.

Brennan, R. G., and T. M. Link. 2007. Hfq structure, function and ligand binding. Curr Opin Microbiol 10(2):125-33.

Brescia, C. C., M. K. Kaw, and D. D. Sledjeski. 2004. The DNA binding protein H-NS binds to and alters the stability of RNA *in vitro* and *in vivo*. J Mol Biol 339(3):505-14.

Brutinel, E. D., C. A. Vakulskas, K. M. Brady, and T. L. Yahr. 2008. Characterization of ExsA and of ExsA-dependent promoters required for expression of the *Pseudomonas aeruginosa* type III secretion system. Mol Microbiol 68(3):657-71.

Burghout, P., F. Beckers, E. de Wit, R. van Boxtel, G. R. Cornelis, J. Tommassen, and M. Koster. 2004. Role of the pilot protein YscW in the biogenesis of the YscC secretin in *Yersinia enterocolitica*. J Bacteriol 186(16):5366-75.

Butler, T. 2009. Plague into the 21st century. Clin Infect Dis 49(5):736-42.

Carter, J. D., and A. P. Hudson. 2009. Reactive arthritis: clinical aspects and medical management. Rheum Dis Clin North Am 35(1):21-44.

Castillo, A., W. Nasser, G. Condemine, and S. Reverchon. 1998. The PecT repressor interacts with regulatory regions of pectate lyase genes in *Erwinia chrysanthemi*. Biochim Biophys Acta 1442(2-3):148-60.

Cathelyn, J. S., S. D. Crosby, W. W. Lathem, W. E. Goldman, and V. L. Miller. 2006. RovA, a global regulator of *Yersinia pestis*, specifically required for bubonic plague. Proc Natl Acad Sci U S A 103(36):13514-9.

Cathelyn, J. S., D. W. Ellison, S. J. Hinchliffe, B. W. Wren, and V. L. Miller. 2007. The RovA regulons of *Yersinia enterocolitica* and *Yersinia pestis* are distinct: evidence that many RovA-regulated genes were acquired more recently than the core genome. Mol Microbiol 66(1):189-205.

Chang, A. C., and S. N. Cohen. 1978. Construction and characterization of amplifiable multicopy DNA cloning vehicles derived from the P15A cryptic miniplasmid. J Bacteriol 134(3):1141-56.

Chao, Y., and J. Vogel. 2010. The role of Hfq in bacterial pathogens. Curr Opin Microbiol 13(1):24-33.

Chatterjee, A., Y. Cui, and A. K. Chatterjee. 2002. RsmA and the quorum-sensing signal, N-[3-oxohexanoyl]-L-homoserine lactone, control the levels of *rsmB* RNA in *Erwinia carotovora* subsp. *carotovora* by affecting its stability. J Bacteriol 184(15):4089-95.

Cirillo, D. M., R. H. Valdivia, D. M. Monack, and S. Falkow. 1998. Macrophage-dependent induction of the *Salmonella* pathogenicity island 2 type III secretion system and its role in intracellular survival. Mol Microbiol 30(1):175-88.

Cohn, M. T., H. Ingmer, F. Mulholland, K. Jorgensen, J. M. Wells, and L. Brondsted. 2007. Contribution of conserved ATP-dependent proteases of *Campylobacter jejuni* to stress tolerance and virulence. Appl Environ Microbiol 73(24):7803-13.

Condemine, G., A. Castillo, F. Passeri, and C. Enard. 1999. The PecT repressor coregulates synthesis of exopolysaccharides and virulence factors in *Erwinia chrysanthemi*. Mol Plant Microbe Interact 12(1):45-52.

Coombes, B. K., M. E. Wickham, M. J. Lowden, N. F. Brown, and B. B. Finlay. 2005. Negative regulation of *Salmonella* pathogenicity island 2 is required for contextual control of virulence during typhoid. Proc Natl Acad Sci U S A 102(48):17460-5.

Cordeiro, T. N., J. Garcia, J. I. Pons, S. Aznar, A. Juarez, and M. Pons. 2008. A single residue mutation in Hha preserving structure and binding to H-NS results in loss of H-NS mediated gene repression properties. FEBS Lett 582(20):3139-44.

Cornelis, G. R. 1993. Role of the transcription activator *virF* and the histone-like protein YmoA in the thermoregulation of virulence functions in yersiniae. Zentralbl Bakteriol 278(2-3):149-64.

Cornelis, G. R. 2002a. *Yersinia* type III secretion: send in the effectors. J Cell Biol 158(3):401-8.

Cornelis, G. R. 2002b. The *Yersinia* Ysc-Yop 'type III' weaponry. Nat Rev Mol Cell Biol 3(10):742-52.

Cornelis, G. R. 2006. The type III secretion injectisome. Nat Rev Microbiol 4(11):811-25.

Cornelis, G. R., C. Sluiters, I. Delor, D. Geib, K. Kaniga, C. Lambert de Rouvroit, M. P. Sory, J. C. Vanooteghem, and T. Michiels. 1991. *ymoA*, a *Yersinia enterocolitica* chromosomal gene modulating the expression of virulence functions. Mol Microbiol 5(5):1023-34.

Cornelis, G., C. Sluiters, C. L. de Rouvroit, and T. Michiels. 1989. Homology between *virF*, the transcriptional activator of the *Yersinia* virulence regulon, and AraC, the *Escherichia coli* arabinose operon regulator. J Bacteriol 171(1):254-62.

Cornelis, G., J. C. Vanootegem, and C. Sluiters. 1987. Transcription of the *yop* regulon from *Y. enterocolitica* requires trans acting pYV and chromosomal genes. Microb Pathog 2(5):367-79.

Cotter, S. E., N. K. Surana, and J. W. St Geme, 3rd. 2005. Trimeric autotransporters: a distinct subfamily of autotransporter proteins. Trends Microbiol 13(5):199-205.

Cui, Y., A. Chatterjee, Y. Liu, C. K. Dumenyo, and A. K. Chatterjee. 1995. Identification of a global repressor gene, *rsmA,* of *Erwinia carotovora* subsp. *carotovora* that controls extracellular enzymes, N-(3-oxohexanoyl)-L-homoserine lactone, and pathogenicity in soft-rotting *Erwinia* spp. J Bacteriol 177(17):5108-15.

Cui, Y., A. Mukherjee, C. K. Dumenyo, Y. Liu, and A. K. Chatterjee. 1999. *rsmC* of the soft-rotting bacterium *Erwinia carotovora* subsp. *carotovora* negatively controls extracellular enzyme and harpin(Ecc) production and virulence by modulating levels of regulatory RNA (*rsmB*) and RNA-binding protein (RsmA). J Bacteriol 181(19):6042-52.

Dame, R. T., C. Wyman, and N. Goosen. 2001. Structural basis for preferential binding of H-NS to curved DNA. Biochimie 83(2):231-4.

Datsenko, K. A., and B. L. Wanner. 2000. One-step inactivation of chromosomal genes in *Escherichia coli* K-12 using PCR products. Proc Natl Acad Sci U S A 97(12):6640-5.

de la Cruz, F., M. Carmona, and A. Juarez. 1992. The Hha protein from *Escherichia coli* is highly homologous to the YmoA protein from *Yersinia enterocolitica*. Mol Microbiol 6(22):3451-2.

Derbise, A., B. Lesic, D. Dacheux, J. M. Ghigo, and E. Carniel. 2003. A rapid and simple method for inactivating chromosomal genes in *Yersinia*. FEMS Immunol Med Microbiol 38(2):113-6.

Dersch, P., and R. R. Isberg. 1999. A region of the *Yersinia pseudotuberculosis* invasin protein enhances integrin-mediated uptake into mammalian cells and promotes self-association. EMBO J 18(5):1199-213.

Dersch, P., and R. R. Isberg. 2000. An immunoglobulin superfamily-like domain unique to the *Yersinia pseudotuberculosis* invasin protein is required for stimulation of bacterial uptake via integrin receptors. Infect Immun 68(5):2930-8.

Diepold, A., M. Amstutz, S. Abel, I. Sorg, U. Jenal, and G. R. Cornelis. 2010. Deciphering the assembly of the *Yersinia* type III secretion injectisome. EMBO J 29(11):1928-40.

Dillon, S. C., and C. J. Dorman. 2010. Bacterial nucleoid-associated proteins, nucleoid structure and gene expression. Nat Rev Microbiol 8(3):185-95.

Dorman, C. J. 2004. H-NS: a universal regulator for a dynamic genome. Nat Rev Microbiol 2(5):391-400.

Dube, P. 2009. Interaction of *Yersinia* with the gut: mechanisms of pathogenesis and immune evasion. Curr Top Microbiol Immunol 337:61-91.

Dubey, A. K., C. S. Baker, T. Romeo, and P. Babitzke. 2005. RNA sequence and secondary structure participate in high-affinity CsrA-RNA interaction. RNA 11(10):1579-87.

Duong, N., S. Osborne, V. H. Bustamante, A. M. Tomljenovic, J. L. Puente, and B. K. Coombes. 2007. Thermosensing coordinates a cis-regulatory module for transcriptional activation of the intracellular virulence system in *Salmonella enterica* serovar Typhimurium. J Biol Chem 282(47):34077-84.

Eichelberg, K., and J. E. Galan. 1999. Differential regulation of *Salmonella typhimurium* type III secreted proteins by pathogenicity island 1 (SPI-1)-encoded transcriptional activators InvF and *hilA*. Infect Immun 67(8):4099-105.

Eitel, J., and P. Dersch. 2002. The YadA protein of *Yersinia pseudotuberculosis* mediates high-efficiency uptake into human cells under environmental conditions in which invasin is repressed. Infect Immun 70(9):4880-91.

Eitel, J., T. Heise, U. Thiesen, and P. Dersch. 2005. Cell invasion and IL-8 production pathways initiated by YadA of *Yersinia pseudotuberculosis* require common signalling molecules (FAK, c-Src, Ras) and distinct cell factors. Cell Microbiol 7(1):63-77.

El Tahir, Y., and M. Skurnik. 2001. YadA, the multifaceted *Yersinia* adhesin. Int J Med Microbiol 291(3):209-18.

Ellison, D. W., M. B. Lawrenz, and V. L. Miller. 2004. Invasin and beyond: regulation of *Yersinia* virulence by RovA. Trends Microbiol 12(6):296-300.

Ellison, D. W., and V. L. Miller. 2006. H-NS represses inv transcription in *Yersinia enterocolitica* through competition with RovA and interaction with YmoA. J Bacteriol 188(14):5101-12.

Ellison, D. W., B. Young, K. Nelson, and V. L. Miller. 2003. YmoA negatively regulates expression of invasin from *Yersinia enterocolitica*. J Bacteriol 185(24):7153-9.

Fahlen, T. F., R. L. Wilson, J. D. Boddicker, and B. D. Jones. 2001. Hha is a negative modulator of transcription of *hilA*, the *Salmonella enterica* serovar Typhimurium invasion gene transcriptional activator. J Bacteriol 183(22):6620-9.

Fang, F. C., and S. Rimsky. 2008. New insights into transcriptional regulation by H-NS. Curr Opin Microbiol 11(2):113-20.

Fantappie, L., M. M. Metruccio, K. L. Seib, F. Oriente, E. Cartocci, F. Ferlicca, M. M. Giuliani, V. Scarlato, and I. Delany. 2009. The RNA chaperone Hfq is involved in stress response and virulence in *Neisseria meningitidis* and is a pleiotropic regulator of protein expression. Infect Immun 77(5):1842-53.

Fass, E., and E. A. Groisman. 2009. Control of *Salmonella* pathogenicity island-2 gene expression. Curr Opin Microbiol 12(2):199-204.

Fortune, D. R., M. Suyemoto, and C. Altier. 2006. Identification of CsrC and characterization of its role in epithelial cell invasion in *Salmonella enterica* serovar Typhimurium. Infect Immun 74(1):331-9.

Francis, M. S., H. Wolf-Watz, and A. Forsberg. 2002. Regulation of type III secretion systems. Curr Opin Microbiol 5(2):166-72.

Fremaux, B., C. Prigent-Combaret, and C. Vernozy-Rozand. 2008. Long-term survival of Shiga toxin-producing *Escherichia coli* in cattle effluents and environment: an updated review. Vet Microbiol 132(1-2):1-18.

Gallegos, M. T., R. Schleif, A. Bairoch, K. Hofmann, and J. L. Ramos. 1997. Arac/XylS family of transcriptional regulators. Microbiol Mol Biol Rev 61(4):393-410.

Geissmann, T. A., and D. Touati. 2004. Hfq, a new chaperoning role: binding to messenger RNA determines access for small RNA regulator. EMBO J 23(2):396-405.

Geng, J., Y. Song, L. Yang, Y. Feng, Y. Qiu, G. Li, J. Guo, Y. Bi, Y. Qu, W. Wang, X. Wang, Z. Guo, R. Yang, and Y. Han. 2009. Involvement of the post-transcriptional regulator Hfq in *Yersinia pestis* virulence. PLoS One 4(7):e6213.

Ginocchio, C. C., S. B. Olmsted, C. L. Wells, and J. E. Galan. 1994. Contact with epithelial cells induces the formation of surface appendages on *Salmonella typhimurium*. Cell 76(4):717-24.

Girschick, H. J., L. Guilherme, R. D. Inman, K. Latsch, M. Rihl, Y. Sherer, Y. Shoenfeld, H. Zeidler, S. Arienti, and A. Doria. 2008. Bacterial triggers and autoimmune rheumatic diseases. Clin Exp Rheumatol 26(1 Suppl 48):S12-7.

Giuliodori, A. M., F. Di Pietro, S. Marzi, B. Masquida, R. Wagner, P. Romby, C. O. Gualerzi, and C. L. Pon. 2010. The *cspA* mRNA is a thermosensor that modulates translation of the cold-shock protein CspA. Mol Cell 37(1):21-33.

Goranson, J., A. K. Hovey, and D. W. Frank. 1997. Functional analysis of *exsC* and *exsB* in regulation of exoenzyme S production by *Pseudomonas aeruginosa*. J Bacteriol 179(5):1646-54.

Grassl, G. A., E. Bohn, Y. Muller, O. T. Buhler, and I. B. Autenrieth. 2003. Interaction of *Yersinia enterocolitica* with epithelial cells: invasin beyond invasion. Int J Med Microbiol 293(1):41-54.

Grutzkau, A., C. Hanski, H. Hahn, and E. O. Riecken. 1990. Involvement of M cells in the bacterial invasion of Peyer's patches: a common mechanism shared by *Yersinia enterocolitica* and other enteroinvasive bacteria. Gut 31(9):1011-5.

Guan, T. Y., and R. A. Holley. 2003. Pathogen survival in swine manure environments and transmission of human enteric illness--a review. J Environ Qual 32(2):383-92.

Gudapaty, S., K. Suzuki, X. Wang, P. Babitzke, and T. Romeo. 2001. Regulatory interactions of Csr components: the RNA binding protein CsrA activates *csrB* transcription in *Escherichia coli*. J Bacteriol 183(20):6017-27.

Guerrier-Takada, C., K. Gardiner, T. Marsh, N. Pace, and S. Altman. 1983. The RNA moiety of ribonuclease P is the catalytic subunit of the enzyme. Cell 35(3 Pt 2):849-57.

Gutierrez, P., Y. Li, M. J. Osborne, E. Pomerantseva, Q. Liu, and K. Gehring. 2005. Solution structure of the carbon storage regulator protein CsrA from *Escherichia coli*. J Bacteriol 187(10):3496-501.

Hansen, A. M., and J. B. Kaper. 2009. Hfq affects the expression of the LEE pathogenicity island in enterohaemorrhagic *Escherichia coli*. Mol Microbiol 73(3):446-65.

Hanski, C., M. Naumann, H. Hahn, and E. O. Riecken. 1989. Determinants of invasion and survival of *Yersinia enterocolitica* in intestinal tissue. An *in vivo* study. Med Microbiol Immunol 178(5):289-96.

Hartz, D., D. S. McPheeters, and L. Gold. 1989. Selection of the initiator tRNA by *Escherichia coli* initiation factors. Genes Dev 3(12A):1899-912.

Hasegawa, H., A. Chatterjee, Y. Cui, and A. K. Chatterjee. 2005. Elevated temperature enhances virulence of *Erwinia carotovora* subsp. *carotovora* strain EC153 to plants and stimulates production of the quorum sensing signal, N-acyl homoserine lactone, and extracellular proteins. Appl Environ Microbiol 71(8):4655-63.

Heesemann, J., A. Sing, and K. Trulzsch. 2006. *Yersinia*'s stratagem: targeting innate and adaptive immune defense. Curr Opin Microbiol 9(1):55-61.

Heise, T., and P. Dersch. 2006. Identification of a domain in *Yersinia* virulence factor YadA that is crucial for extracellular matrix-specific cell adhesion and uptake. Proc Natl Acad Sci U S A 103(9):3375-80.

Heise, T., and P. Dersch. 2007. Interaktion mit Wirtszellen – individuell. BIO*spektrum* (13. Jahrgang):258/259.

Herbst, K., M. Bujara, A. K. Heroven, W. Opitz, M. Weichert, A. Zimmermann, and P. Dersch. 2009. Intrinsic thermal sensing controls proteolysis of *Yersinia* virulence regulator RovA. PLoS Pathog 5(5):e1000435.

Heroven, A. K., K. Bohme, M. Rohde, and P. Dersch. 2008. A Csr-type regulatory system, including small non-coding RNAs, regulates the global virulence regulator RovA of *Yersinia pseudotuberculosis* through RovM. Mol Microbiol 68(5):1179-95.

Heroven, A. K., K. Bohme, H. Tran-Winkler, and P. Dersch. 2007. Regulatory elements implicated in the environmental control of invasin expression in enteropathogenic *Yersinia*. Adv Exp Med Biol 603:156-66.

Heroven, A. K., and P. Dersch. 2006. RovM, a novel LysR-type regulator of the virulence activator gene *rovA,* controls cell invasion, virulence and motility of *Yersinia pseudotuberculosis*. Mol Microbiol 62(5):1469-83.

Heroven, A. K., G. Nagel, H. J. Tran, S. Parr, and P. Dersch. 2004. RovA is autoregulated and antagonizes H-NS-mediated silencing of invasin and rovA expression in *Yersinia pseudotuberculosis*. Mol Microbiol 53(3):871-88.

Heroven, A. K., and P. Dersch. 2010. A global regulatory network, implicating regulatory RNAs, controls virulence gene expression in pathogenic yersiniae. Pp. 1-17: Res. Adv. in Molecular Microbiology.

Hoe, N. P., and J. D. Goguen. 1993. Temperature sensing in *Yersinia pestis*: translation of the LcrF activator protein is thermally regulated. J Bacteriol 175(24):7901-9.

Hoe, N. P., F. C. Minion, and J. D. Goguen. 1992. Temperature sensing in *Yersinia pestis*: regulation of yopE transcription by lcrF. J Bacteriol 174(13):4275-86.

Hoiczyk, E., A. Roggenkamp, M. Reichenbecher, A. Lupas, and J. Heesemann. 2000. Structure and sequence analysis of *Yersinia* YadA and *Moraxella* UspAs reveal a novel class of adhesins. EMBO J 19(22):5989-99.

Hovey, A. K., and D. W. Frank. 1995. Analyses of the DNA-binding and transcriptional activation properties of ExsA, the transcriptional activator of the *Pseudomonas aeruginosa* exoenzyme S regulon. J Bacteriol 177(15):4427-36.

Humair, B., N. Gonzalez, D. Mossialos, C. Reimmann, and D. Haas. 2009. Temperature-responsive sensing regulates biocontrol factor expression in *Pseudomonas fluorescens* CHA0. ISME J 3(8):955-65.

Hurst, M. R., S. A. Becher, S. D. Young, T. L. Nelson, and T. R. Glare. 2010. *Yersinia entomophaga* sp. *nov*. isolated from the New Zealand grass grub *Costelytra zealandica*. Int J Syst Evol Microbiol.

Isberg, R. R., and P. Barnes. 2001. Subversion of integrins by enteropathogenic *Yersinia*. J Cell Sci 114(Pt 1):21-28.

Isberg, R. R., Z. Hamburger, and P. Dersch. 2000. Signaling and invasin-promoted uptake via integrin receptors. Microbes Infect 2(7):793-801.

Jackson, M. W., E. Silva-Herzog, and G. V. Plano. 2004. The ATP-dependent ClpXP and Lon proteases regulate expression of the *Yersinia pestis* type III secretion system via regulated proteolysis of YmoA, a small histone-like protein. Mol Microbiol 54(5):1364-78.

Jang, M. H., M. N. Kweon, K. Iwatani, M. Yamamoto, K. Terahara, C. Sasakawa, T. Suzuki, T. Nochi, Y. Yokota, P. D. Rennert, T. Hiroi, H. Tamagawa, H. Iijima, J. Kunisawa, Y. Yuki, and H. Kiyono. 2004. Intestinal villous M cells: an antigen entry site in the mucosal epithelium. Proc Natl Acad Sci U S A 101(16):6110-5.

Johansson, J., S. Eriksson, B. Sonden, S. N. Wai, and B. E. Uhlin. 2001. Heteromeric interactions among nucleoid-associated bacterial proteins: localization of StpA-stabilizing regions in H-NS of *Escherichia coli*. J Bacteriol 183(7):2343-7.

Johansson, J., P. Mandin, A. Renzoni, C. Chiaruttini, M. Springer, and P. Cossart. 2002. An RNA thermosensor controls expression of virulence genes in *Listeria monocytogenes*. Cell 110(5):551-61.

Johansson, J., and B. E. Uhlin. 1999. Differential protease-mediated turnover of H-NS and StpA revealed by a mutation altering protein stability and stationary-phase survival of *Escherichia coli*. Proc Natl Acad Sci U S A 96(19):10776-81.

Jonas, K., and O. Melefors. 2009. The *Escherichia coli* CsrB and CsrC small RNAs are strongly induced during growth in nutrient-poor medium. FEMS Microbiol Lett 297(1):80-6.

Jones, B. D. 2005. *Salmonella* invasion gene regulation: a story of environmental awareness. J Microbiol 43 Spec No:110-7.

Journet, L., K. T. Hughes, and G. R. Cornelis. 2005. Type III secretion: a secretory pathway serving both motility and virulence (review). Mol Membr Biol 22(1-2):41-50.

Kage, H., A. Takaya, M. Ohya, and T. Yamamoto. 2008. Coordinated regulation of expression of *Salmonella* pathogenicity island 1 and flagellar type III secretion systems by ATP-dependent ClpXP protease. J Bacteriol 190(7):2470-8.

Kajfasz, J. K., A. R. Martinez, I. Rivera-Ramos, J. Abranches, H. Koo, R. G. Quivey, Jr., and J. A. Lemos. 2009. Role of Clp proteins in expression of virulence properties of *Streptococcus mutans*. J Bacteriol 191(7):2060-8.

Kang, Y., V. V. Lunin, T. Skarina, A. Savchenko, M. J. Schurr, and T. T. Hoang. 2009. The long-chain fatty acid sensor, PsrA, modulates the expression of *rpoS* and the type III secretion *exsCEBA* operon in *Pseudomonas aeruginosa*. Mol Microbiol 73(1):120-36.

Kawamoto, H., Y. Koide, T. Morita, and H. Aiba. 2006. Base-pairing requirement for RNA silencing by a bacterial small RNA and acceleration of duplex formation by Hfq. Mol Microbiol 61(4):1013-22.

Kim, M. S., S. H. Bae, S. H. Yun, H. J. Lee, S. C. Ji, J. H. Lee, P. Srivastava, S. H. Lee, H. Chae, Y. Lee, B. S. Choi, D. K. Chattoraj, and H. M. Lim. 2005. Cnu, a novel oriC-binding protein of *Escherichia coli*. J Bacteriol 187(20):6998-7008.

Kirjavainen, V., H. Jarva, M. Biedzka-Sarek, A. M. Blom, M. Skurnik, and S. Meri. 2008. *Yersinia enterocolitica* serum resistance proteins YadA and ail bind the complement regulator C4b-binding protein. PLoS Pathog 4(8):e1000140.

Koretke, K. K., P. Szczesny, M. Gruber, and A. N. Lupas. 2006. Model structure of the prototypical non-fimbrial adhesin YadA of *Yersinia enterocolitica*. J Struct Biol 155(2):154-61.

Koslover, D. J., A. J. Callaghan, M. J. Marcaida, E. F. Garman, M. Martick, W. G. Scott, and B. F. Luisi. 2008. The crystal structure of the *Escherichia coli* RNase E apoprotein and a mechanism for RNA degradation. Structure 16(8):1238-44.

Koster, M., W. Bitter, H. de Cock, A. Allaoui, G. R. Cornelis, and J. Tommassen. 1997. The outer membrane component, YscC, of the Yop secretion machinery of *Yersinia enterocolitica* forms a ring-shaped multimeric complex. Mol Microbiol 26(4):789-97.

Kulshina, N., N. J. Baird, and A. R. Ferre-D'Amare. 2009. Recognition of the bacterial second messenger cyclic diguanylate by its cognate riboswitch. Nat Struct Mol Biol 16(12):1212-7.

Laemmli, U. K. 1970. Cleavage of structural proteins during the assembly of the head of bacteriophage T4. Nature 227(5259):680-5.

Lambert de Rouvroit, C., C. Sluiters, and G. R. Cornelis. 1992. Role of the transcriptional activator, VirF, and temperature in the expression of the pYV plasmid genes of *Yersinia enterocolitica*. Mol Microbiol 6(3):395-409.

Lapouge, K., M. Schubert, F. H. Allain, and D. Haas. 2008. Gac/Rsm signal transduction pathway of gamma-proteobacteria: from RNA recognition to regulation of social behaviour. Mol Microbiol 67(2):241-53.

Lawhon, S. D., J. G. Frye, M. Suyemoto, S. Porwollik, M. McClelland, and C. Altier. 2003. Global regulation by CsrA in *Salmonella typhimurium*. Mol Microbiol 48(6):1633-45.

Lawrenz, M. B., and V. L. Miller. 2007. Comparative analysis of the regulation of *rovA* from the pathogenic yersiniae. J Bacteriol 189(16):5963-75.

Le Derout, J., I. V. Boni, P. Regnier, and E. Hajnsdorf. 2010. Hfq affects mRNA levels independently of degradation. BMC Mol Biol 11:17.

Lee, E. R., J. L. Baker, Z. Weinberg, N. Sudarsan, and R. R. Breaker. 2010. An allosteric self-splicing ribozyme triggered by a bacterial second messenger. Science 329(5993):845-8.

Lee, N. L., W. O. Gielow, and R. G. Wallace. 1981. Mechanism of *araC* autoregulation and the domains of two overlapping promoters, Pc and PBAD, in the L-arabinose regulatory region of *Escherichia coli*. Proc Natl Acad Sci U S A 78(2):752-6.

Lehnen, D., C. Blumer, T. Polen, B. Wackwitz, V. F. Wendisch, and G. Unden. 2002. LrhA as a new transcriptional key regulator of flagella, motility and chemotaxis genes in *Escherichia coli*. Mol Microbiol 45(2):521-32.

Lenz, D. H., M. B. Miller, J. Zhu, R. V. Kulkarni, and B. L. Bassler. 2005. CsrA and three redundant small RNAs regulate quorum sensing in *Vibrio cholerae*. Mol Microbiol 58(4):1186-202.

Lenz, D. H., K. C. Mok, B. N. Lilley, R. V. Kulkarni, N. S. Wingreen, and B. L. Bassler. 2004. The small RNA chaperone Hfq and multiple small RNAs control quorum sensing in *Vibrio harveyi* and *Vibrio cholerae*. Cell 118(1):69-82.

Li, B., and R. Yang. 2008. Interaction between *Yersinia pestis* and the host immune system. Infect Immun 76(5):1804-11.

Li, Y., and S. Altman. 2003. A specific endoribonuclease, RNase P, affects gene expression of polycistronic operon mRNAs. Proc Natl Acad Sci U S A 100(23):13213-8.

Link, T. M., P. Valentin-Hansen, and R. G. Brennan. 2009. Structure of *Escherichia coli* Hfq bound to polyriboadenylate RNA. Proc Natl Acad Sci U S A 106(46):19292-7.

Ljungberg, P., M. Valtonen, V. P. Harjola, S. S. Kaukoranta-Tolvanen, and M. Vaara. 1995. Report of four cases of *Yersinia pseudotuberculosis* septicemia and a literature review. Eur J Clin Microbiol Infect Dis 14(9):804-10.

Loh, E., O. Dussurget, J. Gripenland, K. Vaitkevicius, T. Tiensuu, P. Mandin, F. Repoila, C. Buchrieser, P. Cossart, and J. Johansson. 2009. A trans-acting riboswitch controls expression of the virulence regulator PrfA in *Listeria monocytogenes*. Cell 139(4):770-9.

Lucchini, S., G. Rowley, M. D. Goldberg, D. Hurd, M. Harrison, and J. C. Hinton. 2006. H-NS mediates the silencing of laterally acquired genes in bacteria. PLoS Pathog 2(8):e81.

Mackie, G. A. 1998. Ribonuclease E is a 5'-end-dependent endonuclease. Nature 395(6703):720-3.

Madrid, C., C. Balsalobre, J. Garcia, and A. Juarez. 2007. The novel Hha/YmoA family of nucleoid-associated proteins: use of structural mimicry to modulate the activity of the H-NS family of proteins. Mol Microbiol 63(1):7-14.

Madrid, C., J. M. Nieto, and A. Juarez. 2002. Role of the Hha/YmoA family of proteins in the thermoregulation of the expression of virulence factors. Int J Med Microbiol 291(6-7):425-32.

Majdalani, N., C. K. Vanderpool, and S. Gottesman. 2005. Bacterial small RNA regulators. Crit Rev Biochem Mol Biol 40(2):93-113.

Manoil, C., and J. Beckwith. 1986. A genetic approach to analyzing membrane protein topology. Science 233(4771):1403-8.

Marra, A., and R. R. Isberg. 1996. Common entry mechanisms. Bacterial pathogenesis. Curr Biol 6(9):1084-6.

Marra, A., and R. R. Isberg. 1997. Invasin-dependent and invasin-independent pathways for translocation of *Yersinia pseudotuberculosis* across the Peyer's patch intestinal epithelium. Infect Immun 65(8):3412-21.

Martin, R. G., and J. L. Rosner. 2001. The AraC transcriptional activators. Curr Opin Microbiol 4(2):132-7.

Matsumoto, H., and G. M. Young. 2009. Translocated effectors of *Yersinia*. Curr Opin Microbiol 12(1):94-100.

Mayer, O., L. Rajkowitsch, C. Lorenz, R. Konrat, and R. Schroeder. 2007. RNA chaperone activity and RNA-binding properties of the *E. coli* protein StpA. Nucleic Acids Res 35(4):1257-69.

Mayer, O., C. Waldsich, R. Grossberger, and R. Schroeder. 2002. Folding of the td pre-RNA with the help of the RNA chaperone StpA. Biochem Soc Trans 30(Pt 6):1175-80.

McFeeters, R. L., A. S. Altieri, S. Cherry, J. E. Tropea, D. S. Waugh, and R. A. Byrd. 2007. The high-precision solution structure of *Yersinia* modulating protein YmoA provides insight into interaction with H-NS. Biochemistry 46(49):13975-82.

Mercante, J., K. Suzuki, X. Cheng, P. Babitzke, and T. Romeo. 2006. Comprehensive alanine-scanning mutagenesis of *Escherichia coli* CsrA defines two subdomains of critical functional importance. J Biol Chem 281(42):31832-42.

Mikulskis, A. V., and G. R. Cornelis. 1994. A new class of proteins regulating gene expression in enterobacteria. Mol Microbiol 11(1):77-86.

Mikulskis, A. V., I. Delor, V. H. Thi, and G. R. Cornelis. 1994. Regulation of the *Yersinia enterocolitica* enterotoxin Yst gene. Influence of growth phase, temperature, osmolarity, pH and bacterial host factors. Mol Microbiol 14(5):905-15.

Miller, J. H. 1992. A Short Course in Bacterial Genetics. Cold Spring Harbor, NY: Cold Spring Harbor Laboratory Press.

Mitobe, J., T. Morita-Ishihara, A. Ishihama, and H. Watanabe. 2009. Involvement of RNA-binding protein Hfq in the osmotic-response regulation of *invE* gene expression in *Shigella sonnei*. BMC Microbiol 9:110.

Mondragon, V., B. Franco, K. Jonas, K. Suzuki, T. Romeo, O. Melefors, and D. Georgellis. 2006. pH-dependent activation of the BarA-UvrY two-component system in *Escherichia coli*. J Bacteriol 188(23):8303-6.

Morishita, R., A. Kawagoshi, T. Sawasaki, K. Madin, T. Ogasawara, T. Oka, and Y. Endo. 1999. Ribonuclease activity of rat liver perchloric acid-soluble protein, a potent inhibitor of protein synthesis. J Biol Chem 274(29):20688-92.

Morita, M., M. Kanemori, H. Yanagi, and T. Yura. 1999a. Heat-induced synthesis of sigma32 in *Escherichia coli*: structural and functional dissection of *rpoH* mRNA secondary structure. J Bacteriol 181(2):401-10.

Morita, M. T., Y. Tanaka, T. S. Kodama, Y. Kyogoku, H. Yanagi, and T. Yura. 1999b. Translational induction of heat shock transcription factor sigma32: evidence for a built-in RNA thermosensor. Genes Dev 13(6):655-65.

Morschhauser, J., V. Vetter, T. Korhonen, B. E. Uhlin, and J. Hacker. 1993. Regulation and binding properties of S fimbriae cloned from *E. coli* strains causing urinary tract infection and meningitis. Zentralbl Bakteriol 278(2-3):165-76.

Mourino, M., C. Balsalobre, C. Madrid, J. M. Nieto, A. Prenafeta, F. J. Munoa, and A. Juarez. 1998. Osmolarity modulates the expression of the Hha protein from *Escherichia coli*. FEMS Microbiol Lett 160(2):225-9.

Mourino, M., C. Madrid, C. Balsalobre, A. Prenafeta, F. Munoa, J. Blanco, M. Blanco, J. E. Blanco, and A. Juarez. 1996. The Hha protein as a modulator of expression of virulence factors in *Escherichia coli*. Infect Immun 64(7):2881-4.

Muller, C. M., G. Schneider, U. Dobrindt, L. Emody, J. Hacker, and B. E. Uhlin. 2010. Differential effects and interactions of endogenous and horizontally acquired H-NS-like proteins in pathogenic *Escherichia coli*. Mol Microbiol 75(2):280-93.

Murros-Kontiainen, A. E., M. Fredriksson-Ahomaa, H. Korkeala, P. Johansson, R. Rahkila, and J. Bjorkroth. 2010a. *Yersinia nurmii* sp. nov. Int J Syst Evol Microbiol.

Murros-Kontiainen, A. E., P. Johansson, T. Niskanen, M. Fredriksson-Ahomaa, H. Korkeala, and J. Bjorkroth. 2010b. *Yersinia pekkanenii* sp. nov. Int J Syst Evol Microbiol.

Nagel, G., A. K. Heroven, J. Eitel, and P. Dersch. 2003. Function and regulation of the transcriptional activator RovA of *Yersinia pseudotuberculosis*. Adv Exp Med Biol 529:285-7.

Nagel, G., A. Lahrz, and P. Dersch. 2001. Environmental control of invasin expression in *Yersinia pseudotuberculosis* is mediated by regulation of RovA, a transcriptional activator of the SlyA/Hor family. Mol Microbiol 41(6):1249-69.

Narberhaus, F. 2010. Translational control of bacterial heat shock and virulence genes by temperature-sensing mRNAs. RNA Biol 7(1):84-9.

Nasser, W., S. Reverchon, R. Vedel, and M. Boccara. 2005. PecS and PecT coregulate the synthesis of HrpN and pectate lyases, two virulence determinants in *Erwinia chrysanthemi* 3937. Mol Plant Microbe Interact 18(11):1205-14.

Navarre, W. W., M. McClelland, S. J. Libby, and F. C. Fang. 2007. Silencing of xenogeneic DNA by H-NS-facilitation of lateral gene transfer in bacteria by a defense system that recognizes foreign DNA. Genes Dev 21(12):1456-71.

Neutra, M. R., A. Frey, and J. P. Kraehenbuhl. 1996. Epithelial M cells: gateways for mucosal infection and immunization. Cell 86(3):345-8.

Niemann, H. H., W. D. Schubert, and D. W. Heinz. 2004. Adhesins and invasins of pathogenic bacteria: a structural view. Microbes Infect 6(1):101-12.

Nieto, J. M., C. Madrid, E. Miquelay, J. L. Parra, S. Rodriguez, and A. Juarez. 2002. Evidence for direct protein-protein interaction between members of the enterobacterial Hha/YmoA and H-NS families of proteins. J Bacteriol 184(3):629-35.

Nieto, J. M., C. Madrid, A. Prenafeta, E. Miquelay, C. Balsalobre, M. Carrascal, and A. Juarez. 2000. Expression of the hemolysin operon in *Escherichia coli* is modulated by a nucleoid-protein complex that includes the proteins Hha and H-NS. Mol Gen Genet 263(2):349-58.

Nishino, K., M. Hayashi-Nishino, and A. Yamaguchi. 2009. H-NS modulates multidrug resistance of *Salmonella enterica* serovar Typhimurium by repressing multidrug efflux genes *acrEF*. Antimicrob Agents Chemother 53(8):3541-3.

Nishino, K., and A. Yamaguchi. 2004. Role of histone-like protein H-NS in multidrug resistance of *Escherichia coli*. J Bacteriol 186(5):1423-9.

Noom, M. C., W. W. Navarre, T. Oshima, G. J. Wuite, and R. T. Dame. 2007. H-NS promotes looped domain formation in the bacterial chromosome. Curr Biol 17(21):R913-4.

Norrander, J., T. Kempe, and J. Messing. 1983. Construction of improved M13 vectors using oligodeoxynucleotide-directed mutagenesis. Gene 26(1):101-6.

Nummelin, H., M. C. Merckel, J. C. Leo, H. Lankinen, M. Skurnik, and A. Goldman. 2004. The *Yersinia* adhesin YadA collagen-binding domain structure is a novel left-handed parallel beta-roll. EMBO J 23(4):701-11.

Oellerich, M. F., C. A. Jacobi, S. Freund, K. Niedung, A. Bach, J. Heesemann, and K. Trulzsch. 2007. *Yersinia enterocolitica* infection of mice reveals clonal invasion and abscess formation. Infect Immun 75(8):3802-11.

Olekhnovich, I. N., and R. J. Kadner. 2006. Crucial roles of both flanking sequences in silencing of the hilA promoter in *Salmonella enterica*. J Mol Biol 357(2):373-86.

Olekhnovich, I. N., and R. J. Kadner. 2007. Role of nucleoid-associated proteins Hha and H-NS in expression of *Salmonella enterica* activators HilD, HilC, and RtsA required for cell invasion. J Bacteriol 189(19):6882-90.

Ono, S., M. D. Goldberg, T. Olsson, D. Esposito, J. C. Hinton, and J. E. Ladbury. 2005. H-NS is a part of a thermally controlled mechanism for bacterial gene regulation. Biochem J 391(Pt 2):203-13.

Oshima, T., S. Ishikawa, K. Kurokawa, H. Aiba, and N. Ogasawara. 2006. *Escherichia coli* histone-like protein H-NS preferentially binds to horizontally acquired DNA in association with RNA polymerase. DNA Res 13(4):141-53.

Paglia, M. G., S. D'Arezzo, A. Festa, C. Del Borgo, L. Loiacono, A. Antinori, G. Antonucci, and P. Visca. 2005. *Yersinia pseudotuberculosis* septicemia and HIV. Emerg Infect Dis 11(7):1128-30.

Papenfort, K., and J. Vogel. 2010. Regulatory RNA in bacterial pathogens. Cell Host Microbe 8(1):116-27.

Park, H. S., Y. Ostberg, J. Johansson, E. G. Wagner, and B. E. Uhlin. 2010. Novel role for a bacterial nucleoid protein in translation of mRNAs with suboptimal ribosome-binding sites. Genes Dev 24(13):1345-50.

Paytubi, S., C. Madrid, N. Forns, J. M. Nieto, C. Balsalobre, B. E. Uhlin, and A. Juarez. 2004. YdgT, the Hha paralogue in *Escherichia coli*, forms heteromeric complexes with H-NS and StpA. Mol Microbiol 54(1):251-63.

Pepe, J. C., J. L. Badger, and V. L. Miller. 1994. Growth phase and low pH affect the thermal regulation of the *Yersinia enterocolitica inv* gene. Mol Microbiol 11(1):123-35.

Pepe, J. C., and V. L. Miller. 1993. The biological role of invasin during a *Yersinia enterocolitica* infection. Infect Agents Dis 2(4):236-41.

Pepe, J. C., M. R. Wachtel, E. Wagar, and V. L. Miller. 1995. Pathogenesis of defined invasion mutants of *Yersinia enterocolitica* in a BALB/c mouse model of infection. Infect Immun 63(12):4837-48.

Pernestig, A. K., D. Georgellis, T. Romeo, K. Suzuki, H. Tomenius, S. Normark, and O. Melefors. 2003. The *Escherichia coli* BarA-UvrY two-component system is needed for efficient switching between glycolytic and gluconeogenic carbon sources. J Bacteriol 185(3):843-53.

Pernestig, A. K., O. Melefors, and D. Georgellis. 2001. Identification of UvrY as the cognate response regulator for the BarA sensor kinase in *Escherichia coli*. J Biol Chem 276(1):225-31.

Perry, R. D., and J. D. Fetherston. 1997. *Yersinia pestis*--etiologic agent of plague. Clin Microbiol Rev 10(1):35-66.

Petrova, O. E., and K. Sauer. 2010. The novel two-component regulatory system BfiSR regulates biofilm development by controlling the small RNA *rsmZ* through CafA. J Bacteriol 192(20):5275-88.

Pfeiffer, V., A. Sittka, R. Tomer, K. Tedin, V. Brinkmann, and J. Vogel. 2007. A small non-coding RNA of the invasion gene island (SPI-1) represses outer membrane protein synthesis from the *Salmonella* core genome. Mol Microbiol 66(5):1174-91.

Pridmore, R. D. 1987. New and versatile cloning vectors with kanamycin-resistance marker. Gene 56(2-3):309-12.

Prosseda, G., M. Falconi, M. Giangrossi, C. O. Gualerzi, G. Micheli, and B. Colonna. 2004. The *virF* promoter in *Shigella*: more than just a curved DNA stretch. Mol Microbiol 51(2):523-37.

Pujol, C., and J. B. Bliska. 2005. Turning *Yersinia pathogenesis* outside in: subversion of macrophage function by intracellular yersiniae. Clin Immunol 114(3):216-26.

Ramamurthi, K. S., and O. Schneewind. 2002. Type iii protein secretion in *yersinia* species. Annu Rev Cell Dev Biol 18:107-33.

Rasmussen, A. A., M. Eriksen, K. Gilany, C. Udesen, T. Franch, C. Petersen, and P. Valentin-Hansen. 2005. Regulation of *ompA* mRNA stability: the role of a small regulatory RNA in growth phase-dependent control. Mol Microbiol 58(5):1421-9.

Reimmann, C., C. Valverde, E. Kay, and D. Haas. 2005. Posttranscriptional repression of GacS/GacA-controlled genes by the RNA-binding protein RsmE acting together with RsmA in the biocontrol strain *Pseudomonas fluorescens* CHA0. J Bacteriol 187(1):276-85.

Revell, P. A., and V. L. Miller. 2000. A chromosomally encoded regulator is required for expression of the *Yersinia enterocolitica inv* gene and for virulence. Mol Microbiol 35(3):677-85.

Rinnenthal, J., B. Klinkert, F. Narberhaus, and H. Schwalbe. 2010. Direct observation of the temperature-induced melting process of the *Salmonella* fourU RNA thermometer at base-pair resolution. Nucleic Acids Res 38(11):3834-47.

Rodriguez, S., J. M. Nieto, C. Madrid, and A. Juarez. 2005. Functional replacement of the oligomerization domain of H-NS by the Hha protein of *Escherichia coli*. J Bacteriol 187(15):5452-9.

Rogers, M. T., R. Zimmerman, and M. E. Scott. 2009. Histone-like nucleoid-structuring protein represses transcription of the *ehx* operon carried by locus of enterocyte effacement-negative Shiga toxin-expressing *Escherichia coli*. Microb Pathog 47(4):202-11.

Roggenkamp, A., N. Ackermann, C. A. Jacobi, K. Truelzsch, H. Hoffmann, and J. Heesemann. 2003. Molecular analysis of transport and oligomerization of the *Yersinia enterocolitica* adhesin YadA. J Bacteriol 185(13):3735-44.

Rohde, J. R., J. M. Fox, and S. A. Minnich. 1994. Thermoregulation in *Yersinia enterocolitica* is coincident with changes in DNA supercoiling. Mol Microbiol 12(2):187-99.

Rohde, J. R., X. S. Luan, H. Rohde, J. M. Fox, and S. A. Minnich. 1999. The *Yersinia enterocolitica* pYV virulence plasmid contains multiple intrinsic DNA bends which melt at 37 degrees C. J Bacteriol 181(14):4198-204.

Romeo, T. 1998. Global regulation by the small RNA-binding protein CsrA and the non-coding RNA molecule CsrB. Mol Microbiol 29(6):1321-30.

Rosner, B. M., K. Stark, and D. Werber. 2010. Epidemiology of reported *Yersinia enterocolitica* infections in Germany, 2001-2008. BMC Public Health 10:337.

Rosqvist, R., S. Hakansson, A. Forsberg, and H. Wolf-Watz. 1995. Functional conservation of the secretion and translocation machinery for virulence proteins of yersiniae, salmonellae and shigellae. EMBO J 14(17):4187-95.

Roth, M. J., N. Tanese, and S. P. Goff. 1988. Gene product of Moloney murine leukemia virus required for proviral integration is a DNA-binding protein. J Mol Biol 203(1):131-9.

Ruckdeschel, K., A. Deuretzbacher, and R. Haase. 2008. Crosstalk of signalling processes of innate immunity with *Yersinia* Yop effector functions. Immunobiology 213(3-4):261-9.

Sambrook J., Fritsch E. and T. Maniatis. 1989. Molecular Cloning. Cold Spring Harbor, NY: Cold Spring Harbor Laboratory Press.

Sambrook, J., E. Fritsch, and T. Maniatis. 1989. Molecular Cloning. Cold Spring Harbor, NY: Cold Spring Harbor Laboratory Press.

Sansonetti, P. 2002. Host-pathogen interactions: the seduction of molecular cross talk. Gut 50 Suppl 3:III2-8.

Sansonetti, P. J., and A. Phalipon. 1999. M cells as ports of entry for enteroinvasive pathogens: mechanisms of interaction, consequences for the disease process. Semin Immunol 11(3):193-203.

Schagger, H. 2006. Tricine-SDS-PAGE. Nat Protoc 1(1):16-22.

Schiano, C. A., L. E. Bellows, and W. W. Lathem. 2010. The small RNA chaperone Hfq is required for the virulence of *Yersinia pseudotuberculosis*. Infect Immun 78(5):2034-44.

Schmid, Y., G. A. Grassl, O. T. Buhler, M. Skurnik, I. B. Autenrieth, and E. Bohn. 2004. *Yersinia enterocolitica* adhesin A induces production of interleukin-8 in epithelial cells. Infect Immun 72(12):6780-9.

Schubert, M., K. Lapouge, O. Duss, F. C. Oberstrass, I. Jelesarov, D. Haas, and F. H. Allain. 2007. Molecular basis of messenger RNA recognition by the specific bacterial repressing clamp RsmA/CsrA. Nat Struct Mol Biol 14(9):807-13.

Schuck, A., A. Diwa, and J. G. Belasco. 2009. RNase E autoregulates its synthesis in *Escherichia coli* by binding directly to a stem-loop in the *rne* 5' untranslated region. Mol Microbiol 72(2):470-8.

Schutz, M., E. M. Weiss, M. Schindler, T. Hallstrom, P. F. Zipfel, D. Linke, and I. B. Autenrieth. 2010. Trimer stability of YadA is critical for virulence of *Yersinia enterocolitica*. Infect Immun 78(6):2677-90.

Sebbane, F., N. Lemaitre, D. E. Sturdevant, R. Rebeil, K. Virtaneva, S. F. Porcella, and B. J. Hinnebusch. 2006. Adaptive response of *Yersinia pestis* to extracellular effectors of innate immunity during bubonic plague. Proc Natl Acad Sci U S A 103(31):11766-71.

Seif, E., and S. Altman. 2008. RNase P cleaves the adenine riboswitch and stabilizes *pbuE* mRNA in *Bacillus subtilis*. RNA 14(6):1237-43.

Shakhnovich, E. A., B. M. Davis, and M. K. Waldor. 2009. Hfq negatively regulates type III secretion in EHEC and several other pathogens. Mol Microbiol 74(2):347-63.

Shao, F. 2008. Biochemical functions of *Yersinia* type III effectors. Curr Opin Microbiol 11(1):21-9.

Sharma, V. K., and R. L. Zuerner. 2004. Role of *hha* and *ler* in transcriptional regulation of the *esp* operon of enterohemorrhagic *Escherichia coli* O157:H7. J Bacteriol 186(21):7290-301.

Sherman, P. M., J. C. Ossa, and E. Wine. 2010. Bacterial infections: new and emerging enteric pathogens. Curr Opin Gastroenterol 26(1):1-4.

Silphaduang, U., M. Mascarenhas, M. Karmali, and B. K. Coombes. 2007. Repression of intracellular virulence factors in *Salmonella* by the Hha and YdgT nucleoid-associated proteins. J Bacteriol 189(9):3669-73.

Silva-Herzog, E., F. Ferracci, M. W. Jackson, S. S. Joseph, and G. V. Plano. 2008. Membrane localization and topology of the *Yersinia pestis* YscJ lipoprotein. Microbiology 154(Pt 2):593-607.

Silva, A. J., S. Z. Sultan, W. Liang, and J. A. Benitez. 2008. Role of the histone-like nucleoid structuring protein in the regulation of *rpoS* and RpoS-dependent genes in *Vibrio cholerae*. J Bacteriol 190(22):7335-45.

Simonet, M., S. Richard, and P. Berche. 1990. Electron microscopic evidence for *in vivo* extracellular localization of *Yersinia pseudotuberculosis* harboring the pYV plasmid. Infect Immun 58(3):841-5.

Simonet, M., B. Riot, N. Fortineau, and P. Berche. 1996. Invasin production by *Yersinia pestis* is abolished by insertion of an IS200-like element within the *inv* gene. Infect Immun 64(1):375-9.

Sittka, A., V. Pfeiffer, K. Tedin, and J. Vogel. 2007. The RNA chaperone Hfq is essential for the virulence of *Salmonella typhimurium*. Mol Microbiol 63(1):193-217.

Skurnik, M., and P. Toivanen. 1992. LcrF is the temperature-regulated activator of the *yadA* gene of *Yersinia enterocolitica* and *Yersinia pseudotuberculosis*. J Bacteriol 174(6):2047-51.

Song, T., D. Sabharwal, and S. N. Wai. 2010. VrrA mediates Hfq-dependent regulation of OmpT synthesis in *Vibrio cholerae*. J Mol Biol 400(4):682-8.

Sorger-Domenigg, T., E. Sonnleitner, V. R. Kaberdin, and U. Blasi. 2007. Distinct and overlapping binding sites of *Pseudomonas aeruginosa* Hfq and RsmA proteins on the non-coding RNA RsmY. Biochem Biophys Res Commun 352(3):769-73.

Spreter, T., C. K. Yip, S. Sanowar, I. Andre, T. G. Kimbrough, M. Vuckovic, R. A. Pfuetzner, W. Deng, A. C. Yu, B. B. Finlay, D. Baker, S. I. Miller, and N. C. Strynadka. 2009. A conserved structural motif mediates formation of the periplasmic rings in the type III secretion system. Nat Struct Mol Biol 16(5):468-76.

Stebbins, C. E., and J. E. Galan. 2001. Structural mimicry in bacterial virulence. Nature 412(6848):701-5.

Steffen, P., B. Voss, M. Rehmsmeier, J. Reeder, and R. Giegerich. 2006. RNAshapes: an integrated RNA analysis package based on abstract shapes. Bioinformatics 22(4):500-3.

Stoebel, D. M., A. Free, and C. J. Dorman. 2008. Anti-silencing: overcoming H-NS-mediated repression of transcription in Gram-negative enteric bacteria. Microbiology 154(Pt 9):2533-45.

Studier, F. W., A. H. Rosenberg, J. J. Dunn, and J. W. Dubendorff. 1990. Use of T7 RNA polymerase to direct expression of cloned genes. Methods Enzymol 185:60-89.

Suggs, S. V., R. B. Wallace, T. Hirose, E. H. Kawashima, and K. Itakura. 1981. Use of synthetic oligonucleotides as hybridization probes: isolation of cloned cDNA sequences for human beta 2-microglobulin. Proc Natl Acad Sci U S A 78(11):6613-7.

Sun, Y. C., A. Koumoutsi, and C. Darby. 2009. The response regulator PhoP negatively regulates *Yersinia pseudotuberculosis* and *Yersinia pestis* biofilms. FEMS Microbiol Lett 290(1):85-90.

Suzuki, K., P. Babitzke, S. R. Kushner, and T. Romeo. 2006. Identification of a novel regulatory protein (CsrD) that targets the global regulatory RNAs CsrB and CsrC for degradation by RNase E. Genes Dev 20(18):2605-17.

Timmermans, J., and L. Van Melderen. 2009. Conditional essentiality of the *csrA* gene in *Escherichia coli*. J Bacteriol 191(5):1722-4.

Timmermans, J., and L. Van Melderen. 2010. Post-transcriptional global regulation by CsrA in bacteria. Cell Mol Life Sci 67(17):2897-908.

Toivanen, A., and P. Toivanen. 2004. Reactive arthritis. Best Pract Res Clin Rheumatol 18(5):689-703.

Tolstorukov, M. Y., K. M. Virnik, S. Adhya, and V. B. Zhurkin. 2005. A-tract clusters may facilitate DNA packaging in bacterial nucleoid. Nucleic Acids Res 33(12):3907-18.

Tomljenovic-Berube, A. M., D. T. Mulder, M. D. Whiteside, F. S. Brinkman, and B. K. Coombes. 2010. Identification of the regulatory logic controlling *Salmonella* pathoadaptation by the SsrA-SsrB two-component system. PLoS Genet 6(3):e1000875.

Torres, A. G., G. N. Lopez-Sanchez, L. Milflores-Flores, S. D. Patel, M. Rojas-Lopez, C. F. Martinez de la Pena, M. M. Arenas-Hernandez, and Y. Martinez-Laguna. 2007. Ler and H-NS, regulators controlling expression of the long polar fimbriae of *Escherichia coli* O157:H7. J Bacteriol 189(16):5916-28.

Torres, A. G., T. M. Slater, S. D. Patel, V. L. Popov, and M. M. Arenas-Hernandez. 2008. Contribution of the Ler- and H-NS-regulated long polar fimbriae of *Escherichia coli* O157:H7 during binding to tissue-cultured cells. Infect Immun 76(11):5062-71.

Towbin, H., T. Staehelin, and J. Gordon. 1979. Electrophoretic transfer of proteins from polyacrylamide gels to nitrocellulose sheets: procedure and some applications. Proc Natl Acad Sci U S A 76(9):4350-4.

Tran, H. J., A. K. Heroven, L. Winkler, T. Spreter, B. Beatrix, and P. Dersch. 2005. Analysis of RovA, a transcriptional regulator of *Yersinia pseudotuberculosis* virulence that acts through antirepression and direct transcriptional activation. J Biol Chem 280(51):42423-32.

Trosky, J. E., A. D. Liverman, and K. Orth. 2008. *Yersinia* outer proteins: Yops. Cell Microbiol 10(3):557-65.

Trulzsch, K., M. F. Oellerich, and J. Heesemann. 2007. Invasion and dissemination of *Yersinia enterocolitica* in the mouse infection model. Adv Exp Med Biol 603:279-85.

Uliczka, F., T. Kornprobst, J. Eitel, D. Schneider, and P. Dersch. 2009. Cell invasion of *Yersinia pseudotuberculosis* by invasin and YadA requires protein kinase C, phospholipase C-gamma1 and Akt kinase. Cell Microbiol 11(12):1782-801.

Urbanowski, M. L., E. D. Brutinel, and T. L. Yahr. 2007. Translocation of ExsE into Chinese hamster ovary cells is required for transcriptional induction of the *Pseudomonas aeruginosa* type III secretion system. Infect Immun 75(9):4432-9.

Vakulskas, C. A., K. M. Brady, and T. L. Yahr. 2009. Mechanism of transcriptional activation by *Pseudomonas aeruginosa* ExsA. J Bacteriol 191(21):6654-64.

Vallis, A. J., T. L. Yahr, J. T. Barbieri, and D. W. Frank. 1999. Regulation of ExoS production and secretion by *Pseudomonas aeruginosa* in response to tissue culture conditions. Infect Immun 67(2):914-20.

Viboud, G. I., and J. B. Bliska. 2005. *Yersinia* outer proteins: role in modulation of host cell signaling responses and pathogenesis. Annu Rev Microbiol 59:69-89.

Viegas, S. C., V. Pfeiffer, A. Sittka, I. J. Silva, J. Vogel, and C. M. Arraiano. 2007. Characterization of the role of ribonucleases in *Salmonella* small RNA decay. Nucleic Acids Res 35(22):7651-64.

Vogel, J. 2009. A rough guide to the non-coding RNA world of *Salmonella*. Mol Microbiol 71(1):1-11.

Waldminghaus, T., A. Fippinger, J. Alfsmann, and F. Narberhaus. 2005. RNA thermometers are common in alpha- and gamma-proteobacteria. Biol Chem 386(12):1279-86.

Waldminghaus, T., L. C. Gaubig, B. Klinkert, and F. Narberhaus. 2009. The *Escherichia coli* ibpA thermometer is comprised of stable and unstable structural elements. RNA Biol 6(4):455-63.

Waldminghaus, T., N. Heidrich, S. Brantl, and F. Narberhaus. 2007. FourU: a novel type of RNA thermometer in *Salmonella*. Mol Microbiol 65(2):413-24.

Waldminghaus, T., J. Kortmann, S. Gesing, and F. Narberhaus. 2008. Generation of synthetic RNA-based thermosensors. Biol Chem 389(10):1319-26.

Watarai, M., T. Tobe, M. Yoshikawa, and C. Sasakawa. 1995. Contact of *Shigella* with host cells triggers release of Ipa invasins and is an essential function of invasiveness. EMBO J 14(11):2461-70.

Waters, C. M., J. T. Wu, M. E. Ramsey, R. C. Harris, and B. L. Bassler. 2010. Control of the type 3 secretion system in *Vibrio harveyi* by quorum sensing through repression of ExsA. Appl Environ Microbiol 76(15):4996-5004.

Wattiau, P., and G. R. Cornelis. 1994. Identification of DNA sequences recognized by VirF, the transcriptional activator of the *Yersinia yop* regulon. J Bacteriol 176(13):3878-84.

Wei, B. L., A. M. Brun-Zinkernagel, J. W. Simecka, B. M. Pruss, P. Babitzke, and T. Romeo. 2001. Positive regulation of motility and *flhDC* expression by the RNA-binding protein CsrA of *Escherichia coli*. Mol Microbiol 40(1):245-56.

Weilbacher, T., K. Suzuki, A. K. Dubey, X. Wang, S. Gudapaty, I. Morozov, C. S. Baker, D. Georgellis, P. Babitzke, and T. Romeo. 2003. A novel sRNA component of the carbon storage regulatory system of *Escherichia coli*. Mol Microbiol 48(3):657-70.

WHO. 2009. Human plague: review of regional morbidity and mortality, 2004-2009. Wkly Epidemiol Rec 85(6):40-5.

Wong, K. W., and R. R. Isberg. 2005. Emerging views on integrin signaling via Rac1 during invasin-promoted bacterial uptake. Curr Opin Microbiol 8(1):4-9.

Yahr, T. L., and D. W. Frank. 1994. Transcriptional organization of the trans-regulatory locus which controls exoenzyme S synthesis in *Pseudomonas aeruginosa*. J Bacteriol 176(13):3832-38.

Yahr, T. L., and M. C. Wolfgang. 2006. Transcriptional regulation of the *Pseudomonas aeruginosa* type III secretion system. Mol Microbiol 62(3):631-40.

Zuker, M. 2003. Mfold web server for nucleic acid folding and hybridization prediction. Nucleic Acids Res 31(13):3406-15.

Supplementary Material

1. Plasmid constructions

1.1 Construction of plasmid pKB4

To complement gene deletions, the coding sequence of *ymoA* was introduced into the low copy vector pHSG575. The insert was amplified using primer 1 and 2. Vector pHSG575 and the PCR product were digested with *Sal*I and *Bam*HI and ligated, generating pKB4.

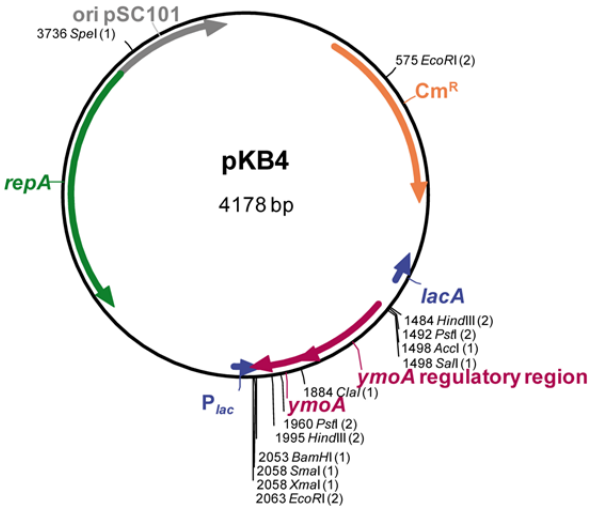

Fig. S1. Plasmid map of pKB4. The coding sequence of *ymoA* was inserted into the *Bam*HI/*Sal*I restriction sites of pHSG575 multiple cloning site, interrupting the *lacA* gene. In black, restriction sites preceded by nucleotide number of the cleavage site with respect to the plasmid origin, ( ) indicates number of restriction sites.

1.2 Construction of plasmids pKB13, pKB14 and pKB18

pKB13, pKB14 and pKB18 were constructed to measure the transcription-independent *lcrF* translation of the P_{BAD} promoter followed by the intergenic region between *yscW* and *lcrF* with different sequence deletions. Primers 3 and 6 were used to synthesize the insert for pKB14. The pKB18 insert was amplified with primers 6 and 7. For pKB13, the insert was generated by a three-step-PCR to delete nucleotides -41 to 30 in relation to the *lcrF* start codon. Therefore, an upstream fragment was generated with primers 3 and 4. The downstream fragment was synthesized using primers 5 and 6. In the last step, the resulting insert was amplified in reaction containing up- and downstream fragment with primers 3 and 6. All inserts were digested with *Eco*RI and *Nhe*I and ligated into the pBAD18-*lacZ* (481) linearized with the same restriction enzymes.

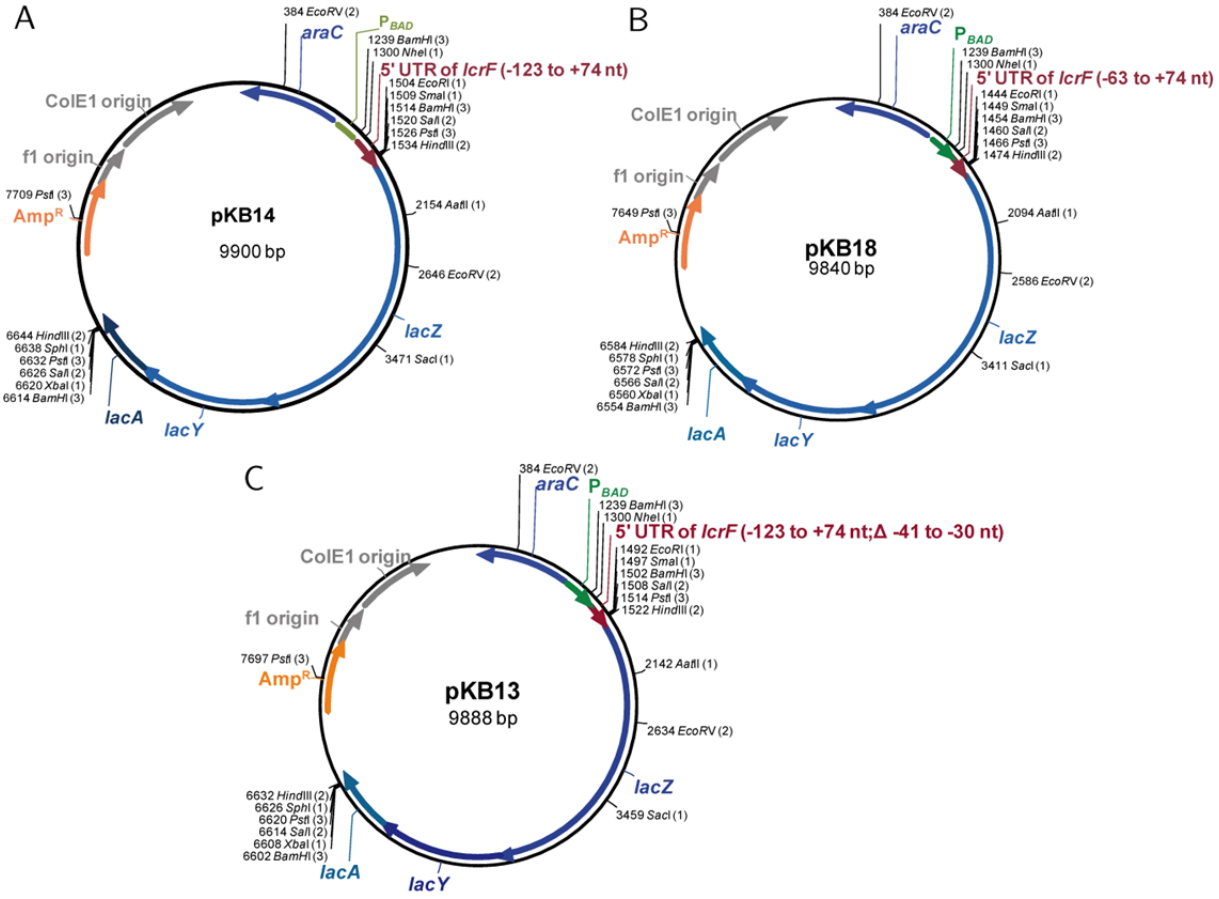

Fig. S2. Plasmid maps of pKB14, pKB18 and pKB13. A. The 5' UTR of *lcrF* from (A) nucleotide -123 to +74 (B) -63 to + 74 and (C) -123 to +74 with a deletion from position -41 to -30 relative to the *lcrF* start codon was introduced into the *Eco*RI-*Nhe*I sites of pBAD18-*lacZ* (481). In black, restriction sites preceded by nucleotide number of the cleavage site with respect to the plasmid origin. ( ) indicates number of restriction sites.

1.3 Construction of plasmid pKB20

To determine the *csrC* expression of construct harboring the first 71 nucleotides after the transcription start, a fragment was synthesized using primers 8 and 9. The insert was digested with *Eco*RI and *Sal*I and introduced into the similar linearized *lacZ* reporter gene vector pHT124.

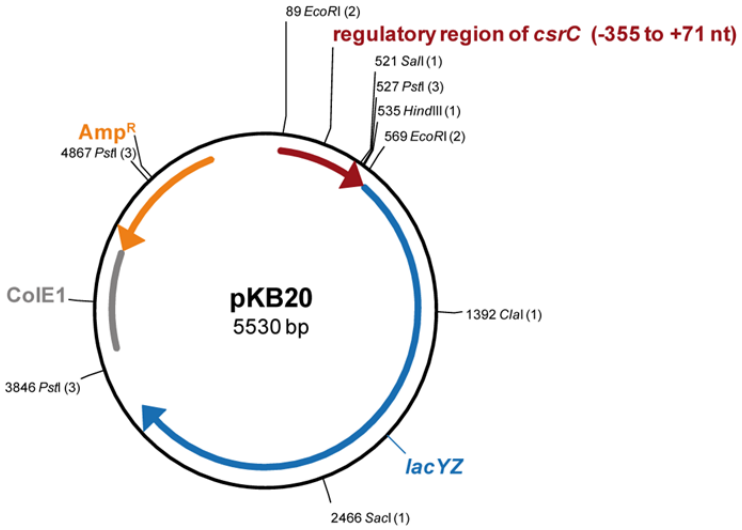

Fig. S3. Plasmid map of pKB20. The promoter region of *csrC* from positions -355 to +71 nt relative to the transcription start was inserted into vector pHT124 using restriction sites *EcoR*I and *Sal*I. In black, restriction sites preceded by nucleotide number of the cleavage site with respect to the plasmid origin, ( ) indicates number of restriction sites.

1.4 Construction of plasmid pKB17

For the expression of *csrC* with a deletion at nucleotides +24 to +57 relative the transcription start, a fragment was generated with primers 10 and 9 and digested with *EcoR*I and *Sal*I. The insert was introduced into the *lacZ* reporter gene vector pHT124 linearized with the same restriction enzymes.

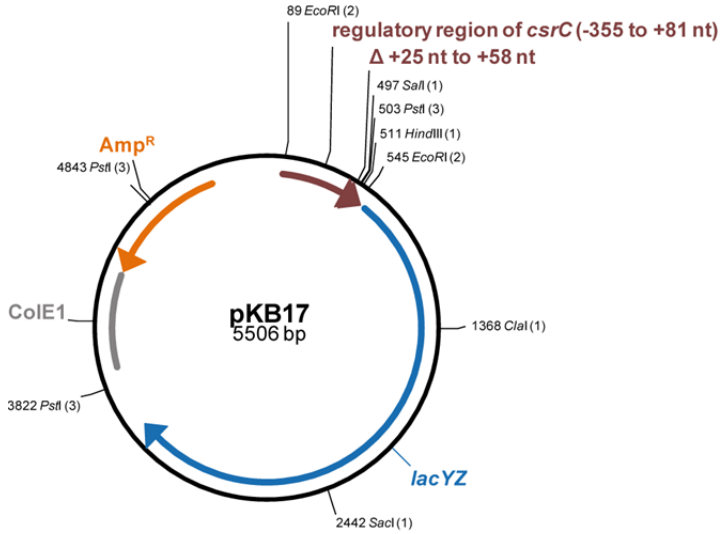

Fig. S4. Plasmid map of pKB17. The promoter region of *csrC* from positions -355 to +81 nt relative to the transcription start with a deletion at positions +24 to +57 nt was inserted into vector pHT124 using restriction sites *EcoR*I and *Sal*I. In black, restriction sites preceded by nucleotide number of the cleavage site with respect to the plasmid origin, ( ) indicates number of restriction sites.

1.5 Construction of plasmids pKB34 and pKB38 to pKB43

To measure the influence of YmoA on the *yscW* promoter region translational promoter deletion fusions were constructed. Therefore, fragments comprising the *yscW* promoter region, the *yscW* gene, 5' region of *lcrF* and *lcrF* gene were generated producing an *yscW* upstream region to position -573 (pKB34), -466 (pKB39), -368 (pKB40), -267 (pKB41), -171 (pKB42), -73 (pKB43) and -8 (pKB38) with primer pairs 11/12, 15/12, 16/12, 17/12, 18/12, 19/12 and 14/12, respectively. The inserts were digested with *Pst*I and ligated into the similarly linearized and dephosphorylated vector pTS02, which fuses the fragment in frame to a *lacZ* reporter gene.

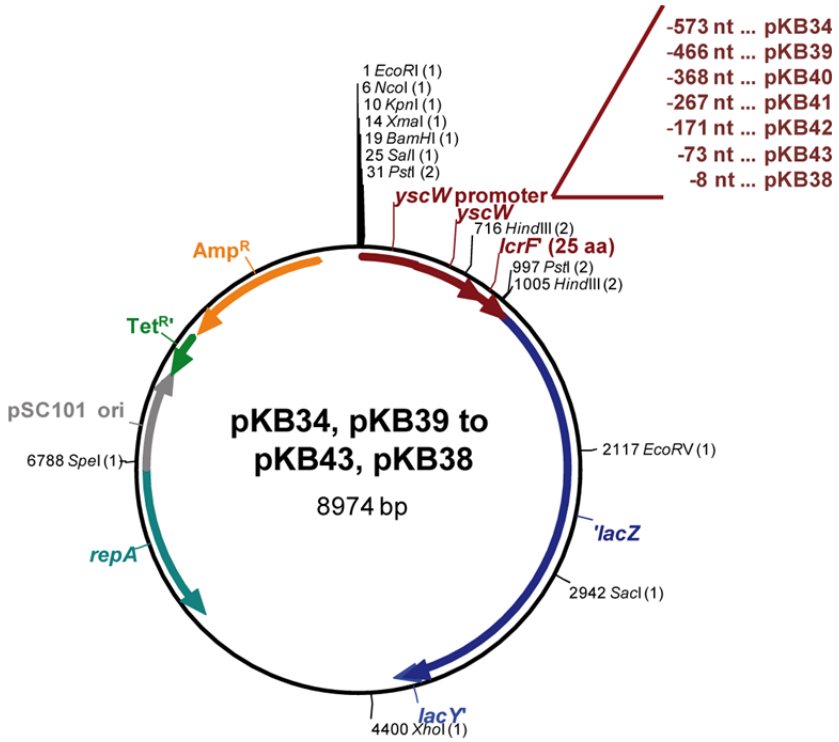

Fig. S5. Plasmid maps of pKB34, pKB39 to pKB43 and pKB38. Promoter deletion fusion with *yscW*/*lcrF* regions from positions -573 (pKB34), -466 (pKB39), -368 (pKB40), -267 (pKB41), -171 (pKB42), -73 (pKB43) and -8 (pKB38) upstream of the *yscW* gene were fused to the *lacZ* gene of vector pTS02 at the *Pst*I restriction site. In black, restriction sites preceded by nucleotide number of the cleavage site with respect to the plasmid origin, ( ) indicates number of restriction sites.

1.6 Construction of plasmid pKB35

To determine the impact of Hfq on the *yscW* gene expression, the promoter region of *yscW* and the following five codons of the *yscW* gene were fused to the reporter gene *lacZ* in vector pTS02. Therefore an insert was amplified with primers 11 and 13. After digestion with *Pst*I, it was ligated into the corresponding restriction site of the linearized and dephosporylated vector.

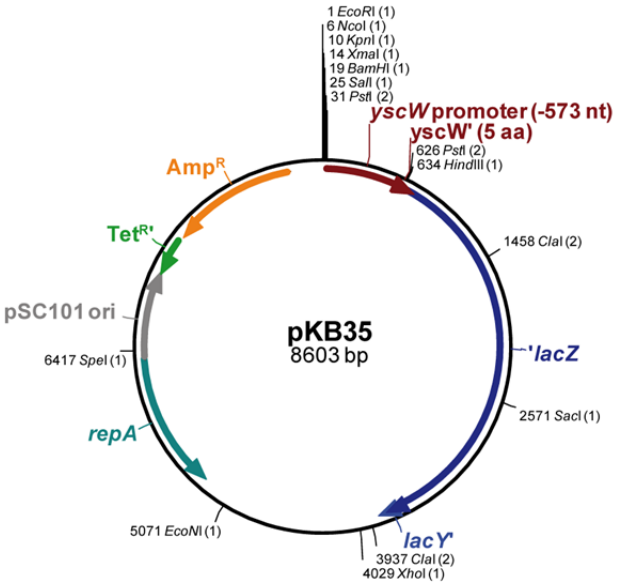

Fig. S6. Plasmid map of pKB35. The promoter region of *yscW* and five codons of the *yscW* gene were introduced into pTS02 at the *Pst*I site for translational fusion to a *lacZ* reporter gene. In black, restriction sites preceded by nucleotide number of the cleavage site with respect to the plasmid origin, ( ) indicates number of restriction sites.

1.7 Construction of plasmids pKB45 and pKB46

Plasmids pKB45 and pKB46 were constructed to examine the effect of H-NS on *csrC* expression. For this purpose, the regulatory region of *csrC* and 4 nt (pKB45) or 81 nt (pKB46) downstream of the transcription start were amplified with primer pairs 20/21 or 20/22, respectively. Generated fragments were digested with *Pst*I and inserted into the corresponding restriction site of the linearized and dephosphorylated vector pTS03.

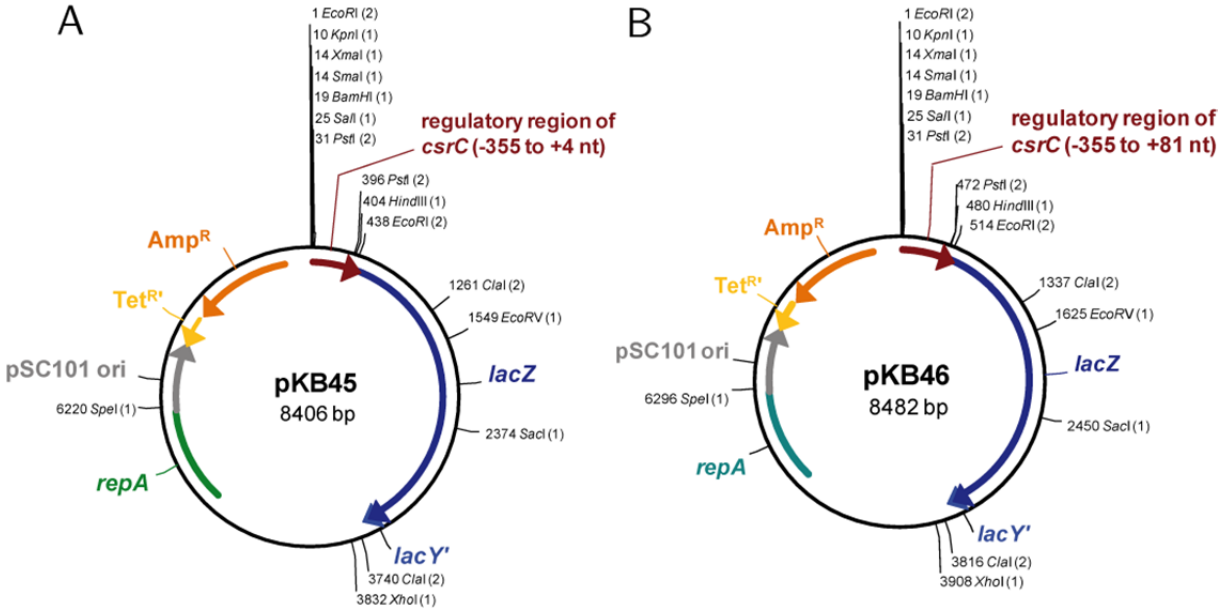

Fig. S7. Plasmid maps of pKB45 and pKB46. The promoter region of *csrC* and 4 nt or 81 nt of the sequence 3' of the transcriptional start site was introduced into pTS03 at the *Pst*I site, generating pKB45 and pKB46, respectively. In black, restriction sites preceded by nucleotide number of the cleavage site with respect to the plasmid origin, ( ) indicates number of restriction sites.

1.8 Construction of plasmid pKB47

To express *csrC* independently from transcription, a P_{tet} promoter was fused to the *csrC* gene by PCR using primers 23 and 24. The insert was digested by *Sal*I and *Bam*HI and ligated into the linearized vector pHSG575 cleaved with the same restriction enzymes.

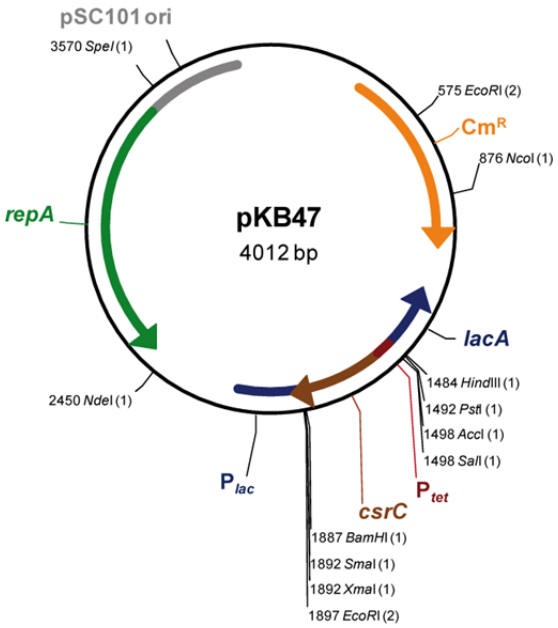

Fig. S8. Plasmid map of pKB47. A fragment carrying the sequence of P_{tet} and the *csrC* gene was introduced into the *Pst*I site of pHSG575. In black, restriction sites preceded by nucleotide number of the cleavage site with respect to the plasmid origin, ( ) indicates number of restriction sites.

1.9 Construction of plasmids pKB49 and pKB59

To compare the synthesis of RNA from a *csrC* wild type gene and *csrC* harboring a deletion from position +24 to +57 relative to the transcription start. An insert carrying the *csrC* gene and its regulatory region was synthesized by primers 27 and 28, digested with *Bam*HI and *Sal*I and ligated into pHSG576, generating pKB59. Deletion of the region deletion from position +24 to +57 within the *csrC* gene was accomplished by three-step-PCR. First, the upstream region was amplified by primers 25 and 27, where primer contained the mutated region. In the following, primers 26 and 28 were used to generate a downstream fragment, in which primer 26 missed the nucleotides to be deleted. In a third step, up- and downstream fragment were mixed with primers 25 and 28 to generate the entire insert. This was digested with *Sal*I and *Bam*HI and introduced into pHSG576 resulting in pKB49.

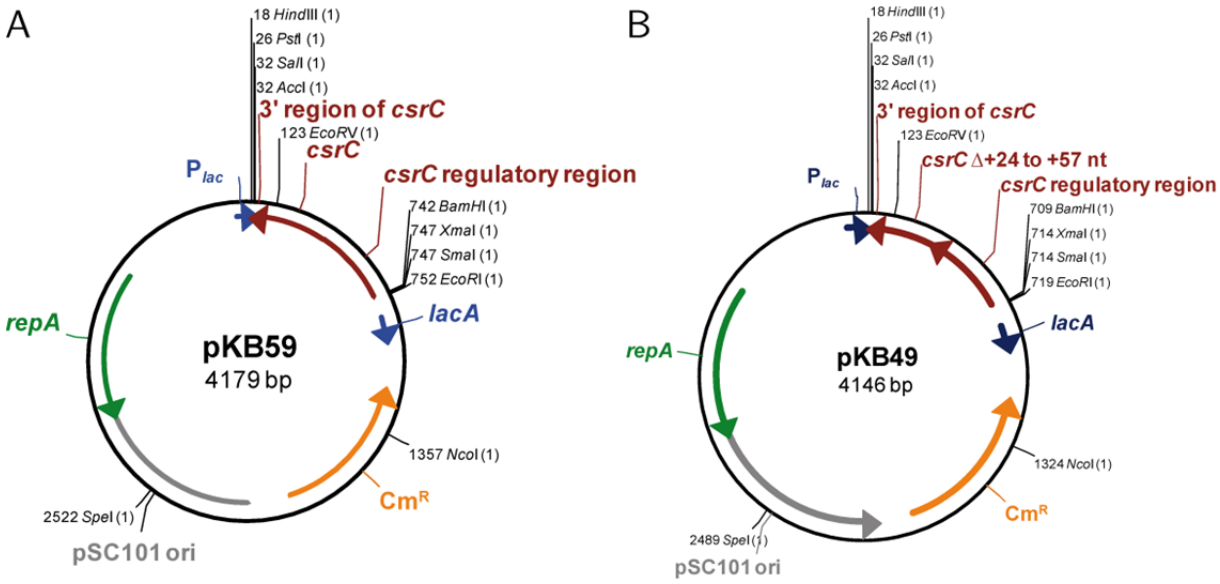

Fig. S9. Plasmid maps of pKB59 and pKB49. Fragments harboring the regulatory region of *csrC* and (A) the wild type *csrC* gene or (B) *csrC* missing the region from position +24 to +57 relative to the transcription start were inserted into vector pHSG576 generating pKB59 and pKB49, respectively. In black, restriction sites preceded by nucleotide number of the cleavage site with respect to the plasmid origin, ( ) indicates number of restriction sites.

1.10 Construction of plasmid pKB60

Expression of *csrA* from a low copy vector was essential to prevent toxic effects of the CsrA protein. The coding region of *csrA* was amplified using primers 29 and 30. The insert was digested with *Sal*I and *Bam*HI and ligated into the linearized vector pHSG576.

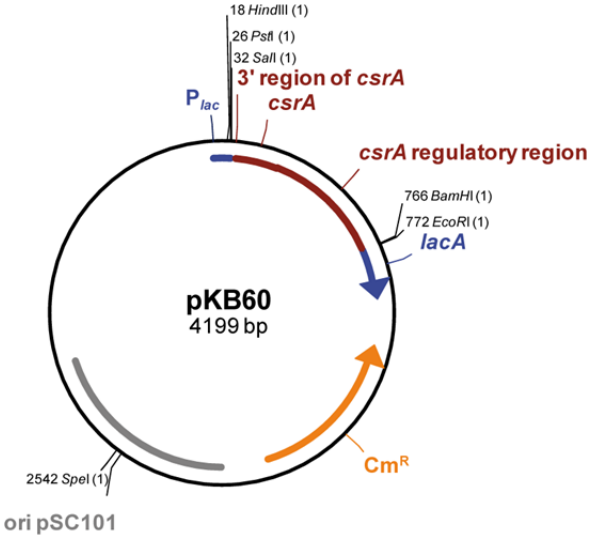

Fig. S10. Plasmid maps of pKB60. The coding sequence of *csrA* was ligated into the *Bam*HI and *Sal*I sites of pHSG576. In black, restriction sites preceded by nucleotide number of the cleavage site with respect to the plasmid origin, ( ) indicates number of restriction sites.

1.11 Construction of plasmid pKB63

To monitor the transcription activity of the *csrA* regulatory region, the promoter sequence of *csrA* and five codons of *csrA* was amplified using primers 31 and 32. The insert was digested

with *Pst*I and ligated into the linearized, dephosphorylated vector pTS02. This fuses the *csrA* coding region in frame to a *lacZ* reporter gene generating pKB63.

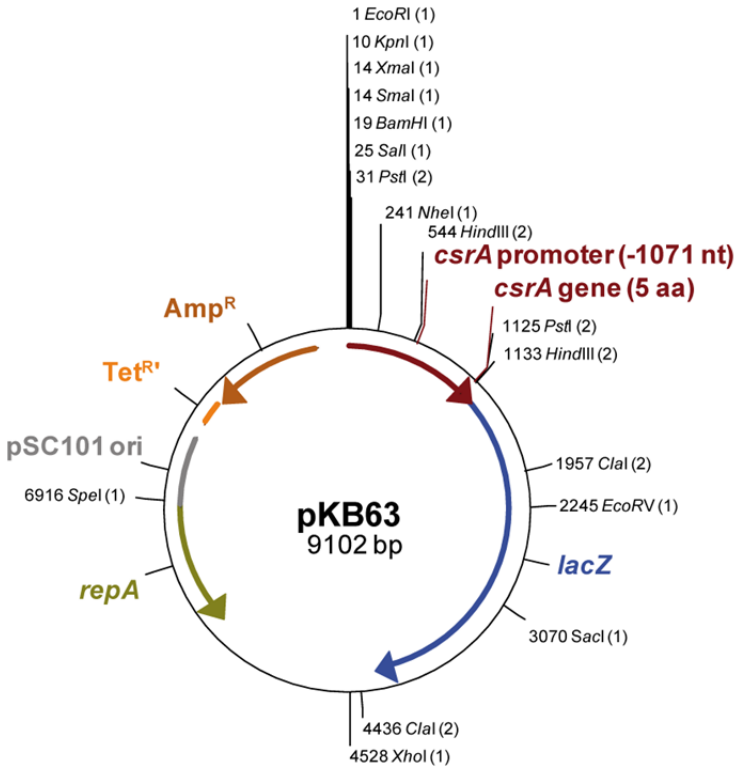

Fig. S11. Plasmid maps of pKB63. An insert harboring the promoter sequence of *csrA* and the first 5 codons of *csrA* was fused to *lacZ* reporter gene of vector pTS02 at the *Pst*I site. In black, restriction sites preceded by nucleotide number of the cleavage site with respect to the plasmid origin, ( ) indicates number of restriction sites.